



**US Army Corps
of Engineers**
Waterways Experiment
Station

Technical Report ITL-99-1
January 1999

Computer Aided Structural Engineering Project

Development of an Improved Numerical Model for Concrete-to-Soil Interfaces in Soil-Structure Interaction Analyses

Report 1

Preliminary Study

*by Jesús E. Gómez, George M. Filz, Virginia Polytechnic Institute
and State University*

Robert M. Ebeling, WES



Approved For Public Release; Distribution Is Unlimited

DTIC QUALITY INSPECTED 3

Prepared for Headquarters, U.S. Army Corps of Engineers

19990126 055

The contents of this report are not to be used for advertising, publication, or promotional purposes. Citation of trade names does not constitute an official endorsement or approval of the use of such commercial products.

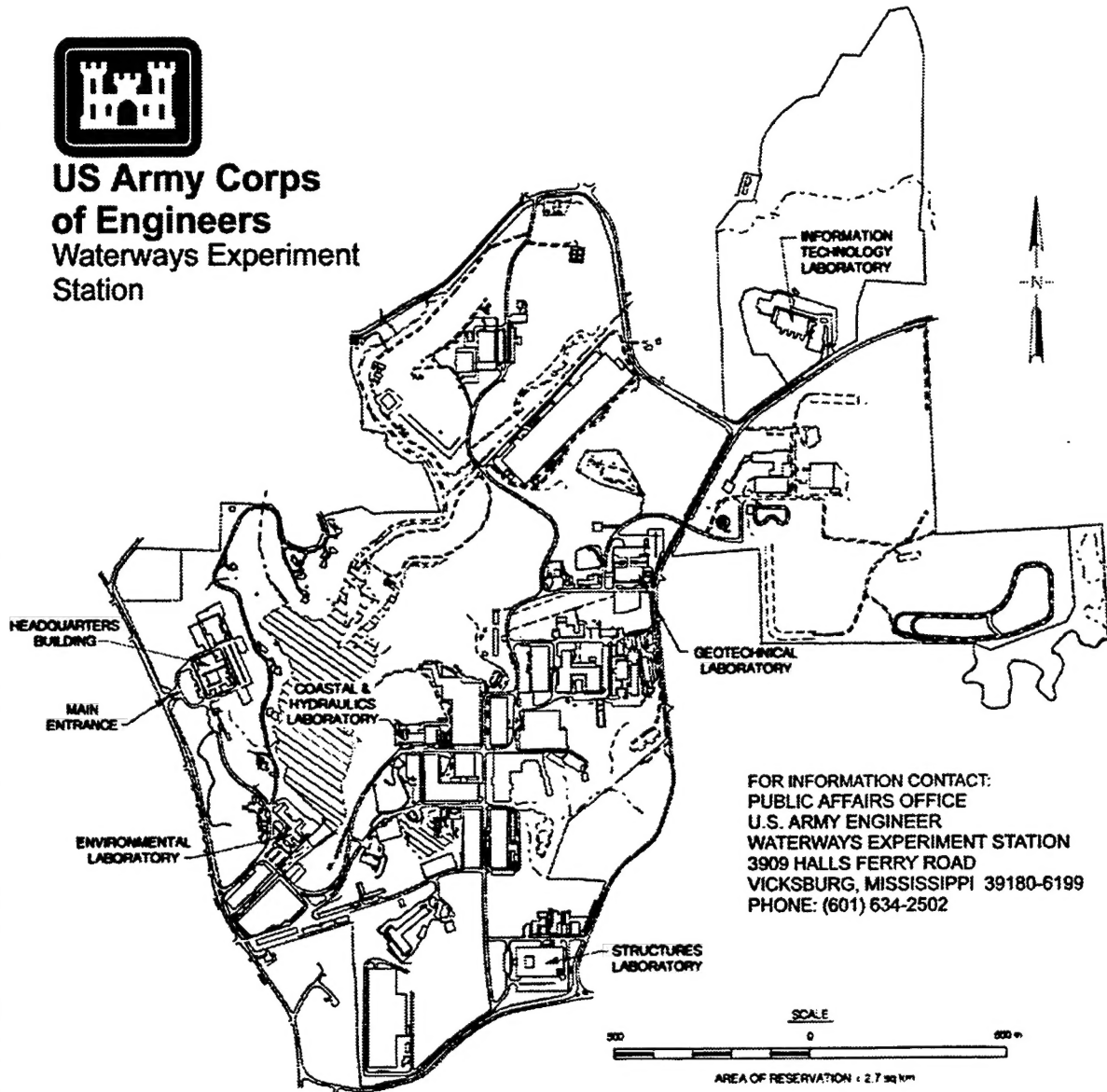
The findings of this report are not to be construed as an official Department of the Army position, unless so designated by other authorized documents.



PRINTED ON RECYCLED PAPER



**US Army Corps
of Engineers**
Waterways Experiment
Station



FOR INFORMATION CONTACT:
PUBLIC AFFAIRS OFFICE
U.S. ARMY ENGINEER
WATERWAYS EXPERIMENT STATION
3909 HALLS FERRY ROAD
VICKSBURG, MISSISSIPPI 39180-6199
PHONE: (601) 634-2502

Waterways Experiment Station Cataloging-in-Publication Data

Gomez, Jesus E.

Development of an improved numerical model for concrete-to-soil interfaces in soil-structure interaction analyses. Report 1, Preliminary study / by Jesus E. Gomez, George M. Filz, Robert M. Ebeling ; prepared for U.S. Army Corps of Engineers.

153 p. : ill. ; 28 cm. — (Technical report ; ITL-99-1 rept.1)

Includes bibliographical references.

Report 1 of a series.

1. Soil-structure interaction — Mathematical models. 2. Locks (Hydraulic engineering) I. Filz, George Michael, 1953- II. Ebeling, Robert M., 1954- III. United States. Army. Corps of Engineers. IV. U.S. Army Engineer Waterways Experiment Station. V. Information Technology Laboratory (U.S. Army Engineer Waterways Experiment Station) VI. Computer Aided Structural Engineering Project (U.S.) V. Title. VI. Series: Technical report (U.S. Army Engineer Waterways Experiment Station) ; ITL-99-1 rept.1.

TA7 W34 no.ITL-99-1 rept.1

Contents

| | |
|---|----|
| Preface | vi |
| 1—Introduction | 1 |
| 1.1 Background | 1 |
| 1.2 Interface Behavior in SSI Analyses | 2 |
| 1.2.1 The North Lock Wall at McAlpine Locks | 2 |
| 1.2.2 Limitations of existing interface models | 7 |
| 1.2.3 Improvements to existing models | 11 |
| 1.3 Project Scope | 12 |
| 1.3.1 Interface testing | 12 |
| 1.3.2 Development of interface model | 12 |
| 1.4 Report Organization | 13 |
| 2—Literature Review | 14 |
| 2.1 Interface Testing | 14 |
| 2.1.1 Direct Shear Box (DSB) devices | 14 |
| 2.1.2 Direct Simple Shear (DSS) devices | 15 |
| 2.1.3 Other devices | 17 |
| 2.1.4 Summary of previous findings on interface testing and interface behavior | 18 |
| 2.1.5 The Large Displacement Shear Box (LDSB) | 20 |
| 2.2 Interface Modeling | 20 |
| 2.2.1 Interface elements | 21 |
| 2.2.2 Interface constitutive models | 23 |
| 2.2.3 The hyperbolic model | 24 |
| 2.3 SSI Analyses of Retaining Walls | 28 |
| 2.3.1 Review of previous work | 28 |
| 2.3.2 Simplified procedure for calculating the downdrag force | 30 |
| 2.4 Summary | 35 |
| 3—Laboratory Testing | 40 |
| 3.1 Soil Properties | 40 |
| 3.1.1 Triaxial testing | 41 |
| 3.1.2 Hyperbolic parameters from triaxial tests | 41 |
| 3.2 Concrete Specimen | 45 |
| 3.2.1 Materials | 49 |

| | | |
|-------|--|-----|
| 3.2.2 | Preparation of the specimen | 49 |
| 3.2.3 | Surface texture | 52 |
| 3.3 | Testing Procedures | 56 |
| 3.3.1 | The soil box | 56 |
| 3.3.2 | Preparation of the interface | 57 |
| 3.3.3 | The Large Direct Shear Box (LDSB) | 57 |
| 3.3.4 | Test setup | 59 |
| 3.3.5 | Data reduction | 59 |
| 3.4 | Testing Program | 60 |
| 3.4.1 | Types of interface testing performed | 60 |
| 3.4.2 | Testing parameters | 62 |
| 3.5 | Results of Interface Tests | 62 |
| 3.5.1 | Initial loading tests | 62 |
| 3.5.2 | Staged shear tests | 65 |
| 3.5.3 | Shear reversals | 70 |
| 3.5.4 | Unload-reload tests | 70 |
| 3.6 | Summary | 79 |
| 4— | Extended Hyperbolic Model | 82 |
| 4.1 | Hyperbolic Model for Initial Loading | 82 |
| 4.1.1 | Determination of hyperbolic parameters: Clough and Duncan (1971) procedure | 83 |
| 4.1.2 | SID criterion for the determination of hyperbolic parameters | 86 |
| 4.1.3 | Evaluation of the model against results of initial loading tests ... | 86 |
| 4.2 | Hyperbolic Model Extended to Shear Stress Reversals | 88 |
| 4.2.1 | Formulation | 88 |
| 4.2.2 | Evaluation of the model against results of shear reversal tests ... | 92 |
| 4.3 | Hyperbolic Model Extended to Unload-Reload Cycles | 97 |
| 4.3.1 | Formulation | 97 |
| 4.3.2 | Determination of the model parameter values | 99 |
| 4.3.3 | Evaluation of the model against results of unload-reload interface tests | 103 |
| 4.3.4 | Limitations of the hyperbolic model extended to unload-reload cycles | 108 |
| 4.3.5 | Optional beta-formulation for repeated unload-reload cycles in the first quadrant | 108 |
| 4.4 | Hyperbolic Model Extended to Staged Shear | 113 |
| 4.4.1 | Formulation | 113 |
| 4.4.2 | Hyperbolic parameters for staged shear | 114 |
| 4.4.3 | Evaluation of the model against results of staged tests | 116 |
| 4.5 | Advantages and Limitations of the Extended Hyperbolic Model | 116 |
| 4.6 | Summary | 122 |
| 5— | Summary and Conclusions | 127 |
| 5.1 | Summary of Activities | 127 |
| 5.1.1 | Literature review | 128 |
| 5.1.2 | Laboratory testing | 129 |
| 5.1.3 | Extended hyperbolic model | 130 |

| | |
|----------------------------|-----|
| 5.2 Conclusions | 131 |
| 5.3 Recommended Work | 132 |
| References | 134 |
| Appendix A: Notation | A1 |
| SF 298 | |

Preface

The work described herein summarizes the results of a preliminary study which, when completed, will lead to the development of an improved numerical model for concrete-to-soil interfaces for use in soil-structure interaction analyses. These improvements will extend the accuracy of current interface models to include unload-reload and staged shear interface behavior. Accurate unload-reload concrete-to-soil interface behavior is important to cases involving the partial or complete submergence of a lock and its backfill, commonly referred to as a post-construction rise in the groundwater level. The resulting interface numerical model is intended for implementation in the incremental construction soil-structure interaction program SOILSTRUCT. Funding for this research was provided by the Computer-Aided Structural Engineering Project sponsored by Headquarters, U. S. Army Corps of Engineers (HQUSACE), as part of the Civil Works Research and Development Program on Structural Engineering (CWR&D). The work was performed under Civil Works Work Unit 31589, "Computer-Aided Structural Engineering (CASE)," for which Dr. Robert Hall, Structures Laboratory (SL), U.S. Army Engineer Waterways Experiment Station (WES), is Problem Area Leader and Mr. H. Wayne Jones, Information Technology Laboratory (ITL), WES, is the Principal Investigator. The HQUSACE Technical Monitor is Mr. Lucian Guthrie, CECW-ED.

The work was performed at Virginia Polytechnic Institute and State University, Blacksburg, by Mr. Jesús E. Gómez, doctoral student, and Dr. George M. Filz, Associate Professor, under the guidance and supervision of Dr. Robert M. Ebeling, Computer-Aided Engineering Division (CAED), ITL. The research consisted of performing large-scale sand-to-concrete interface tests, researching current interface models for primary shear loading, and developing a preliminary interface model for staged shear primary loading and unloading-reloading. A survey of existing concrete retaining walls was carried out by Mr. Gómez. The concrete specimen for interface testing was prepared by Mr. Gómez and Mr. Derrick Shelton at the Structures Laboratory at Virginia Tech. Mr. Gómez performed the large-scale interface test program at the Geotechnical Laboratory at Virginia Tech. The preliminary version of the new interface model was developed by Mr. Gómez and Dr. Filz, with contributions by Dr. Ebeling. This report was prepared by Mr. Gómez, Dr. Filz, and Dr. Ebeling under the direct supervision of Mr. H. Wayne Jones, Chief, CAED, ITL, and Dr. N. Radhakrishnan, Director, ITL.

At the time of publication of this report, Director of WES was Dr. Robert W. Whalin. Commander was COL Robin R. Cababa, EN.

The contents of this report are not to be used for advertising, publication, or promotional purposes. Citation of trade names does not constitute an official endorsement or approval of the use of such commercial products.

1 Introduction

1.1 Background

Soil-Structure Interaction (SSI) analyses have proven to be a powerful tool for use in analyzing, designing, and monitoring geotechnical structures. A substantial amount of the geotechnical literature of the last 30 years has dealt with the development or improvement of techniques for SSI analyses of retaining walls, piles, anchors, etc. These analyses may be performed to address key issues concerning the behavior of the structure in the design stage, and often provide a means for evaluation of instrumentation data from the completed structure.

SSI analyses are particularly useful in problems of complex geometry and loading conditions such as lock walls. In these cases, simple analyses are not adequate to characterize the behavior of the soil-structure system. Factors such as the placement of the backfill, filling of the lock with water, changes in the water table elevation behind the wall, temperature fluctuations, etc., play an important role in the behavior of the structure.

The first clear evidence of the importance of these factors was provided by the analyses of the Port Allen and Old River locks performed by Clough and Duncan (1969). Extensive instrumentation data suggested deformation patterns of the locks that seemed unreasonable, and were therefore considered as produced by instrumentation errors. Clough and Duncan (1969 and 1971) showed that close modeling of the construction stages of the lock and the use of a simple but adequate constitutive model for the soil and for the soil-to-structure interface yielded results in close agreement with the measured data. For their analyses they used the hyperbolic model for soils proposed by Duncan and Chang (1970) following previous work by Kondner (1963) and Kondner and Zelasko (1963). The adequacy of this simple stress-strain model for use in SSI analyses is discussed in section 4.1 of Ebeling, Peters, and Mosher (1997). This model has been extended to interface behavior as described by Clough and Duncan (1971).

Several important contributions followed the pioneering work of Clough and Duncan. Studies of the Red River Lock and Dam No. 1 (Ebeling et al. 1993; Ebeling and Mosher 1996; and Ebeling, Peters, and Mosher 1997), the North Lock Wall at McAlpine Locks (Ebeling and Wahl 1997), and Locks 27 (Ebeling, Pace, and Morrison 1997) are good examples of state-of-the-art techniques

available for SSI analyses. These studies showed that the behavior of the soil-structure interface has a significant influence on the magnitudes of the loads acting against the lock wall. They also illustrated that the pre- and post-construction stress paths followed by interface elements often involve simultaneous changes in normal and shear stresses, as well as shear stress reversals.

The hyperbolic interface model developed by Clough and Duncan (1971) is a very useful tool for SSI analyses. It is easy to implement and the parameters involved in the hyperbolic fit to laboratory data have a physical meaning. Although it models interface behavior in the primary loading stage very closely, it has not been extended to accurately model simultaneous changes in shear and normal stresses, reduction of shear stress, reversals in the direction of shear, or unload-reload cycles at the interface.

The purpose of the research described in this report is to develop test data and perform preliminary modeling. This will lead ultimately to the development of an improved numerical model for soil-structure interfaces that can handle a wide variety of stress paths. This research is being performed in two phases. The results of the first phase are summarized in this report. Development of the final version of the improved interface model will be completed during the second phase of research. Implementation of this improved model in SSI analyses of lock walls will allow a more realistic evaluation of the vertical and horizontal forces that act on this type of structure.

1.2 Interface Behavior in SSI Analyses

Based on SSI analyses of four hypothetical earth retaining structures, Ebeling, Duncan, and Clough (1990) concluded that the interface shear stiffness has a significant influence on the distribution of forces on the structure. They performed two different analyses of the same structure using the expected maximum and minimum values of shear stiffness of the backfill-to-structure interface. A difference of 12.5 percent was found between the values of friction angle mobilized at the base of the structure for the two analyses. Further evidence of the importance of interface behavior in SSI analyses has been provided in a study of the North Lock Wall at McAlpine Locks (Ebeling and Wahl 1997).

1.2.1 The North Lock Wall at McAlpine Locks

The North Lock Wall at McAlpine Locks (Ebeling and Wahl 1997) has been designed as a monolith of roller-compacted concrete (RCC) directly founded on rock as illustrated in Figure 1-1. The lock wall will be 22.25 m (73 ft) high with a dense granular backfill extending from the new RCC lock to the existing lock wall as shown in the figure. The analyses were performed using the finite

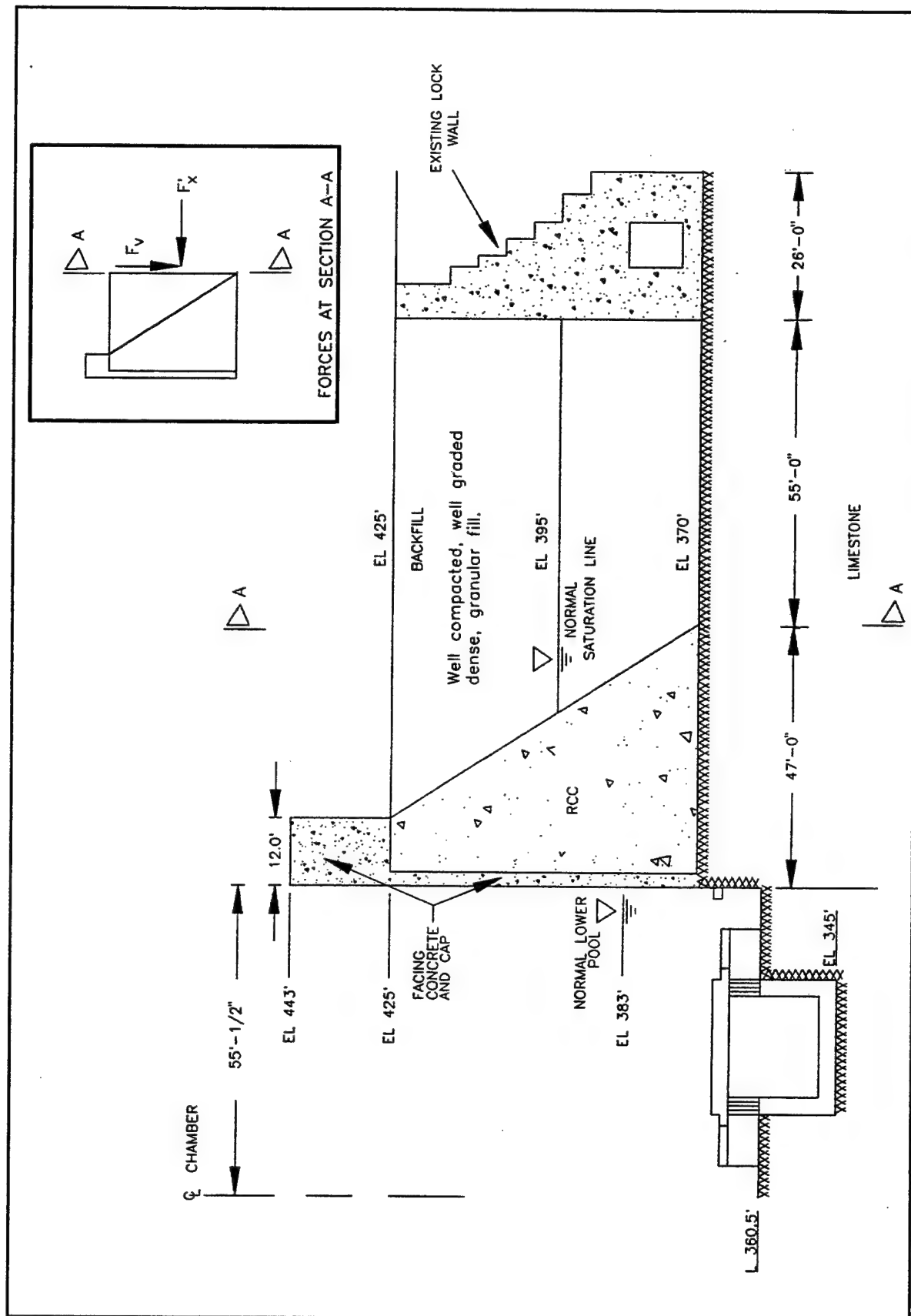


Figure 1-1. Typical section, north wall of new RCC McAlpine Lock (adapted from Ebeling and Wahl 1997) (1 ft = 0.305 m)

element program SOILSTRUCT-ALPHA (Ebeling, Duncan, and Clough 1990), which is an updated version of SOILSTRUCT (Clough and Duncan 1969) that allows for separation between the base of the wall and the foundation.

The analyses performed for the North Lock Wall were completed in three phases: (a) gravity turn-on analysis prior to construction of the new lock, (b) incremental construction of the new lock and concurrent backfill placement, and (c) postconstruction submergence of the backfill and flooding of the lock chamber. The lock-to-backfill, lock-to-rock, and backfill-to-rock interfaces were modeled using Goodman, Taylor, and Brekke (1968) one-dimensional interface elements. The hyperbolic models proposed by Duncan and Chang (1970) and Clough and Duncan (1971) were used for the backfill and the interfaces, respectively.

Table 1-1 shows the results of the analyses in terms of the effective horizontal and vertical forces F'_x and F_v per unit length, acting on section A-A represented in Figure 1-1.¹ The vertical force F_v represents the downdrag on section A-A caused by the settlement of the backfill.

| Table 1-1 Summary of Results of SSI Analyses for the North Lock at McAlpine Locks (adapted from Ebeling and Wahl 1997) | | | | | |
|---|---|--|---|-------------------------|-------------------------|
| Condition | Effective Overburden, kN per m Run Of Wall | F'_x, kN per m Run Of Wall | F_v, kN per m Run Of Wall | K_h | K_v |
| After backfilling | 2,782 | 1,217 | 167 | 0.437 | 0.060 |
| After submergence | 2,515 | 1,155 | 99 | 0.459 | 0.039 |

The earth pressure coefficients K_h and K_v , also shown in Table 1-1, are a convenient way to quantify the effective horizontal and vertical forces acting on section A-A. They represent the ratio of these forces to the *effective overburden* and are calculated as follows (Ebeling and Wahl 1997):

$$\text{Effective Overburden} = \int_{EI370}^{EI425} \sigma'_v dy \quad (1-1)$$

$$K_h = \frac{F'_x}{\text{Effective Overburden}} \quad (1-2)$$

$$K_v = \frac{F_v}{\text{Effective Overburden}} \quad (1-3)$$

where σ'_v = effective vertical stress acting along section A-A.

¹ For convenience, symbols are listed and defined in the Notation (Appendix A).

The earth pressure coefficients K_h and K_v are useful for consistent comparison between results of analyses at different operational stages of the lock wall, and even between retaining walls of different geometry and loading conditions. The vertical earth pressure coefficient K_v is also used in a simplified procedure to estimate the downdrag on retaining walls founded on rock. This simplified procedure (Appendix F in Engineer Circular (EC) 1110-2-291, Stability Analysis of Concrete Structures (Headquarters, U.S. Army Corps of Engineers (HQUSACE), 1997)) is described in detail in Chapter 2.

The results in Table 1-1 show that, after backfilling and prior to inundation, the magnitude of the downdrag on the wall is substantial and amounts to 6 percent of the effective overburden. The mechanism for generation of this downdrag during backfilling is illustrated in Figure 1-2a. The initial horizontal position of the surface of a compacted lift is shown. As the backfill placement progresses, the weight of the newly placed and compacted lifts compresses the underlying backfill. The relative movement between the compressing backfill and the wall generates shear stresses at the backfill-to-structure interface. The final configuration of the lift illustrates the nonuniform compression of the backfill due to the restraint imposed by the interface shear stresses.

Filz (1992) and Filz and Duncan (1997) showed that the distribution of the backfill-to-structure interface shear stresses is not uniform along the height of the wall. For walls founded on relatively incompressible materials, such as the rock-founded North Lock Wall, there is no settlement at the bottom of the backfill due to the absence of underlying compressible material. The top of the backfill does not settle if no further loads are applied after completion of backfilling with soils that do not creep. The maximum interface shear stress occurs at some intermediate point between the top and bottom of the backfill.

Table 1-1 also shows the results of the analyses considering a postconstruction submergence of the backfill. There is a substantial reduction of the vertical shear force and the vertical earth pressure coefficient K_v with respect to the analysis before submergence. The mechanism for this reduction of shear stresses is illustrated in Figure 1-2b. As the groundwater level in the backfill rises, there is a decrease in the effective stresses and, in the absence of hydrocompression, an upward movement of the backfill. As the backfill in contact with the wall rises, the shear stresses at the interface decrease.

The magnitude of the vertical shear forces acting on the back of the wall may have a significant impact on the stability of the structure. These vertical shear forces have a stabilizing effect that could produce economies if accounted for in the design of the structure. Reliable calculation of these forces requires an adequate constitutive model for the interface response to conditions such as those represented in Figure 1-2.

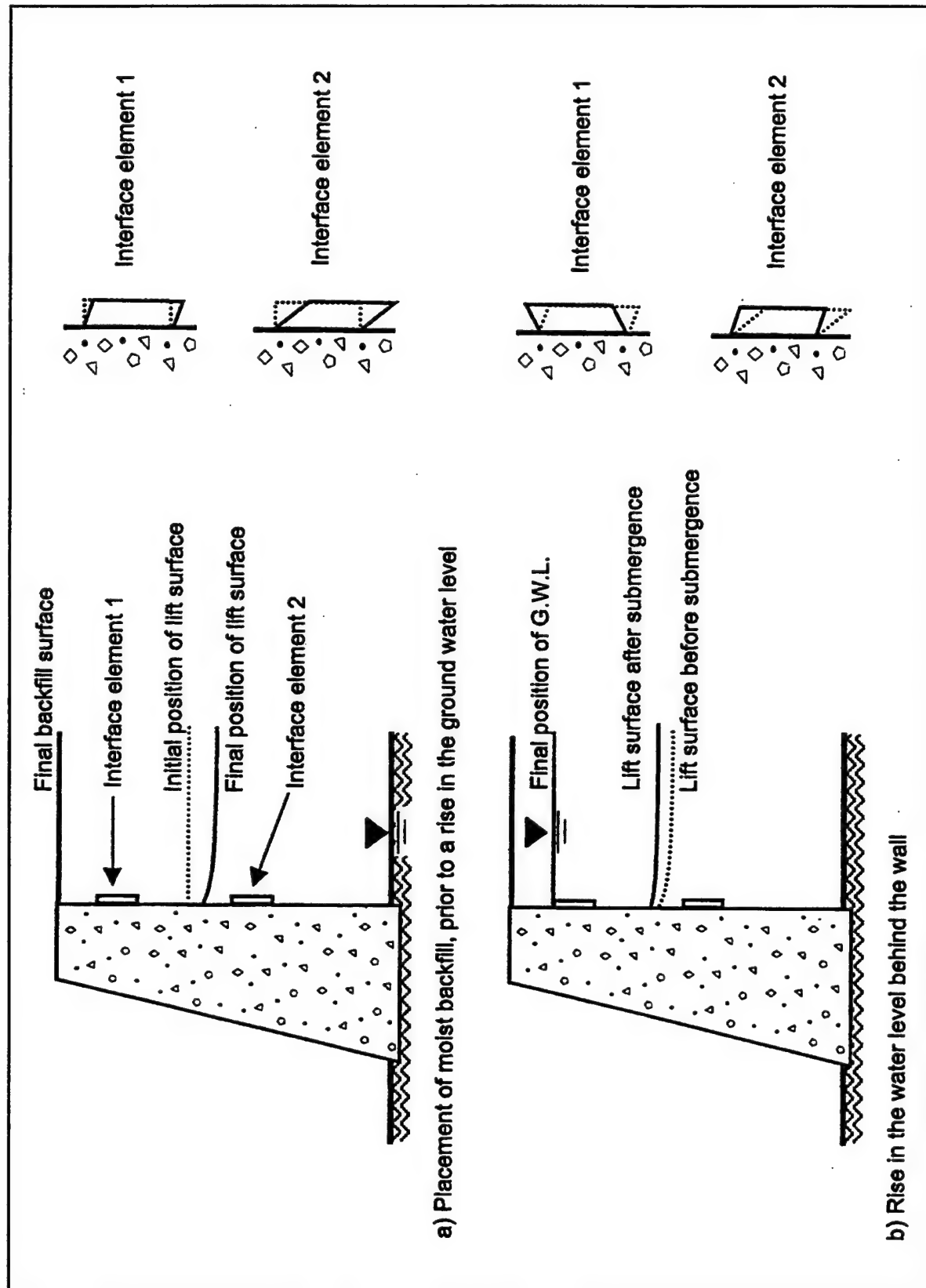


Figure 1-2. Simplified illustration of the mechanism of downdrag and shear reversal in a typical lock wall

1.2.2 Limitations of existing interface models

Two interface elements are represented in the simplified lock wall scheme of Figure 1-2. The normal and shear stresses acting on these elements change simultaneously during backfill placement and subsequent submergence of the backfill. Figure 1-3a shows the typical field stress paths followed by these elements during placement of the backfill. Element 1, which is located close to the top of the backfill, follows the stress path A-B. Element 2, which is located at midheight of the backfill, is subjected to larger normal and shear stresses at the end of the backfill placement and may follow a stress path such as A-C. It also undergoes larger interface displacements than element 1.

Although the Clough and Duncan (1971) hyperbolic interface model works well for a typical laboratory stress path such as the one shown in Figure 1-3a, the response of the interface to the actual field stress path may differ substantially from that predicted by the model. Laboratory shear tests can be performed to determine the interface response to stress paths such as the one represented in Figure 1-3b.

Figure 1-4a shows the stress paths that may be followed by the two interface elements in Figure 1-2 during inundation of the backfill. Element 2 may follow the stress path C-E. The shear stresses acting on element 2 decrease simultaneously with the normal stresses. The stress path for element 1 is represented by line B-D. Element 1 undergoes a larger displacement along the interface because the thickness of the underlying backfill subject to rebound is larger. Due to this large displacement and the low initial shear stress acting on element 1, inundation of the backfill may induce a reversal in the direction of shear. Further fluctuations in the water table behind the lock wall may induce unload-reload cycles on the interface.

Two different SSI analyses were performed for the North Lock Wall at McAlpine Locks considering partial submergence of the backfill. Figure 1-5 shows the two different interface responses used for these analyses. In the stiff unload interface model, shown in Figure 1-5a for a constant effective normal stress, the shear stiffness during the reversal is assumed equal to the initial shear stiffness K_{st} . Changes in effective normal stress occurred in the interface elements as the water table rose in the backfill. This resulted, in turn, in a change in the interface shear stiffness used during unloading of the interface elements. In the soft unload interface model, shown in Figure 1-5b for a constant effective normal stress, the primary loading curve is maintained as the interface constitutive relationship during unloading. The results of the two SSI analyses are summarized in Table 1-2. These results show that the vertical shear forces acting on the wall after partial submergence of the backfill are significantly lower for the stiff interface response model during unloading compared to the results for the soft interface response. The computed effective base pressure below the heel of the lock wall (results not shown) is lower for the SSI analysis using the stiffer interface model during postconstruction, partial submergence of the backfill. This behavior is attributed to both the lower shear force and slightly larger

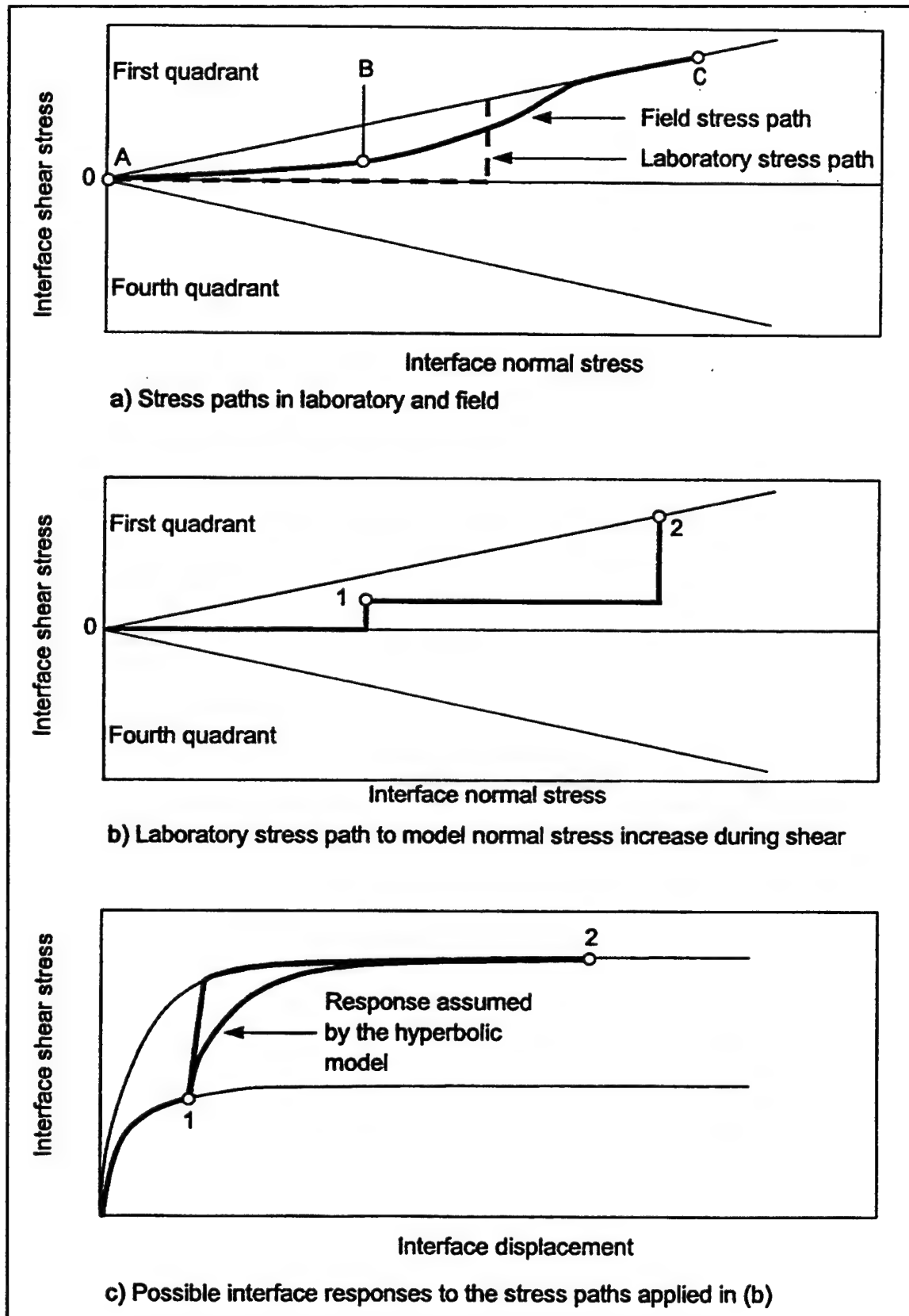


Figure 1-3. Interface responses to stress paths with changing shear and normal stresses

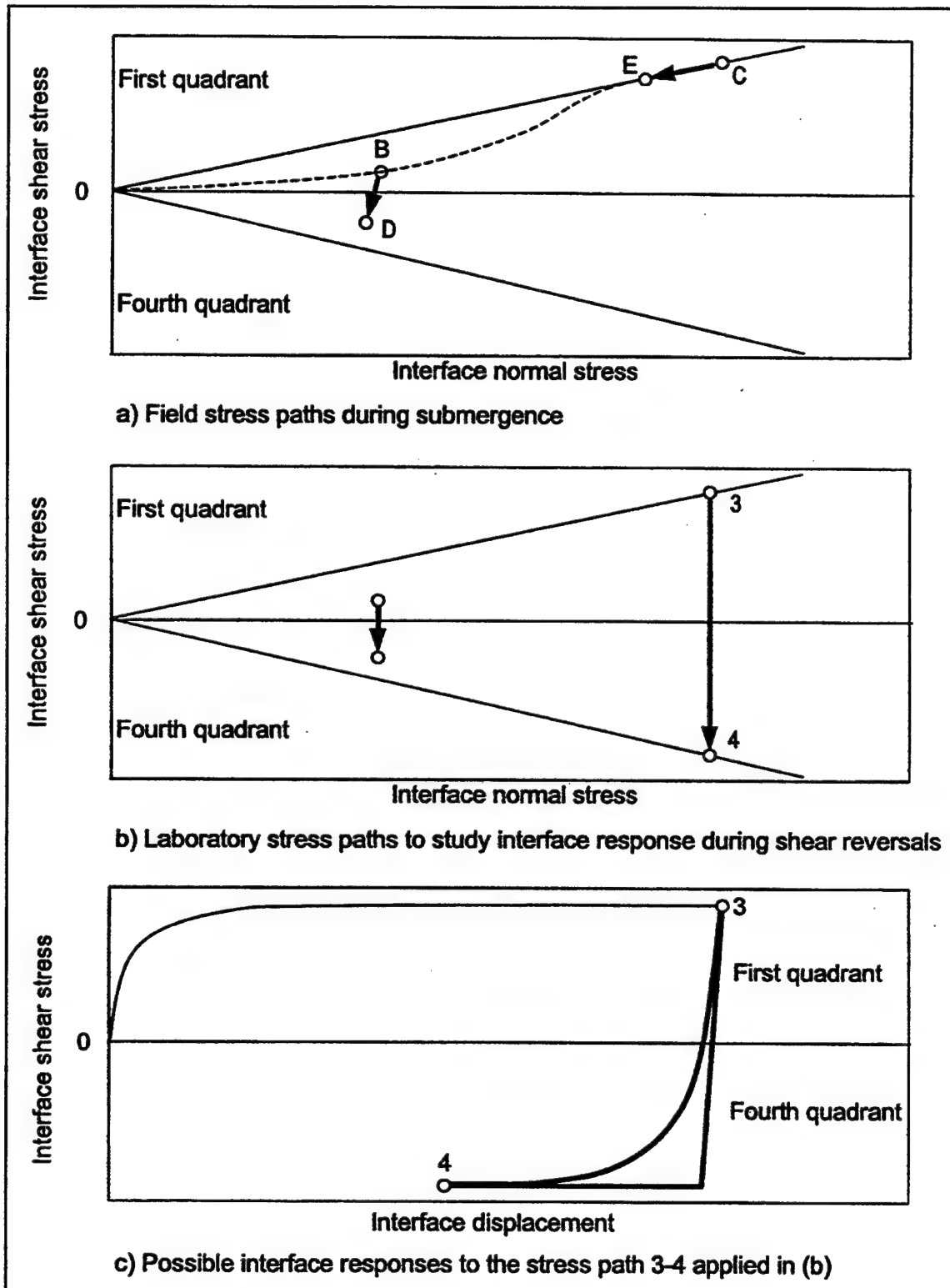


Figure 1-4. Interface responses to reversals of shear stress

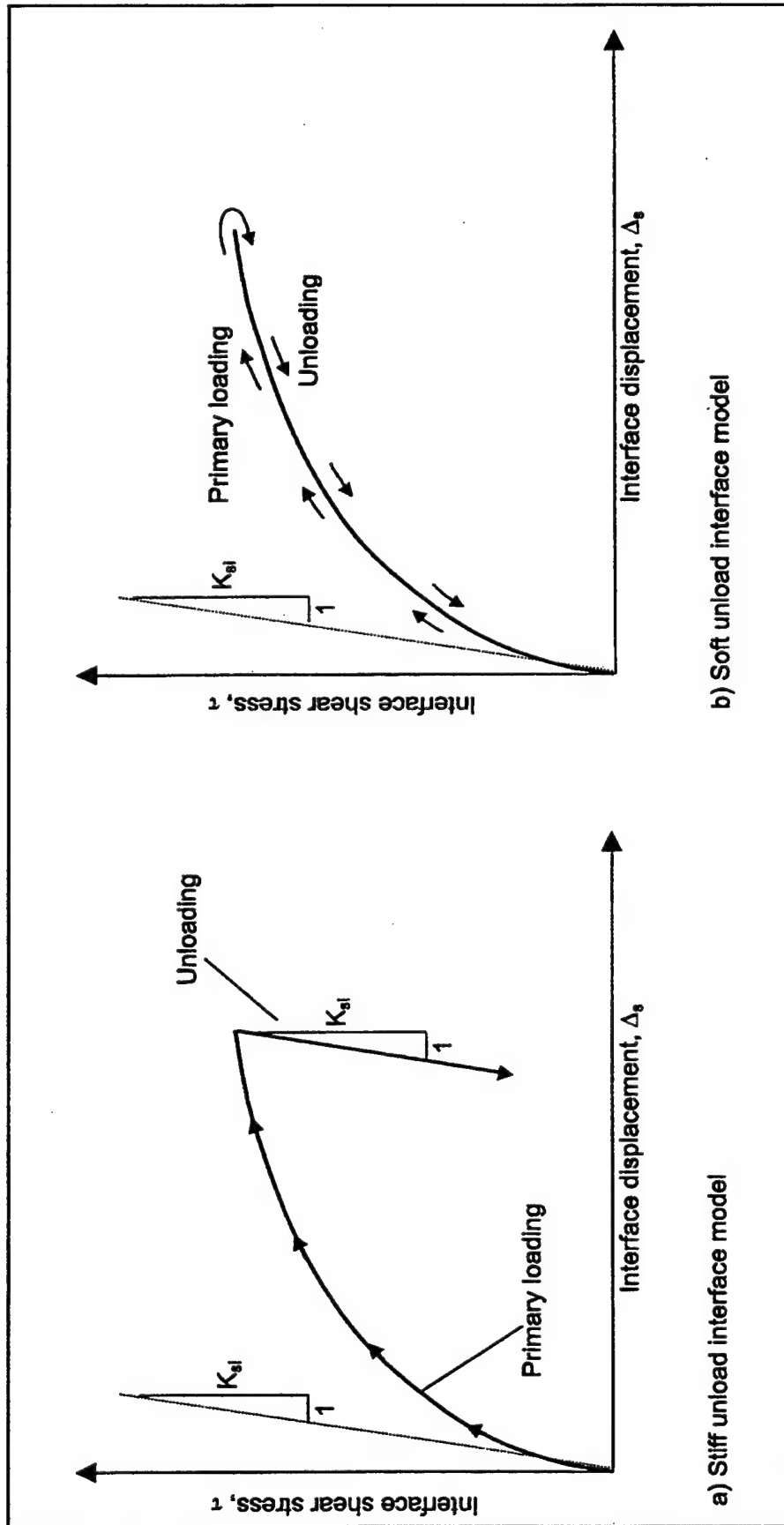


Figure 1-5. Two models for interface shear stress-displacement response under unloading (adapted from Ebeling and Wahl 1997)

horizontal earth pressure force acting on the back of the lock wall for the SSI analysis with the stiff interface model.

Table 1-2
Comparison of Results of SSI Analyses at Section A-A for Two Different Models of Interface Response to Unloading (adapted from Ebeling and Wahl 1997)

| Condition | Effective Overburden, kN per m Run of Wall | F_v , kN per m Run of Wall | F_h , kN per m Run of Wall | K_h | K_v |
|---------------|--|------------------------------|------------------------------|-------|-------|
| "Stiff" model | 2,515 | 1,155 | 99 | 0.459 | 0.039 |
| "Soft" model | 2,515 | 1,131 | 130 | 0.450 | 0.052 |

Knowledge is limited about the actual interface response to shear stress reversals, unload and reload cycles, or simultaneous change in shear and normal stresses. One of the most significant works on the response of concrete-to-soil interfaces was performed by Peterson et al. (1976). Their results, along with those reported in Clough and Duncan (1969), have been the main source of information on interface response for SSI analyses of lock walls. Peterson et al. (1976) used a 101.6- by 101.6-mm (4- by 4-in.) shear box to test combinations of different concrete surfaces and sands. The most important variables analyzed were roughness of the concrete surface and gradation and relative density of the sand. Their work has three main limitations: (a) the frequency of the reported data points collected during interface testing is in general not adequate to model the behavior during shear reversals, (b) no tests were performed to model simultaneous changes in normal and shear stresses, and (c) end effects due to the small dimensions of the shear box may have influenced the results, especially with respect to the initial stiffness during shear load reversals.

1.2.3 Improvements to existing models

In order to introduce improvements in the existing interface models, it is necessary to perform laboratory tests that model stress paths such as those described in the preceding section. Figure 1-3b shows a laboratory stress path designed to probe the yield surface. In the laboratory test the interface is sheared initially under a constant normal stress, then the normal stress is increased instantaneously and shearing is progressed to failure. This type of loading is referred to as *staged shear* throughout this report. Two possible responses of the interface to the staged shear stress path are shown in Figure 1-3c. The response commonly assumed in the hyperbolic model is parallel to the initial loading curve. Figure 1-4b shows laboratory stress paths that can be followed to study the response of the interface under a reversal in shear stresses. Two possible responses of the interface to the stress path 3-4 in Figure 1-4b are illustrated in Figure 1-4c.

The results of a series of such tests will allow the development of an improved numerical model that can be used in SSI analyses. It is anticipated that the improved model will be an extension to the existing hyperbolic model developed

by Clough and Duncan (1971). This new model will be implemented in the finite element code SOILSTRUCT and will be calibrated against the results of a pilot-scale test using the Instrumented Retaining Wall (IRW) at Virginia Polytechnic Institute and State University, Blacksburg (Virginia Tech) (Sehn and Duncan 1990).

1.3 Project Scope

In order to achieve these research goals, it is necessary to perform laboratory testing on soil-to-concrete interfaces, develop an improved numerical model based on the results of these tests, implement the new model in the program SOILSTRUCT, and calibrate the model against the results of large-scale tests performed using the IRW at Virginia Tech. At the time this Phase 1 report was prepared, several soil-to-concrete tests had been completed and preliminary development of an improved numerical model had been accomplished. This work, which is discussed in subsequent chapters, comprises the scope of the Phase 1 report.

1.3.1 Interface testing

Virginia Tech's Large Displacement Shear Box (LDSB) was used to perform the soil-to-concrete interface shear tests. The LDSB was used previously to test clay-geomembrane interfaces (Shallenberger and Filz 1996). Several modifications to the original configuration of the LDSB were necessary to permit the kind of soil-to-concrete interface testing necessary for this project. For this Phase 1 investigation, the tests were performed on the interface between a uniform dense sand and concrete. The purpose of these tests was to observe the response of the interface to stress paths such as those shown in Figures 1-3b and 1-4b. The details of sample preparation, testing procedures, and results are described in this report.

Additional tests will be performed to investigate the influence of the following variables on interface behavior: density, gradation, and angularity of sand. A plan for performing these tests is included in this Phase 1 report, and the complete series of test results will be presented in the final (Phase II) report of this investigation.

1.3.2 Development of interface model

A preliminary improved numerical model was developed according to the results of the interface tests between the uniform dense sand and the concrete, performed for this phase of the investigation. This preliminary model is based on the hyperbolic formulation developed by Clough and Duncan (1971), which has been extended to model shear reversals, load-unload cycles, and staged shear. It was found that the model gives accurate approximations of the interface response

under these loading conditions. However, it has not been evaluated against results of tests performed on other types of interfaces.

A more complete version of this model will evolve as the laboratory testing progresses and as other variables are investigated. It is anticipated that the IRW test will supply valuable information for calibration of the model. The more complete version of the model will be included in the final report of this investigation.

1.4 Report Organization

This report describes the work completed to date for this investigation. The report is organized in three main sections. The literature review is presented in Chapter 2, which contains a description of previous work on interface testing, interface modeling, and SSI analyses.

Chapter 3 contains a complete description of the testing equipment, testing procedures, and results of laboratory testing performed on the soil and on the soil-to-concrete interface. The basic properties of the soil used for the interface testing, results of triaxial tests, and hyperbolic modeling for this soil are presented. A description of the preparation method and characteristics of the concrete surface is also included. Detailed descriptions of the interface test procedures, sample preparation, and results obtained are presented.

The hyperbolic fit to the data from the interface tests is presented in Chapter 4. A preliminary interface model that is applicable to primary loading under constant or changing normal stress, as well to reversals in the shear direction, is described. Finally, limitations of the proposed preliminary model are discussed.

A discussion of the results obtained so far and preliminary conclusions are included in Chapter 5. A brief description of the planned laboratory and analytical work is also presented.

2 Literature Review

The literature review presented in this chapter includes the topics considered relevant for this Phase 1 report: interface testing, constitutive models of interface behavior, and SSI analyses of retaining walls. Further revision of the available literature will be carried out as needed for the second phase of this investigation.

2.1 Interface Testing

Several studies have been published regarding laboratory interface testing. Most often, interface tests were performed to determine the soil-to-structure friction angle for design of geotechnical structures, such as retaining walls, buried culverts, piles, etc. In some cases, parameters for constitutive modeling of interface response were determined from laboratory tests that model field loading conditions.

Interface tests have been performed on many types of soil-to-structure, soil-to-rock, and rock-to-rock interfaces. In this section, emphasis is given to previous studies of soil-to-concrete and sand-to-steel interfaces. The results of tests performed on both types of interfaces provide valuable insights into fundamental aspects of interface behavior.

2.1.1 Direct Shear Box (DSB) devices

Early systematic efforts to obtain data on the behavior of soil-to-structure interfaces were carried out by Potyondy (1961), Clough and Duncan (1971), and Peterson et al. (1976), among others. Their tests were performed using a slightly modified Direct Shear Box (DSB) in which a concrete specimen occupied one of the halves of the shear box. In most cases, the soil sample was prepared against a concrete specimen situated at the bottom. The tests were typically performed by first increasing the normal pressure to a desired value, then shearing the interface under constant normal stress to a maximum displacement of typically 12.5 mm (0.5 in.).

The work performed by Peterson et al. (1976) appears to be the most complete study of the fundamental factors that influence interface behavior. They

performed a large number of sand-to-concrete interface tests using a 102- by 102-mm (4- by 4-in.) DSB. In their tests, the interface was inundated and sheared, under drained conditions and constant normal load, to a maximum displacement of 12.5 mm (0.5 in.). They analyzed the influence of normal stress, interface roughness, and soil characteristics on the interface behavior, and developed a database of sand-to-concrete interface friction angles.

Peterson et al. (1976) also demonstrated the convenience of the Clough and Duncan (1971) hyperbolic formulation to model interface behavior. They developed a set of hyperbolic parameter values, which have been used as an important source of data for SSI analyses up to the present time (Ebeling et al. 1993; Ebeling and Mosher, 1996; Ebeling, Pace and Morrison 1997; Ebeling, Peters and Mosher 1997; Ebeling and Wahl 1997).

The DSB presents two important advantages: wide availability and relatively simple test setup and sample preparation procedures. Consequently, it has been the common choice for interface testing in research and practice. A summary of published works describing interface testing performed using DSB-type devices is presented in Table 2-1. Other applications of the DSB include testing on interfaces such as soil to geomembrane, soil to geotextile, and geomembrane to geotextile. Commercial devices have been developed for larger interface areas of up to 305 by 305 mm (12 by 12 in.), which can also be used for soil-to-concrete testing.

Traditional DSB devices present several limitations. The maximum relative displacement that can be attained in a conventional DSB is limited; hence, the determination of the interface residual strength becomes difficult. Additionally, end effects, induced by the presence of the rigid walls of the soil container, may introduce errors in the test results.

Kishida and Uesugi (1987), Fakharian and Evgin (1995), and Evgin and Fakharian (1996) have pointed out that the actual sliding displacement Δ_{act} between the soil particles and the concrete cannot be directly measured in the DSB, as illustrated in Figure 2-1. The displacement Δ_{meas} measured between the soil box and the concrete specimen, includes the sliding displacement at the interface, as well as the deformation Δ_{dis} of the sand mass due to distortion under the applied shear stresses.

2.1.2 Direct Simple Shear (DSS) devices

Direct Simple Shear (DSS) devices have been intensively employed for interface testing during the last two decades, primarily on sand-to-steel and clay-to-steel interfaces. Sand-to-steel tests have yielded interesting results regarding the general behavior of interfaces. Many of these results are applicable to sand-to-concrete interfaces as well. A summary of the previous work on interface behavior, where testing was performed in DSS apparatuses, is presented in Table 2-2.

Table 2-1
Previous Work on Direct Shear Testing of Sand-to-Concrete and Sand-to-Steel Interfaces

| Source | Type of Interface and Dimensions | Type of Loading | Summary |
|--|--|---|---|
| Potyondy (1961) | Sand-to-concrete Sand-to-steel | Monotonic shear under constant normal stress | <ul style="list-style-type: none"> Developed a database of interface friction parameter values for interfaces between sand and concrete of varying roughness |
| Clough and Duncan (1971) | Sand-to-concrete | Monotonic shear under constant normal stress | <ul style="list-style-type: none"> Developed a hyperbolic formulation for modeling interface response |
| Peterson et al. (1976) and Kulhawy and Peterson (1979) | Sand-to-concrete 102 mm x 102 mm | Monotonic shear and shear reversal under constant normal stress | <ul style="list-style-type: none"> Analyzed the relationship between the interface response and the interface roughness, soil type, and soil density and gradation Added important contributions to the database of parameters for the Clough and Duncan (1971) hyperbolic formulation |
| Acar, Durgunoglu, and Tumay (1982) | Sand-to-concrete Sand-to-steel | Monotonic shear under constant normal stress | <ul style="list-style-type: none"> Studied the relationship between void ratio of the sand and interface friction angle Presented a relationship between void ratio and hyperbolic parameter values for Clough and Duncan (1971) formulation for the interface used in their tests |
| Desai, Drumm, and Zaman (1985) | Sand-to-concrete 305 mm x 305 mm | Cyclic shear under constant normal stress | <ul style="list-style-type: none"> Developed the <i>Cyclic Multi-Degree-of-Freedom</i> (CYMDOF) device for interface testing Studied the influence on interface response of the following factors: displacement and shear stress amplitude, number of loading cycles, and initial density of the sand |
| Bosscher and Ortiz (1987) | Sand-to-concrete Sand-to-rock | Cyclic shear under constant normal stress | <ul style="list-style-type: none"> Studied the relationship between interface roughness and interface friction angle Assessed the effect of roughness on damping ratio of the interface |
| Lee et al. (1989) | Sand-to-concrete 100 mm x 100 mm | Monotonic shear under constant normal stress | <ul style="list-style-type: none"> Developed a set of hyperbolic parameters for the response of the interface used in their tests |
| Hryciw and Irsyam (1993) | Sand-to-ribbed steel 267 mm x 76 mm | Monotonic and cyclic shear under constant normal stress | <ul style="list-style-type: none"> Studied the mechanisms of dilation and shear band formation at the interface Studied the influence of rib geometry and spacing, and soil density on the interface response |

One of the main advantages of DSS devices is the ability to measure separately the total interface displacements Δ_{meas} and the soil distortion Δ_{dis} as illustrated in Figure 2-1. According to Uesugi and Kishida (1986b), the horizontal deformation due to distortion of the sand mass is an important component of the total displacement measured in the DSS device.

DSS devices have important limitations for interface testing: (a) nonuniform distribution of stresses at the interface (Kishida and Uesugi 1987), (b) complicated sample preparation, and (c) limited maximum total displacement, which does not exceed 25.4 mm (1 in.).

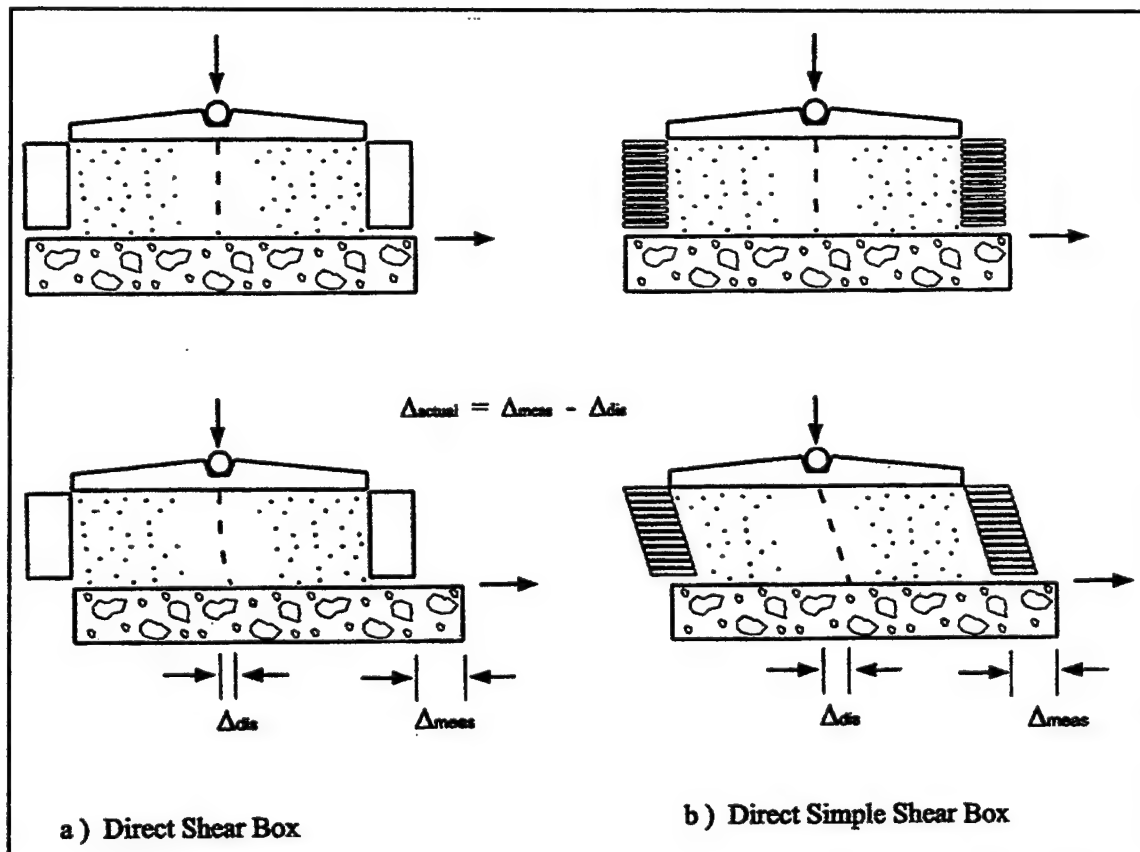


Figure 2-1. Distortion of the sand mass during interface tests in the DSB and DSS devices

2.1.3 Other devices

In order to overcome the limitations of the conventional apparatuses for interface testing, several investigators have developed special devices. Brummund and Leonards (1973) developed an annular device in which a cylindrical specimen of the structural material was embedded in sand. During testing, the specimen of structural material was pulled along its axis to failure, under a confining pressure applied on the boundary of the sand sample. This device was created in an attempt to model the behavior of a pile shaft. The sample preparation for this type of test is complicated, and the normal stresses at the interface are difficult to control and depend on the relative stiffness between the structural specimen and the sand (Kishida and Uesugi 1987).

Ring shear devices have been used by Huck and Saxena (1981) and Yoshimi and Kishida (1981) for sand-to-concrete and sand-to-steel interface testing. According to Stark, Williamson, and Eid (1996), the advantages of ring shear devices are unlimited interface displacement, making possible the determination of residual interface shear strengths; shearing along the same interface throughout the test; and no eccentric loading during shear.

Table 2-2
Previous Work on Direct Simple Shear Testing of Sand-to-Concrete and Sand-to-Steel Interfaces

| Source | Type of Interface and Dimensions | Type of Loading | Summary |
|---|---|---|---|
| Uesugi and Kishida (1986a and 1986b) | Sand-to-steel 100 mm x 40 mm | Monotonic shear under constant normal stress | <ul style="list-style-type: none"> Concluded that distortion of the sand sample is an important component of the total displacement |
| Kishida and Uesugi (1987) | Sand-to-steel 400 mm x 100 mm | Monotonic shear under constant normal stress | <ul style="list-style-type: none"> Found a direct relationship between steel roughness and interface friction coefficient |
| Uesugi, Kishida, and Tsubakihara (1988) | Sand-to-steel 400 mm x 100 mm | Monotonic shear and shear reversal under constant normal stress | <ul style="list-style-type: none"> Found that slippage and rolling of sand particles occur during shear, on rough steel surface Found that only slippage occurs on smooth steel surface Found that large volume changes of sand occur near the contact with the steel surface Reported shear band formation on rough surfaces, not on smooth surfaces |
| Uesugi, Kishida, and Tsubakihara (1989) | Sand-to-steel 100 mm x 40 mm | Cyclic shear under constant normal stress | <ul style="list-style-type: none"> Confirmed observations on shear band formation by Uesugi, Kishida, and Tsubakihara (1988) |
| Uesugi, Kishida, and Uchikawa (1990) | Sand-to-concrete 100 mm x 40 mm | Cyclic shear under constant normal stress | <ul style="list-style-type: none"> Observed similar behavior as in sand-to-steel interfaces Found that large volume changes of the sand occur in the vicinity of the concrete surface Observed shear band formation Reported that actual sliding displacement between sand particles and concrete is small Found a direct relationship between concrete roughness and friction coefficient |
| Evgin and Fakharian (1996) | Sand-to-steel 100 mm x 100 mm | Monotonic shear under constant normal stiffness | <ul style="list-style-type: none"> Developed the <i>Cyclic 3-D Simple Shear Interface</i> (C3DSSI), from a previous DSB version by Fakharian and Evgin (1996), capable of applying shear stresses in two orthogonal directions |
| Fakharian and Evgin (1997) | Sand-to-steel 100 mm x 100 mm | Cyclic shear with constant normal stiffness | <ul style="list-style-type: none"> Studied the interface shear strength degradation during cyclic shear under constant normal stiffness |
| Desai and Rigby (1997) | Clay-to-steel and clay-to-rock 165-mm diameter | Cyclic shear under constant normal stress | <ul style="list-style-type: none"> Presented the CYMDOF-P device, with pore pressure measurement capabilities, which is still under development. |

The following are principal disadvantages of the ring shear device:

- (a) complicated sample preparation procedures, especially for sand-to-concrete interfaces (Kishida and Uesugi 1987); (b) relatively narrow soil samples, which may induce scale effects in some interface tests; (c) nonuniform radial distribution of shear stresses (Stark, Williamson and Eid 1996); and (d) unknown actual sliding displacement at the interface in the case of rigid ring shear devices.

2.1.4 Summary of previous findings on interface testing and interface behavior

There seems to be no universal agreement on procedures and data interpretation for interface testing. Furthermore, little progress on the

understanding of the behavior of sand-to-concrete interfaces has occurred since the works of Clough and Duncan (1971) and Peterson et al. (1976). However, several observations, which have been substantiated in more recent investigations, may be considered of special interest for this research:

- a. The Clough and Duncan (1971) hyperbolic formulation is an adequate model for the behavior of interfaces under constant normal stress and monotonic shearing (Peterson et al. 1976; Acar, Durgunoglu, and Tumay 1982; Lee et al. 1989).
- b. The main factors affecting interface behavior under monotonic loading are interface roughness, soil density, particle angularity, and normal stress (Peterson et al. 1976; Bosscher and Ortiz 1987; Hryciw and Irsyam 1993; Uesugi and Kishida 1986a; Kishida and Uesugi 1987; Uesugi, Kishida, and Tsubakihara 1988).
- c. In all the studies reviewed, displacement softening behavior was reported in interface tests between dense sand and structural materials.
- d. The interface peak friction angle increases steadily with increasing interface roughness until a maximum is reached (Peterson et al. 1976; Bosscher and Ortiz 1987; Uesugi and Kishida 1986a; Kishida and Uesugi 1987; Uesugi, Kishida, and Uchikawa 1990). This maximum is very close to or slightly lower than the internal peak friction angle of the sand. The roughness value at which this maximum value is reached is commonly referred to as the *critical roughness*. There are, however, a number of criteria to quantify the interface roughness, of which none seems to have been adopted universally. Therefore, the critical roughness values are given in units that are not consistent among different investigators.
- e. Dilation occurs during shear of a dense sand-to-concrete or dense sand-to-steel interface (Peterson et al. 1976). The dilative deformations of sand in contact with a rough surface are usually large, and take place in a thin zone within the soil adjacent to the interface (Hryciw and Irsyam 1993; Uesugi, Kishida, and Tsubakihara 1988). Dilation is followed by the development of large displacements along the interface. In loose sand samples, compression occurs during shear also followed by large displacements. This zone of large volumetric changes and interface displacements is commonly known as the *shear band*. Shear band formation has not been observed on smooth interfaces.
- f. Interface behavior during cyclic shear is affected by interface roughness, soil density, particle angularity, normal stress, displacement- and stress-amplitude, and number of loading cycles (Desai, Drumm, and Zaman, 1985; Uesugi, Kishida, and Tsubakihara 1989; Uesugi, Kishida, and Uchikawa 1990).

- g. Distortions of the sand mass above the interface are significant; consequently, the actual displacement at the interface cannot be determined in DSB devices (Uesugi and Kishida 1986a and 1986b).

2.1.5 The Large Displacement Shear Box (LDSB)

The LDSB is essentially a DSB-type device especially designed to handle interfaces as large as 711 by 406 mm (28 by 16 in.) (Shallenberger and Filz 1996). The device is capable of attaining interface displacements as large as 305 mm (12 in.) and has been used extensively for testing of interfaces between clay and High-Density Polyethylene (HDPE). The soil sample is prepared in a soil box and pressed against a moveable upper assembly containing the specimen of HDPE or structural material. An isolated test section 305 mm by 305 mm in the upper assembly, located at the center of the interface, allows the measurement of normal and shear stresses away from the edges.

Shallenberger and Filz (1996) pointed out the advantages of the LDSB over conventional devices: (a) end effects are negligible, (b) the maximum displacement of 305 mm (12 in.) allows the determination of the interface residual shear strength, and (c) no eccentric normal loads are generated during shear.

The principal disadvantage of this apparatus is that sample preparation is a time-consuming process due to the large size of the interface. Additionally, the distortion deformations of the soil sample cannot be measured; therefore, the actual interface displacements are not known.

The large displacement capabilities of the LDSB, which permit staged tests with several steps of normal pressure increments, and its reduced end effects are the main reasons for its use in this investigation. Several modifications were implemented in the device to accommodate sand-to-concrete interfaces and perform shear stress reversals. A more detailed description of the LDSB will be provided later in this report.

2.2 Interface Modeling

In SSI analyses, the soil-structure interface is represented by means of interface elements. Several kinds of interface elements have been developed to model the behavior of the interface under certain loading conditions. When an interface element is developed for a particular problem, an appropriate constitutive relationship must be adopted. This constitutive model should be based on the results of a testing program performed to determine the interface response under the expected loading conditions.

A literature review on interface elements and interface constitutive models has been performed for this Phase 1 report, and is summarized in the following

sections. It includes the most significant contributions that are considered pertinent for the work presented in this report.

2.2.1 Interface elements

Interface elements were first introduced by Goodman, Taylor, and Brekke (1968) for finite element analysis of jointed rock masses. They were soon extended to SSI analyses of retaining walls by Clough and Duncan (1971) and Duncan and Clough (1971). The adoption of interface elements represented a significant improvement over previous methods, which assumed either of two conditions: a perfectly rough interface with no slip between soil and structure, or a perfectly smooth interface with no shear stresses developed (Clough and Duncan 1971).

The element developed by Goodman, Taylor and Brekke (1968) is commonly referred to as *joint element* (JE) or *zero-thickness interface element*. It is a 4-node element of zero thickness as illustrated in Figure 2-2. In their derivation of the joint element stiffness matrix, they used a very simple constitutive law consisting of constant values for both the shear stiffness and the normal stiffness:

$$k_n \cdot \Delta_n = \sigma_n \quad (2-1)$$

$$k_s \cdot \Delta_s = \tau \quad (2-2)$$

where

k_n = normal interface stiffness

Δ_n = displacement normal to the interface

σ_n = normal stress acting on the interface

k_s = interface shear stiffness

Δ_s = displacement along the interface

τ = interface shear stress

In this formulation, coupling effects between tangential and normal displacements along the interface are excluded, as evidenced by zero off-diagonal elements in the stiffness matrix.

Clough and Duncan (1971) observed that compressive stresses normal to the interface would induce overlapping among soil and structural elements adjacent to the interface. To minimize this effect, they proposed assigning a high value of normal stiffness to the joint element under compression. Similarly, for interface

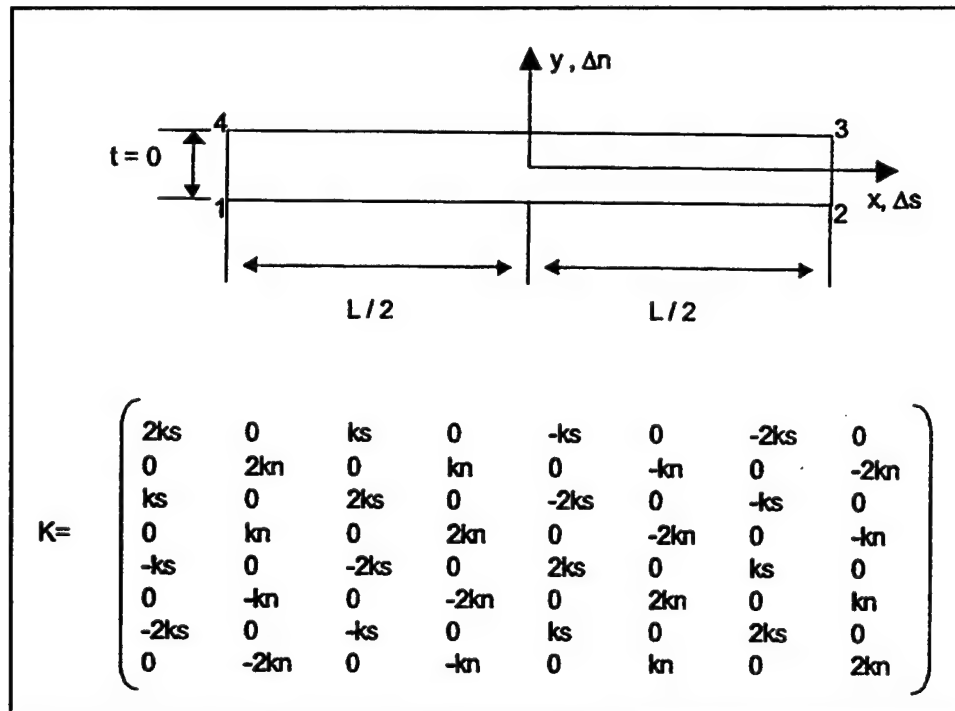


Figure 2-2. Goodman, Taylor, and Brekke (1968) zero thickness interface element and corresponding element stiffness matrix

elements under tension, they proposed assigning a small value of normal stiffness to minimize the development of tensile stresses at the interface.

A continuous development of improved joint elements has taken place since the original formulation by Goodman, Taylor, and Brekke (1968). Heuze and Barbour (1982) presented a review of the historical development of joint elements for analyses of jointed rock masses; most were linear and one-dimensional and did not include rotational degrees of freedom. A limited number of joint elements were developed to model displacement softening and dilation at the joints.

Morrison (1995) also presented a comprehensive review of previous investigations of interface elements. Many of the studies he reviewed described numerical integration problems arising from the use of interface elements of high normal stiffness adjacent to softer soil elements. Morrison studied an interface element formulation with relative degrees-of-freedom proposed by Wilson (1977) to minimize such numerical problems. Morrison showed that the Wilson (1977) formulation is not necessary if Newton-Raphson iteration is used to find the interface displacements resulting from each load increment.

Heuze and Barbour (1982) presented a zero-thickness axisymmetric joint element for finite element analyses of footings on rock, underground openings, and excavations, where dilation effects play an important role. Although no coupling terms are included in the formulation of the element, the dilation

induced normal stresses are determined explicitly based on the stiffness of the surrounding rock and the dilation angle. Yuan and Chua (1992) presented a more general formulation of the Heuze and Barbour axisymmetric element.

Matsui and San (1989) proposed an elastoplastic joint element to model interface behavior of rock joints. It accounts for the generation of normal stresses during shear, due to fully restrained dilation of the joint, in a way similar to that of Heuze and Barbour (1982).

Desai et al. (1984) and Zaman, Desai, and Drumm (1984) presented the *thin layer interface element*. It is based on the idea that interface behavior is controlled by a narrow band of soil adjacent to the interface with different properties from the surrounding materials. The thin layer element is treated mathematically as any other element of the finite element mesh and is assigned special constitutive relations. The Desai et al. (1984) thin layer element prevents overlapping between structural and geological materials due to its finite thickness. Desai, Muqtadir and Scheele (1986) implemented the thin layer element in interaction analyses of grouted anchors-soil systems.

Wong, Kulhawy, and Ingraffea (1989) implemented a three-dimensional (3-D) version of the thin layer interface element for SSI analyses of drilled shafts under generalized loading.

2.2.2 Interface constitutive models

A number of interface constitutive models have been developed by different authors. Depending on the type of analysis performed, the interface behavior may be represented by a quasi-linear or a nonlinear model. Quasi-linear models consider a constant value of stiffness over a range of interface displacements, until yield is reached. After yield, a low constant value of stiffness is usually assigned to the interface. Quasi-linear models have been used by Goodman, Taylor, and Brekke (1968); Desai, Muqtadir, and Scheele (1986); Matsui and San (1989); and Wong, Kulhawy, and Ingraffea (1989).

In nonlinear models, the interface shear stress-displacement relationship is represented by a mathematical function of higher degree. The interface shear stiffness changes during shear, depending on the magnitude of the displacement and any other factor included in the model. Nonlinear models have been used by Clough and Duncan (1971); Zaman, Desai, and Drumm (1984); and Desai, Drumm and Zaman (1985) among others.

Clough and Duncan (1971) developed the hyperbolic model for interfaces. This model has been used extensively in SSI analyses and design of geotechnical structures, especially for analyses of lock wall behavior (Ebeling et al. 1993; Ebeling and Mosher 1996; Ebeling, Peters and Mosher 1997; Ebeling and Wahl 1997; and Ebeling, Pace and Morrison 1997). The hyperbolic model, described in detail in the next section, often provides an accurate approximation of the

interface response under monotonic loading at constant normal stress. It has not been extended to cyclic loading, or to staged shear.

Zaman, Desai, and Drumm (1984) developed a constitutive model for cyclic loading of interfaces. It is based on a polynomial formulation that included the effects of the number of cycles, amplitude of shear displacements, and normal stress on interface response.

Desai, Drumm, and Zaman (1985) presented a *modified Ramberg-Osgood* model for interfaces under cyclic loading. The model accounts for shear stress reversals, hardening, or degradation effects with number of load cycles, normal stress, relative density of the sand, and maximum displacement amplitude. Uesugi and Kishida (1985) observed that the modified Ramburg-Osgood model yields inconsistent results for shear stresses close to failure.

In all these interface models the interface yield stress is determined by the Mohr-Coulomb criterion (Goodman, Taylor, and Brekke 1968; Clough and Duncan 1971; Zaman, Desai, and Drumm 1984; Desai, Muqtadir, and Scheele 1986; and Wong, Kulhawy, and Ingraffea 1989).

Postpeak displacement softening has been included in the formulation of some quasi-linear models that are used in conjunction with iterative finite element procedures (Wong, Kulhawy, and Ingraffea 1989). Esterhuizen (1997) presented a nonlinear constitutive formulation for clay-HDPE interfaces that accounts for work-softening behavior of the interface.

Coupling between normal and shear deformations is not included in any of the constitutive formulations found in the literature. Changes in normal stress during shear due to restrained dilation of rock joints are accounted for in the models proposed by Heuze and Barbour (1982) and Matsui and San (1989). This was accomplished by including an explicit formulation relating changes in normal stresses with shear displacement, dilation angle, and elastic properties of the adjacent rock mass.

2.2.3 The hyperbolic model

Duncan and Chang (1970) presented a hyperbolic model for soil behavior following previous work by Kondner (1963) and Kondner and Zelasko (1963). The hyperbolic model was extended to interfaces by Clough and Duncan (1969 and 1971) and implemented into the Goodman, Taylor, and Brekke (1968) joint element formulation.

Figure 2-3 illustrates the basic aspects of the Clough and Duncan (1971) hyperbolic model for interfaces. A hyperbola, shown as a solid line in Figure 2-3a, was used to fit a set of data from an interface shear test. The equation of the hyperbola can be written as:

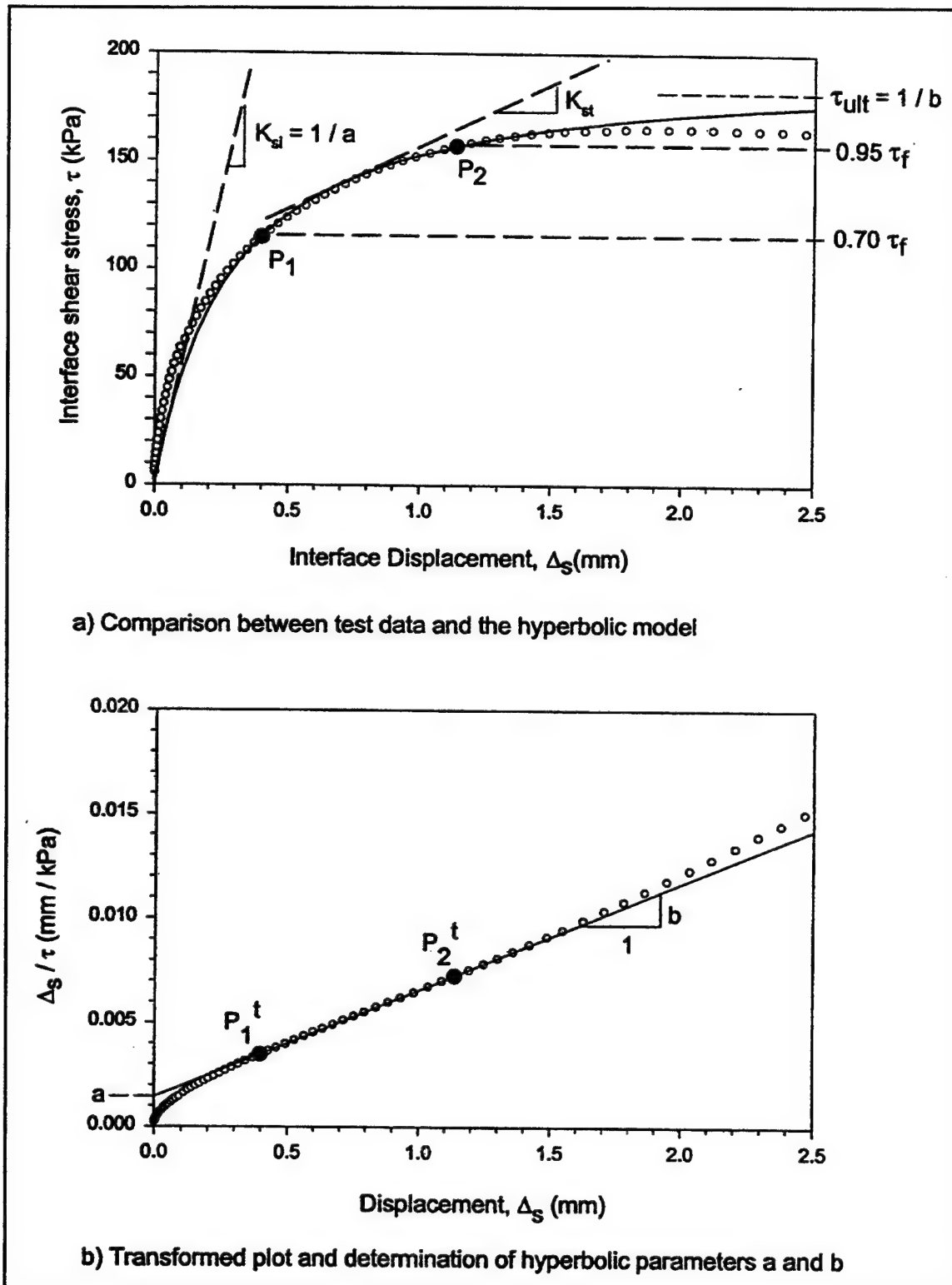


Figure 2-3. Application of the Clough and Duncan (1971) interface hyperbolic model to a typical set of test data

$$\tau = \frac{\Delta_s}{a + b \cdot \Delta_s} \quad (2-3)$$

in which a and b are the parameters evaluated to fit the hyperbola to the experimental data. Equation 2-3 can be rewritten as

$$\frac{\Delta_s}{\tau} = a + b \cdot \Delta_s \quad (2-4)$$

Figure 2-3b shows the same test data of Figure 2-3a, plotted in terms of Δ_s/τ and Δ_s . This is called the *transformed plot*. If the interface shear stress-displacement behavior follows a hyperbolic relationship, the transformed plot will be a straight line. The hyperbolic parameters a and b of Equation 2-4 will be the intercept and slope of this straight line, respectively. The actual interface test data do not exactly follow a hyperbolic relationship, and the transformed plot must then be fitted to a straight line in order to determine the hyperbolic parameters a and b .

Duncan and Chang (1970) observed that the transformed plot for strength test data in soils diverged from a straight line, both at low and high values of strain. They concluded that the best fit to the data was obtained when the hyperbola intersected the test data at 70 and 95 percent of the strength. Clough and Duncan (1971) adopted this same criterion for interface shear tests. Figure 2-3a shows points P_1 and P_2 corresponding to a mobilized strength of 70 and 95 percent respectively. Points P_1' and P_2' are the corresponding representations of P_1 and P_2 in the transformed plot. A straight line is drawn between P_1' and P_2' and the hyperbolic parameters a and b of Equation 2-4 are found as illustrated in the figure.

The hyperbolic shear stress-displacement relationship, calculated from Equation 2-3, is presented in Figure 2-3a. It can be noted that the model intersects the test data at points P_1 and P_2 .

One of the advantages of the Clough and Duncan (1971) model is that the hyperbolic parameters a and b are physically meaningful. The value of a is the reciprocal of the initial shear stiffness K_{si} of the interface. The value of b is the reciprocal of the asymptotic shear stress value τ_{ult} of the hyperbola. The value of τ_{ult} is larger than the actual interface shear strength τ_f . To address this discrepancy, Clough and Duncan defined the failure ratio R_f as:

$$\tau_f = R_f \cdot \tau_{ult} \quad (2-5)$$

Clough and Duncan proposed that the value of initial interface stiffness be calculated using the following expression:

$$K_{si} = K_I \cdot \gamma_w \cdot \left(\frac{\sigma_n}{P_a} \right)^n \quad (2-6)$$

where

K_I = dimensionless stiffness number

γ_w = unit weight of water

p_a = atmospheric pressure

n = dimensionless stiffness exponent

From a series of interface tests under different normal stresses, the hyperbolic parameter a , and consequently K_{st} , can be evaluated for each normal stress. The stiffness number K_I and stiffness exponent n can then be calculated by fitting K_{st} and σ_n data to Equation 2-6.

For interfaces without an adhesion intercept, the shear strength of the interface τ_f can be expressed as:

$$\tau_f = \sigma_n \cdot \tan \delta \quad (2-7)$$

where δ is the angle of interface friction, which can be also determined from a series of interface shear tests at different normal stresses σ_n . Finally, by substituting Equations 2-5, 2-6, and 2-7 into Equation 2-3, the following hyperbolic expression is obtained:

$$\tau = \frac{\Delta_s}{\frac{1}{K_I \cdot \gamma_w \cdot \left(\frac{\sigma_n}{p_a}\right)^n} + \frac{R_f \cdot \Delta_s}{\sigma_n \cdot \tan \delta}} \quad (2-8)$$

For incremental analyses, it is necessary to determine the tangent stiffness value K_{st} at any point during shear. By differentiating Equation 2-8 with respect to Δ_s , the following expression is obtained:

$$K_{st} = K_I \cdot \gamma_w \cdot \left(\frac{\sigma_n}{p_a}\right)^n \cdot \left(1 - \frac{R_f \cdot \tau}{\sigma_n \cdot \tan \Delta}\right)^2 \quad (2-9)$$

If the stress level SL is defined as:

$$SL = \frac{\tau}{\sigma_n \cdot \tan \delta} \quad (2-10)$$

the tangent stiffness K_{st} can be expressed as:

$$K_{st} = K_I \cdot \gamma_w \cdot \left(\frac{\sigma_n}{p_a}\right)^n \cdot (1 - R_f \cdot SL)^2 \quad (2-11)$$

Important advantages of the Clough and Duncan (1971) hyperbolic model are as follows:

- a. Nonlinearity of the interface shear stress-displacement relationship is well represented by Equations 2-8 or 2-11.
- b. The hyperbolic parameters have a clear physical meaning.
- c. The method is easy to implement in SSI analyses.

It can be observed that the hyperbola in Figure 2-3 fits the interface test data well, especially above a stress level SL of 50 percent. However, the initial stiffness K_{si} given by the hyperbola is lower than the actual K_{si} of the test data. In general, the value of K_{si} obtained from the hyperbolic formulation differs from the actual initial shear stiffness of the interface. A similar divergence is found between values of initial stiffness in soils obtained from the Duncan and Chang (1970) hyperbolic model and those obtained from triaxial testing. According to Stark, Ebeling, and Vettel (1994), it is important that the hyperbolic model used in SSI analyses fits the test data from the initial stages of shear. In their models they used the data points corresponding to 70 and 95 percent of the strength (Duncan et al. 1980) to develop an initial approximation for the hyperbolic model. The final hyperbolic model was completed by adjusting the hyperbolic parameters by trial and error until an appropriate fit to the data at low strains was obtained.

In spite of its popularity, the Clough and Duncan (1971) hyperbolic model for interfaces has some important limitations regarding its use in SSI analyses of earth retaining structures, such as lock walls. The hyperbolic formulation does not model displacement softening of the interface and does not include any coupling effects between shear and normal displacements. It has not been extended to cases in which the shear and normal stresses both change, and it has not been fully implemented for cases of cyclic loading and shear stress reversals.

2.3 SSI Analyses of Retaining Walls

2.3.1 Review of previous work

The first systematic SSI analyses of retaining wall behavior were presented by Clough and Duncan (1969, 1971) and Duncan and Clough (1971). They used the hyperbolic constitutive relationship by Duncan and Chang (1970) to model the behavior of the backfill and extended it to model the behavior of the wall-to-soil interfaces. Relative movement at the interfaces was achieved by the use of the joint element developed by Goodman, Taylor, and Brekke (1968).

In their analyses of Port Allen and Old River U-frame locks, Clough and Duncan (1969) and Duncan and Clough (1971) demonstrated the importance of close modeling of the construction stages of the lock and backfill placement.

They demonstrated that a simple linear elastic model for the soil and gravity turn-on analyses are not adequate to model the behavior of the soil-lock system. They also proved that the downdrag or vertical shear force exerted by the backfill on the wall has an important influence on the behavior of U-frame locks. Their work was the key to understanding basic and, at that time, unknown aspects of the behavior of lock walls.

Clough and Duncan (1971) presented a systematic approach to SSI analyses of retaining wall behavior. They observed the importance of modeling the different stages of construction of the wall and placement of the backfill in SSI analyses. They found, when closely modeling the stages of placement of the backfill, that the resulting horizontal and vertical loads acting on the wall were substantially larger than those obtained using classical earth pressure theories. The results of these analyses were consistent with some previous experimental work and field observations.

Ebeling, Duncan, and Clough (1990) compared results from conventional equilibrium (CE) and finite element (FE) analyses of several hypothetical gravity walls founded on rock. Their analyses were performed with the backfill-placement analysis option incorporated in SOILSTRUCT (Clough and Duncan 1969). A range of possible values of shear stiffness was assumed at the interfaces between the wall and the backfill, and between the backfill and the rock. Ebeling, Duncan, and Clough concluded that the magnitude of downdrag force is significantly affected by the concrete-to-backfill and rock-to-backfill shear stiffness values. They also concluded that CE analyses neglect the true process of soil-structure interaction and tend to yield very conservative results.

Ebeling et al. (1992) performed analyses of several hypothetical gravity walls founded on rock. Their work was based on several representative examples of existing lock walls. Ebeling et al. found that CE analyses are very conservative because they do not account for the stabilizing effect of the downdrag forces generated by settlement of the backfill. At the time of their work, it was not known whether these vertical shear forces persisted under field conditions, and if they could be relied upon for the stability of the structure. They also indicated that the behavior of retaining structures founded on soil might differ substantially from that of structures founded on rock. In soil-founded structures, the concrete-to-foundation interface is not bonded as in the case of concrete-to-rock interfaces, and greater relative interface displacements may occur, inducing more redistribution of the earth pressures.

Ebeling et al. (1993), Ebeling and Mosher (1996), and Ebeling, Peters, and Mosher (1997) presented the results of extensive SSI analyses for the soil-founded Red River Lock and Dam No. 1. A reinforced soil berm was recommended, among other alternatives, as a solution to the problems induced by siltation of the lock. The SSI analysis procedures used for the evaluation of the proposed solution were validated against instrumentation measurements from the lock taken at the end of construction and at several operational stages. Their analyses revealed that important changes in normal stresses may occur at the soil-to-structure interface during backfill placement and operation of the lock, and

underscored the importance of selecting the appropriate interface stiffness values for these loading conditions. They also noted that CE analyses are inadequate for the design of this type of structure.

A simplified procedure was presented in Appendix F of HQUSACE (1997) for evaluating the downdrag force on retaining walls founded on rock. This procedure is described in detail in the following section. It was observed that measurements in existing lock walls, as well as previous experimental data from the IRW facility at Virginia Tech (Filz 1992), showed that downdrag forces were significant and tended to increase with time. For the case of U-frame locks and retaining structures founded on soil, EC 1110-2-291 recommended performing complete SSI analyses. The simplified procedure has also been described in detail by Ebeling, Pace, and Morrison (1997).

As discussed in Section 1.2.1, Ebeling and Wahl (1997) presented the results of SSI analyses of the proposed North Lock Wall at McAlpine Locks. They determined that the downdrag force was significant, and that it could be substantially affected by the response mode of the interface to unload-reload cycles.

Filz and Duncan (1997) and Filz, Duncan, and Ebeling (1997) presented a theory for the quantification of the downdrag forces on the back of nonmoving retaining walls and described previous large-scale retaining wall tests and field measurements. They observed that postconstruction settlement causes an increase in the downdrag on the back of the wall. They cited measurements at Eibach Lock in Germany, where large vertical shear forces were persistent for 10 years under repeated filling and emptying cycles and temperature fluctuations. The measured K_v remained at an approximately constant average value of 0.30. These vertical shear forces cause an important reduction in the lateral earth pressures acting on the wall.

2.3.2 Simplified procedure for calculating the downdrag force

There are some cases in which it is possible to estimate the downdrag force acting on the back of a retaining wall without performing sophisticated SSI analyses. In this section a simplified procedure is presented for calculating the downdrag force as described by Ebeling, Pace, and Morrison (1997). It applies to retaining walls with nonyielding backfills. This is the case for rock-founded gravity retaining walls with engineered backfills that do not creep, such as soils classified as SW, SP, GW, and GP according to the Unified Soil Classification System (American Society for Testing and Materials (ASTM) 1993a). It also applies to select SM backfills with nonplastic fines that do not creep. This method is based on the results of analyses performed on walls with geometrical configurations that are representative of many, but not all, Corps of Engineers rock-founded lock walls.

The simplified procedure was first reported in Engineer Technical Letter (ETL) 1110-2-352 (HQUSACE 1994). Ebeling, Pace, and Morrison (1997)

presented an improved version of the original procedure, based on additional SSI analyses on rock-founded gravity walls (Filz, Duncan, and Ebeling 1997; Ebeling and Filz in preparation). It is also described in Appendix F of HQUSACE (1997). This improved version is applicable to situations in which there is no water table behind the wall or when the groundwater level rises as the backfill is being placed.

The simplified procedure is based on the use of the vertical earth pressure coefficient K_v , defined in Chapter 1 of this report. Combining Equations 1-1 and 1-3, the vertical shear force F_v can be expressed as:

$$F_v = K_v \cdot \int_{heel}^{top} \sigma'_v dy \quad (2-12)$$

Figure 2-4 shows the vertical force F_v acting on a vertical plane, passing through the heel of a retaining wall with a hydrostatic water table. It also shows the diagram of vertical effective stress in the backfill. For this case the vertical shear force can be expressed using the equation presented in ETL 1110-2-352 (HQUSACE 1994):

$$F_v = K_v \cdot \left[\frac{1}{2} \gamma_{moist} (D_1)^2 + \gamma_{moist} (D_1 D_2) + \frac{1}{2} \gamma_b (D_2)^2 \right] \quad (2-13)$$

where

γ_{moist} = moist unit weight of the backfill above the water table

D_1 = thickness of the backfill above the hydrostatic water table

D_2 = thickness of the submerged backfill above the heel of the wall

γ_b = buoyant unit weight of the submerged backfill

Equation 2-13 is valid for a horizontal backfill with no surcharge loads applied. Filz, Duncan, and Ebeling (1997) and Ebeling and Filz (in preparation) expanded Equation 2-13 to include the effects of surcharge and sloping backfill. In the case of rock-founded gravity walls with the inclined backfill surface shown in Figure 2-5a, F_v is calculated using

$$F_v = F_{v,soil} + F_{v,q} \quad (2-14)$$

where

$$F_{v,soil} = K_{v,soil} \cdot \left[\frac{1}{2} \gamma_{moist} (D_1)^2 + \gamma_{moist} (D_1 D_2) + \frac{1}{2} \gamma_b (D_2)^2 \right] \quad (2-15)$$

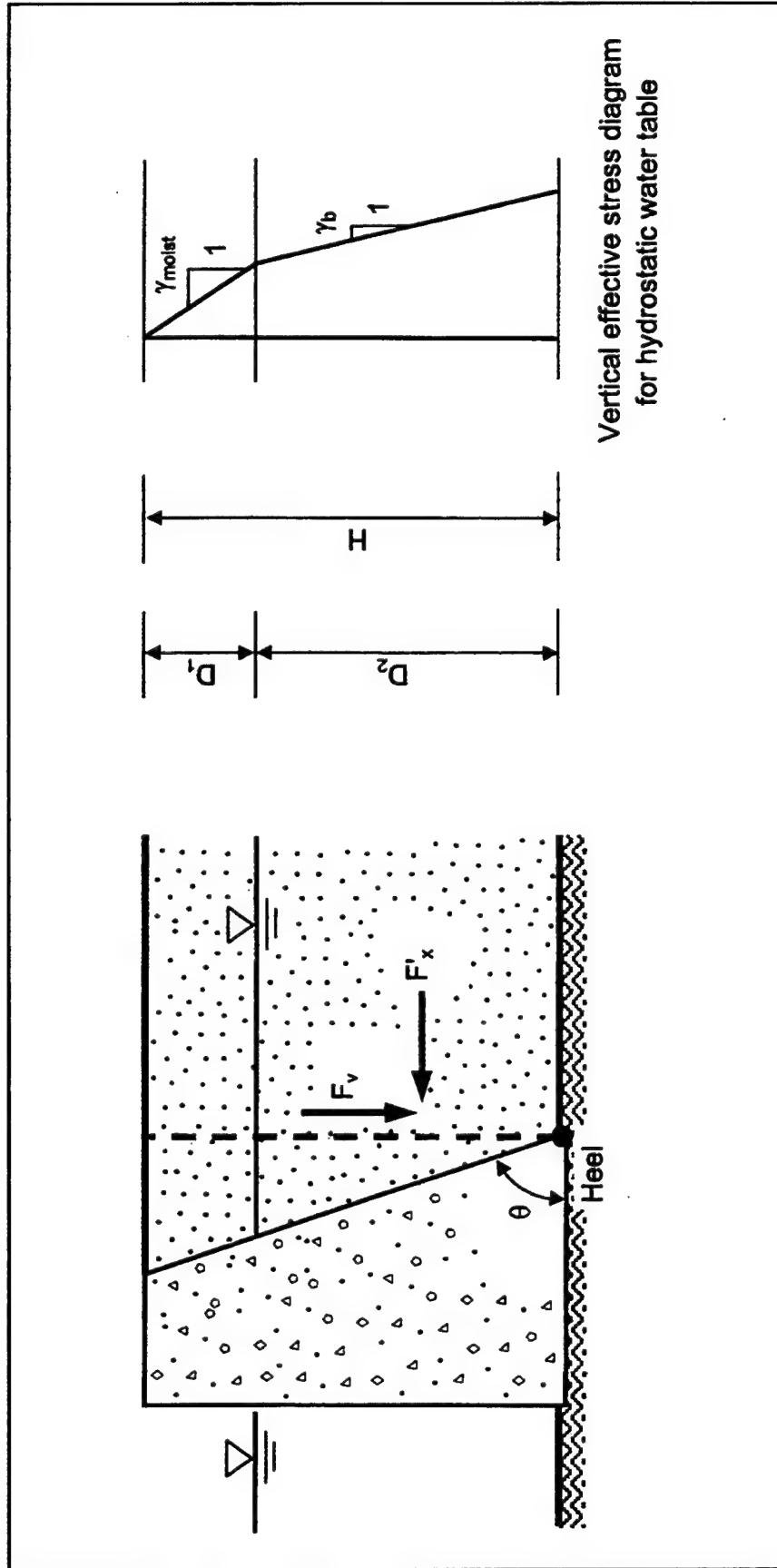


Figure 2-4. Vertical and effective horizontal earth pressure forces on vertical plane extending through the backfill from the heel of the monolith (adapted from ETL 1110-2-352, HQUSACE 1994)

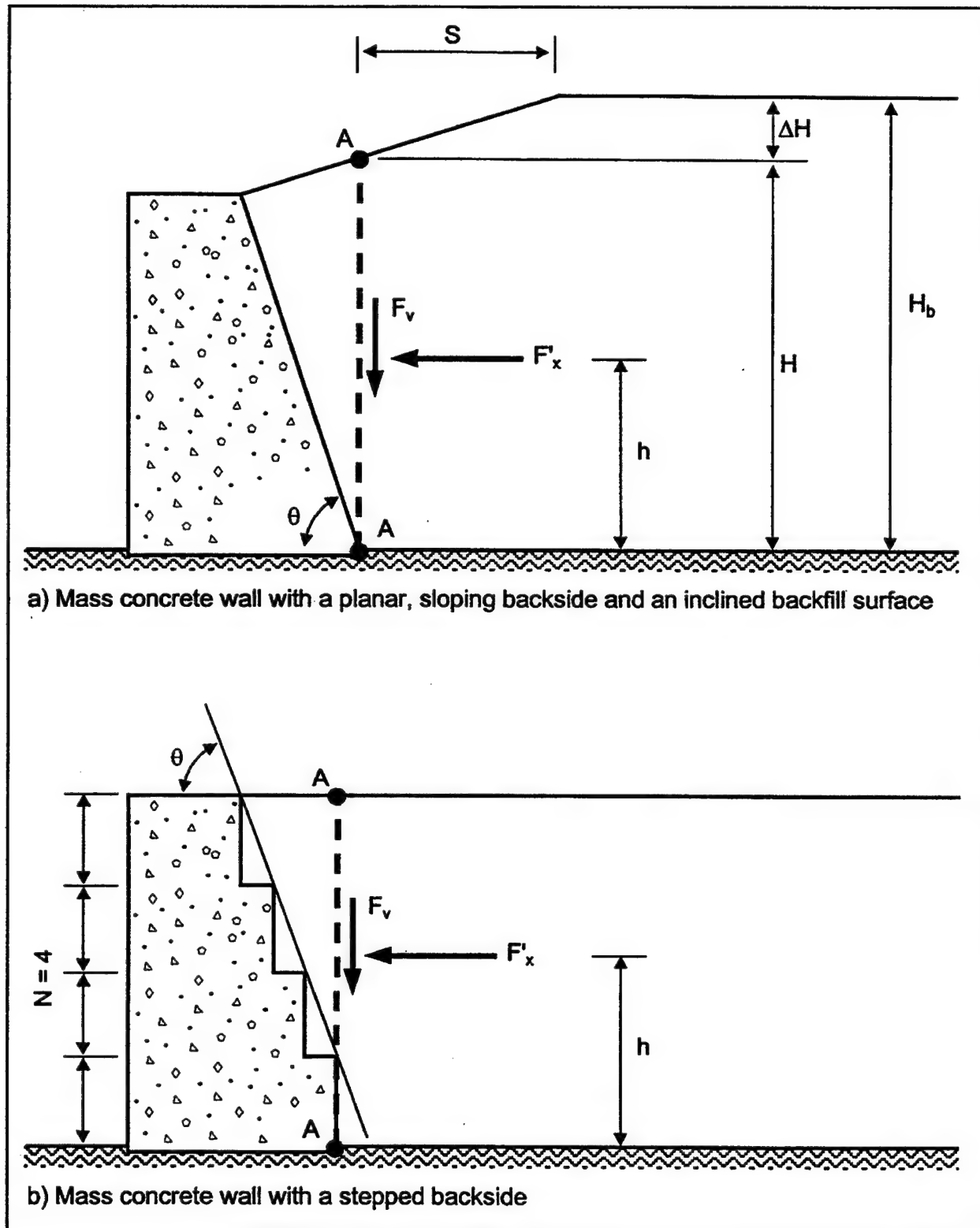


Figure 2-5. Rock-founded retaining wall definition sketches (adapted from Filz, Duncan, and Ebeling 1997)

and

$$F_{v,q} = K_{v,q} \cdot q \cdot H \quad (2-16)$$

where

$K_{v,soil}$ = the vertical shear force coefficient for self-weight of the backfill

$K_{v,q}$ = the vertical shear force coefficient for sloping backfill and surcharge

q = applied surcharge pressure

H = height measured along the vertical plane A-A extending through the backfill as indicated in Figure 2-5a

The surcharge q can be determined from:

$$q = \Delta H \cdot \gamma_{moist} = [H_b - H] \cdot \gamma_{moist} \quad (2-17)$$

where H_b is the total backfill height measured as illustrated in the figure. The vertical shear force coefficient for self-weight of the backfill $K_{v,soil}$ is computed using:

$$K_{v,soil} = (1 - C_\theta \cdot C_N) \cdot K_{v,soil,ref} \quad (2-18)$$

where

C_θ = correction factor for inclination of the back side of a rock-founded gravity wall

C_N = correction factor for the number of steps, N , in the back side of a rock-founded gravity wall

$K_{v,soil,ref}$ = reference value of $K_{v,soil}$ obtained for an inclination of the back of the wall, θ , of 90 deg

Calculation of the value for N is shown in Figure 2-5b.

The vertical shear force coefficient for sloping backfill and surcharge $K_{v,q}$ is given by:

$$K_{v,q} = C_S \cdot K_{v,q,ref} \quad (2-19)$$

where

C_s = correction factor for a rock-founded gravity retaining wall with an inclined backfill surface

$K_{v,q,ref}$ = reference value of $K_{v,q}$ obtained for a value of $S = 0$

S = horizontal distance from the vertical plane through the wall heel to the top of the backfill slope, as shown in Figure 2-5a

Given the density of the backfill and the height H as defined in Figure 2-5a, values for $K_{v,soil,ref}$ and $K_{v,q,ref}$ are obtained from Figures 2-6 and 2-7, respectively, using the curves designated as “design” curves. The data designated as “FEM” are based on the results of complete soil-structure interaction analyses using SOILSTRUCT-ALPHA (Ebeling and Filz, in preparation; or Filz, Duncan, and Ebeling 1997) and are for reference only. Correction factors C_ϕ , C_N , and C_s are given in Figure 2-8.

Filz, Duncan, and Ebeling (1997) presented a complete example calculation for F_v using this simplified procedure for a 9-m- (30-ft-) high, step-tapered, rock-founded gravity wall retaining dense sand with surcharge (no groundwater table). In this example, a 14 percent reduction in base width was obtained by including F_v in the analyses without compromising the design safety requirements. This illustrates the impact of including the downdrag force F_v in equilibrium calculations of a rock-founded gravity wall.

As pointed out by Ebeling, Pace, and Morrison (1997), a rebound of the backfill can occur during a postconstruction rise in the groundwater level behind the wall. This may result in a reduction in the shear force F_v , as reported by Ebeling et al. (1993) and Ebeling and Mosher (1996) from their analyses of the Red River Lock No. 1. Ebeling, Pace, and Morrison (1997) indicated that, in this case, SOILSTRUCT-ALPHA (Ebeling, Duncan, and Clough 1990; Ebeling et al. 1992) can be used to perform the necessary SSI analyses to calculate F_v . These analyses must include the rise in water table and the corresponding “unloading” of the backfill (Ebeling et al. 1993; Ebeling and Mosher 1996). The work performed by Ebeling and Wahl (1997) for the new roller-compacted concrete lock at McAlpine Locks is a good example of this type of analysis.

2.4 Summary

A literature review was carried out for this phase of the investigation. It included previous work on interface testing, interface modeling, and SSI analyses of retaining walls. The review focused on the most relevant issues for this phase of the investigation, and it will be extended, as needed, for the final report.

In the experimental works reviewed, the direct shear box (DSB) and the direct simple shear (DSS) device are the apparatuses most frequently used for testing of sand-to-concrete and sand-to-steel interfaces. Most of the previous work on

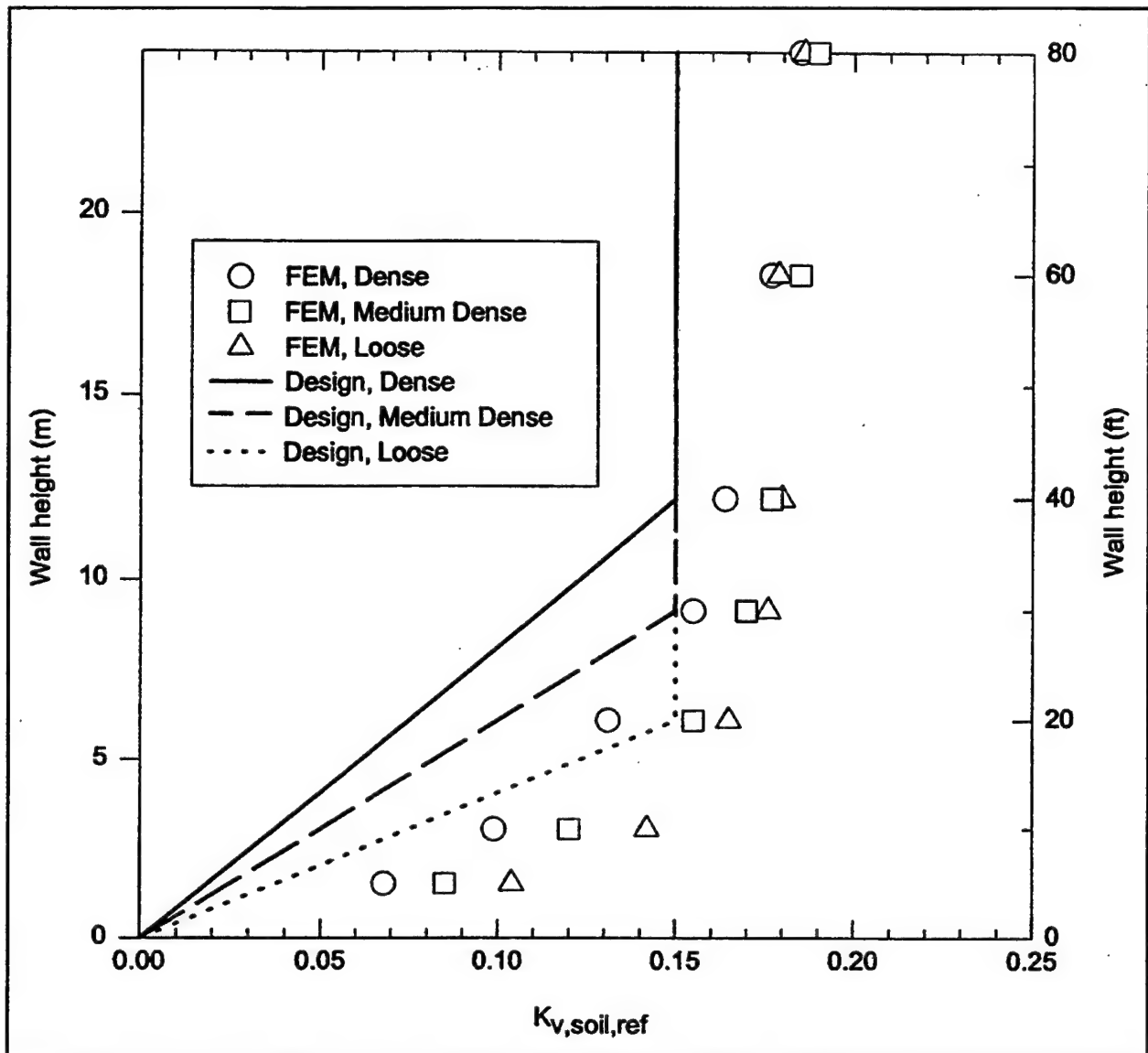


Figure 2-6. Values of $K_{v,soil,ref}$ recommended for design (adapted from Filz, Duncan, and Ebeling 1997)

interface testing corresponds to monotonic shear of the interface, under constant normal stress. Some investigations have been published regarding cyclic shear of interfaces under conditions of constant normal stress or constant normal stiffness. No previous studies were found on the interface response under staged shear.

All of the interface testing devices described in the literature present common limitations. The interface sizes are limited and do not allow the determination of the residual interface strength in all cases. Additionally, end effects may be present, inducing errors in the measurement of the prepeak interface response. The Large Direct Shear Box (LDSB) at Virginia Tech allows testing of interfaces as large as 711 by 406 mm under monotonic or cyclic shear. The size of the interface minimizes end effects and permits maximum interface displacements of 305 mm, allowing the determination of the residual interface strength. The large

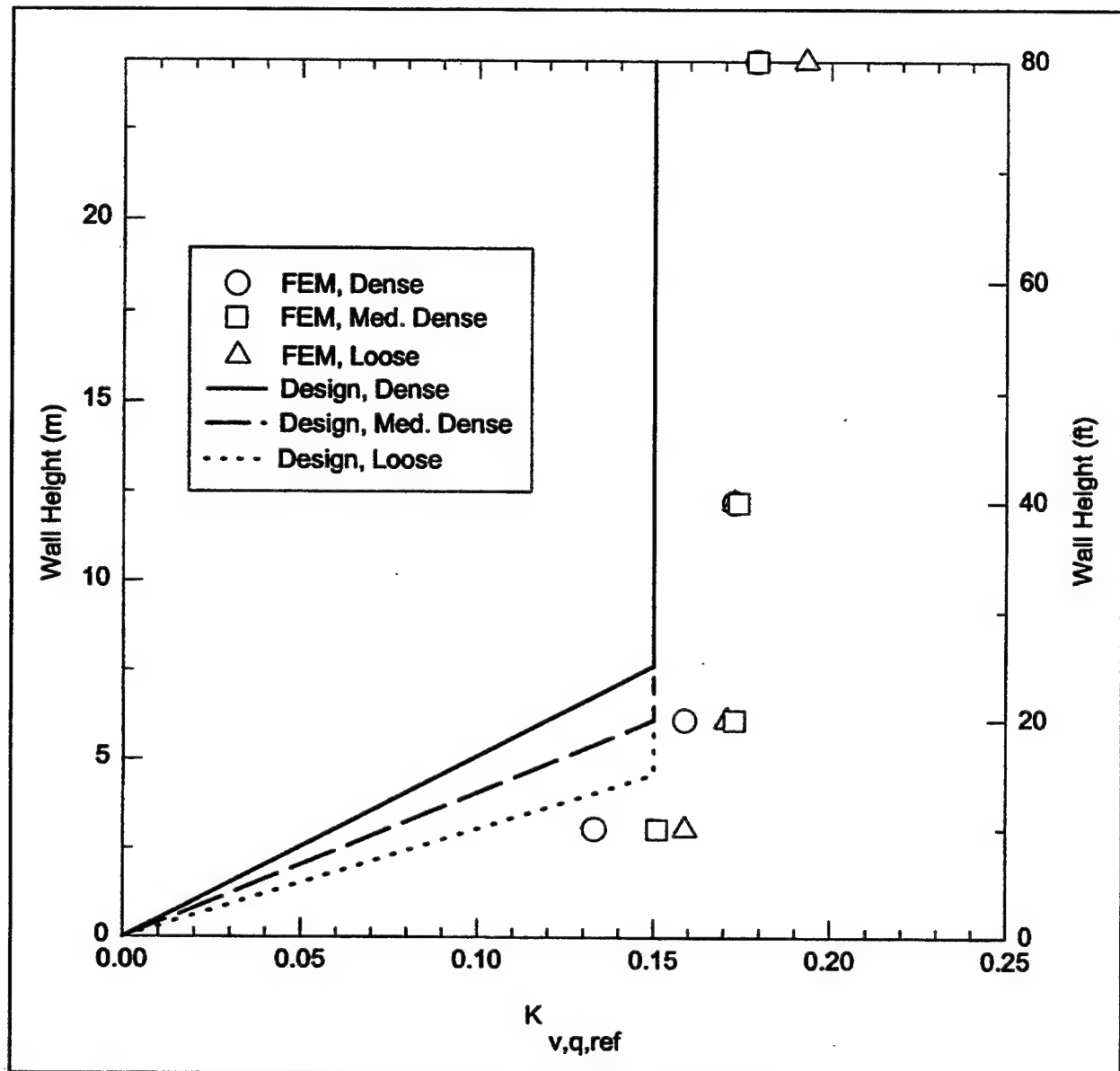


Figure 2-7. Values of $K_{v,q,ref}$ recommended for design (adapted from Filz, Duncan, and Ebeling 1997)

displacement capabilities of the LDSB also make possible shearing of the interface in several stages with changing normal stress.

Two types of elements are commonly implemented for modeling of interfaces: the joint element and the thin layer element. The joint element, developed by Goodman, Taylor, and Brekke (1968), appears to be used most frequently due to the simplicity of its formulation.

Several models of interface response under shearing have been described in the literature. The hyperbolic formulation by Clough and Duncan (1971) was described in detail in this chapter. It has been widely used for modeling the

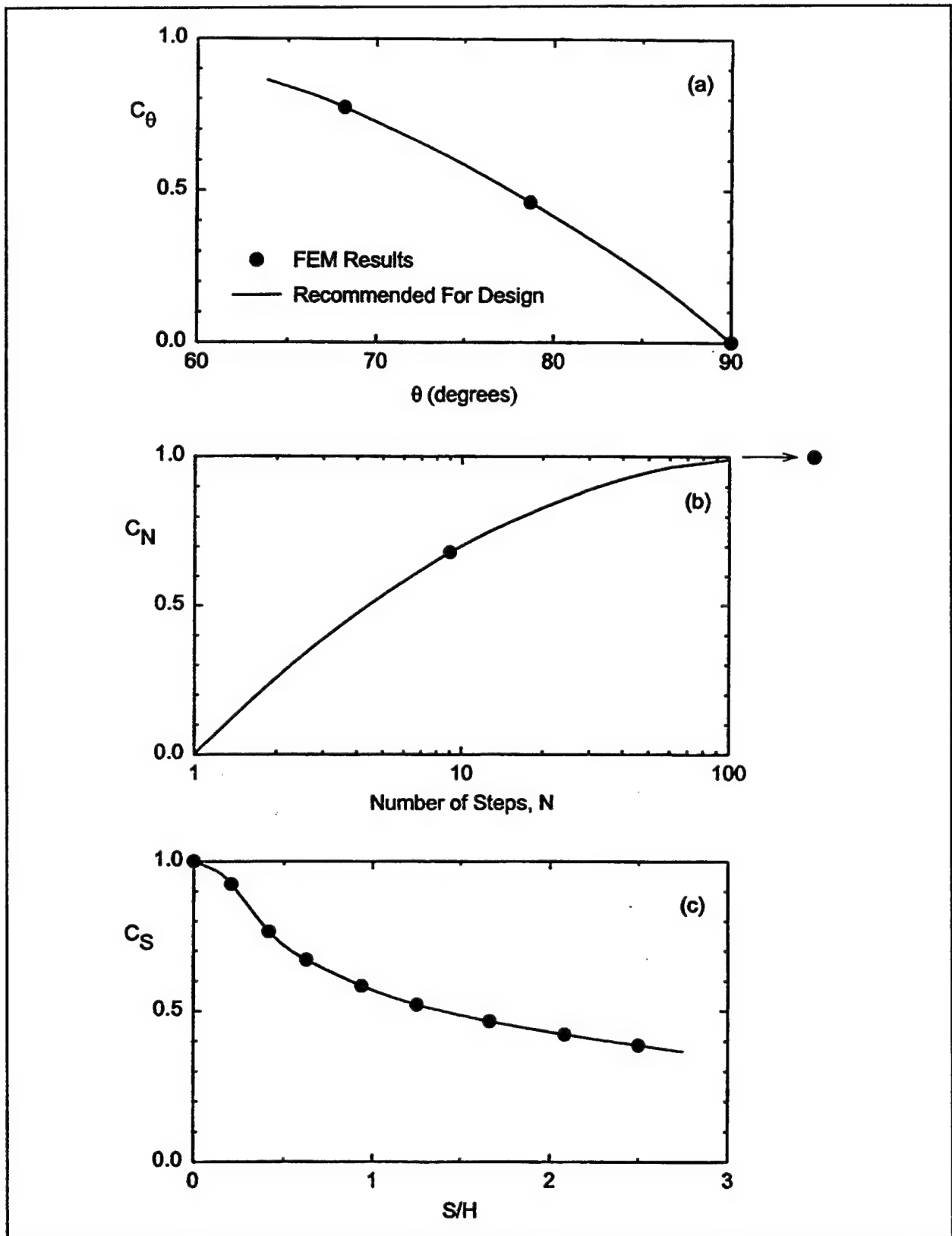


Figure 2-8. Values of the correction factors C_θ , C_N , and C_S (adapted from Filz, Duncan, and Ebeling 1997)

interface response to monotonic shear under constant normal stress. It is a simple model that conveys the most important aspects of interface behavior using parameters that have physical meaning. However, the Clough and Duncan hyperbolic formulation was not developed to model the interface response under cyclic loading or staged shear. None of the other interface models found in this literature review account for simultaneous changes in shear and normal stresses.

Several studies have been published regarding SSI analyses of retaining structures. In the works reviewed, it is concluded that the downdrag force acting on the back of a retaining wall may contribute significantly to the stability of the structure. In typical lock walls, the downdrag develops during fill placement. At this stage, the shear and normal stress acting on the backfill-to-structure interface are changing simultaneously. During submergence and operation of the lock, the shear stresses may be reduced or even reversed. Hence, it is important to model accurately the interface response under staged shear, unloading-reloading, and shear reversals.

A detailed description of a simplified method (Appendix F of HQUSACE 1997) to estimate the downdrag force was presented in this chapter. It is based on a number of SSI analyses of typical lock structures. The simplified method is useful to illustrate the importance of an adequate estimation of the downdrag force in design.

3 Laboratory Testing

A series of shear tests were performed on a soil-to-concrete interface using the Large Displacement Shear Box (LDSB). The objective of the tests was to determine the response of the interface to stress paths such as those illustrated in Figures 1-3b and 1-4b.

Before interface testing, a soil box was designed and fabricated and the LDSB was modified to accommodate soil-to-concrete interfaces. A concrete specimen was prepared with a representative surface texture, according to the results of a survey of existing concrete walls.

All the tests included in this Phase 1 report were performed on the interface between a uniform, rounded, silica sand and the concrete specimen. As discussed in Chapter 1, additional interface tests will be performed on sands of different gradation and angularity to study the influence of these factors on the behavior of sand-to-concrete interfaces. The results of such tests will be included in the final report of this investigation.

This chapter contains a detailed description of the soil properties, preparation and characteristics of the concrete specimen, testing procedures, and results of the interface tests performed for this Phase 1 report. The data obtained from these tests formed the basis for development of the preliminary version of a new extended hyperbolic model, which is discussed in detail in Chapter 4.

3.1 Soil Properties

The interface tests were performed using a fine to medium silica sand, available commercially for in situ density determinations, which will be referred to as Density Sand throughout this report.

A series of laboratory tests were performed to determine the gradation, maximum/minimum density, and specific gravity of the Density Sand. The results are summarized in Table 3-1. The grain size distribution is presented in Figure 3-1. The sand is uniform, with grain sizes ranging from 0.2 to 0.9 mm, and has no fines. It classifies as a poorly graded sand SP (ASTM D2487 (ASTM

Table 3-1
Characteristics of the Density Sand

| Parameter ¹ | Value | Relevant Standard |
|------------------------|------------------------|--------------------|
| D_{10} | 0.3 mm | D2487 (ASTM 1993a) |
| D_{30} | 0.42 mm | |
| D_{60} | 0.55 mm | |
| C_u | 1.8 | |
| C_c | 1.1 | |
| γ_{max} | 17.5 kN/m ³ | D4253 (ASTM 1993c) |
| γ_{min} | 15.1 kN/m ³ | D4254 (ASTM 1991) |
| G_s | 2.65 | D854 (ASTM 1992) |

¹ Parameters are listed and defined in the Notation (Appendix A).

1993a)). Examination under an optical microscope revealed that the grains are subrounded to rounded (ASTM D2488 (ASTM 1993b)), with a length-to-width ratio typically ranging from 1 to 2.

3.1.1 Triaxial testing

A set of drained triaxial (CD) tests was performed to determine the internal friction angle and develop a set of hyperbolic parameters for the Density Sand. The samples were prepared by pluviation to an average relative density of 85%. A manometric pressure of -15 to -20 kPa was kept inside the sample during the test setup, and gradually removed as the cell pressure was increased. The sample was de-aired using CO₂, inundated with de-aired distilled water, and back-pressure saturated. The confining pressure was then increased to the final value, allowing for drainage of the sample. The tests were run at effective confining pressures σ'_3 of 45, 103, and 280 kPa. The strain rate used was 0.25 %/min, which was found appropriate for pore pressure dissipation during previous trials. The results of the tests are presented graphically in Figures 3-2 and 3-3.

During the tests, the samples exhibited dilation under all the confining stresses applied, and strain softening after mobilization of the peak strength. The peak friction angle ϕ'_p was 42.9 degrees, as illustrated in Figure 3-3. The friction angle ϕ'_{cv} at a strain of 15% was 35 degrees.

3.1.2 Hyperbolic parameters from triaxial tests

The hyperbolic formulation by Duncan and Chang (1970) was used to fit the stress-strain data from the triaxial tests. The volumetric-axial strain response was not modeled for the following reasons: (a) dilation occurred almost immediately upon the start of shear, and the initial volumetric compression was negligible; (b) the hyperbolic model does not account for dilation; and (c) the volumetric deformation behavior of the sand is only qualitatively relevant for this phase of the investigation.

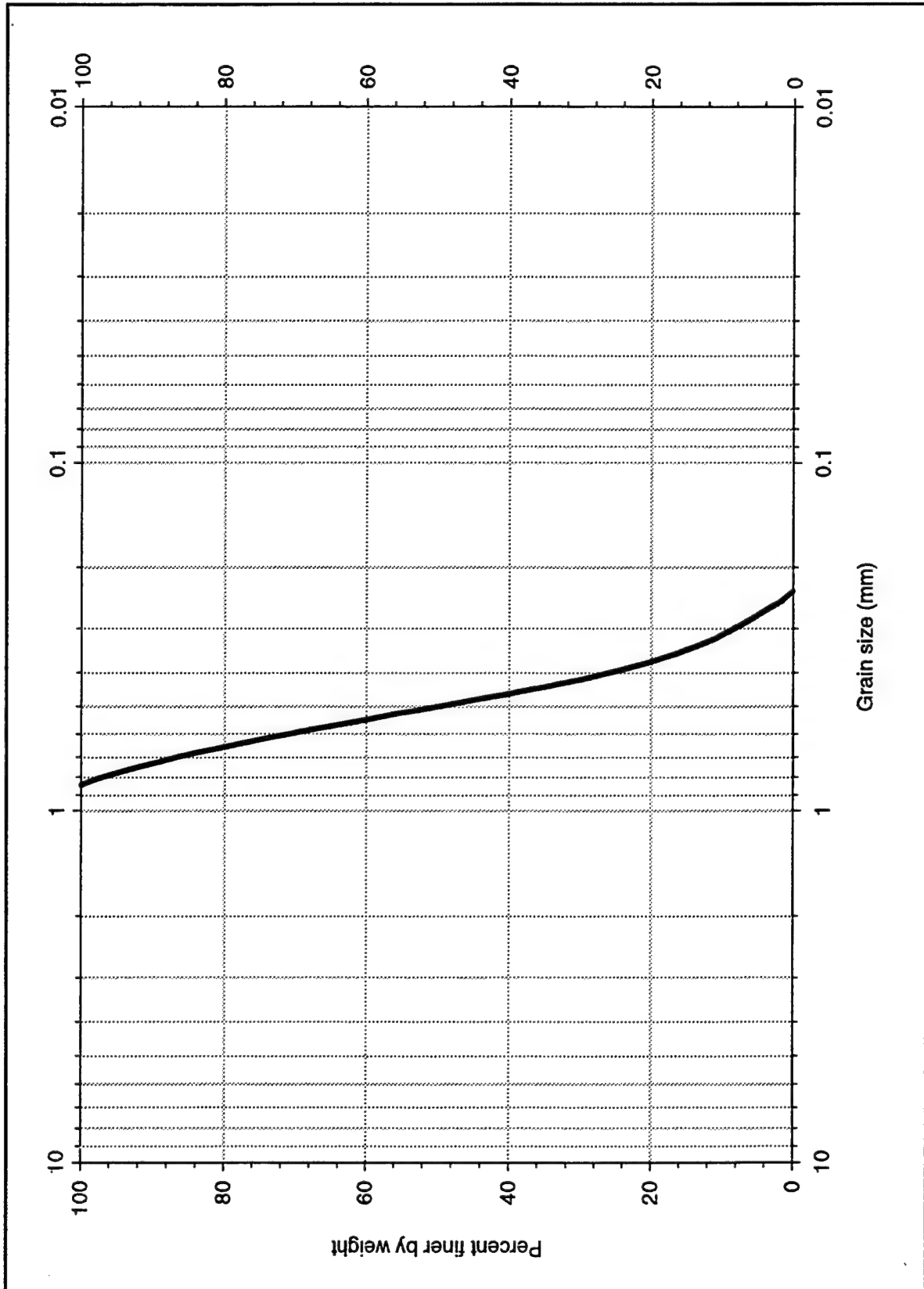


Figure 3-1. Grain size distribution of the Density Sand used for interface testing

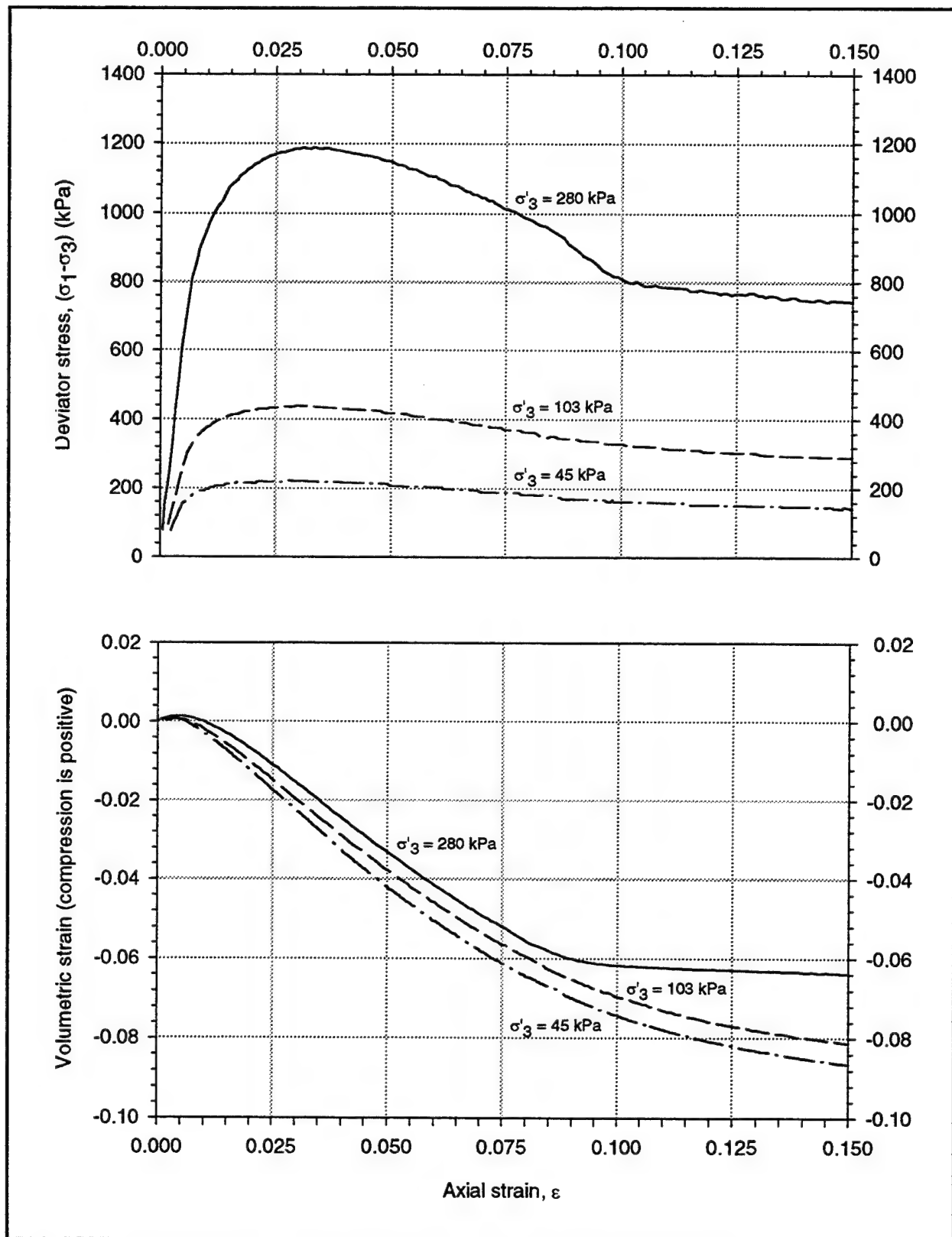


Figure 3-2. Results of consolidated drained triaxial tests on dense Density Sand

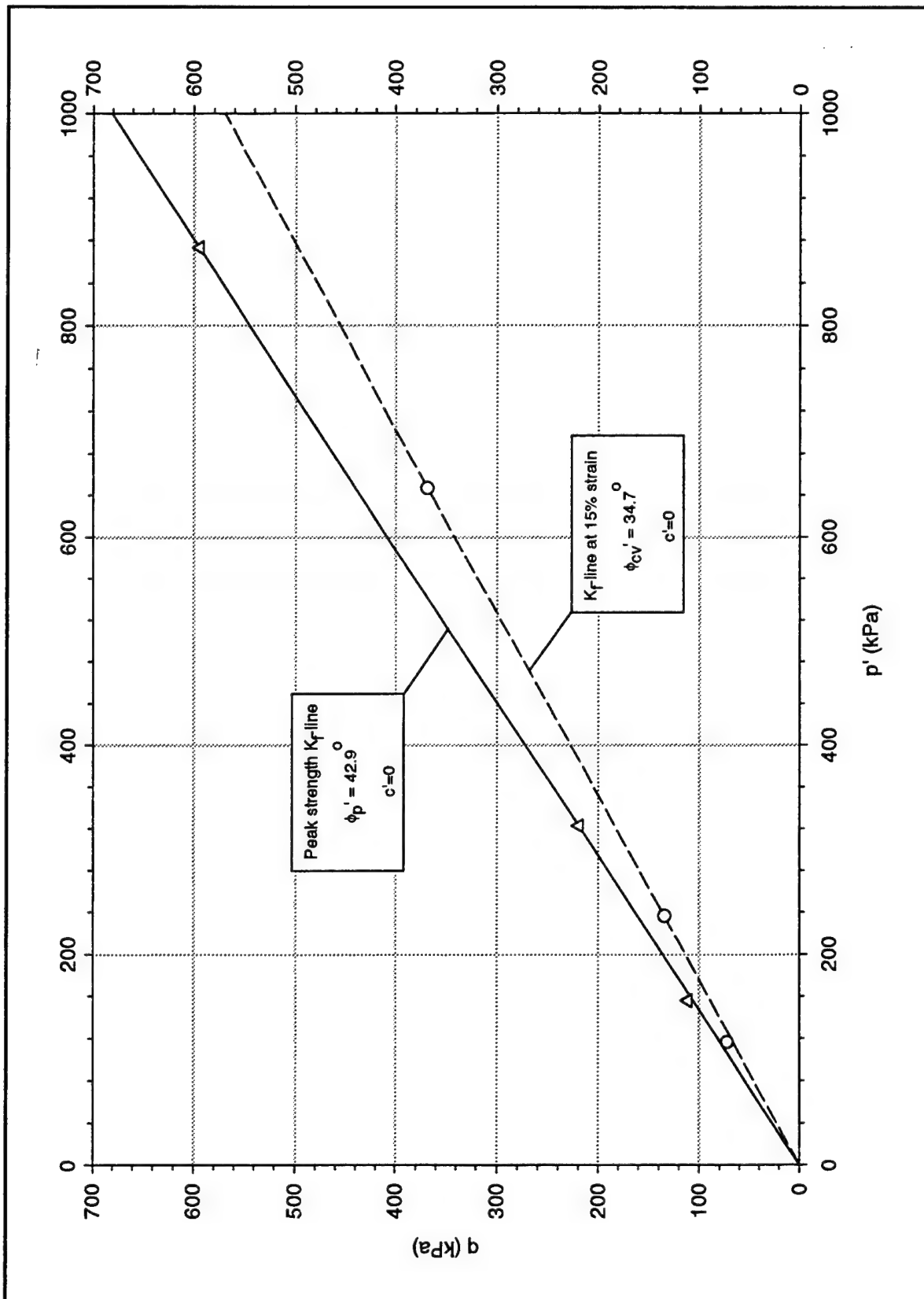


Figure 3-3. K_f lines and determination of strength parameters for dense Density Sand from CD triaxial tests

Figure 3-4 shows the stress-strain data from the tests plotted in transformed coordinates. For each confining stress, a straight line was drawn through the data points corresponding to 70 and 95% of the peak strength. The value of initial tangent modulus E_t was determined as the reciprocal of the intercept a of the line with the ordinates axis. The asymptotic strength $(\sigma_1 - \sigma_3)_{ult}$ was determined as the reciprocal of the slope b . The failure ratio R_f was determined as the ratio of the deviator stress at failure $(\sigma_1 - \sigma_3)_f$ to $(\sigma_1 - \sigma_3)_{ult}$.

Figure 3-5 shows the variation of the initial tangent modulus with confining stress, normalized by atmospheric pressure. A straight line was used to fit the data, and the value of the modulus number K was determined as the normalized initial tangent modulus under atmospheric pressure.

The hyperbolic parameters for the Density Sand are presented in Table 3-2. To assess the validity of these parameters, they are compared with values reported by Duncan et al. (1980) for a similar soil. The sand considered by Duncan et al. (1980) was a fine, rounded, silica sand compacted to a relative density D_R of 100%. The comparison reveals that, with the possible exception of the friction angle, these sets of parameters are very consistent.

| Table 3-2 Hyperbolic Parameters for Density Sand and Fine Silica Sand in Dense Condition | | |
|---|------------------------------|--|
| Hyperbolic Parameters | Density Sand $D_R = 85\%$ | Fine Silica Sand $D_R = 100\%$ (Duncan et al. 1980) |
| K | 1400 | 1400 |
| n | 0.63 | 0.74 |
| R_t | 0.85 | 0.90 |
| ϕ | 43° | 37° |

The hyperbolic parameters for the Density Sand were used to develop a hyperbolic stress-strain relationship for each of the confining pressures used for the tests. The comparison between the test data and the model is presented in Figure 3-6. The hyperbolic model provides a good fit of the laboratory data, especially at the higher stress levels, but it does not model the postpeak strain softening behavior.

3.2 Concrete Specimen

A concrete slab was prepared for the soil-to-concrete interface tests, with dimensions 635 by 305 by 25.4 mm (25 by 16 by 1 in.). The main considerations for the design of the specimen were to obtain a relatively high strength in order to minimize surface wear during shear, create a surface texture representative of field conditions, and minimize internal deformations of the concrete specimen

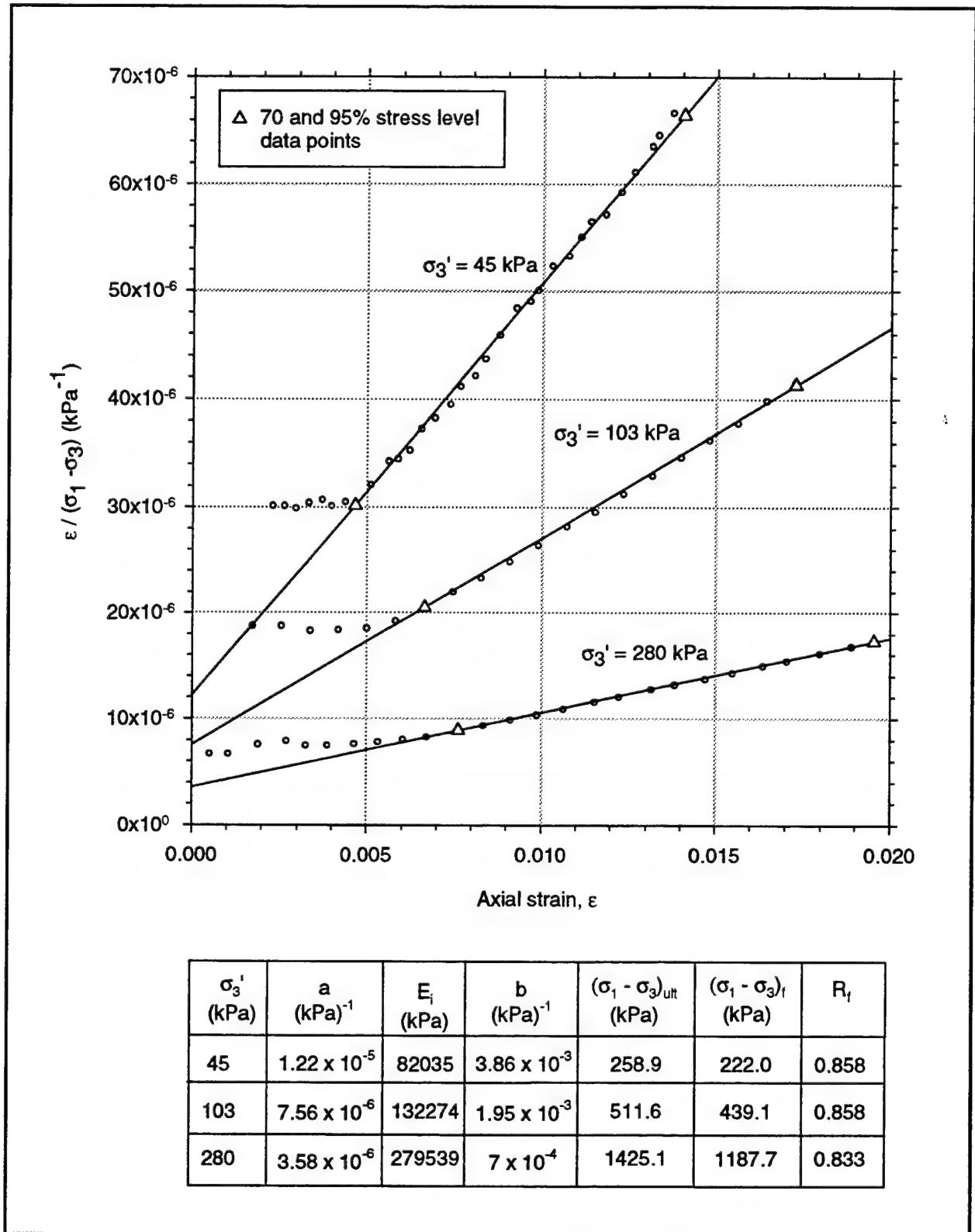


Figure 3-4. Transformed stress-strain plots from triaxial test data on dense Density Sand, and determination of hyperbolic parameter values

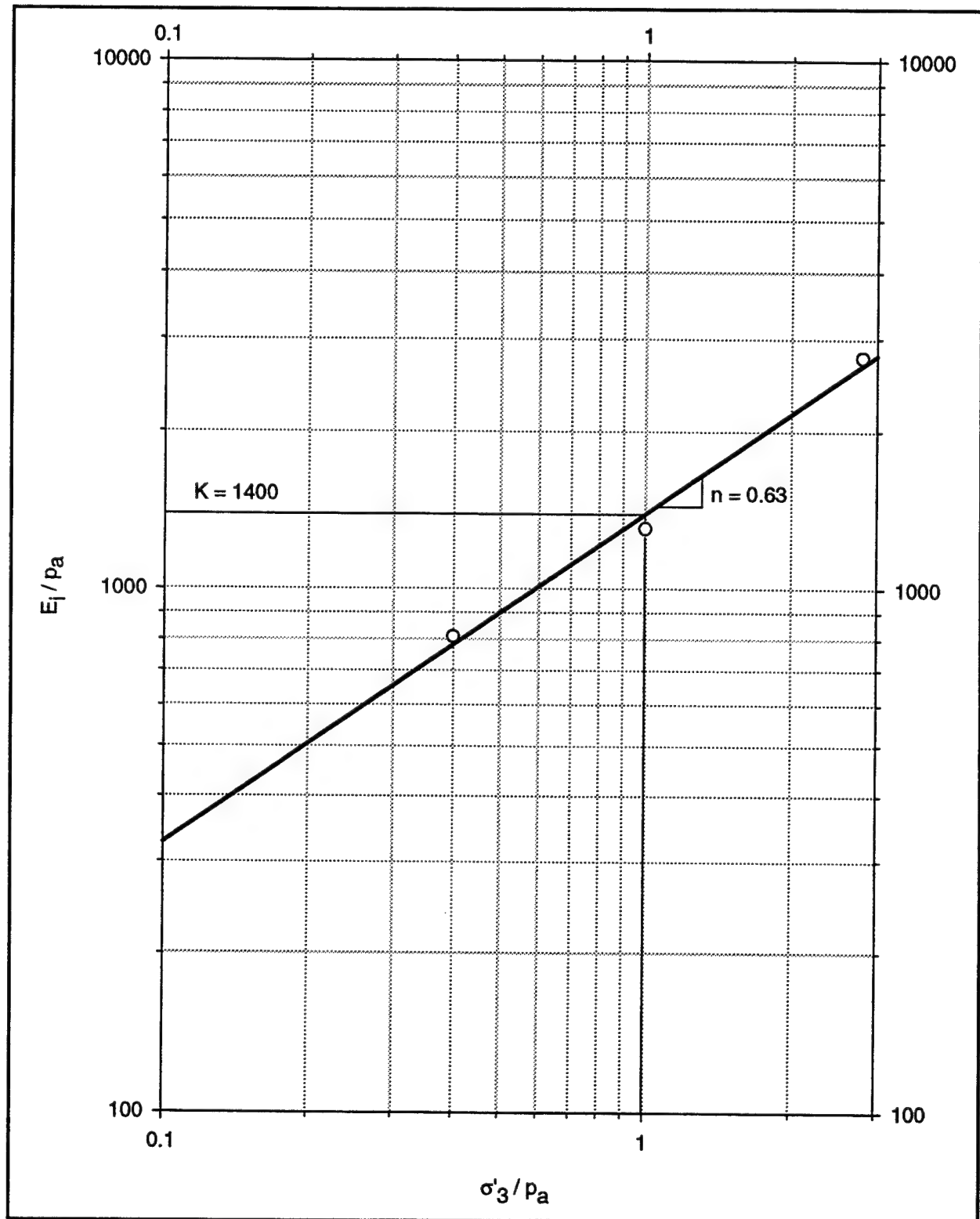


Figure 3-5. Variation of initial tangent modulus E_t with confining pressure σ'_3 and determination of hyperbolic parameters K, n

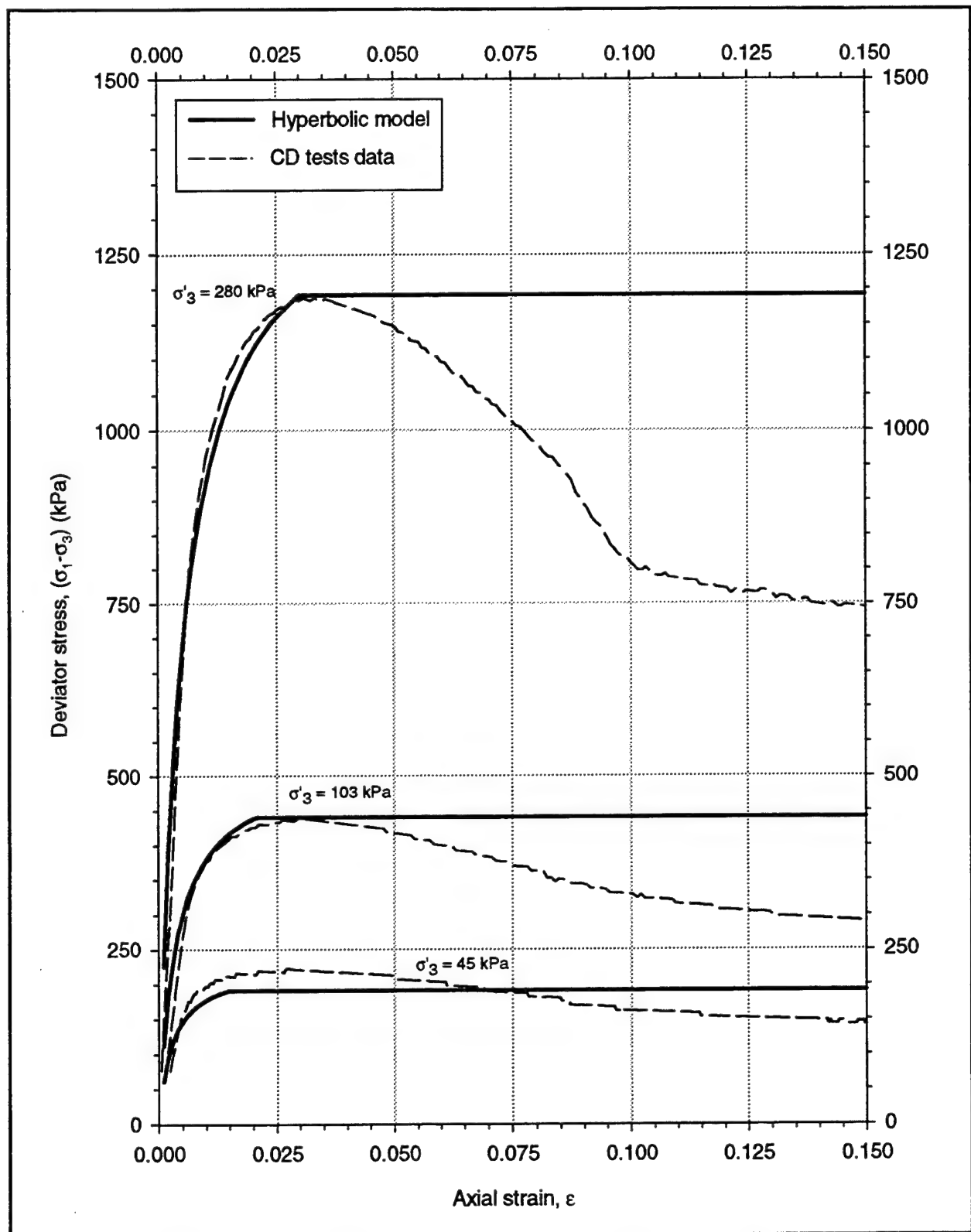


Figure 3-6. Hyperbolic model for dense Density Sand and comparison to CD triaxial test data

during interface shear. To meet these requirements, several trials were required to develop the appropriate mixing and placement procedures for the concrete.

As illustrated in Figure 3-7, the concrete specimen was poured inside an aluminum frame specially fabricated for this testing program, and topped by a 3.2-mm (0.125-in.) steel plate. This system was designed to withstand compressive and tensile forces induced by the interface shear stresses with minimal deformations. The steel plate and aluminum sides of the frame acted as an external reinforcement, minimizing tensile stresses in the concrete during the interface shear tests. A set of threaded, high-strength-steel studs worked as shear connectors between the concrete and the steel plate.

3.2.1 Materials

The fine aggregate for the specimen was a processed, well-graded sand, commercially available for the preparation of concrete. This sand will be referred to as Blacksburg Sand throughout this report. Examination under an optical microscope revealed that the sand grains smaller than 1 mm were predominantly sub-angular, with length-to-width ratios ranging from 1 to 3. The larger grains tended to be more angular and flat (ASTM D2488 (ASTM 1993b)).

The coarse aggregate was a crushed limestone with maximum grain size of 12.5 mm (0.5 in.), which is also commercially available for the preparation of concrete. The coarse aggregate was predominantly angular to subangular. The grain size distribution of the aggregates is presented in Figure 3-8.

In order to obtain an adequate workability without compromising strength, an Air-Entraining Admixture (AEA) and a High-Range Water Reducer (HRWR) were included in the concrete mix. Additionally, a corrosion inhibitor admixture was added to prevent corrosion of the steel components of the concrete frame.

3.2.2 Preparation of the specimen

The concrete was prepared following a rigorous mixing sequence. First, the aggregates were impregnated with the corrosion inhibitor. Then, the AEA, cement, water, and HRWR were added in sequence and thoroughly mixed. The mixing proportions and some physical properties of the concrete are summarized in Table 3-3.

Several trial batches were prepared until a mix with the appropriate physical properties was obtained. Tests were performed to determine the slump, air content, and compressive strength of the concrete, and the results are presented in Table 3-4.

The concrete was carefully placed onto the piece of plyform, inside the aluminum frame, as illustrated in Figure 3-7a. The concrete specimen was vibrated, trimmed, and covered with the steel plate. The plate was then attached to the

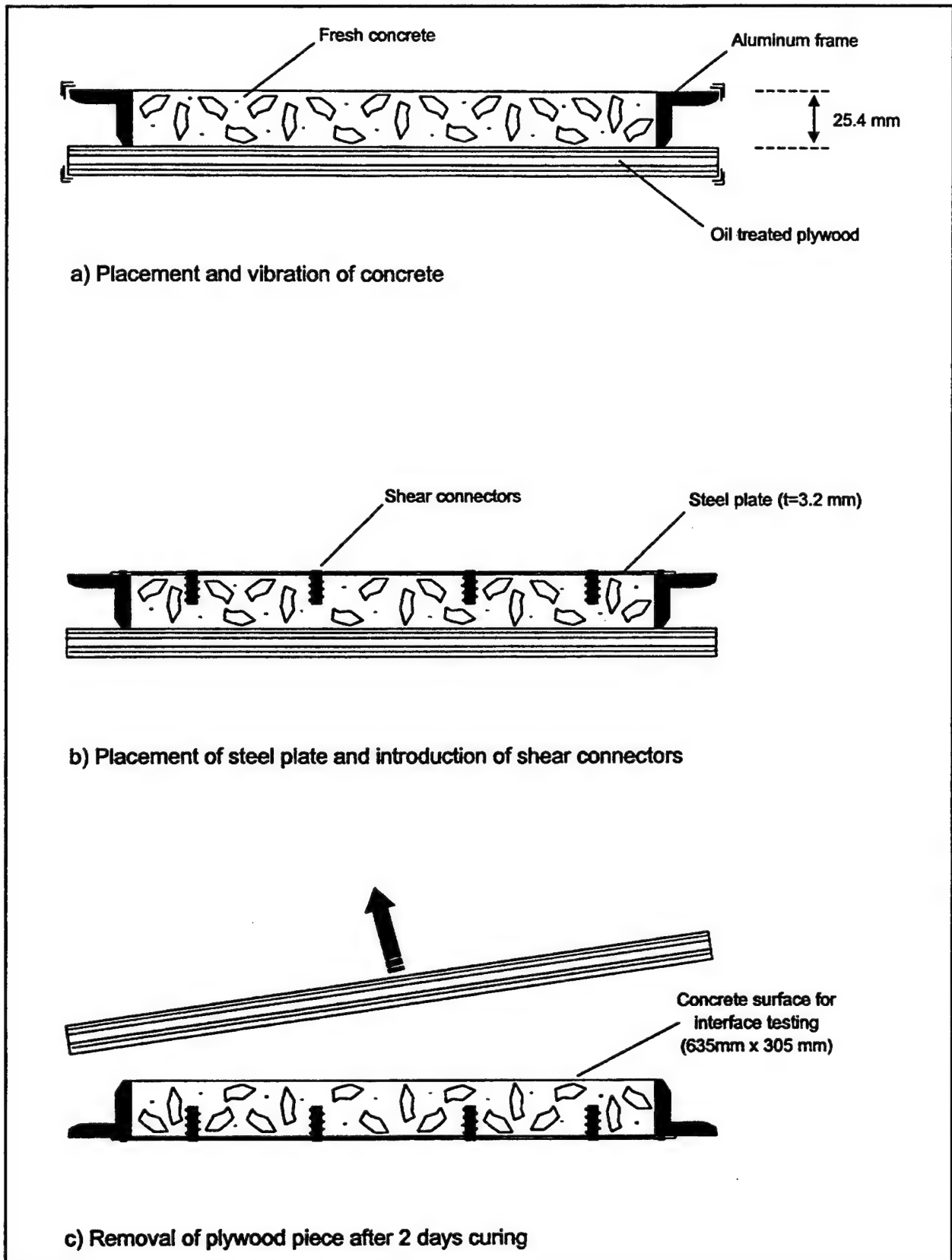


Figure 3-7. Preparation of the concrete specimen

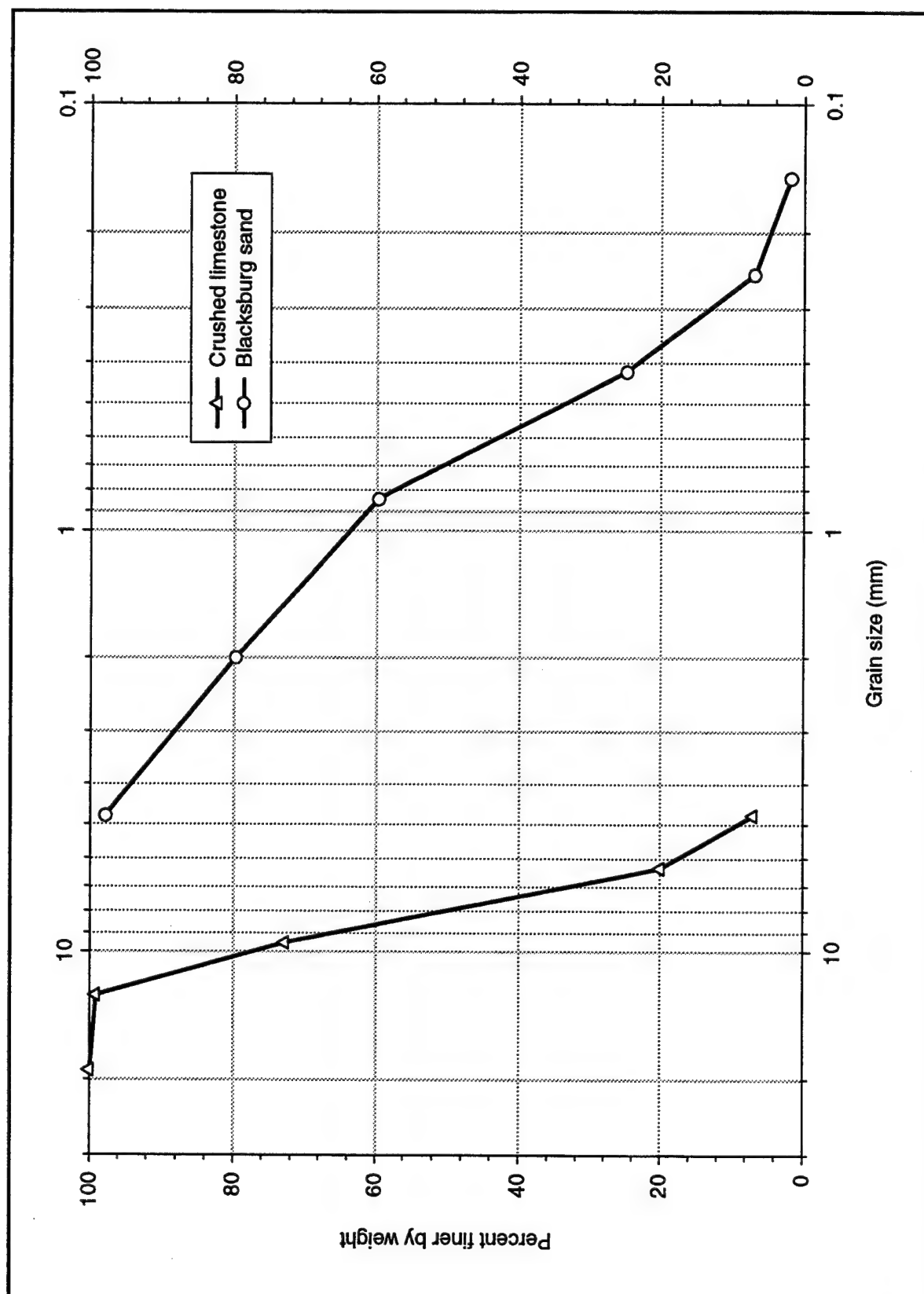


Figure 3-8. Grain size distribution of aggregates used for the preparation of the concrete specimen

| Table 3-3 Mixing Proportions of Concrete | |
|---|--------------------------|
| Coarse aggregate | 600 kg/m ³ |
| Fine aggregate (Blacksburg Sand) | 600 kg/m ³ |
| Type I Portland cement | 264 kg/m ³ |
| Water | 105 kg/m ³ |
| HRWR (Daracem) | 850 ml/m ³ |
| AEA (Daravair) | 530 ml/m ³ |
| Corrosion inhibitor (DCI-S) | 10,420 ml/m ³ |

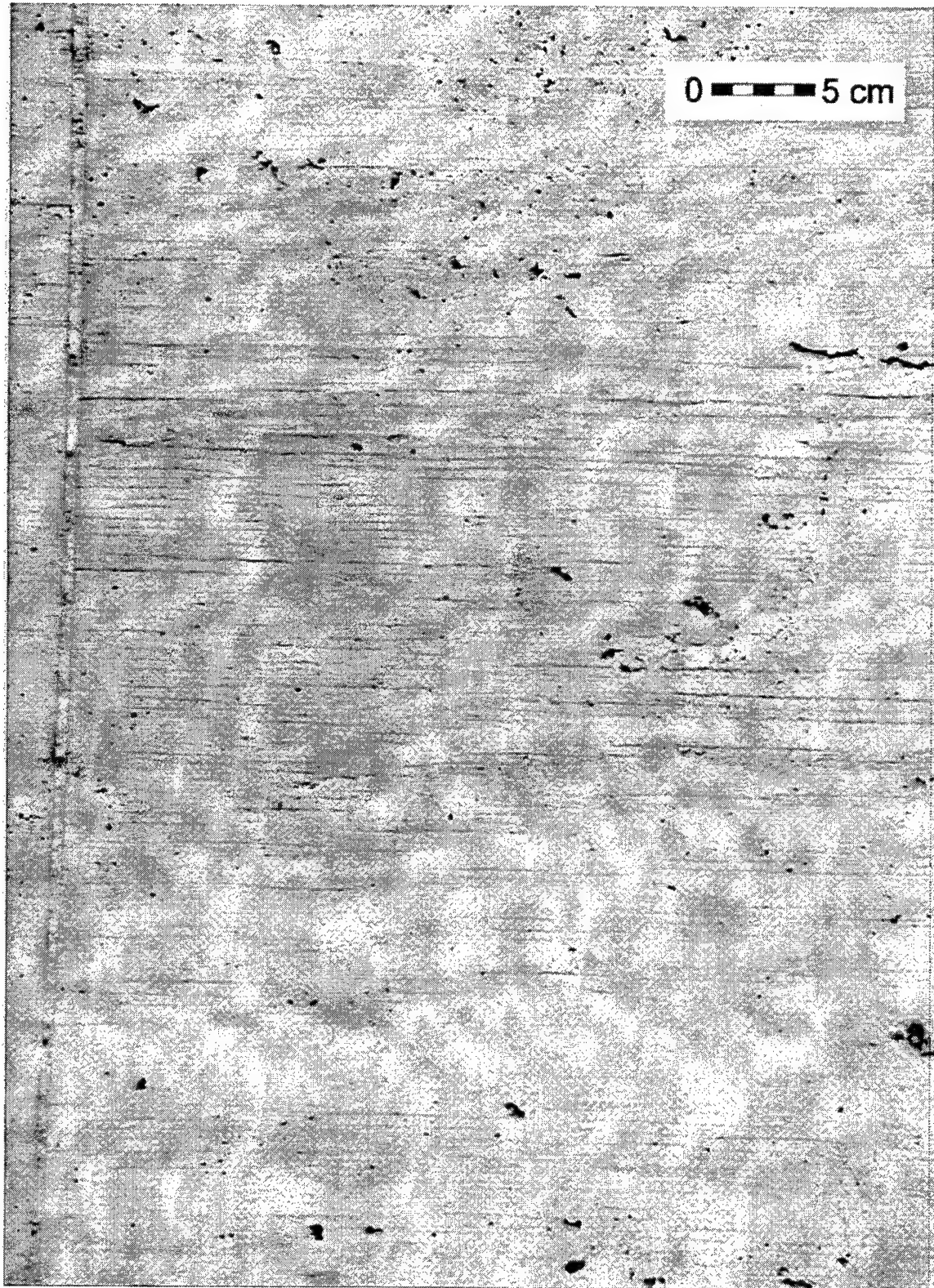
| Table 3-4 Physical Properties of the Concrete Mix | |
|--|------------------------|
| Slump | 180 mm (7 in.) |
| Air content | 7 % |
| Compressive strength | |
| 7 days | 24,700 kPa (3,580 psi) |
| 21 days | 27,450 kPa (3,980 psi) |
| 28 days | 33,100 kPa (4,800 psi) |

aluminum frame as illustrated in Figure 3-7b. The threaded steel studs were screwed in place through the openings in the steel plate, and into the fresh concrete. The assembly was left in place for 2 days, after which the plywood piece was carefully removed, exposing the concrete surface for visual examination. At this point, an assessment was made of the surface texture of the specimen based on the results of the field survey of retaining walls, which is described in the following section. No surface treatment was applied to the specimen after its preparation. Once accepted as representative of field conditions, the specimen was placed in a wet room for a period of 28 days, after which it was removed and used for the interface tests.

3.2.3 Surface texture

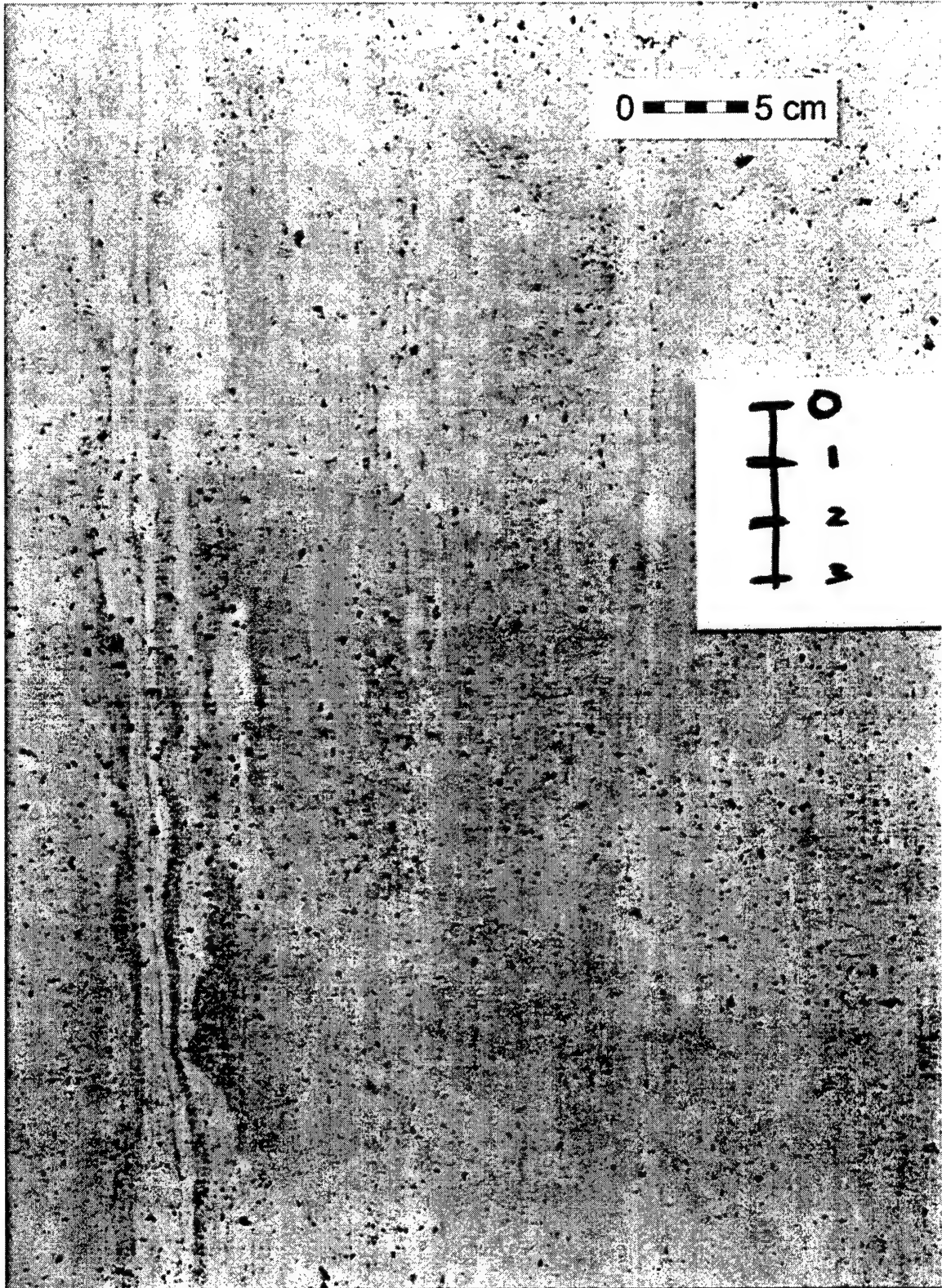
A field survey was performed to establish a range of surface textures representative of existing retaining walls. The survey, carried out throughout southwestern and northern Virginia, focused on mass and reinforced concrete retaining walls ranging from 3 to 7 m (10 to 23 ft) high, where plywood forms were used. For the purposes of this investigation, four main types of surface features were identified: small-scale roughness controlled by fine aggregate of concrete, waviness controlled by the formwork material, pores, and air pockets.

In total, ten retaining walls were surveyed. Two cases, which can be considered representative of all the walls surveyed, are presented in Figure 3-9 at approximately the same scale. Wall A is a mass-concrete retaining wall under construction, 5 m (16 ft) high and 60 m (200 ft) long, poured inside oil-treated plywood forms. The forms were reused up to six times throughout the length of



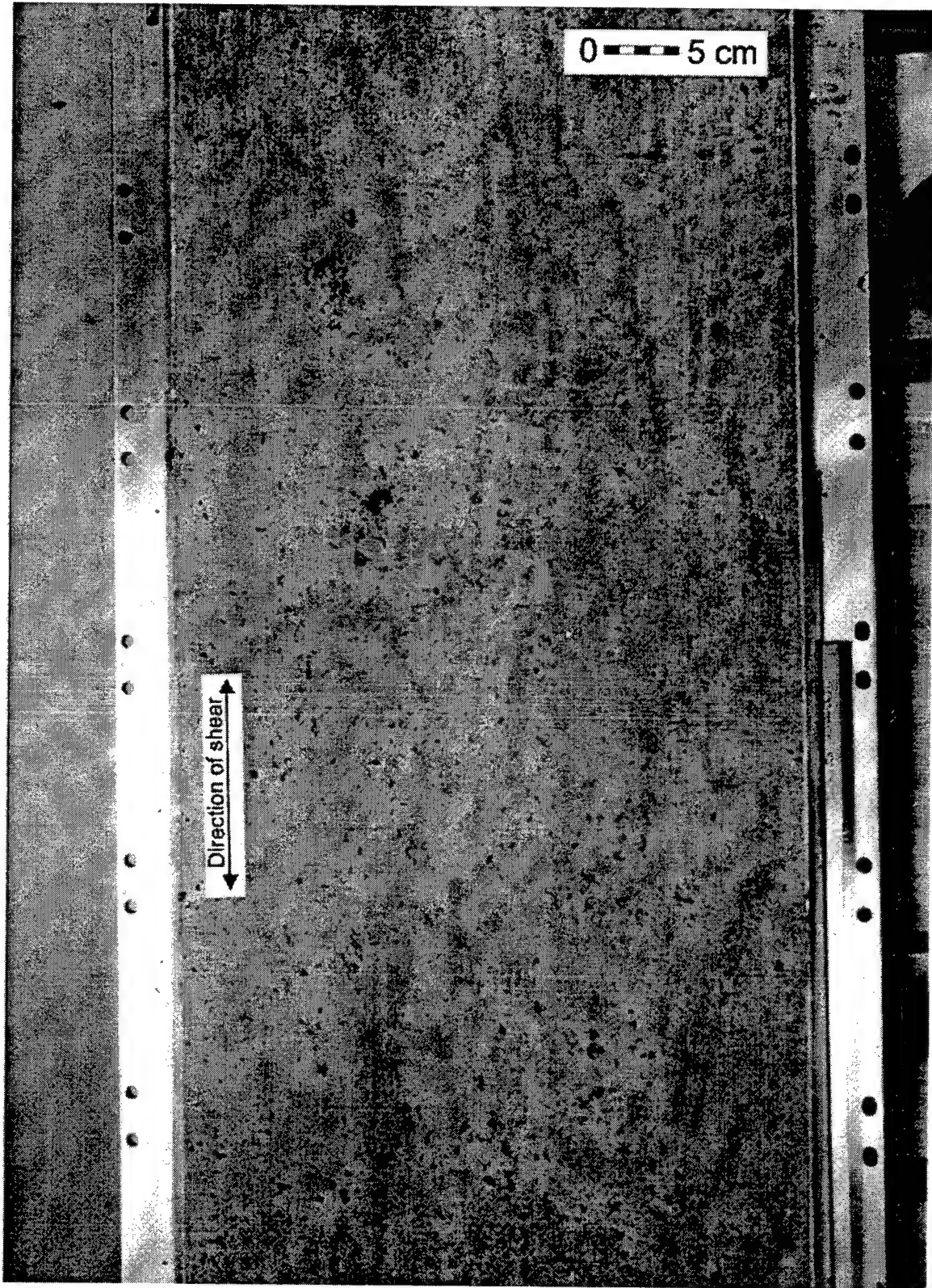
a. Surface texture of wall A

Figure 3-9. Surface texture of representative retaining walls (Sheet 1 of 3)



b. Surface texture of wall B

Figure 3-9. (Sheet 2 of 3)



c. Surface texture of concrete specimen

Figure 3-9. (Sheet 3 of 3)

the wall. The picture shows the average texture of the back of the wall, where the forms had been reused two or three times. The imprint of the plywood pattern, or waviness, is evident and is a significant component of the concrete texture. It was also noted that the waviness increased with the number of times the forms were reused. Although the concrete was vibrated after placement, air pockets are frequent.

Wall B is a 7-m- (22-ft-) high reinforced concrete wall of recent construction. The picture shows the average conditions on the exposed face of the wall before any surface treatment was applied. Here the pattern of the plywood is also evident, although not as marked as in wall A. There is a much higher frequency of air pockets than in wall A.

Figure 3-9c shows the surface of the finished concrete specimen. It has surface features similar to those of the walls surveyed. The imprint of the plywood pattern is clearly visible, suggesting a degree of waviness similar to the field cases. The frequency of air pockets was very difficult to control during the specimen preparation. The final specimen was obtained after several trials, and it presents a frequency of air pockets similar to wall B.

No controls were placed on surface features such as small-scale roughness and porosity, because they are very difficult to measure in the field. However the concrete was prepared using materials and mixing procedures that are common in the industry and highly repeatable, and can also be considered representative of actual construction practices.

3.3 Testing Procedures

3.3.1 The soil box

The sand sample is compacted inside a soil box that was designed and fabricated specially for sand-to-concrete interface testing. Its inner dimensions are 635 by 406 by 25.4 mm (25 by 16 by 1 in.), and it is composed of a bottom plate and sidewalls made entirely of a thermally treated, medium-strength aluminum alloy. The face of the bottom plate in contact with the soil is coated with several layers of polyurethane paint mixed with medium to coarse sand. This prevents slippage of the soil during interface shear testing.

The sidewalls are connected to the bottom plate by a set of structural-steel bolts, which also allow the creation of the gap at the interface as described in Section 3.3.4. These bolts will be referred to as *set bolts* throughout this report.

The volume of the soil box was carefully determined using several procedures. This was important to obtain reliable values of density of the sand sample.

3.3.2 Preparation of the interface

The sand-to-concrete interface is created by compacting the sand sample on top of the concrete specimen, as illustrated in Figure 3-10. The concrete slab is attached to a 750- by 750-mm (30- by 30-in.) vibrating table. The sidewalls of the soil box and an extension collar are placed on top of the slab. Four mounting brackets keep the side walls firmly in place throughout the entire process.

To minimize the friction between the soil and the soil box, the inside of the walls is coated with vacuum grease and covered with a plastic sheeting 0.1 mm thick (4 mil). The soil is carefully placed inside the box to a height of approximately 5 mm above the trimming level, and vibrated under an appropriate load. The load and the extension collar are then removed, and the sample is trimmed as illustrated in Figure 3-10a. The bottom plate is carefully placed on top of the sample and bolted gently to the sidewalls, as illustrated in Figure 3-10b. The set bolts are tightened to generate a pressure of approximately 3.5 to 5 kPa between the bottom plate and the soil, and therefore between the soil and the concrete specimen as well. This low contact pressure maintains the rigidity of the assembly during handling without disturbance to the interface. The assembly is then flipped and placed in position in the LDSB.

3.3.3 The Large Direct Shear Box (LDSB)

The LDSB was developed at Virginia Tech for testing of clay-to-HDPE interfaces (Shallenberger and Filz 1996). Some modifications to the LDSB were implemented to accommodate sand-to-concrete interface testing of the type described in this report. The LDSB is essentially a direct shear box type device with the capability to handle interfaces as large as 711 by 406 mm (28 by 16 in.), allowing a maximum interface displacement of 305 mm (12 in.).

Shallenberger and Filz (1996) pointed out the advantages of the LDSB over conventional devices: (a) end effects are negligible, (b) the maximum displacement of 305 mm (12 in.) allows the determination of the interface residual shear strength, and (c) no eccentric normal loads are generated during shear. Additionally, the large displacement capabilities of the LDSB allow multistage testing, which is a particularly useful feature for the testing program developed in this investigation.

Figure 3-10c illustrates the main components of the device. The concrete specimen is rigidly attached to a moveable upper assembly by a set of structural-steel bolts on each end of the slab. A screw jack transmits the action of a stepper motor to the upper assembly, which can be moved in both forward and reverse directions. The normal stress at the interface is provided by a pneumatic actuator capable of applying a force of up to 200 kN (44,000 lb). During shear, the normal and tangential forces at the interface are measured by load cells as illustrated in the figure. The vertical and horizontal displacements at the interface are monitored by a system of four linear variable displacement transducers (LVDTs), two

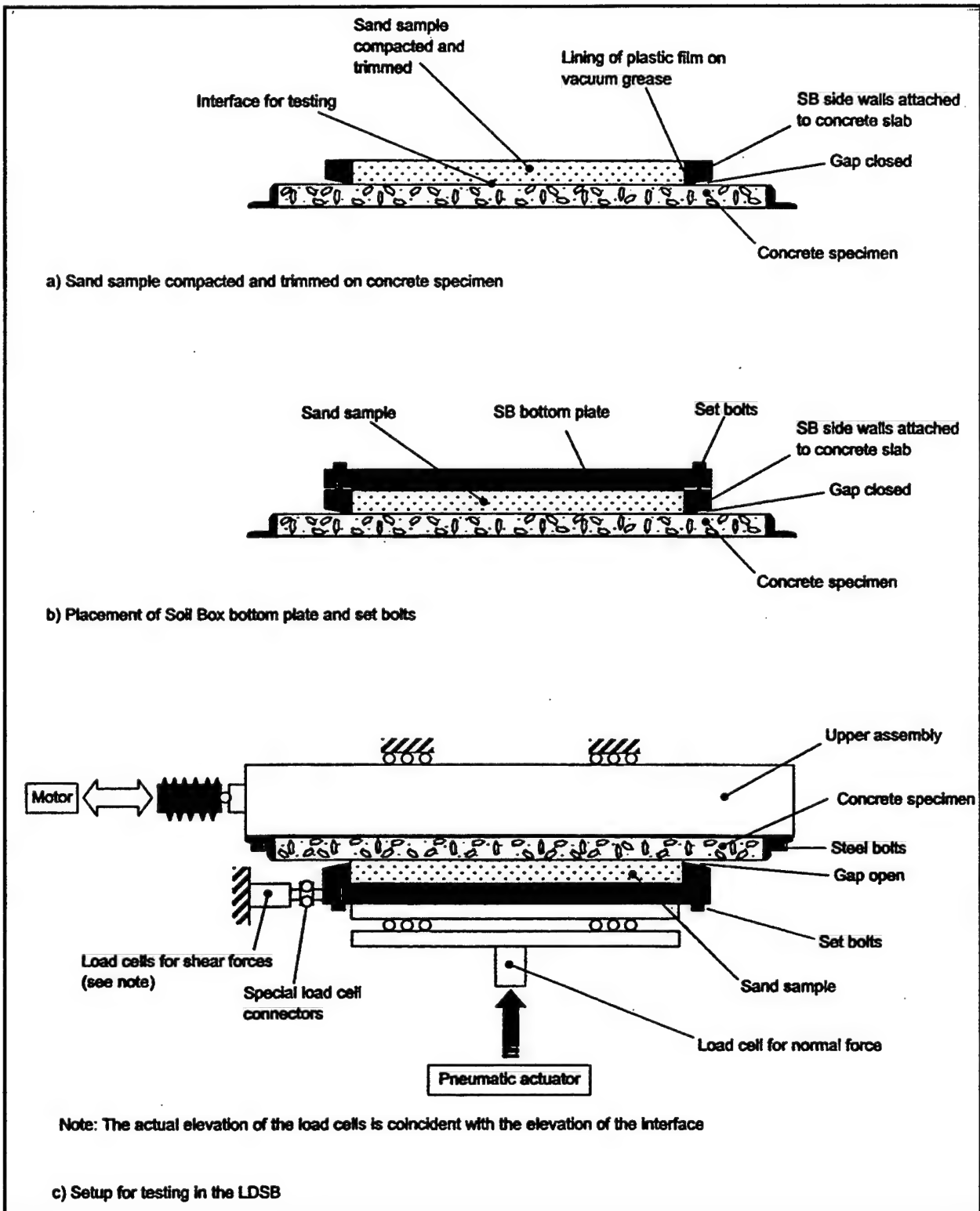


Figure 3-10. Preparation of sand-to-concrete interface and setup for testing

in each direction, located on both sides of the sample and capable of resolving displacements as small as 0.0025 mm (0.0001 in.).

A data acquisition system, connected to a personal computer, constantly monitors and records the readings from the load cells and transducers. The data acquisition program, developed specially for this investigation, converts the readings to units of force or displacement using appropriate calibration factors. Testing features, such as repeated unload-reload cycles between two predefined stress levels, can be programmed or controlled manually.

3.3.4 Test setup

Once the sand-concrete sample is placed in the LDSB, it is lifted by the pneumatic actuator into its final position, and the concrete slab is bolted to the upper assembly. The normal pressure is increased until the initial pressure applied by the set bolts is equaled. At this point, the set bolts become loose and can be turned by hand. The sidewalls are released from the mounting brackets and lowered by turning the set bolts to generate a gap between the sidewalls and the concrete surface. The sidewalls slide gently into position due to their lubricated inner lining. The gap is approximately 3.2 mm (0.125 in.) wide as shown in Figure 3-10c.

During the entire setup operation, the data acquisition system registers vertical and horizontal displacements and loads. These data are checked to prevent any undesired interface displacement or stresses from occurring. After the normal pressure is increased to its final value, the soil box is connected to the load cells by special load cell connectors. These connectors allow lateral movement of the soil box, while restraining longitudinal displacement during shear in the forward or reverse direction. The sample is then ready for testing.

3.3.5 Data reduction

The load and displacement data recorded during the interface tests are processed using a data reduction program developed for the LDSB. The program creates a series of files containing such reduced data as shear stress versus displacement and vertical versus horizontal displacement.

These output files are copied onto a spreadsheet for examination and further manipulation. For clarity of presentation in certain types of tests, a transformation of the coordinate system is carried out as will be explained in Chapter 4.

3.4 Testing Program

3.4.1 Types of interface testing performed

The interface tests performed for this phase of the investigation are summarized in Table 3-5, and illustrated in Figure 3-11. They can be grouped as initial loading tests, staged shear tests, shear reversal tests, and unload-reload tests.

| Table 3-5 Summary of Density Sand-to-Concrete Interface Tests | | | | | |
|--|----------------------|--------------------|--------------------------|---------------|---|
| Type of Test | Sample Number | Test Number | Normal Stress kPa | Figure | Observations |
| Initial loading (virgin shear) | S101 | T101_2 | 15 | 3-12 and 3-13 | — |
| | S102 | T102_5 | 33 | | |
| | S103 | T103_15 | 102 | | |
| | S104 | T104_40 | 274 | | |
| Staged shear | S101 | T101_5 | 15 to 33 | 3-14 | Normal pressure increment applied on residual condition |
| | | T101_15 | 33 to 102 | | |
| | | T101_40 | 102 to 274 | | |
| | S102 | T102_15 | 33 to 102 | 3-15 | Normal pressure increment applied on initial loading |
| | | T102_40 | 102 to 274 | | |
| | S103 | T103_40 | 102 to 274 | 3-16 | |
| Shear reversal | S101 | T101_2 | 15 | 3-19 | Reversals applied after reaching residual condition. Two or three cycles were performed per test. |
| | | T101_5 | 33 | | |
| | | T101_15 | 102 | | |
| | | T101_40 | 274 | | |
| | S102 | T102_5 | 33 | 3-20 | |
| | | T102_15 | 102 | | |
| | | T102_40 | 274 | | |
| | S103 | T103_15 | 102 | 3-21 | |
| Unload-reload | | T103_40 | 274 | | |
| | S104 | T104_40 | 274 | 3-22 | |
| | S201 | T201_5 | 33 | 3-23 | Unload-reload applied during initial loading |
| | S202 | T202_5 | 33 | 3-25 | |
| | S203 | T203_15 | 102 | 3-24 | |

The initial, or virgin, loading shear tests were performed on the newly prepared interface at different normal pressures. In all initial loading tests, shearing continued until the residual strength was mobilized, as illustrated in Figure 3-11a.

The staged shear tests were performed by increasing the normal pressure during shear. The tests modeled conditions in which the normal pressure increment occurs before mobilization of the peak strength, or after development of the residual condition as in Figure 3-11b.

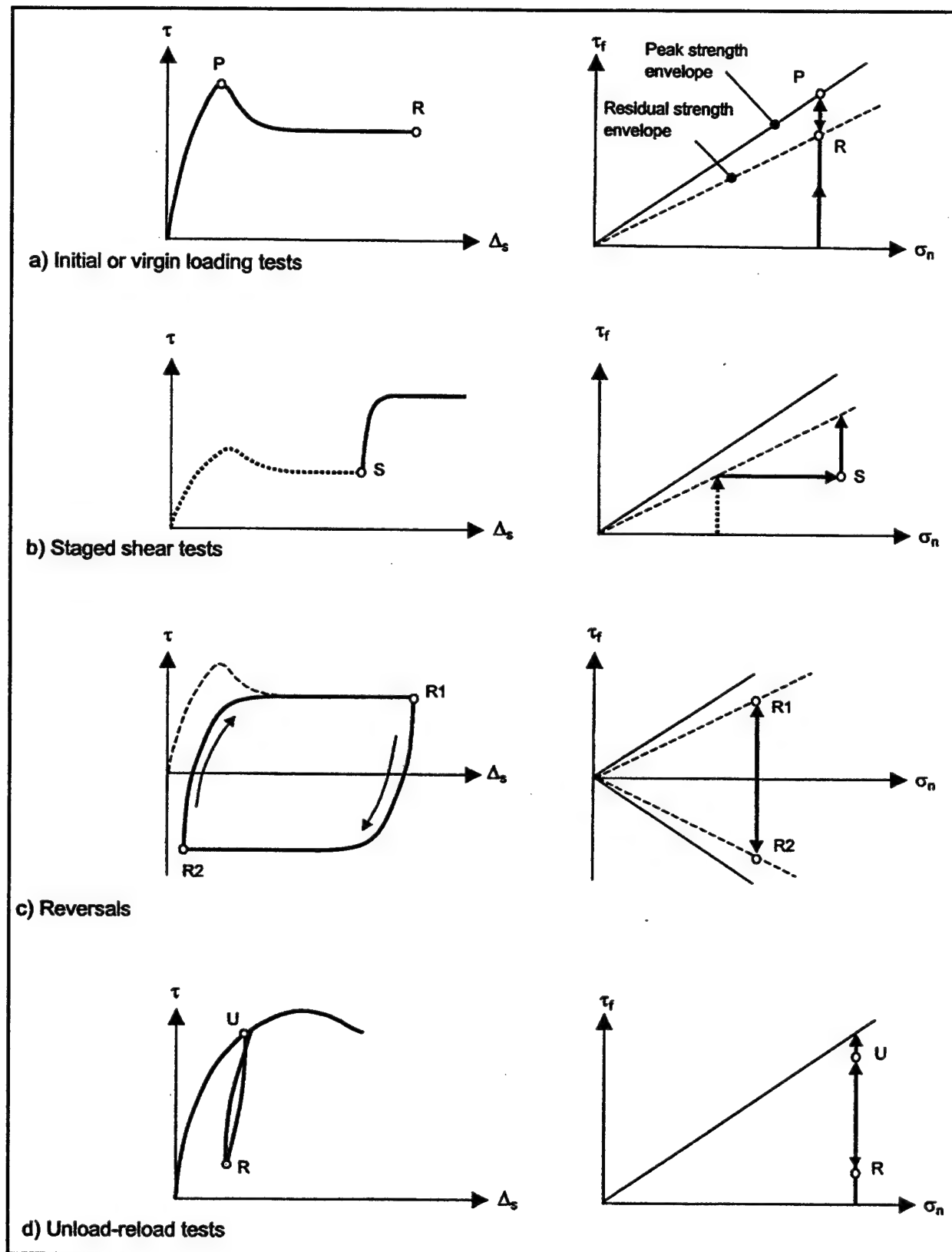


Figure 3-11. Types of shear tests performed on the Density Sand-to concrete interface

The shear reversal tests were usually performed on the interface after completing the tests mentioned previously. Upon mobilization of residual strength, the shear direction was reversed until the residual strength in the opposite direction was attained. This process was repeated until a cycle of shear reversals was completed as illustrated in Figure 3-11c. These tests also allowed the verification of the residual strength values obtained from the virgin shear tests.

Finally, in the unload-reload tests, successive reversals in the shear direction were applied during initial loading of the interface between two predefined stress levels as illustrated in Figure 3-11d.

3.4.2 Testing parameters

All the tests were performed on the interface between the Density Sand and the concrete specimen, as described in previous sections of this chapter. The sand was densified against the concrete specimen by vibration to an average relative density of 75%. All the tests were performed at a displacement rate of 1 mm/min (0.04 in./min), under normal pressures ranging from 15 to 274 kPa (2 to 40 psi). This range of normal stresses is representative of field conditions in most lock walls.

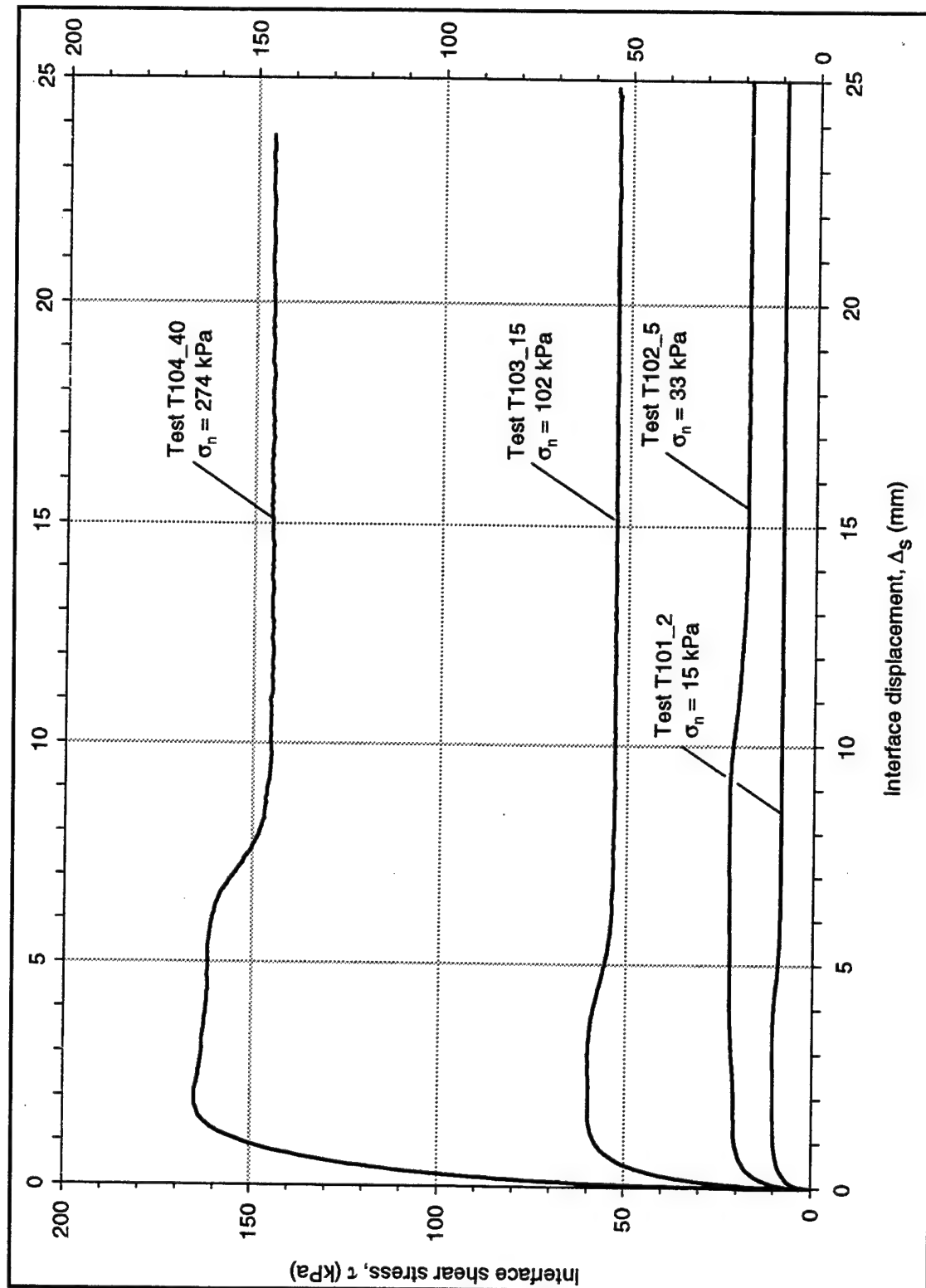
A set of preliminary tests was performed to study the influence of inundation of the interface on the test results. The results showed that inundation does not induce any significant effect on the response of the Density Sand-to-concrete interface. In average, the strength in inundated tests was 3.5 kPa higher than that in dry tests at normal stresses ranging from 100 to 270 kPa. Normal stresses induced by water surface tension between the sand and the concrete may have been responsible for this phenomenon. All subsequent tests were performed in a dry condition.

3.5 Results of Interface Tests

The results of the interface tests performed are presented in Figures 3-12 through 3-25, and will be described in the following sections. The scales used for the plots in the figures are convenient to illustrate the general aspects of the tests, and differ from one group of tests to another. In Chapter 4 the test results are shown in greater detail for the evaluation of the proposed model.

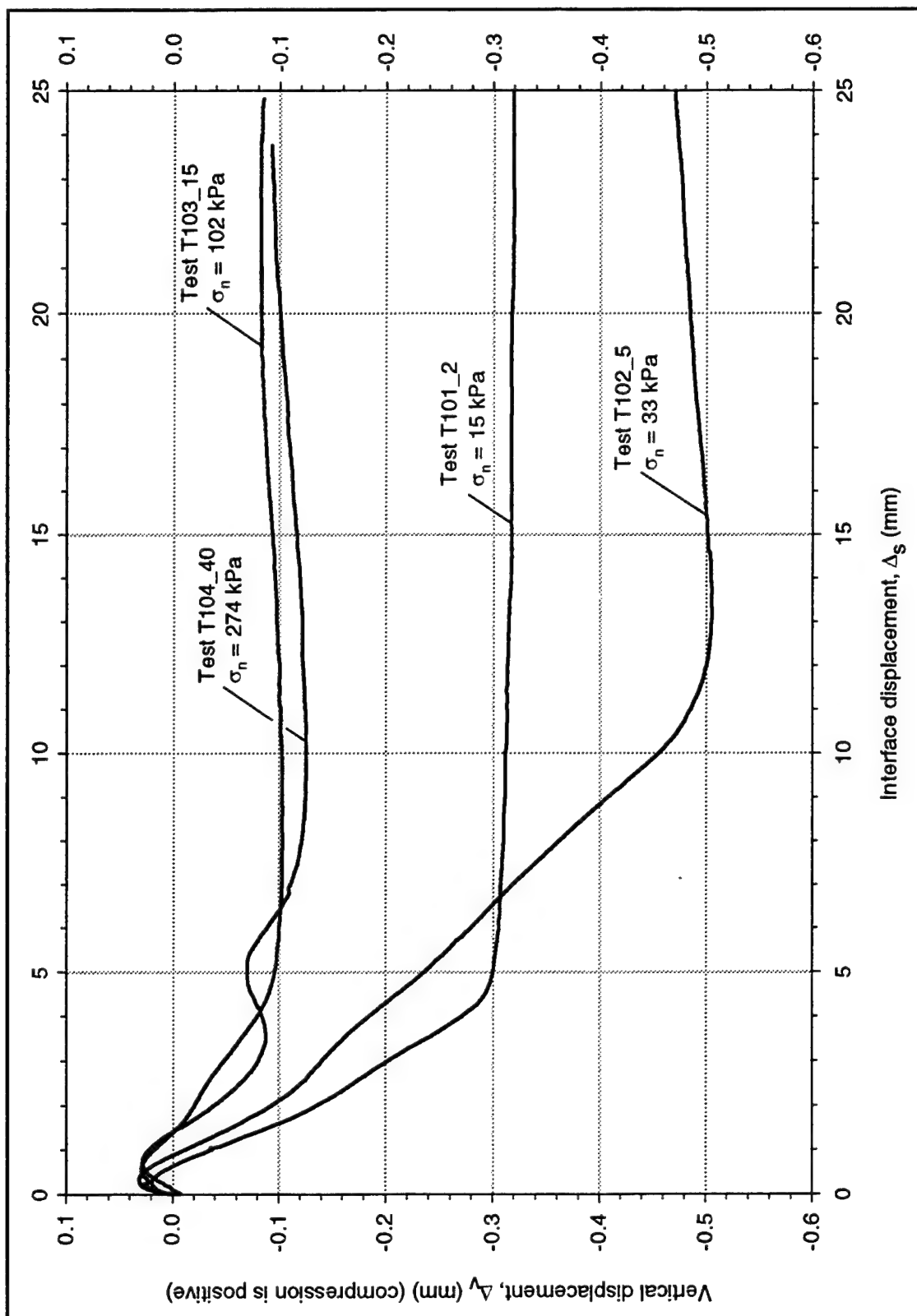
3.5.1 Initial loading tests

A group of four initial shear loading tests were performed on the Density Sand-to-concrete interface. The shear stress versus displacement data are presented in Figure 3-12a. Figure 3-12b shows the vertical versus horizontal displacement data for each of these tests. The shear reversals and subsequent staged



a. Shear stress vs. interface displacement data

63 Figure 3-12. Results of initial loading tests on Density Sand-to-concrete Interface (continued)



b. Vertical vs. horizontal interface displacement data

Figure 3-12. (Concluded)

shear tests, performed on each of these samples after initial loading, are omitted for the sake of clarity and will be discussed in the following sections.

It can be observed that the peak shear strength was mobilized at small displacements of 0.5 to 2 mm. After mobilization of the initial peak strength, the shear stresses remained practically constant before displacement softening took place. This plateau of relatively constant shear stress may exist up to displacements as large as 9 mm as evidenced by Test T102_5.

The vertical versus horizontal deformation data in Figure 3-12b reveal that extension occurred in the normal direction during shear. Based on optical observations of the sand grains during interface shear, Uesugi, Kishida, and Tsubakihara (1988 and 1989), Uesugi, Kishida, and Uchikawa (1990), and Hryciw and Irsyam (1993) indicate that this dilation is produced mostly by normal deformations of a thin shear band developed in the soil adjacent to the concrete surface.

The residual strength was reached at a displacement of 5 to 15 mm. After mobilization of the residual shear strength, no significant normal displacements were detected. It must be noted that the shear stress versus displacement plots reveal that interface displacements of less than 15 mm may not be enough to define the value of the residual strength of this interface.

The peak and residual strength envelopes are presented in Figure 3-13. Some additional data points for the residual strength, corresponding to subsequent reversal cycles, were also included. Both peak and residual strength envelopes were linear for the range of normal stresses considered. The following strength parameters were obtained for initial loading of the Density Sand-to-concrete interface: peak interface friction angle, $\delta_p = 31$ degrees and residual interface friction angle, $\delta_r = 28$ degrees.

The cohesion intercept was zero for both peak and residual strength envelopes. The peak interface friction angle corresponded to approximately 72% of the peak internal friction angle of the Density Sand obtained from the CD triaxial tests. The residual interface friction angle corresponded to 81% of the internal friction angle of the sand measured at 15% strain. It must be noted that the average relative density obtained in the triaxial samples was 85%, which is higher than that obtained in the samples for interface testing. Further triaxial testing at lower relative densities, which will be performed in the next phase of this investigation, will allow a more precise determination of the interface-to-soil friction angle ratio.

3.5.2 Staged shear tests

Two groups of staged shear tests were performed on the Density Sand-to-concrete interface (Table 3-5). Figures 3-14 to 3-16 show the results of tests in which the normal stress increment was applied in steps, during shear in the residual condition. These tests were carried out after the initial loading of the

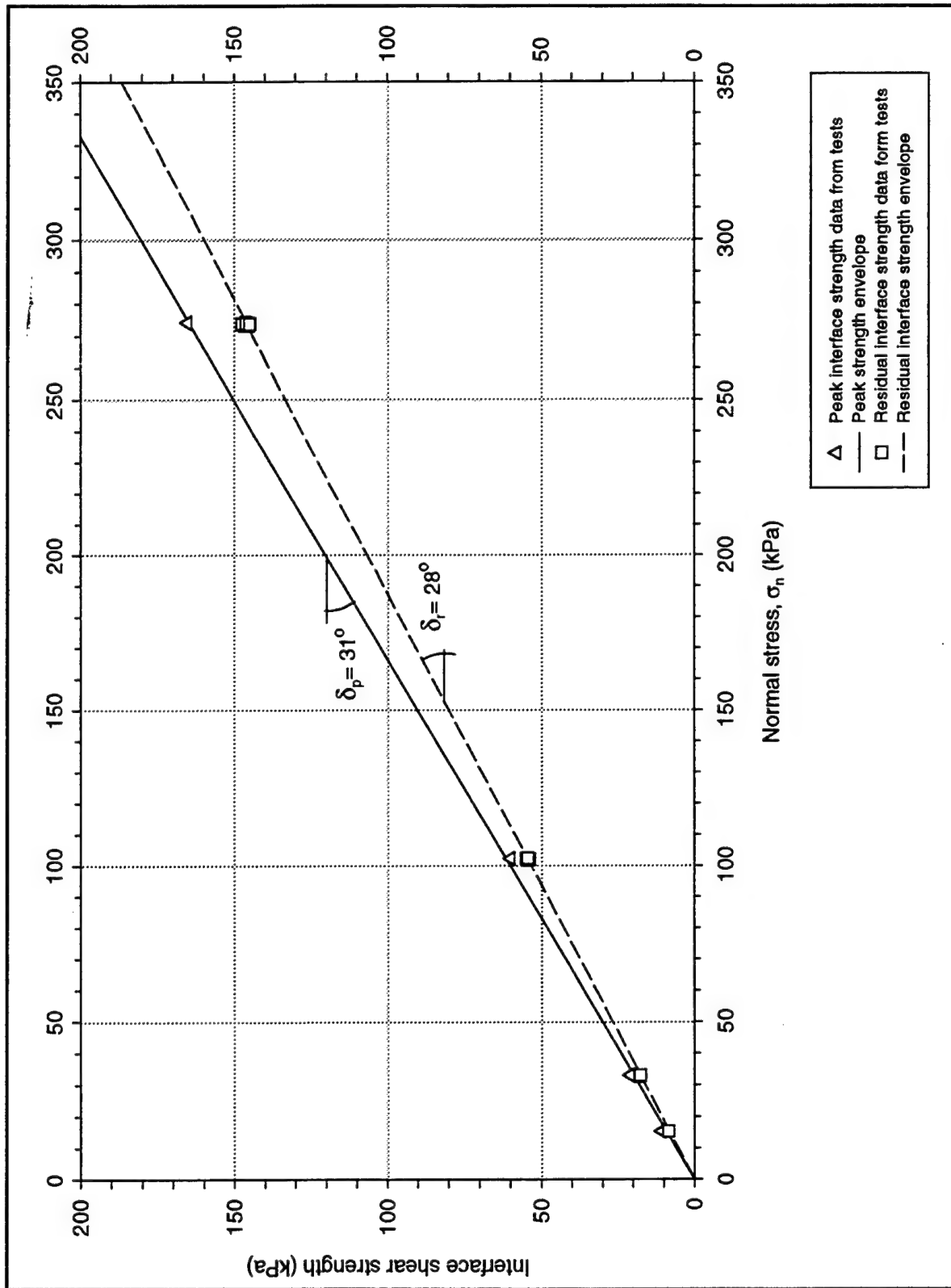


Figure 3-13. Peak and residual shear strength envelopes for initial loading on Density Sand-to-concrete interface

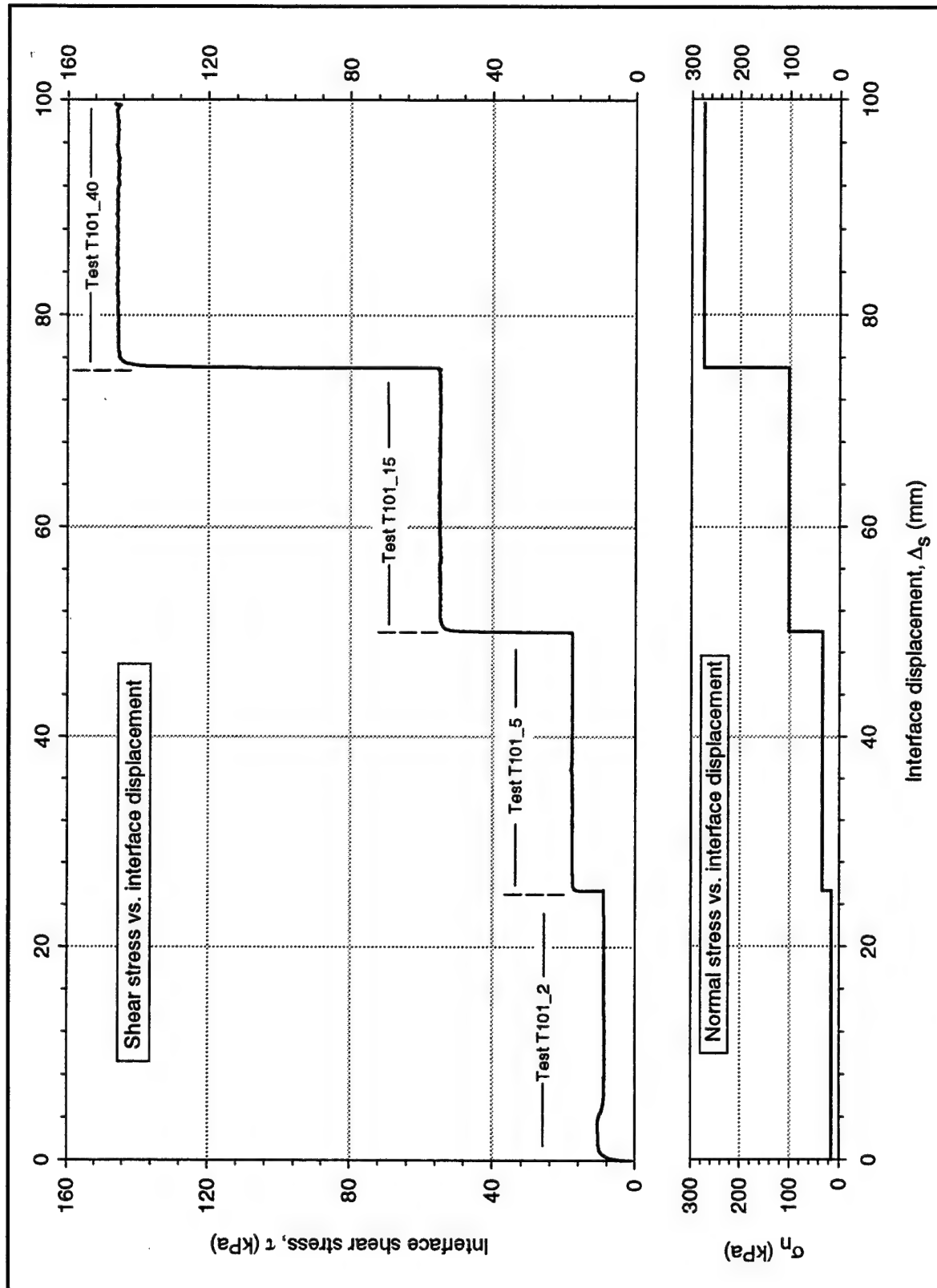


Figure 3-14. Staged tests on Density Sand-to-concrete Interface, sample S101 (data on shear reversals have been omitted)

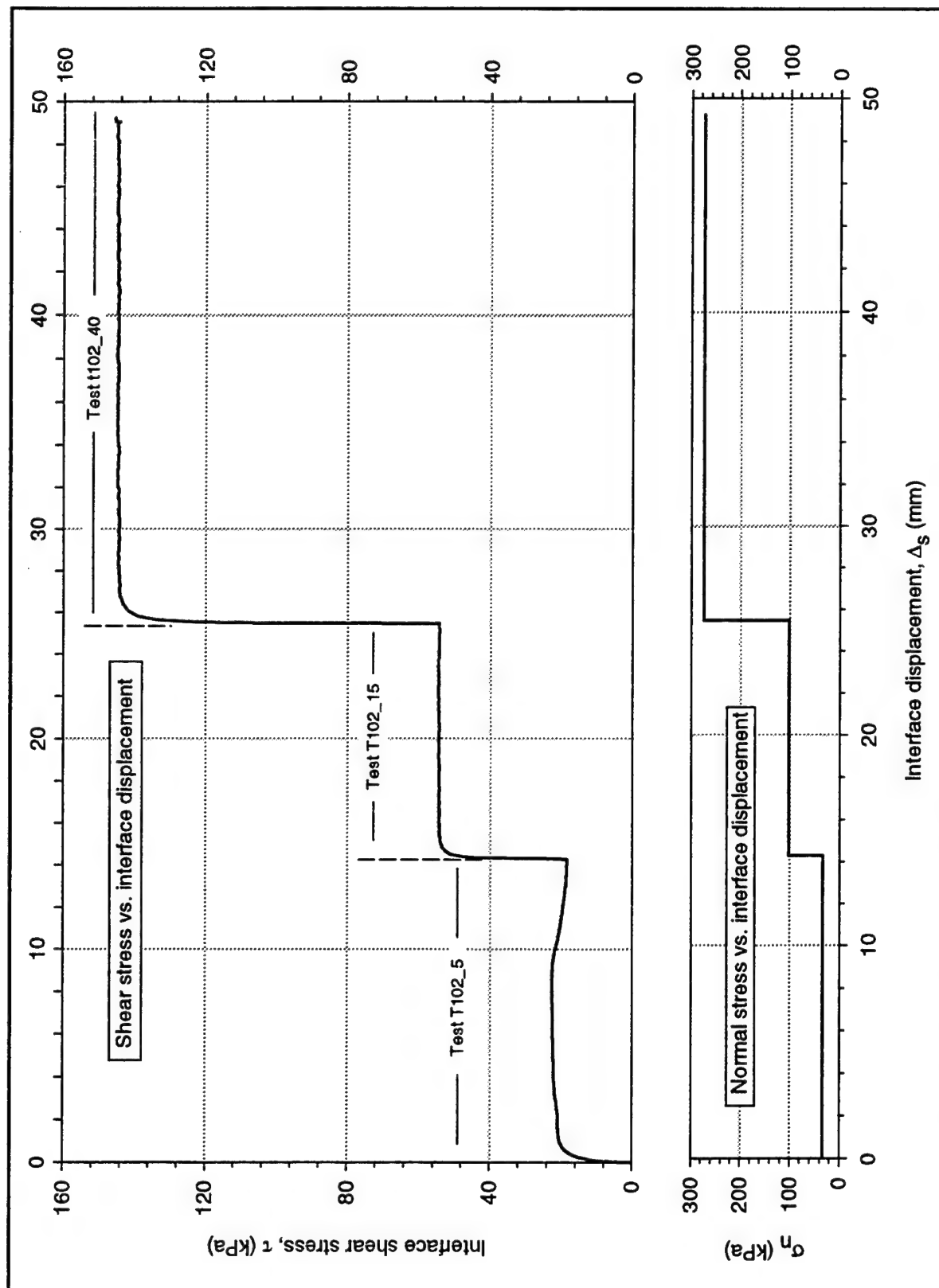


Figure 3-15. Staged tests on Density Sand-to-concrete interface, sample S102 (data on shear reversals have been omitted)

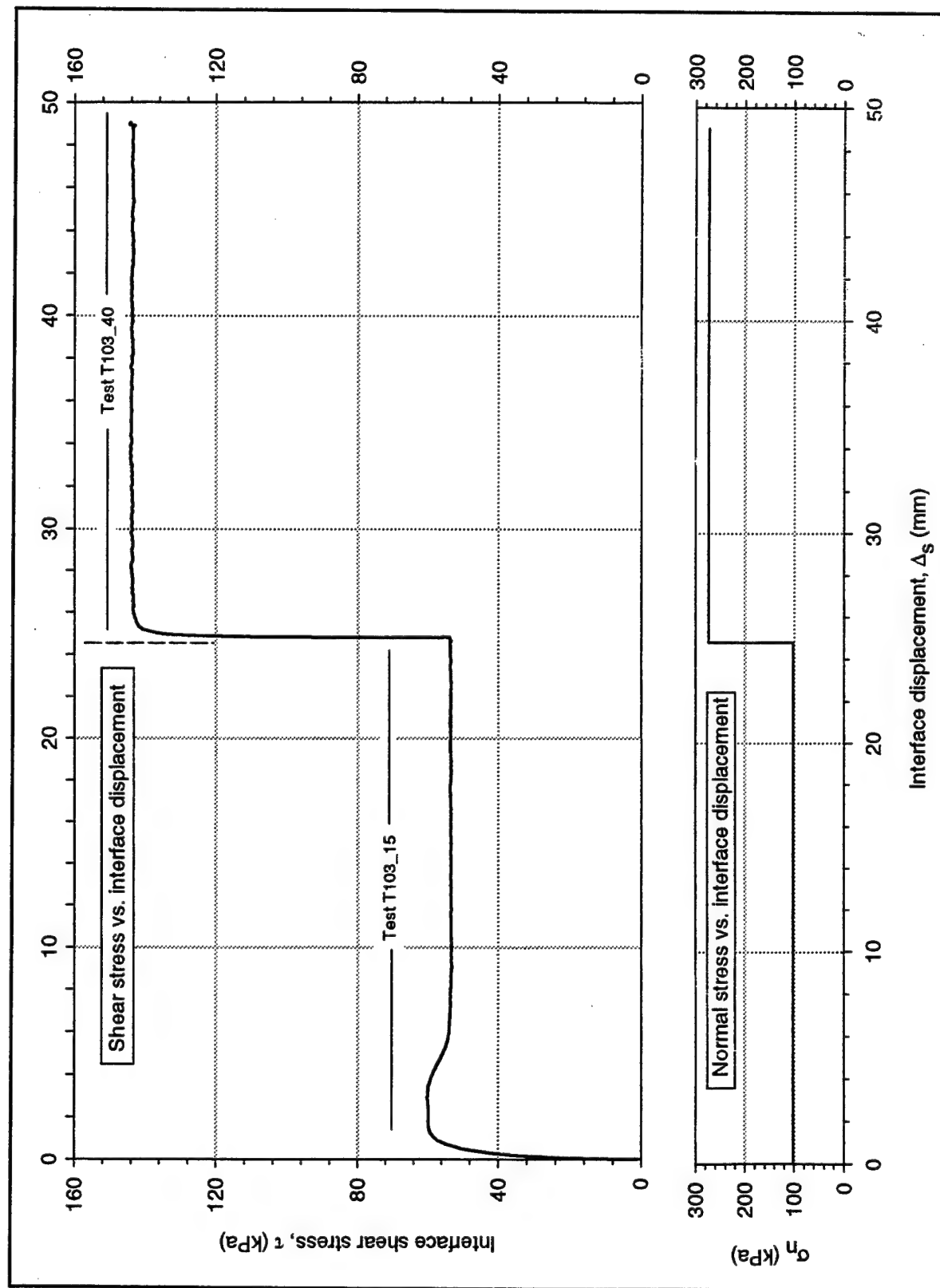


Figure 3-16. Staged tests on Density Sand-to-concrete Interface, sample S103 (data on shear reversals have been omitted)

interface, which was discussed in the previous section. The normal pressure steps followed the sequence: 15 to 33 kPa, 33 to 102 kPa, and 102 to 274 kPa. It can be observed that for the series of tests on sample S101, which was started at a normal pressure of 15 kPa, a total of three normal pressure steps were applied. For the test series on sample S102, two steps were applied, and for S103, only one step was applied. In most of the tests shown, some reversal cycles were performed, and these have been omitted for the sake of clarity.

It can be seen in Figures 3-14 to 3-16 that a peak strength greater than the residual strength occurs only in the initial loading stage. For subsequent stages, the shear stress increases to the residual value and then remains constant until the next normal pressure increment.

Figures 3-17 and 3-18 show the results of a second group of tests in which the normal stress was increased before mobilization of the peak strength. For clarity of presentation, these plots are presented with a magnified interface displacement scale. The corresponding increments of normal stress are also shown in the figures. All the samples were sheared, under constant normal stress and at a displacement rate of 1 mm/min (0.04 in./min), to a shear stress level of 0.6. The relative motion of the interface was then arrested, and the normal pressure increment was applied. Shearing was resumed after the normal pressure increment was completed.

3.5.3 Shear reversals

Shear reversal cycles were applied during or at the end of the interface tests described in the previous sections. For simplicity of presentation, only the results of the shear reversals performed after the initial loading tests have been reproduced in Figures 3-19 to 3-22. In most tests shearing was continued in the reverse direction to the initial position of the interface. The direction of shear was then reversed again, until a full reversal cycle was completed.

It can be observed in Figures 3-19 to 3-22 that, upon reversal, the residual condition was reached at relative displacements of 2.5 to 5 mm measured from the reversal point. The residual strength values and the shear stress-displacement response of the interface were very similar or identical in both directions of shear.

3.5.4 Unload-reload tests

A group of three interface tests was performed that included one unload-reload cycle between two predetermined stress levels during initial loading. As in the previous tests, the Density Sand samples were compacted to an average relative density of 75%. The interface was sheared, under constant normal stress, at a displacement rate of 1 mm/min (0.04 in./min).

Figure 3-23 shows the shear stress versus displacement data from one such test, which was performed under a normal stress of 33 kPa. Figure 3-24 shows

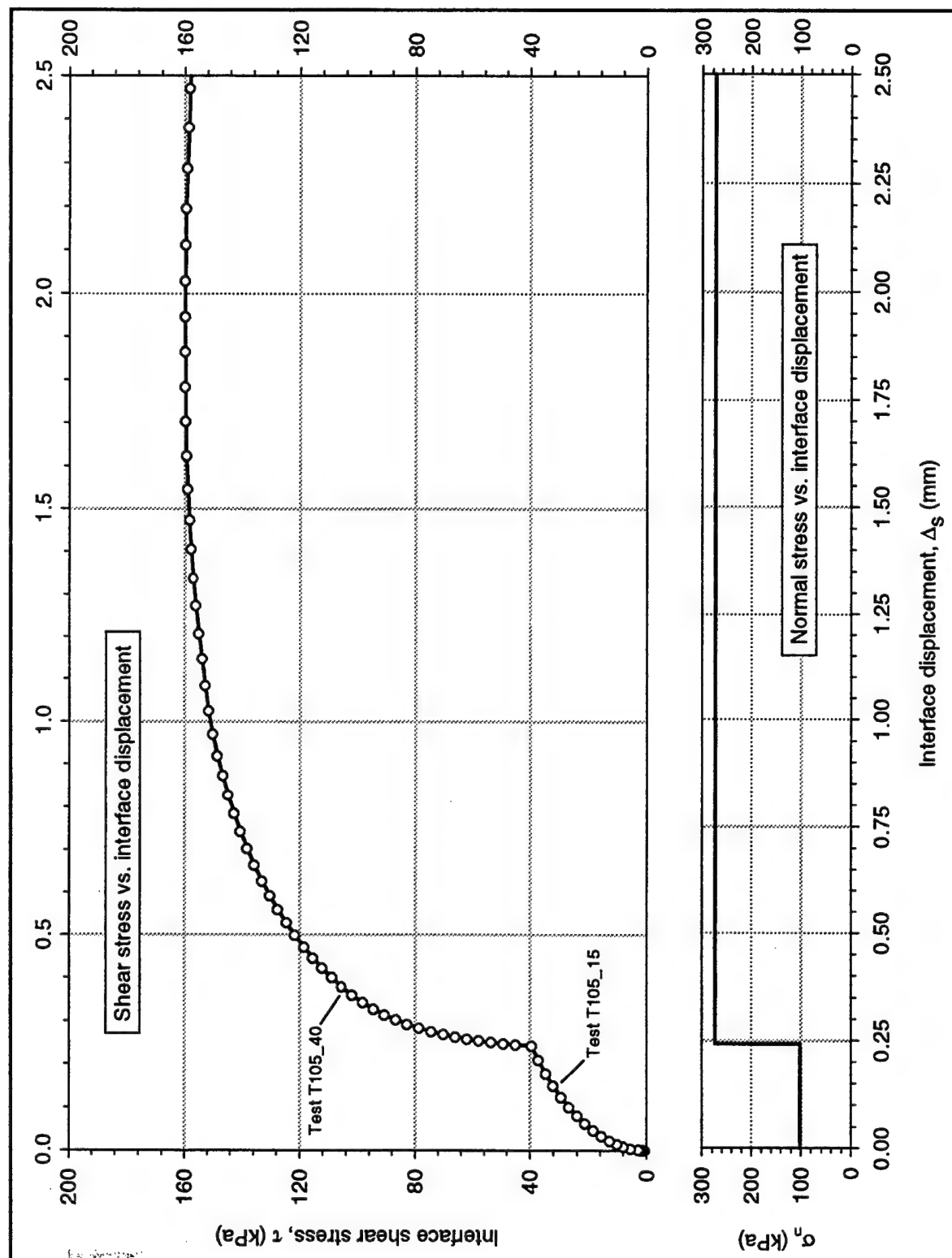


Figure 3-17. Staged test on Density Sand-to-concrete interface, sample S105 (Data on shear reversals have been omitted)

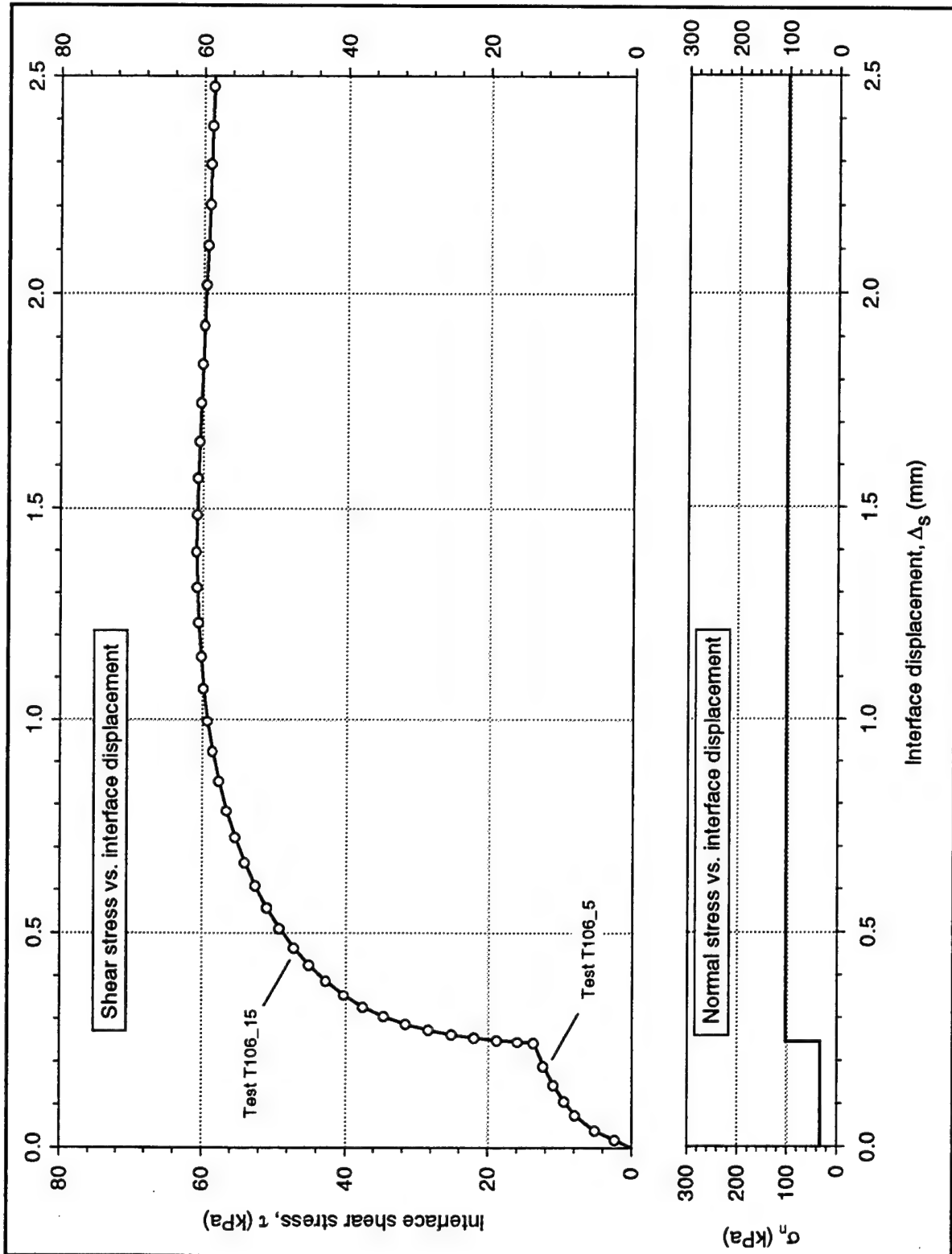


Figure 3-18. Staged test on Density Sand-to-concrete Interface, sample S106 (Data on shear reversals have been omitted)

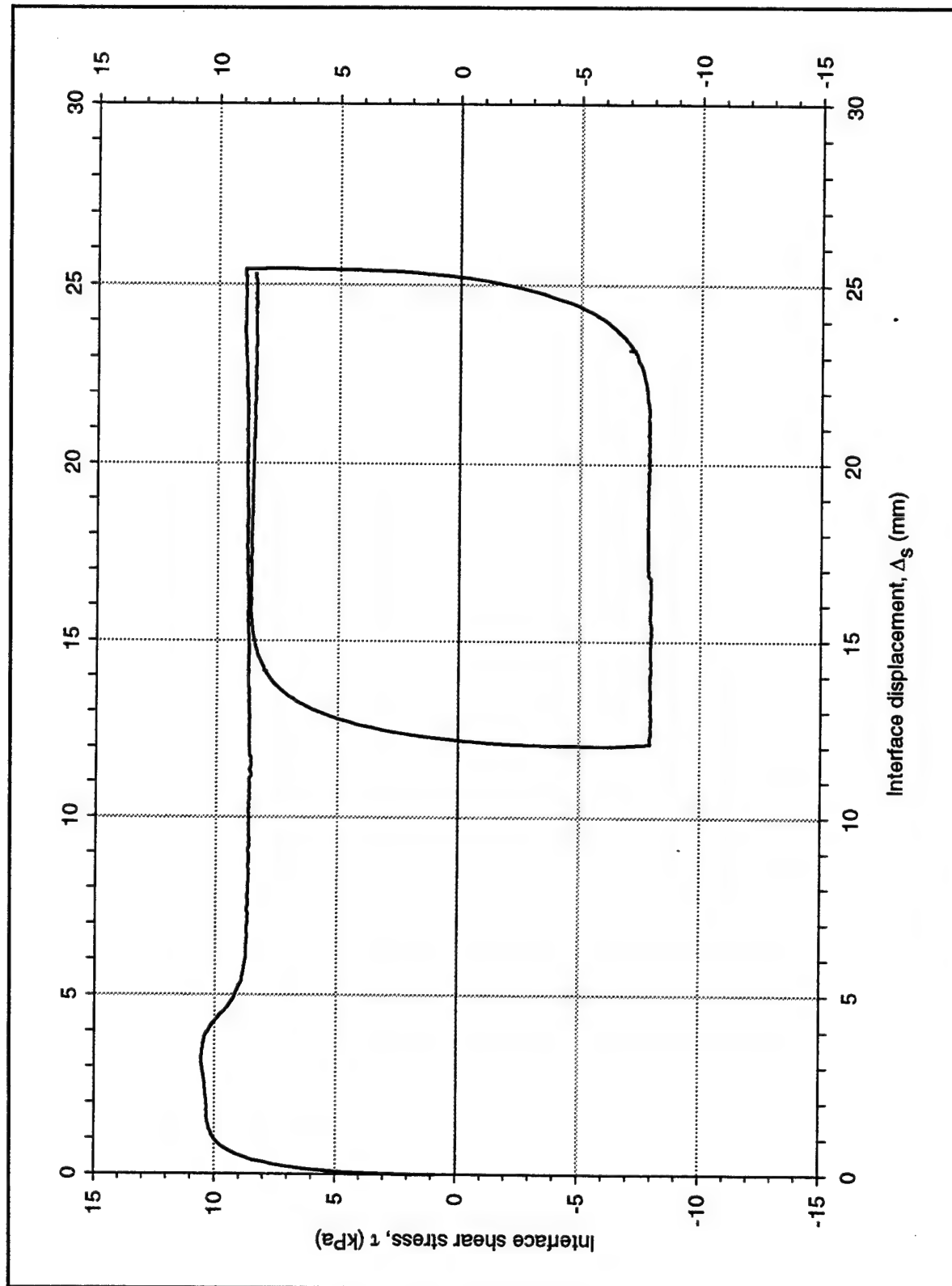


Figure 3-19. Cycle of shear reversals on Density Sand-to-concrete interface, $\sigma_n = 15$ kPa, sample S101

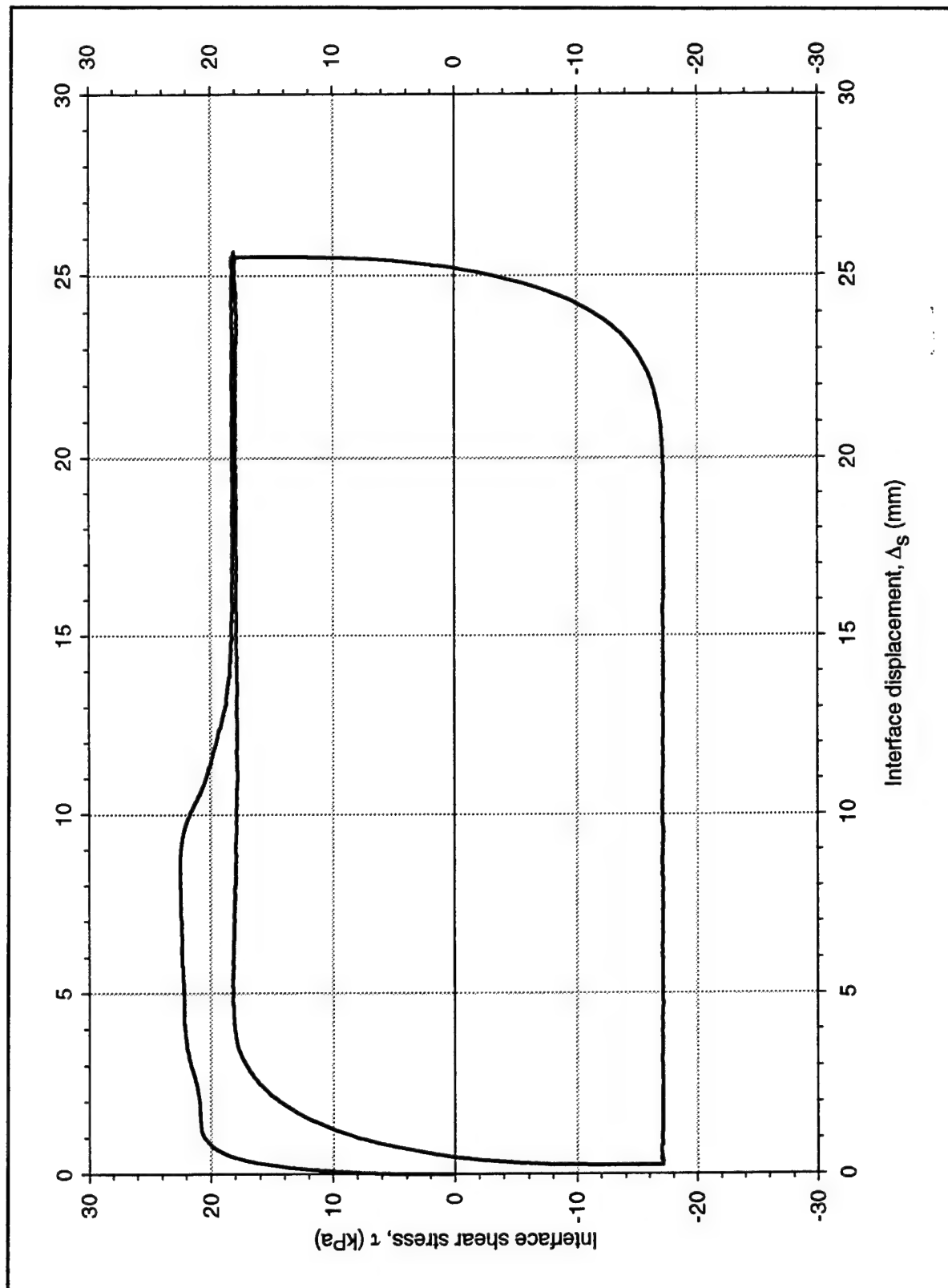


Figure 3-20. Cycle of shear reversals on Density Sand-to-concrete Interface, $\sigma_n = 33\text{kPa}$, sample S102

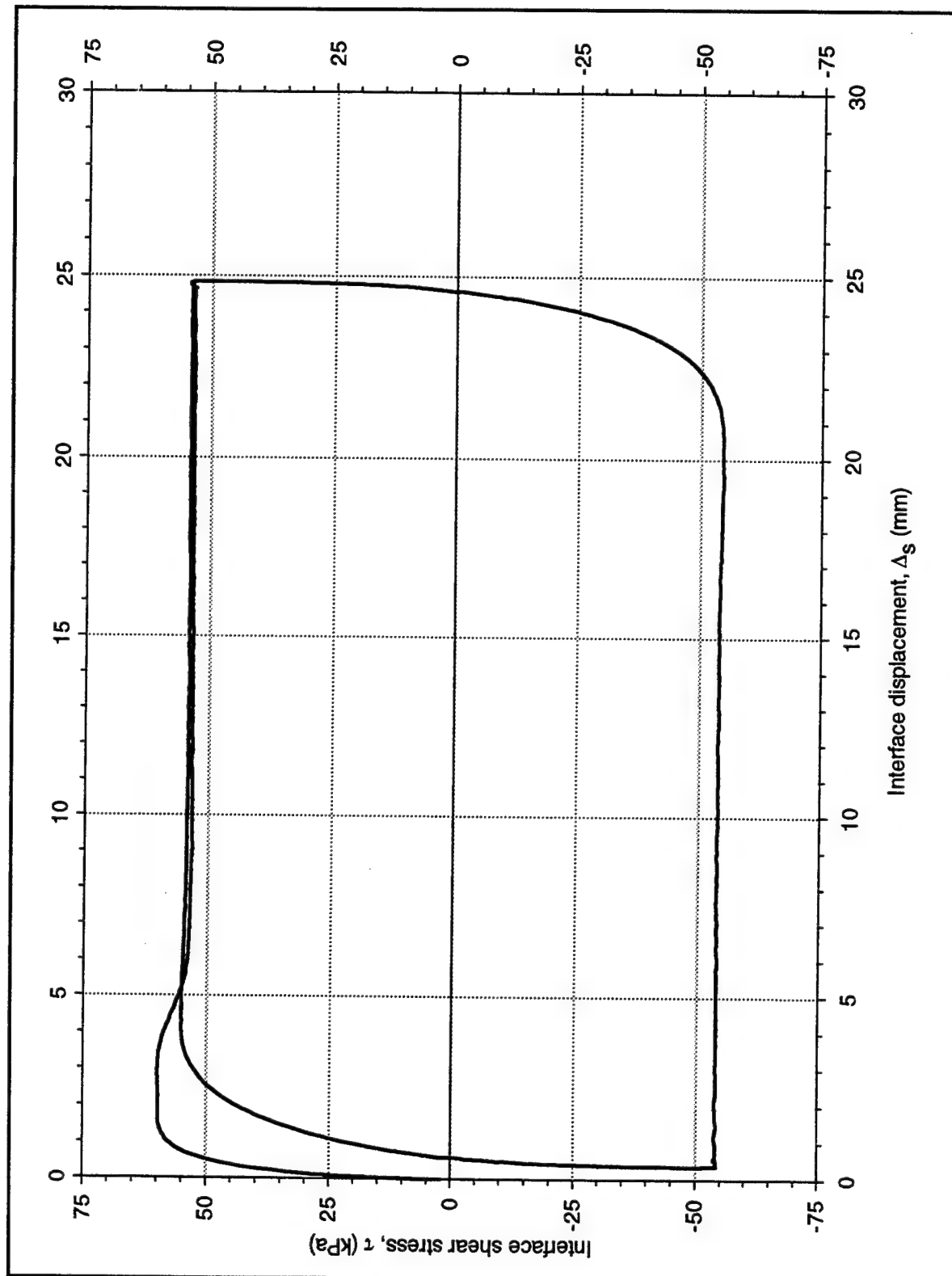


Figure 3-21. Cycle of shear reversals on Density Sand-to-concrete Interface, $\sigma_n = 102$ kPa, sample S103

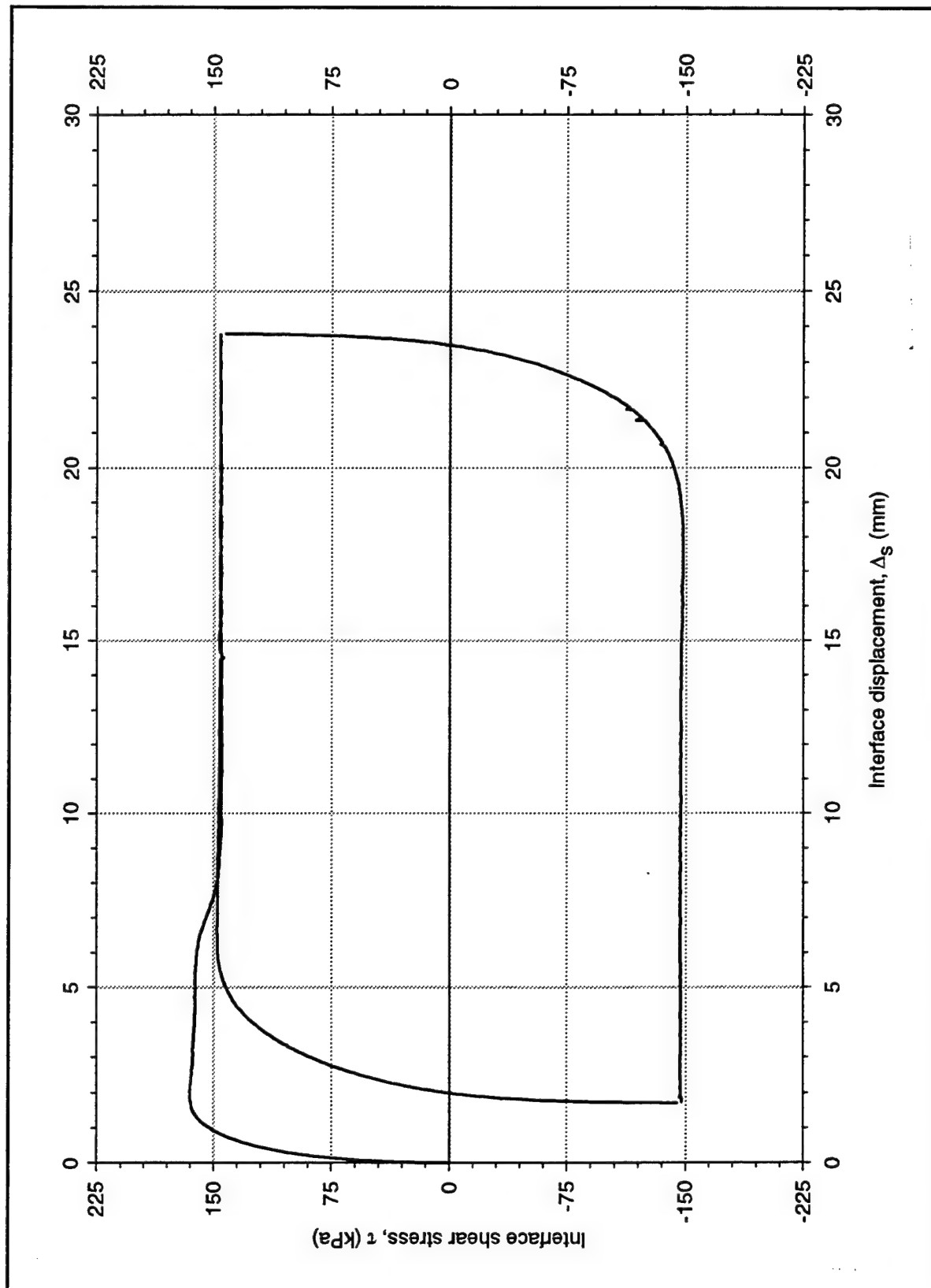


Figure 3-22. Cycle of shear reversals on Density Sand-to-concrete interface, $\sigma_n = 274$ kPa, sample S104

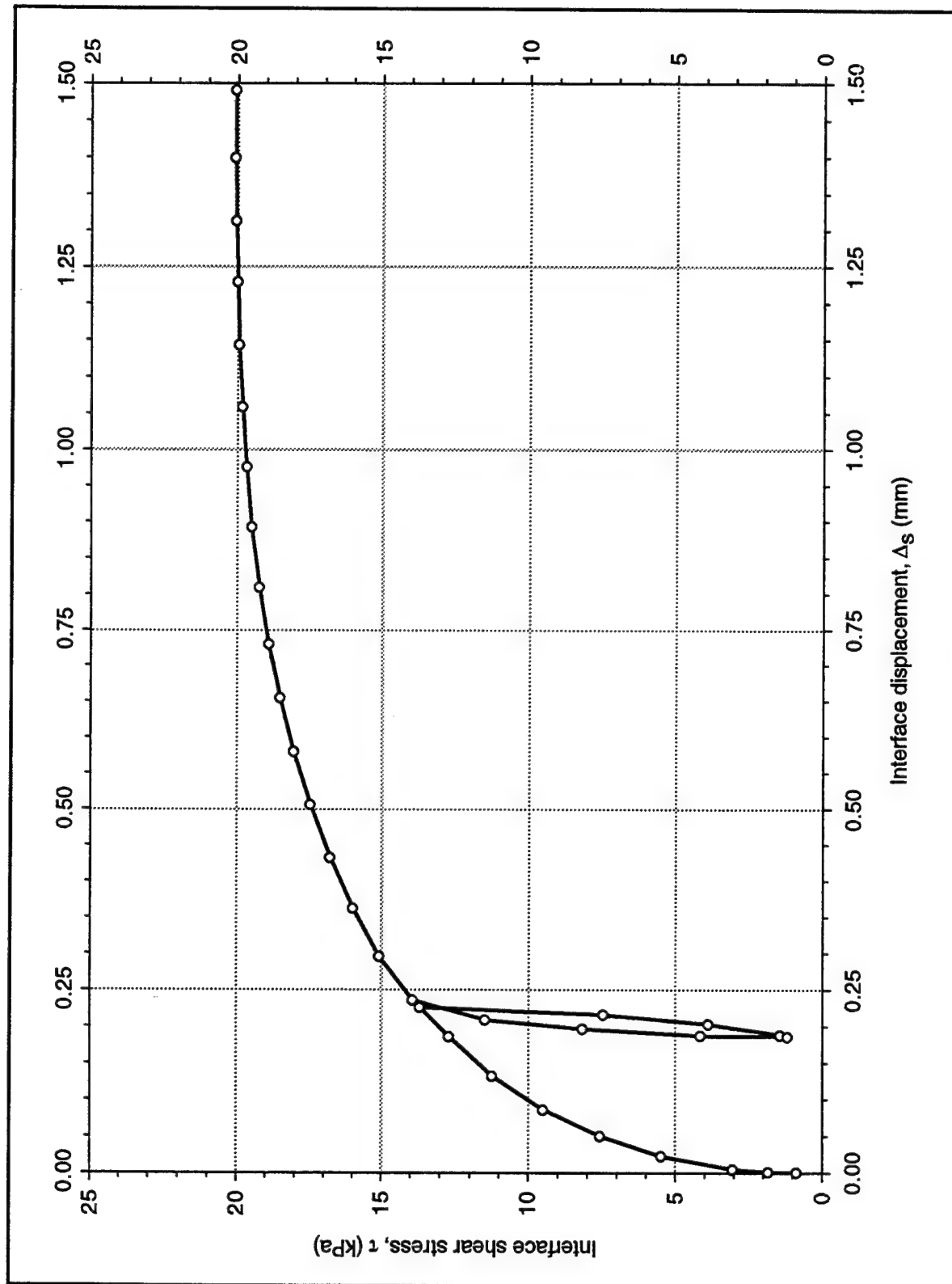


Figure 3-23. Unload-reload cycle on Dense sand-to-concrete Interface, $\sigma_n = 33$ kPa, sample S201

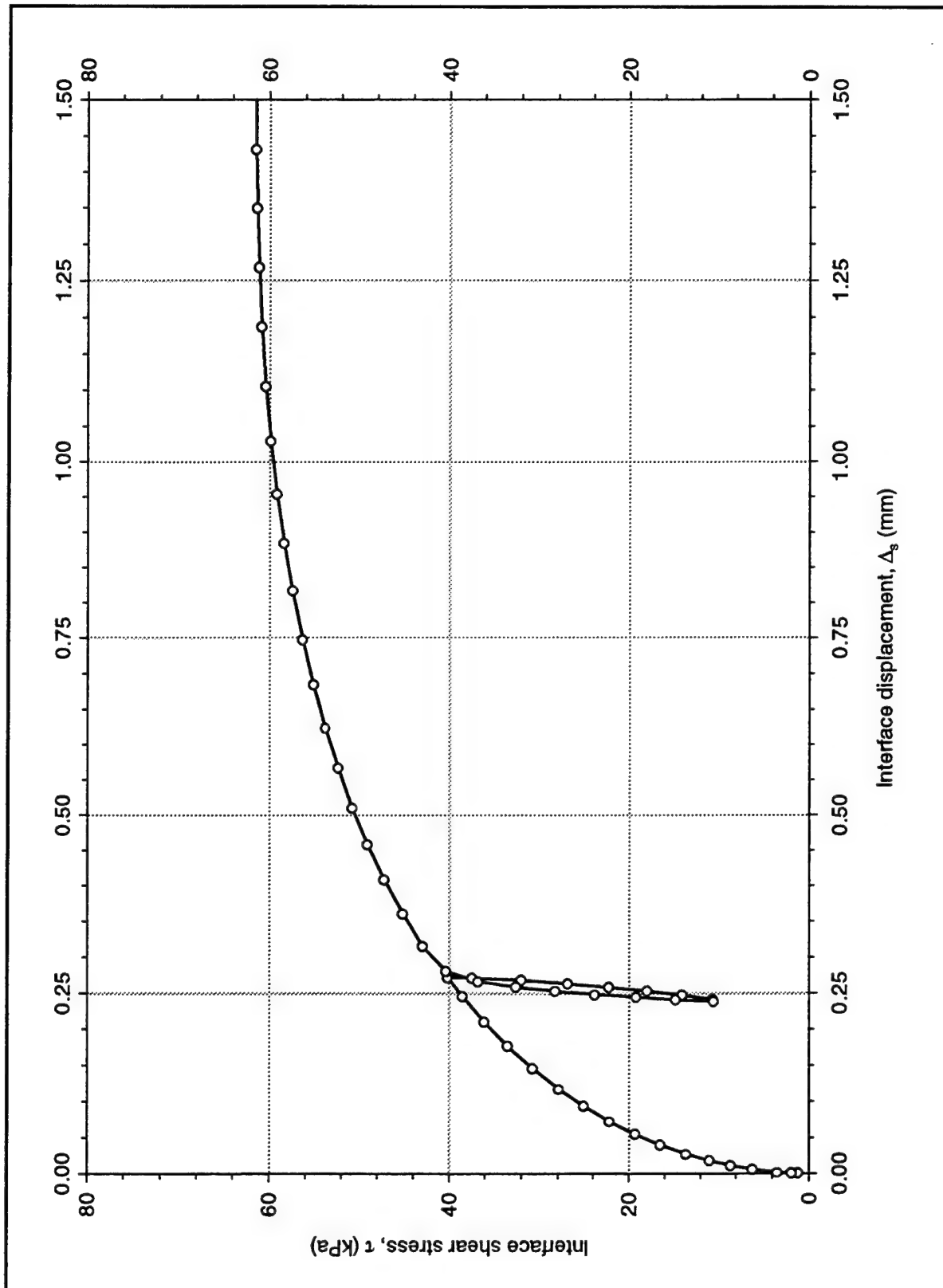


Figure 3-24. Unload-reload cycle on Density sand-to-concrete interface, $\sigma_n = 102$ kPa, sample S203

the results of a similar test performed under a normal stress of 102 kPa. In both tests the unload-reload cycles were applied between stress levels of approximately 0.7 and 0.2. For the test shown in Figure 3-25, the unloading stage was performed between stress levels of 0.7 and -0.7.

3.6 Summary

The following laboratory and field activities were performed during this phase of the investigation:

- a. Modifications to the Large Displacement Shear Box (LDSB).
- b. Design and construction of a soil box and concrete slab.
- c. Selection of the sand for interface tests.
- d. Grain size distribution, minimum/maximum density, specific gravity, and triaxial testing on the Density Sand.
- e. Field survey of existing concrete retaining walls to determine a range of representative surface textures for the concrete specimen.
- f. Development of appropriate testing procedures.
- g. Interface tests following laboratory stress paths that model field conditions in lock walls.

The LDSB was modified specifically to accommodate the soil-to-concrete interface testing for this investigation. A special aluminum soil box was designed and constructed that allows compaction of the sand sample directly onto the concrete specimen, and minimizes the disturbance of the interface during test setup operations.

A field survey of concrete walls was performed. Two representative cases were presented to convey the most common surface features of retaining walls cast against plywood. After a trial-and-error process, a concrete specimen was obtained with surface features similar to those observed in the field. The concrete specimen is contained in a frame, which was designed and constructed to act as an external reinforcement for the concrete and to minimize its deformations during interface shear.

A fine, rounded, silica sand (Density Sand) was selected for interface testing. A series of basic laboratory tests, such as minimum/maximum density and grain size analyses, were performed on the sand. Consolidated, drained, triaxial tests were also performed on the sand to determine its strength parameters.

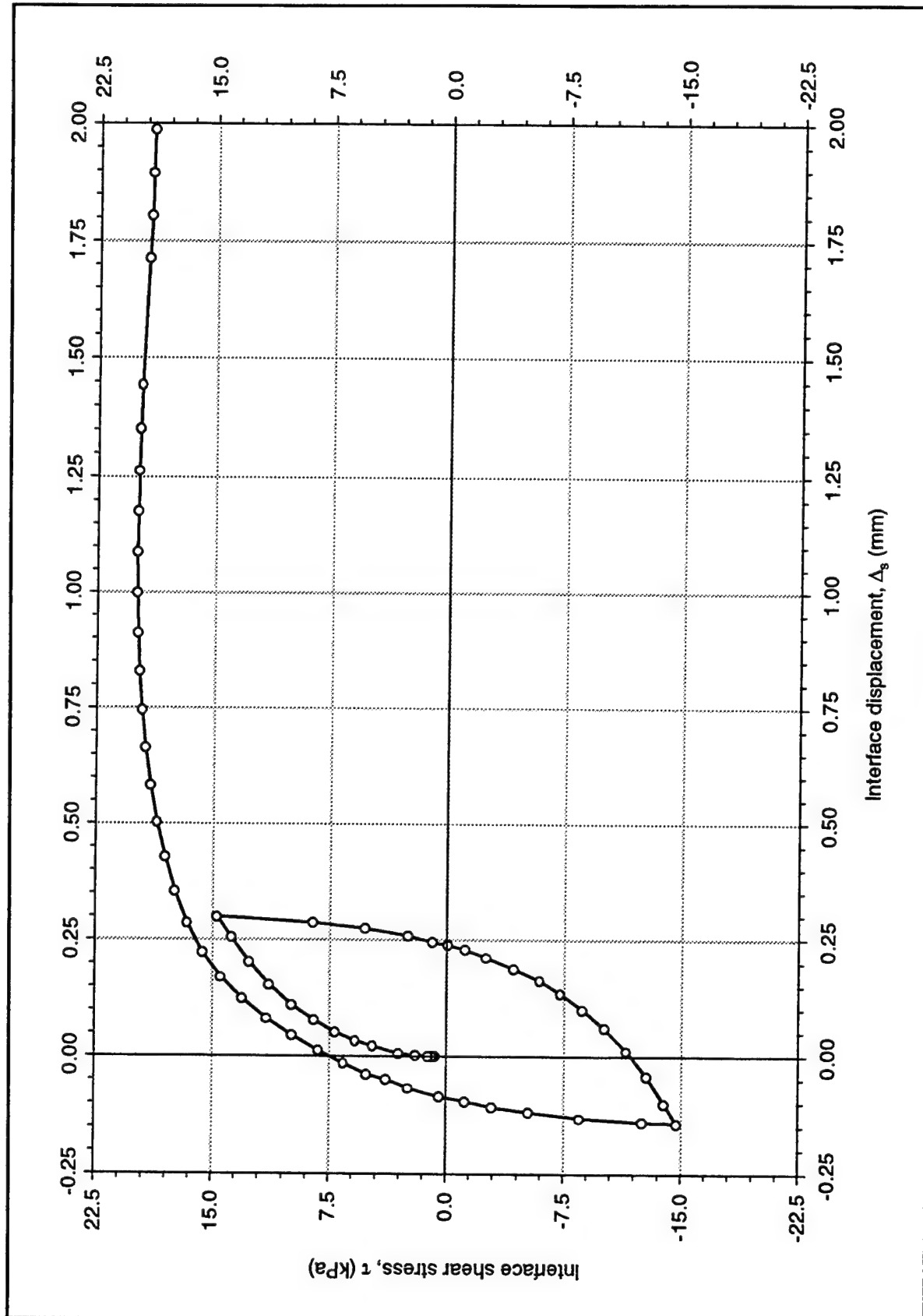


Figure 3-25. Unload-reload cycle on Density sand-to-concrete interface, $\sigma_n = 33$ kPa, sample S202

A set of hyperbolic parameter values were developed for the Density Sand, based on the results of the triaxial tests. The parameters obtained are consistent with values reported by Duncan et al. (1980) for a similar material.

An intensive interface testing program was carried out that included initial loading tests, staged shear tests, reversal tests, and unload-reload tests. The results of these tests are presented in Figures 3-12 to 3-25. All the tests were performed on the dry interface between the Density Sand and the concrete specimen interface, at a displacement rate of 1 mm/min (0.04 in./min). The Density Sand sample was compacted to a relative density of approximately 75% in all tests.

The initial loading tests yielded a peak interface friction angle of 31 degrees, approximately 72 percent of the internal peak friction angle of the sand. After mobilization of the peak strength, displacement softening of the interface occurred in all tests. The residual interface friction angle was approximately 28 degrees.

Staged shear tests were performed by increasing the normal pressure in steps during shear. The staged shear tests provide an approximate model of field stress paths in which both normal and shear stresses change simultaneously.

In the reversal tests, one or several cycles of shear were performed upon mobilization of the residual strength. Similar values of interface residual strength and shear stress-displacement responses were obtained for both directions of shear in all tests.

Several unload-reload tests were performed, where a complete loading cycle was applied between two predetermined stress levels. Both the reversal and the unload-reload tests are representative of field stress paths in which the shear stresses may be reduced, or even reversed, as a consequence of a rise of the water table behind a lock wall.

The interface test results obtained are the basis for the development of the extended hyperbolic model presented in Chapter 4. This extended model is applicable to cases beyond initial loading of the interface at constant normal stress. The extended model covers stress paths such as those applied in the interface tests and those which may occur under field conditions at lock wall interfaces.

4 Extended Hyperbolic Model

A preliminary version of a new hyperbolic model for interfaces was developed for this phase of the investigation. It is based on the Clough and Duncan (1971) hyperbolic formulation, which has been extended herein to model shear stress reversals, unload-reload cycles, and staged shear.

This preliminary version, referred to as the *extended hyperbolic model* throughout this report, was evaluated against the results of the tests performed on the Density Sand-to-concrete interface, which were described in Chapter 3. The model incorporates important aspects of interface response under stress paths such as those presented in Figures 1-3b and 1-4b; yet, it retains the simplicity of the original Clough and Duncan (1971) formulation. The model, however, is in the initial stages of its development, and it is expected that further improvements will be required.

In the first section of this chapter, a new criterion is introduced for the determination of the hyperbolic parameters. In subsequent sections, the formulation of the extended hyperbolic model is presented separately for each type of loading. The accuracy of the model is evaluated against the results of the interface tests described in Chapter 3. Finally, a discussion is presented concerning the advantages and limitations of the new model, and the improvements that may be implemented during the next phase of this research.

4.1 Hyperbolic Model for Initial Loading

The Clough and Duncan (1971) hyperbolic model for interfaces, presented in Chapter 2, was implemented for the initial shear loading of the Density Sand-to-concrete interface. It is shown that, although this hyperbolic formulation may yield overall results that are reasonable, it does not fit the test data accurately at low stress levels. This may lead to difficulties when extending the hyperbolic model to other types of loading, such as unload-reload cycles.

A new criterion for the determination of the hyperbolic parameter values was developed during this investigation. It provides a good fit of the test data at low stress levels.

4.1.1 Determination of hyperbolic parameters: Clough and Duncan (1971) procedure

The transformed plots, shown in Figure 4-1, correspond to the data from the initial loading tests, which were presented in Figure 3-12a. Following the procedure by Clough and Duncan (1971), illustrated in Figure 2-3, a straight line was drawn through the data points corresponding to 70 and 95 percent of the strength. As explained in Chapter 2, the intercept a of this straight line with the vertical axis gives the reciprocal of the initial shear stiffness K_{si} of the interface. The slope b of the straight line gives the reciprocal of the asymptotic shear stress, τ_{ult} . This procedure for the determination of K_{si} and τ_{ult} is referred to as the 70-95% criterion throughout this report. The results of this procedure are presented in the table in Figure 4-1.

The relationship between the initial shear stiffness and the normal stress is presented in Figure 4-2. The initial shear stiffness and normal stress have been normalized by the unit weight of water γ_w and the atmospheric pressure p_a , respectively. Following the procedure presented by Duncan et al. (1980), a best-fit straight line is drawn through all the points. The stiffness number, K_I in Equation 2-6, is the ordinate of this line at a pressure of one atmosphere. The slope of the line gives the stiffness exponent n .

The failure ratio R_f can be calculated for each normal stress from Equation 2-5 if the values of τ_{ult} and τ_f are known. The asymptotic shear stress τ_{ult} is obtained from the transformed plots, as described previously. The shear strength τ_f is calculated from Equation 2-7 using the peak interface friction angle δ_p obtained from the tests (Figure 3-13). The failure ratio R_f , adopted for the model, corresponds to the average of the R_f values obtained for each normal stress.

The values of the hyperbolic parameters, determined according to the 70-95% criterion, are presented in Table 4-1. Table 4-2 summarizes the approximate ranges of values reported by Peterson et al. (1976) for the hyperbolic parameters of two sand-to-concrete interfaces. The surface texture of the concrete specimen in the present investigation is intermediate between the two concrete textures in Table 4-2.

Table 4-1
Hyperbolic Parameters for Initial Loading on Density Sand-to-Concrete Interface ($D_R \sim 75\%$)

| Parameter | 70-95% Criterion | SID Criterion ¹ |
|--|------------------|----------------------------|
| K_I | 35,510 | 63,230 |
| n | 0.71 | 0.584 |
| R_f | 0.846 | 0.93 |
| δ_p | 31.0° | 31.0° |
| ¹ Small initial displacement (Section 4.1.2). | | |

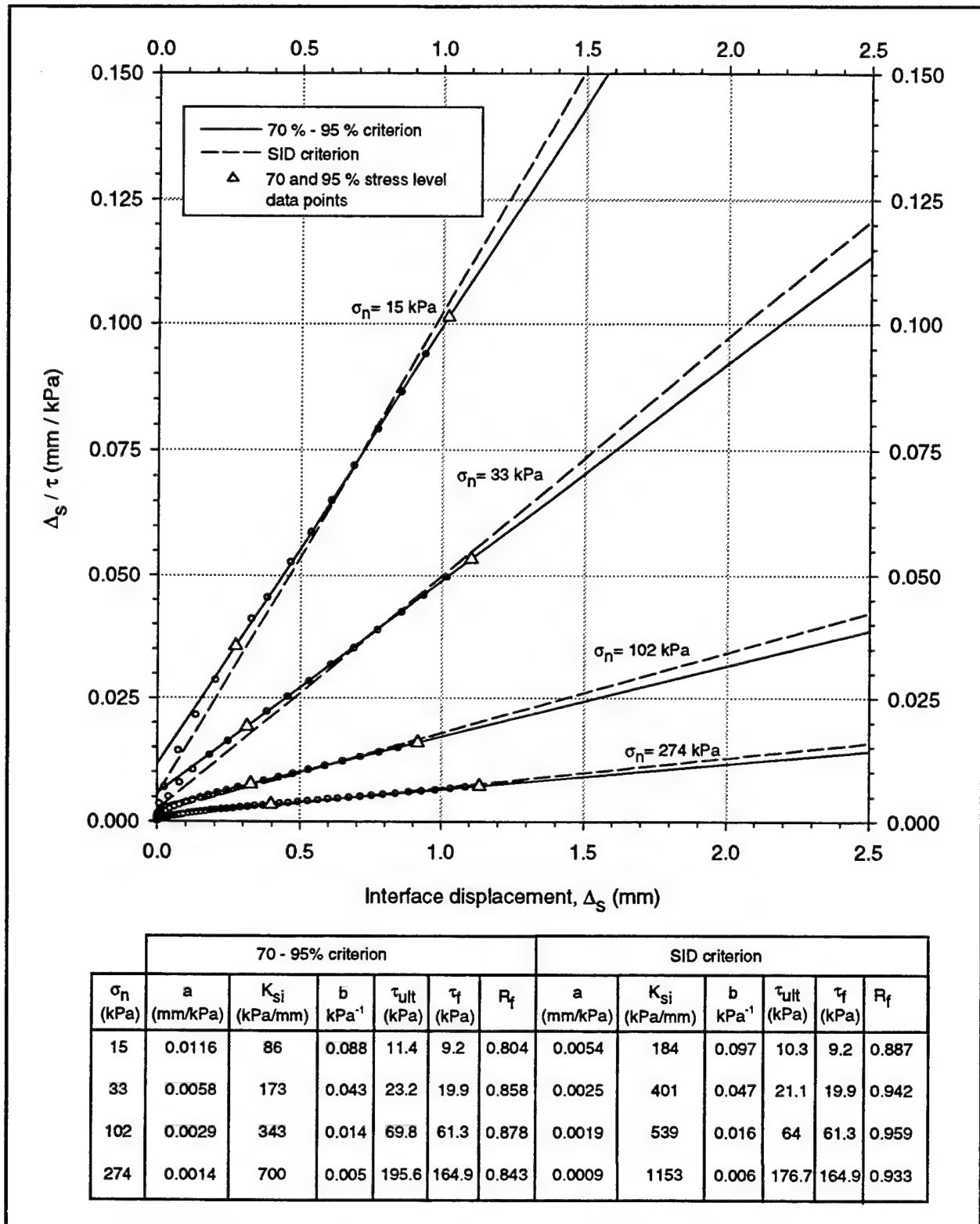


Figure 4-1. Transformed plots for initial loading tests, dense Density Sand-to-concrete interface

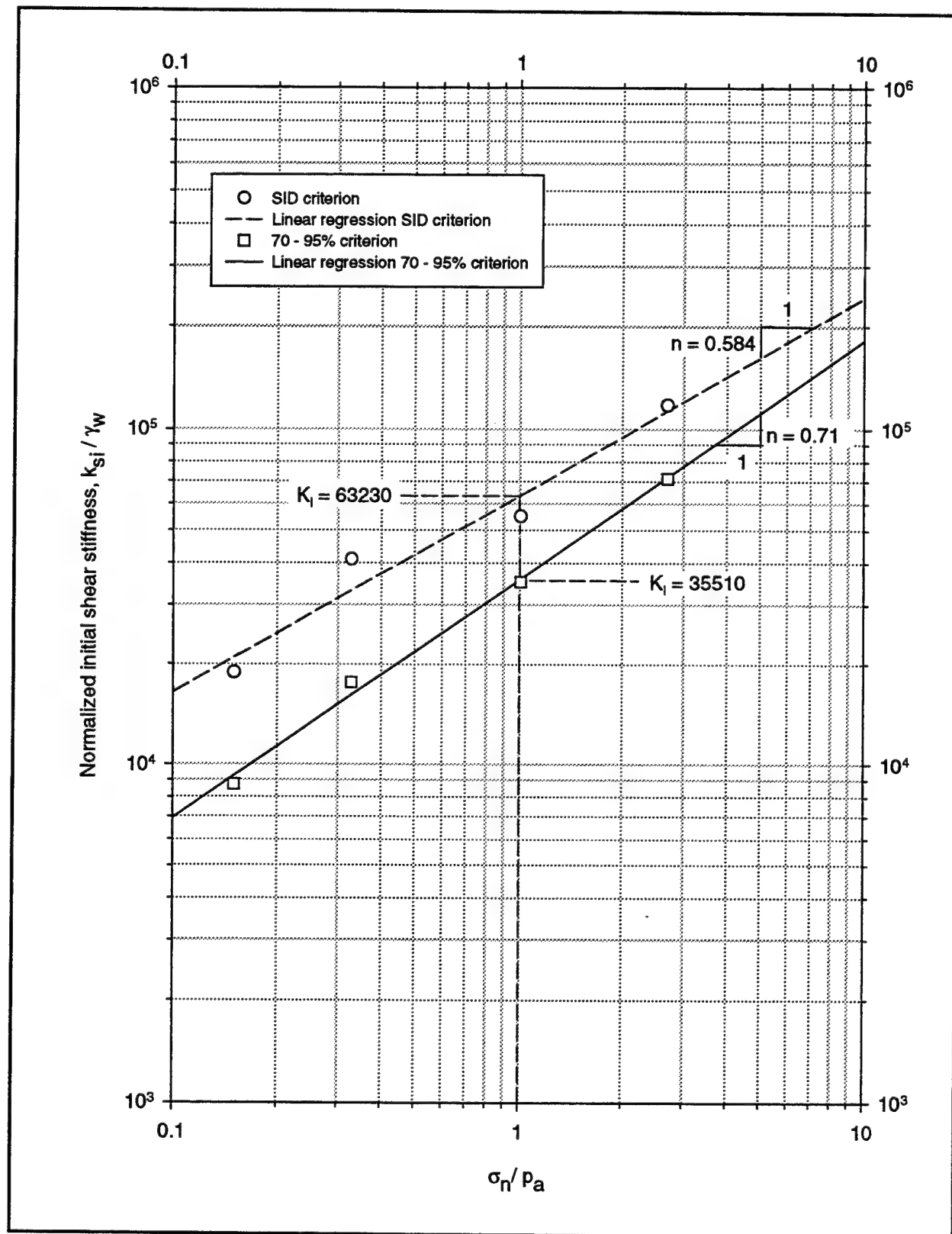


Figure 4-2. Determination of Hyperbolic Parameters K_1 and n for initial loading of dense Density Sand-to-concrete interface

Table 4-2
Hyperbolic Parameters for a Dense, Uniform Sand-to-Concrete
Interface (from Peterson et al. 1976)

| Parameter | Smooth Concrete | Rough Concrete |
|------------|-----------------|----------------|
| K_i | 8,000 - 13,000 | 10,000-12,000 |
| n | 0.85 - 1.18 | 0.7 - 0.72 |
| R_i | 0.4 - 0.6 | 0.3 - 0.8 |
| δ_p | 30.9° | 32.9° |

The hyperbolic parameter values for the Density Sand-to-concrete interface are in general agreement with those reported by Peterson et al. (1976); however, the stiffness number K_i is considerably higher for the Density Sand-to-concrete interface. It is expected that the additional tests to be performed in the next phase of this investigation will help in determining the reasons for the difference.

4.1.2 SID criterion for the determination of hyperbolic parameters

An alternative procedure for determining the hyperbolic parameter values is shown by the dashed lines in Figure 4-1. The *small initial displacement* (SID) criterion, developed during this investigation, consists of finding a best-fit straight line considering all the data points between stress levels of zero and 95%. The values of initial shear stiffness and asymptotic strength are calculated from the intercept and slope of the best-fit line, and are presented in the table included in Figure 4-1.

Since no data points are excluded, this criterion yields K_{si} values closer to the measured initial stiffness of the interface. The corresponding hyperbolic parameters, K_i and n , are calculated as indicated in Figure 4-2. A summary of the SID hyperbolic parameters is presented in Table 4-1.

It may be possible to find a simple correlation between the values of the hyperbolic parameters determined from the 70-95% criterion and the SID criterion. Such a correlation would allow the SID parameters to be estimated from published databases of hyperbolic parameters.

4.1.3 Evaluation of the model against results of initial loading tests

Two sets of hyperbolic model parameter values for initial loading of the interface were developed using the 70-95% and the SID criteria, and are presented in Table 4-1. The interface responses predicted by the models are compared with the test data in Figure 4-3. It can be observed that both models appear to fit the experimental data accurately.

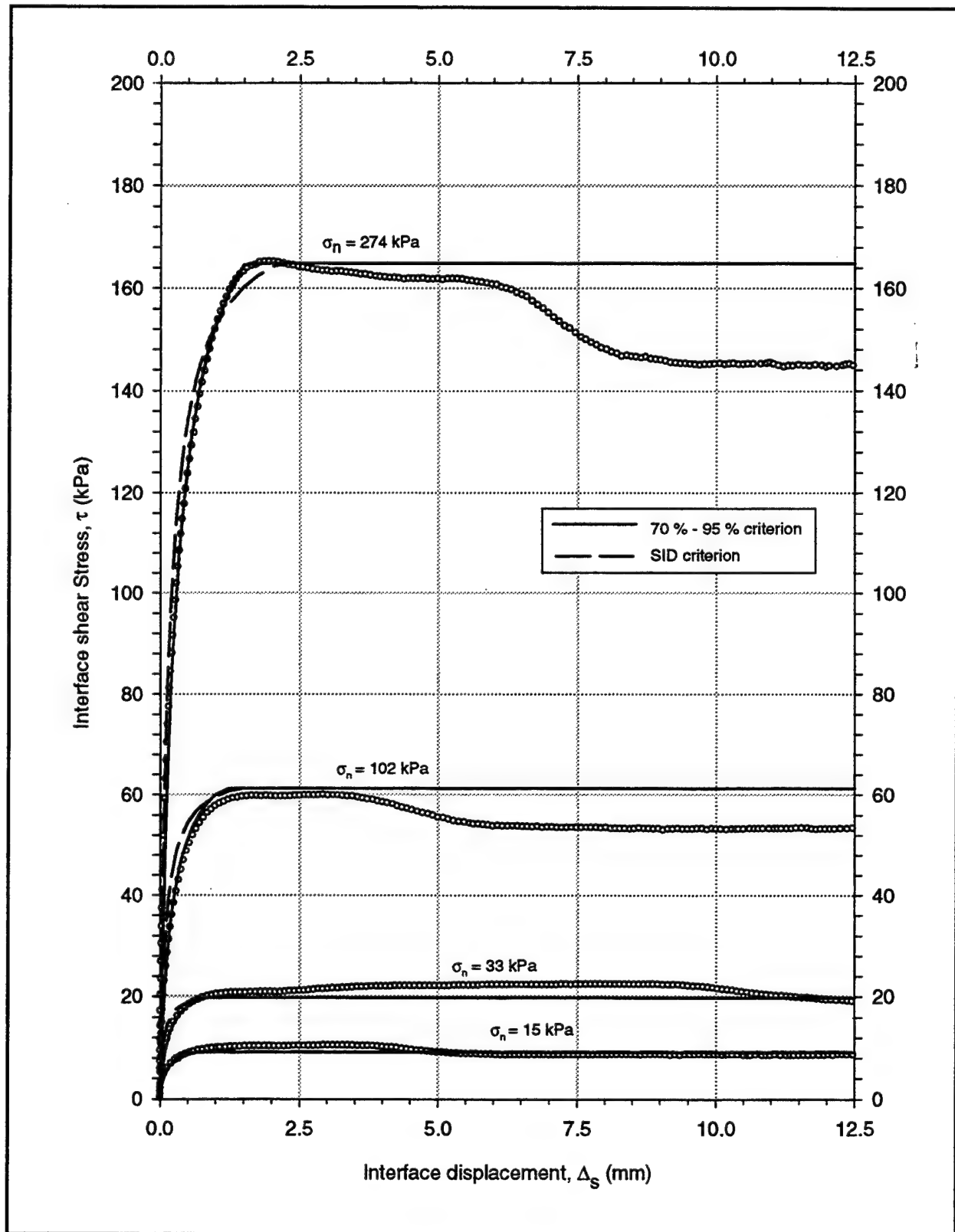


Figure 4-3. Comparison between the hyperbolic model and results of initial loading tests on dense Density Sand-to-concrete interface

Figure 4-4 is an enlargement of Figure 4-3. It can be observed that the Clough and Duncan (1971) hyperbolic model, based on the 70-95% criterion, provides an excellent fit to the test data, especially at stress levels between 50 and 95%. However, the initial shear stiffness K_{si} from the model is lower than the measured shear stiffness of the interface, and for stress levels lower than 50%, the hyperbolic shear stress-displacement relationship lies below the interface test data. As will be shown in the following sections, this characteristic is important when modeling the interface response under unload-reload cycles.

It can also be observed that the SID parameters provide a better approximation of initial stiffness, and give an excellent fit to the interface test data at stress levels lower than 50%. For stress levels higher than 50%, the response from the model is not as accurate, but it is still reasonable.

4.2 Hyperbolic Model Extended to Shear Stress Reversals

4.2.1 Formulation

In this section, the original formulation of the Clough and Duncan (1971) hyperbolic model is extended to the case of shear stress reversals. As defined in Chapter 3, the shear stress reversal loading refers to a change in the direction of shear, once the residual strength is mobilized.

Figure 4-5a illustrates a typical shear reversal test. The interface is sheared past the peak strength until the residual strength is mobilized. The first reversal is applied at point $R1$, with coordinates $(\Delta_{r,1}, \tau_{r,1})$ in the shear stress-displacement plane. Shear progresses in the opposite direction to point $R2$, with coordinates $(\Delta_{r,2}, \tau_{r,2})$, where a second shear reversal is applied. Points such as $R1$ and $R2$ will be referred to as the *shear reversal points* throughout this report.

A set of axes can be defined at each of the reversal points as illustrated in the figure. For the i^{th} reversal, the relative shear and relative displacement, measured along these relative coordinate axes, are defined as:

$$relative\ shear = |\tau - \tau_{r,i}| \quad (4-1)$$

$$relative\ displacement = |\Delta_s - \Delta_{r,i}| \quad (4-2)$$

where i is the shear reversal number. As indicated in Chapter 3, the test results showed that the value of residual shear strength is independent of the shear direction. If both reversals are applied after mobilization of the residual strength, as shown in Figure 4-5a, then the absolute values of $\tau_{r,1}$ and $\tau_{r,2}$ are the same:

$$\tau_f = |\tau_{r,1}| = |\tau_{r,2}| \quad (4-3)$$

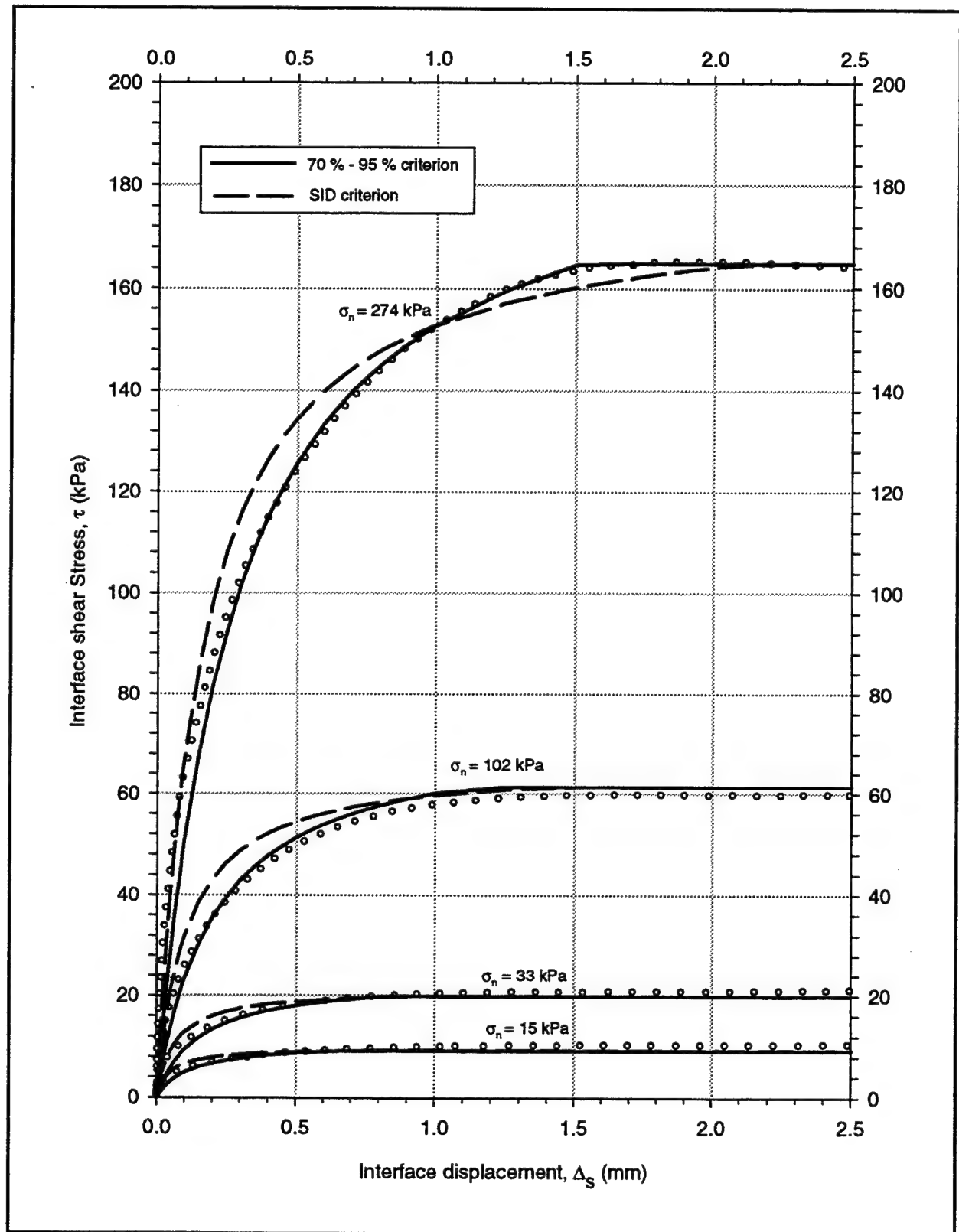


Figure 4-4. Comparison between the hyperbolic model and data from initial loading tests (enlargement of Figure 4-3)

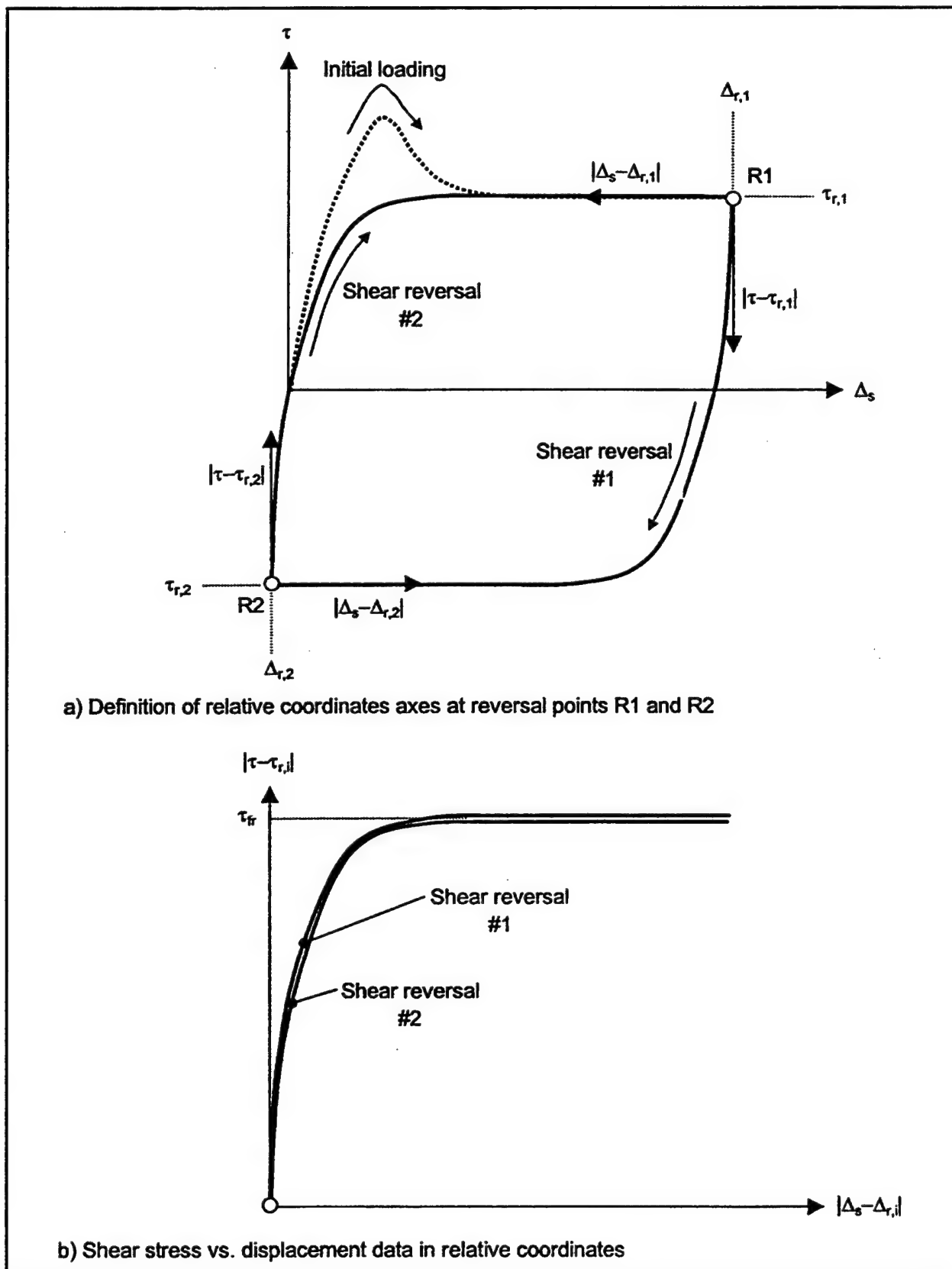


Figure 4-5. Coordinate axes transformation for shear reversals test data

The shear reversal test data are represented in relative coordinates in Figure 4-5b. According to Equation 4-3, the relative strength τ_{fr} , obtained from the plots of relative shear versus relative displacement, can be expressed as:

$$\text{relative shear strength} = \tau_{fr} = 2 \cdot \tau_f \quad (4-4)$$

A hyperbolic relationship, similar to the formulation by Clough and Duncan (1971), can be used to fit the data in the relative coordinate system of Figure 4-5b. Equation 2-4, corresponding to the hyperbolic model for initial loading, can be extended to the i^{th} reversal cycle as follows:

$$\frac{|\Delta_s - \Delta_{r,i}|}{|\tau - \tau_{r,i}|} = a_r + b_r \cdot |\Delta_s - \Delta_{r,i}| \quad (4-5)$$

where a_r is the reciprocal of the initial shear stiffness, K_{sr} , upon reversal; and b_r is the reciprocal of the relative-asymptotic shear stress, τ_{ur} . Equation 4-5 can then be rewritten as:

$$\frac{|\Delta_s - \Delta_{r,i}|}{|\tau - \tau_{r,i}|} = \frac{1}{K_{sr}} + \frac{1}{\tau_{ur}} \cdot |\Delta_s - \Delta_{r,i}| \quad (4-6)$$

The value of τ_{ur} can be related to the relative shear strength τ_{fr} using the following expression:

$$\tau_{ur} = \frac{\tau_{fr}}{R_{fr}} \quad (4-7)$$

where R_{fr} is the failure ratio for shear reversals. If the reversals are applied after mobilization of the residual strength, and considering Equation 4-4, τ_{fr} can then be expressed as:

$$\tau_{fr} = 2 \cdot \sigma_n \cdot \tan \delta_r \quad (4-8)$$

where δ_r is the residual interface friction angle. This equation is valid for interfaces without an adhesion intercept, such as the Density Sand-to-concrete interface.

Equation 2-6 may also be extended to shear stress reversals as follows:

$$K_{sr} = K_{Ir} \cdot \gamma_w \cdot \left(\frac{\sigma_n}{P_a} \right)^{n_r} \quad (4-9)$$

where K_{Ir} is the stiffness number, and n_r is the stiffness exponent for shear reversals. Substituting Equations 4-7, 4-8, and 4-9 into 4-6 gives the following expression:

$$|\tau - \tau_{r,i}| = \frac{|\Delta_s - \Delta_{r,i}|}{\frac{1}{K_{Ir} \cdot \gamma_w \cdot \left(\frac{\sigma_n}{p_a}\right)^{n_r}} + \frac{R_{fr} \cdot |\Delta_s - \Delta_{r,i}|}{2 \cdot \sigma_n \cdot \tan \delta_r}} \quad (4-10)$$

This is the general equation of the hyperbola passing through the i^{th} reversal point of coordinates $(\Delta_{r,i}, \tau_{r,i})$. The absolute shear stress τ can be obtained by rewriting Equation 4-10 as follows:

$$\tau = \tau_{r,i} \pm \frac{|\Delta_s - \Delta_{r,i}|}{\frac{1}{K_{Ir} \cdot \gamma_w \cdot \left(\frac{\sigma_n}{p_a}\right)^{n_r}} + \frac{R_{fr} \cdot |\Delta_s - \Delta_{r,i}|}{2 \cdot \sigma_n \cdot \tan \delta_r}} \quad (4-11)$$

Differentiating Equation 4-11 gives an expression for the tangent stiffness K_{st}

$$K_{st} = K_{Ir} \cdot \gamma_w \cdot \left(\frac{\sigma_n}{p_a}\right)^{n_r} \cdot (1 - R_{fr} \cdot SL_r)^2 \quad (4-12)$$

where SL_r is the relative stress level defined as:

$$SL_r = \frac{|\tau - \tau_{r,i}|}{2 \cdot \sigma_n \cdot \tan \delta_r} \quad (4-13)$$

Combining Equations 2-10 and 4-13:

$$SL_r = \frac{1}{2} |\pm 1 - SL| \quad (4-14)$$

where the first term is positive for unloading and negative for reloading. Finally, combining Equations 4-12 and 4-14:

$$K_{st} = K_{Ir} \cdot \gamma_w \cdot \left(\frac{\sigma_n}{p_a}\right)^{n_r} \cdot \left(1 - \frac{1}{2} \cdot R_{fr} \cdot |\pm 1 - SL|\right)^2 \quad (4-15)$$

4.2.2 Evaluation of the model against results of shear reversal tests

The values of initial shear stiffness upon reversal K_{sr} and relative-asymptotic shear stress τ_w were determined from the transformed plots of relative shear stress and relative displacement presented in Figure 4-6. This figure contains the

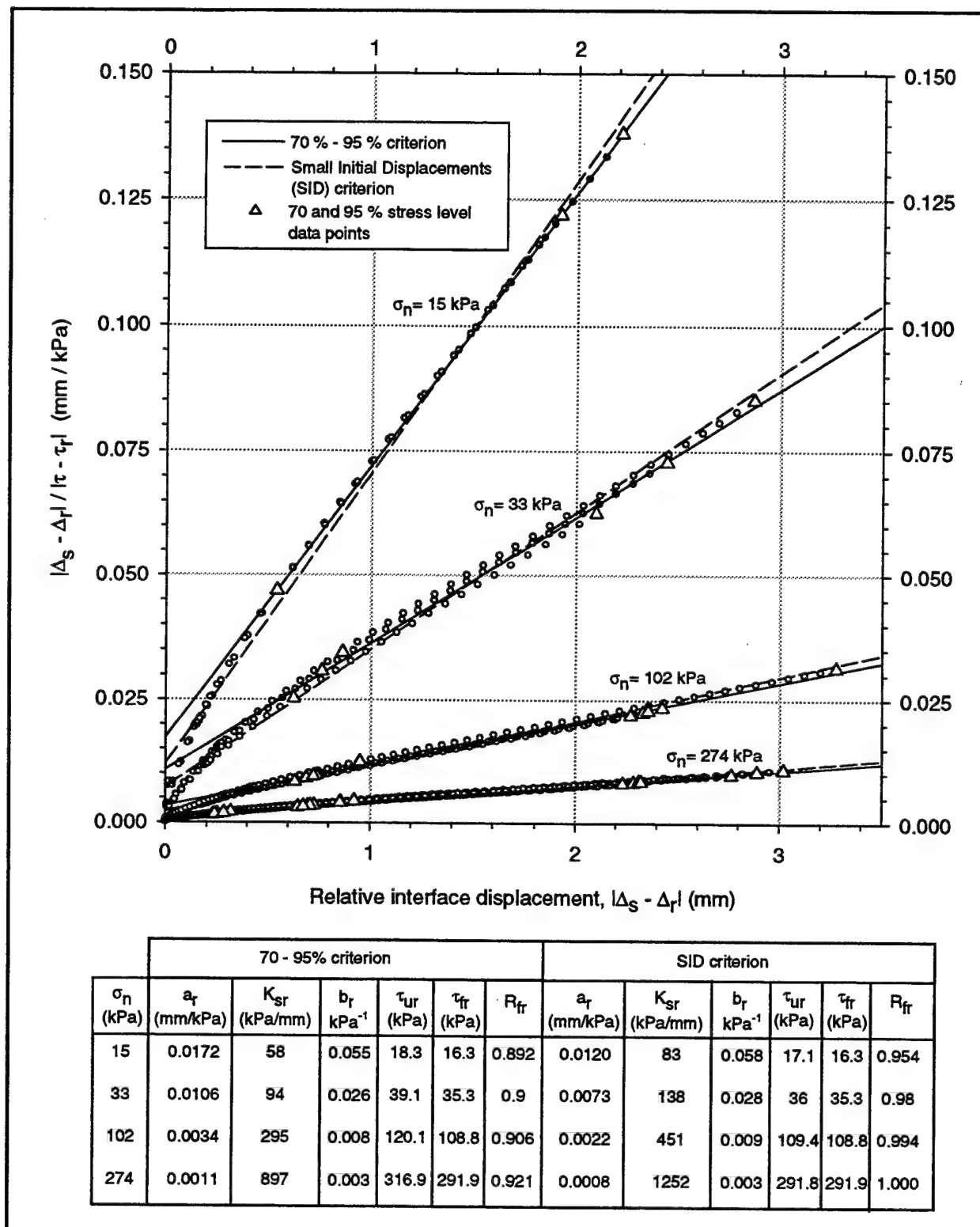


Figure 4-6. Transformed plots for shear reversals tests, dense Density Sand-to-concrete interface

complete sets of data from all the reversal tests performed. Both the 70-95% criterion and the SID criterion were used to define the best-fit lines shown.

In the figure, all the data points that correspond to stress levels of 70 and 95% in each of the tests are clearly identified. In the 70-95% criterion, a linear regression was performed considering only these 70-95% points. In the SID criterion, on the other hand, *all* the data points from the tests were considered for the determination of the best-fit straight lines shown. The table included in Figure 4-6 contains, for each normal stress, the values of initial shear stiffness, relative-asymptotic shear stress, and failure ratio, obtained from each criteria.

Figure 4-7 shows the relationship between the initial stiffness values, obtained from the transformed plots, and the normal stress. The values K_r and n_r are obtained from this plot in a manner identical to that described for initial loading. The values of the hyperbolic parameters for shear reversals are presented in Table 4-3.

| Table 4-3 Hyperbolic Parameters for Shear Reversals on Density Sand-to- Concrete Interface | | |
|---|-------------------------|----------------------|
| Parameter | 70-95% Criterion | SID Criterion |
| K_r | 32,150 | 46,750 |
| n_r | 0.963 | 0.957 |
| R_r | 0.905 | 0.982 |
| δ_r | 28.1° | 28.1° |

The hyperbolic interface response for shear reversals was calculated using the parameter values in Table 4-3. Figure 4-8 shows, in the relative coordinate system, a comparison between the test data and the extended hyperbolic model calculated using both the 70-95% criterion and the SID criterion. For clarity, only three representative sets of data for each normal stress were included in the figure. It can be observed that, using the 70-95% parameters, the resulting hyperbolic model fits the test data very closely, but yields a lower value of K_{sr} than the measured shear stiffness of the interface. The hyperbolic model, based on the SID criterion, gives a very good fit to the test data at relative stress levels below 50 percent.

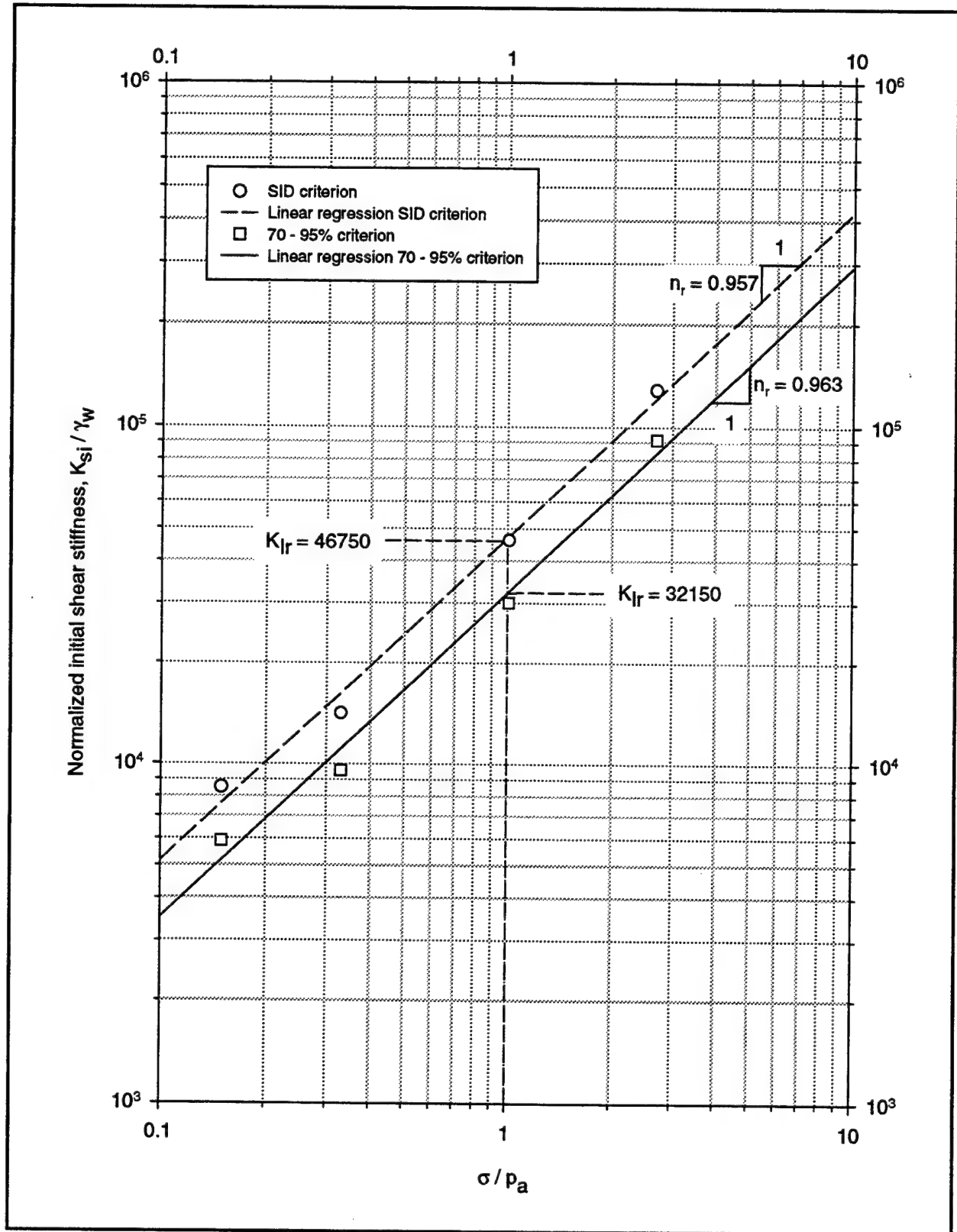


Figure 4-7. Determination of hyperbolic parameters K_h and n_r for shear reversals on Density Sand-to-concrete interface

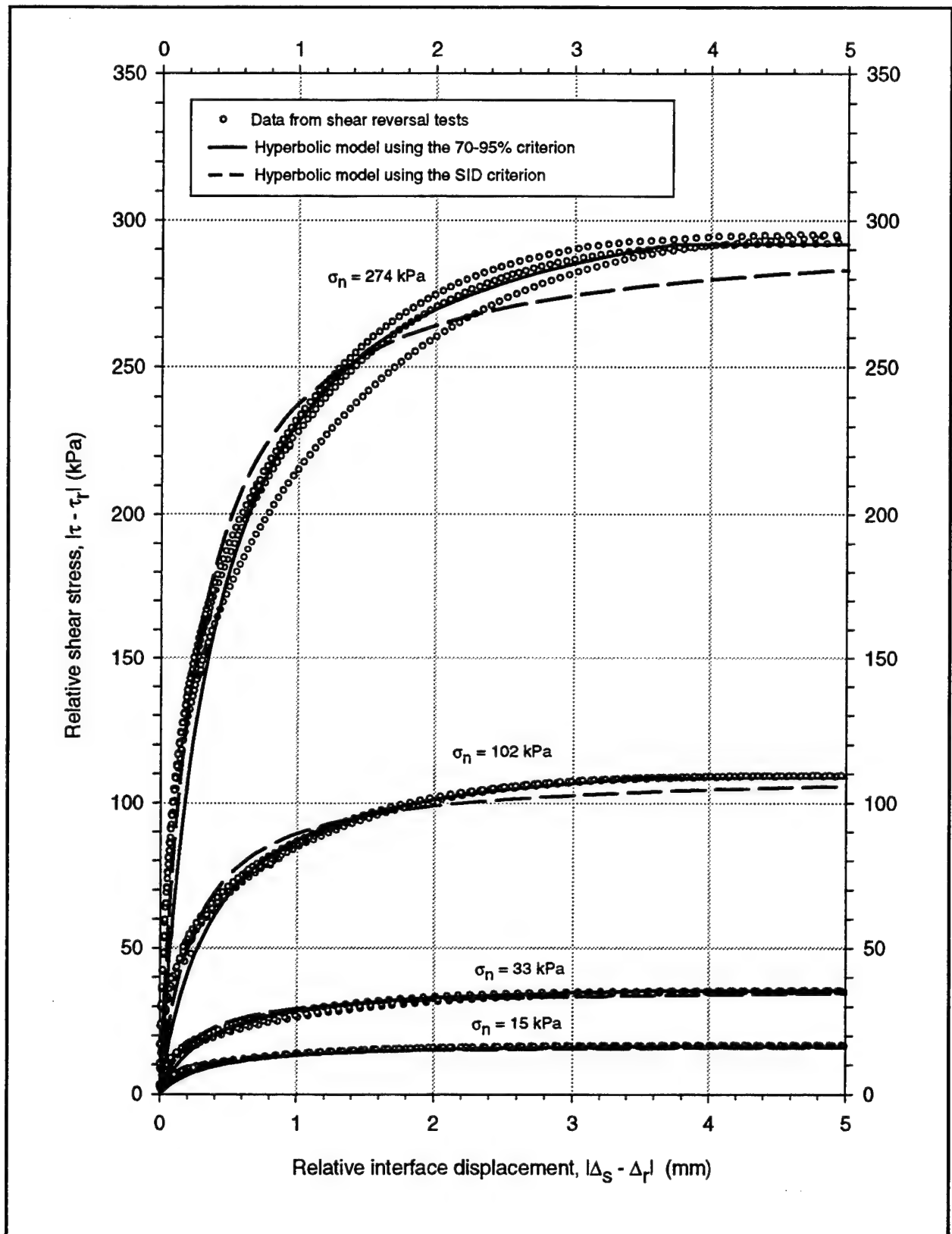


Figure 4-8. Comparison between the hyperbolic model and data from shear reversal tests in relative coordinates

4.3 Hyperbolic Model Extended to Unload-Reload Cycles

4.3.1 Formulation

The formulation given in the previous section is applicable only to shear reversals applied after mobilization of the residual strength. However, it is the guideline for the formulation presented in this section, which applies to the more general case of unloading-reloading at any stress level.

Figure 4-9 shows a typical unload-reload cycle, applied during initial loading of the interface. A set of relative coordinate axes can be defined at the unload- and reload-points, *UL* and *RL*, as illustrated in the figure. The unloading and reloading portions of the stress-displacement curve are assumed to follow a hyperbolic relationship.

Following a derivation similar to that presented in the previous section, the following expression for unloading is obtained:

$$\tau = \tau_{ul} - \frac{|\Delta_s - \Delta_{ul}|}{\frac{1}{K_{Iul} \cdot \gamma_w \cdot \left(\frac{\sigma_n}{p_a}\right)^{n_{ul}}} + \frac{R_{ful} \cdot |\Delta_s - \Delta_{ul}|}{\alpha_{ul} \cdot \sigma_n \cdot \tan \delta}} \quad (4-16)$$

where

τ_{ul} = shear stress at the unload point *UL*

Δ_{ul} = interface displacement at the unload point *UL*

K_{Iul} = stiffness number on unloading

n_{ul} = stiffness exponent on unloading

R_{ful} = failure ratio for unloading

α_{ul} = dimensionless scaling factor for unloading

Similarly, for reloading:

$$\tau = \tau_{rl} + \frac{|\Delta_s - \Delta_{rl}|}{\frac{1}{K_{Irl} \cdot \gamma_w \cdot \left(\frac{\sigma_n}{p_a}\right)^{n_{rl}}} + \frac{R_{frl} \cdot |\Delta_s - \Delta_{rl}|}{\alpha_{rl} \cdot \sigma_n \cdot \tan \delta}} \quad (4-17)$$

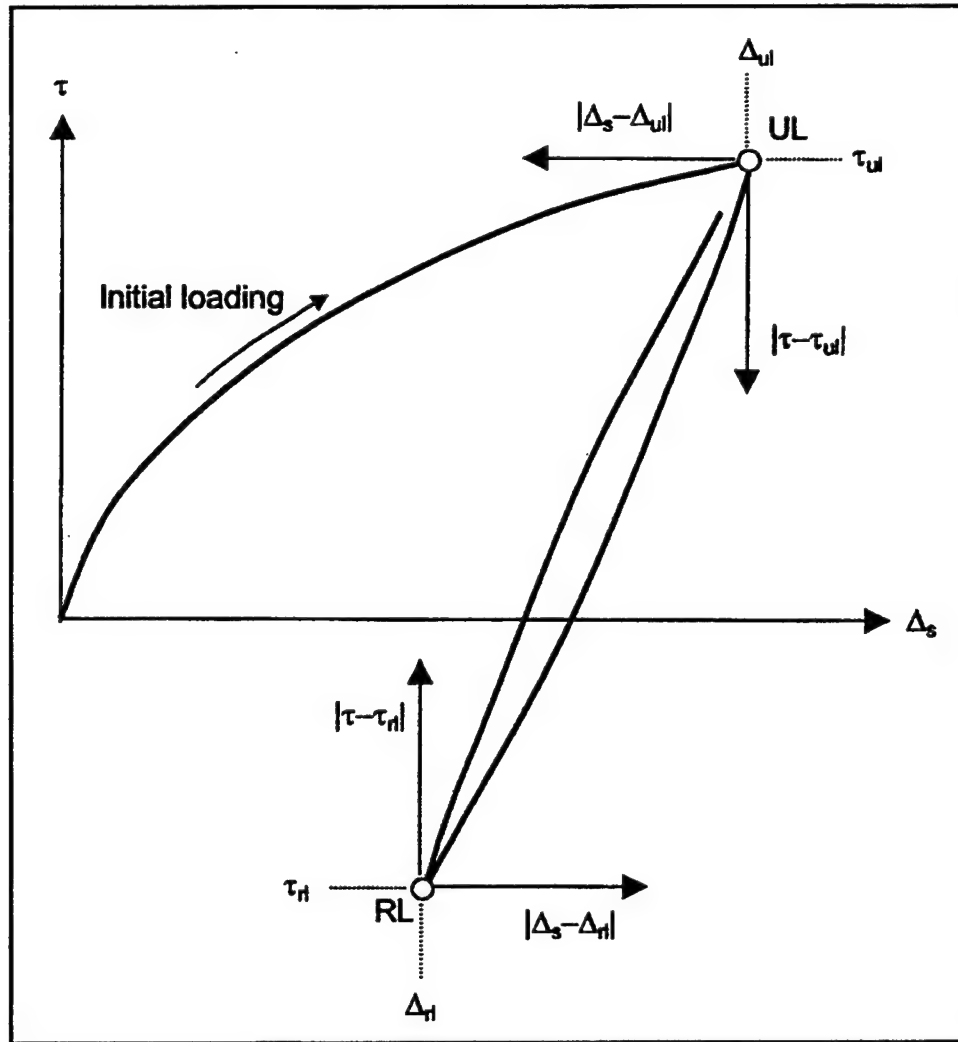


Figure 4-9. Relative coordinate axes for unload-reload cycles

where

τ_{rl} = shear stress at the reload point *RL*

Δ_{rl} = interface displacement at the reload point *RL*

K_{rl} = stiffness number on reloading

n_{rl} = stiffness exponent on reloading

R_{fri} = failure ratio for reloading

α_{rl} = dimensionless scaling factor for reloading

If the hyperbolic parameters K_I , n , R_f , and δ are assumed to have the same values for both unloading and reloading, the following general expression is obtained:

$$\tau = \tau_o \pm \frac{|\Delta_s - \Delta_o|}{\frac{1}{K_{Iur} \cdot \gamma_w \cdot \left(\frac{\sigma_n}{p_a}\right)^{n_{ur}}} + \frac{R_{fur} \cdot |\Delta_s - \Delta_o|}{\alpha \cdot \sigma_n \cdot \tan \delta}} \quad (4-18)$$

where

τ_o = shear stress at the unload or reload point

Δ_o = interface displacement at the unload or reload point

ur = subscript denoting that the parameters have the same values for both unloading and reloading of the interface

α = dimensionless scaling factor

Equation 4-18 is the general expression for hyperbolas passing through unload and reload points.

4.3.2 Determination of the model parameter values

In the new extended model, two basic assumptions are made regarding the values of the hyperbolic parameters:

- a. The initial shear stiffness at the unload and reload points will take one of two possible values, K_{si} or K_{sr} , depending on whether the unloading started before or after mobilization of the peak strength.
- b. The interface friction angle is independent of the direction of shear and can take two possible values, δ_p or δ_r , depending on whether unloading was applied before or after mobilization of the peak strength.

These assumptions are illustrated in Figure 4-10. Two possible unload-reload cycles are considered: unloading-reloading before mobilization of the interface peak strength and unloading-reloading after mobilization of the interface residual strength. If unloading occurs *before* the mobilization of the peak strength, the interface shear stiffness on unloading is assumed to be equal to the initial shear stiffness K_{si} for initial loading. Similarly, the interface friction angle is assumed to be equal to the peak friction angle δ_p . The hyperbolic parameters to be introduced in Equation 4-18 become:

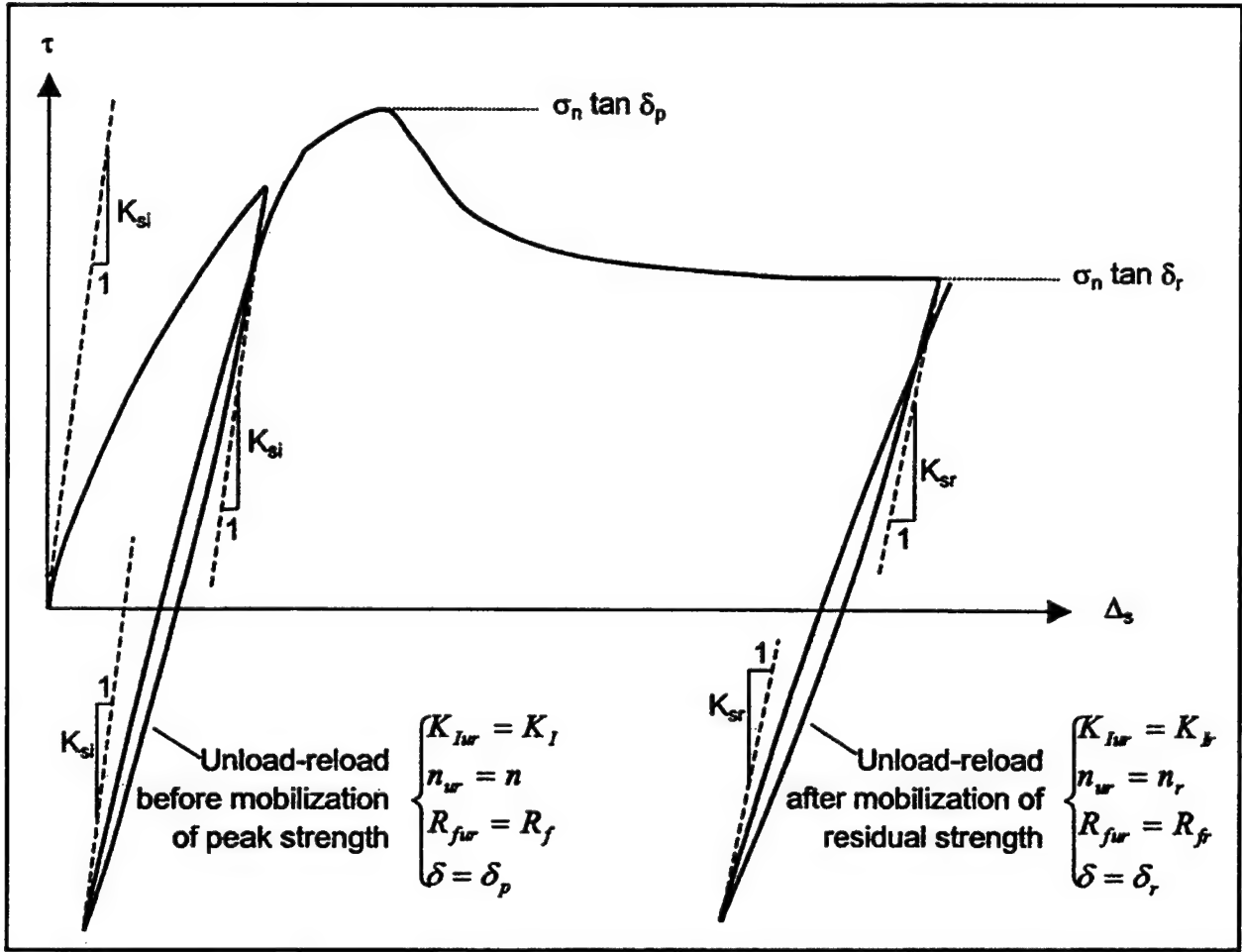


Figure 4-10. Guidelines for selection of hyperbolic parameters for unloading-reloading of interfaces

$$\begin{aligned}
 K_{Iur} &= K_I \\
 n_{ur} &= n \\
 R_{fur} &= R_f \\
 \delta &= \delta_p
 \end{aligned}
 \tag{4-19}$$

On the other hand, if unloading occurs *after* mobilization of the residual strength, then the initial stiffness on unloading is assumed to be equal to the initial stiffness K_{sr} for shear stress reversals, discussed in the previous section. Similarly, the interface friction angle is assumed to be equal to the residual friction angle δ_r . The hyperbolic parameters for the model become:

$$\begin{aligned}
K_{lur} &= K_{lr} \\
n_{ur} &= n_r \\
R_{fur} &= R_{fr} \\
\delta &= \delta_r
\end{aligned}
\tag{4-20}$$

The results of the shear reversal tests support to a reasonable extent the use of the same parameters for both unloading and reloading because the interface response measured in these tests was very similar in both directions of shear.

The parameter α is a *scaling factor* for the hyperbolic shear stress-displacement relationship, as illustrated in Figure 4-11a. Two unload paths from hypothetical interface tests are represented in the figure. Unloading along path 1 starts at point U1, close to mobilization of the interface peak shear strength, and progresses until the shear strength is mobilized in the opposite direction, at U1'. Unloading along path 2 starts midway between zero and the peak shear strength, and progresses until the shear strength is mobilized at U2'. According to the formulation presented in this section, Equation 4-18 becomes:

$$\tau = \tau_o \pm \frac{\frac{|\Delta_s - \Delta_o|}{1 + \frac{R_f \cdot |\Delta_s - \Delta_o|}{K_I \cdot \gamma_w \cdot \left(\frac{\sigma_n}{p_a}\right)^n} + \alpha \cdot \sigma_n \cdot \tan \delta_p}}{\alpha \cdot \sigma_n \cdot \tan \delta_p}
\tag{4-21}$$

Figure 4-11b shows the unloading curves 1 and 2 in relative coordinates, as was done for the shear reversals in the previous section. Both unloading curves, represented by Equation 4-21, have identical shape as the initial loading curve, represented by Equation 2-8, but are enlarged by the scaling factor α . This feature of the extended hyperbolic formulation is found in some models for cyclic loading of soils.

In the *extended Massing models* for cyclic loading of soils, a scaling factor of two is usually assumed (Kramer 1996). This assumption is valid for unloading paths such as 1. However, for unloading paths such as 2, the value of the scaling factor α will be intermediate between 1 and 2 as illustrated in the figure. Based on the work presented by Pyke (1979) for cyclic loading of soils, the following expression for α was developed:

$$\alpha = |\pm 1 - SL_{ur}|
\tag{4-22}$$

where SL_{ur} is the stress level at the unload or reload points, and the first term is negative for unloading and positive for reloading.

The formulation of the extended hyperbolic model is represented by Equations 4-18 and 4-22. For its application, the hyperbolic parameter values,

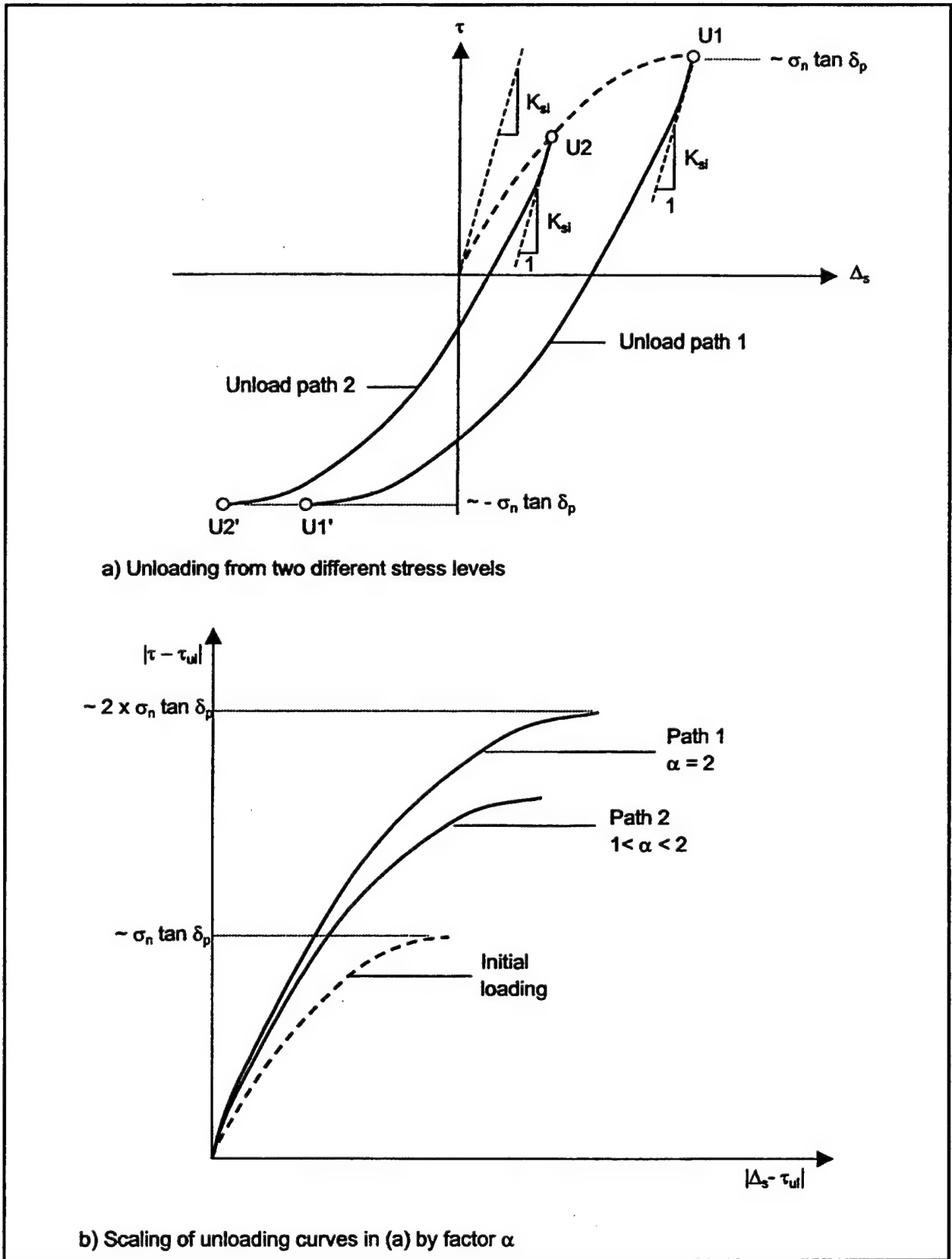


Figure 4-11. Scaling of τ - Δ_s relationship during unload by factor α in the extended hyperbolic model

corresponding to initial loading and shear reversals, must be determined from interface tests and introduced in Equation 4-18 following the guidelines presented in Figure 4-10 and in Equations 4-19 and 4-20. As discussed in the following section, it is recommended that the hyperbolic parameter values be determined using the SID criterion developed during this investigation.

4.3.3 Evaluation of the model against results of unload-reload interface tests

The results of the unload-reload tests performed on the Density Sand-to-concrete interface, described in Chapter 3, are reproduced in Figures 4-12 to 4-14. The interface response under the type of loading applied in the tests was modeled using the formulation described in the previous section, and the modeling results are shown in the figures.

Figure 4-12 shows the data from test T202_5, which was performed under a constant normal stress of 33 kPa. Unloading was initiated at a stress level of 0.7, during initial loading of the interface and before mobilization of the peak strength, and progressed until reaching a stress level of -0.7, where reloading started. The interface response was simulated using Equations 4-18, 4-19, and 4-22 and the SID hyperbolic parameters for initial loading presented in Table 4-1.

It can be observed that the extended hyperbolic model produces reasonable agreement with the data. It can also be observed that the interface shear stiffness, upon unloading and reloading, is slightly higher than the value K_{si} assumed by the model; however, this does not seriously affect the overall performance of the model.

Figures 4-13 and 4-14 show the data from tests T201_5 and T203_15, which were performed under constant normal stresses of 33 and 102 kPa, respectively. An unload-reload cycle, contained within the first quadrant of the shear stress-displacement plane, was applied between stress levels of 0.7 and 0.1 in both tests. The hyperbolic interface response, given by Equations 4-18, 4-19, and 4-22, has also been included in the figures. The interface response predicted by the model is in good agreement with the test data.

As discussed in previous sections, the SID criterion approximates the actual initial shear stiffness values better than the 70-95% criterion. Figure 4-15 shows modeling results using the 70-95% parameter values for analysis of the same unload-reload cycle presented in Figure 4-12. It can be observed that the interface response obtained using the 70-95% parameter values is much softer than the measured interface response and does not fit the test data accurately. Similar results were obtained for the other unload-reload cycles presented in the previous section. It may be concluded that the extended hyperbolic formulation produces good results if the SID parameters are used.

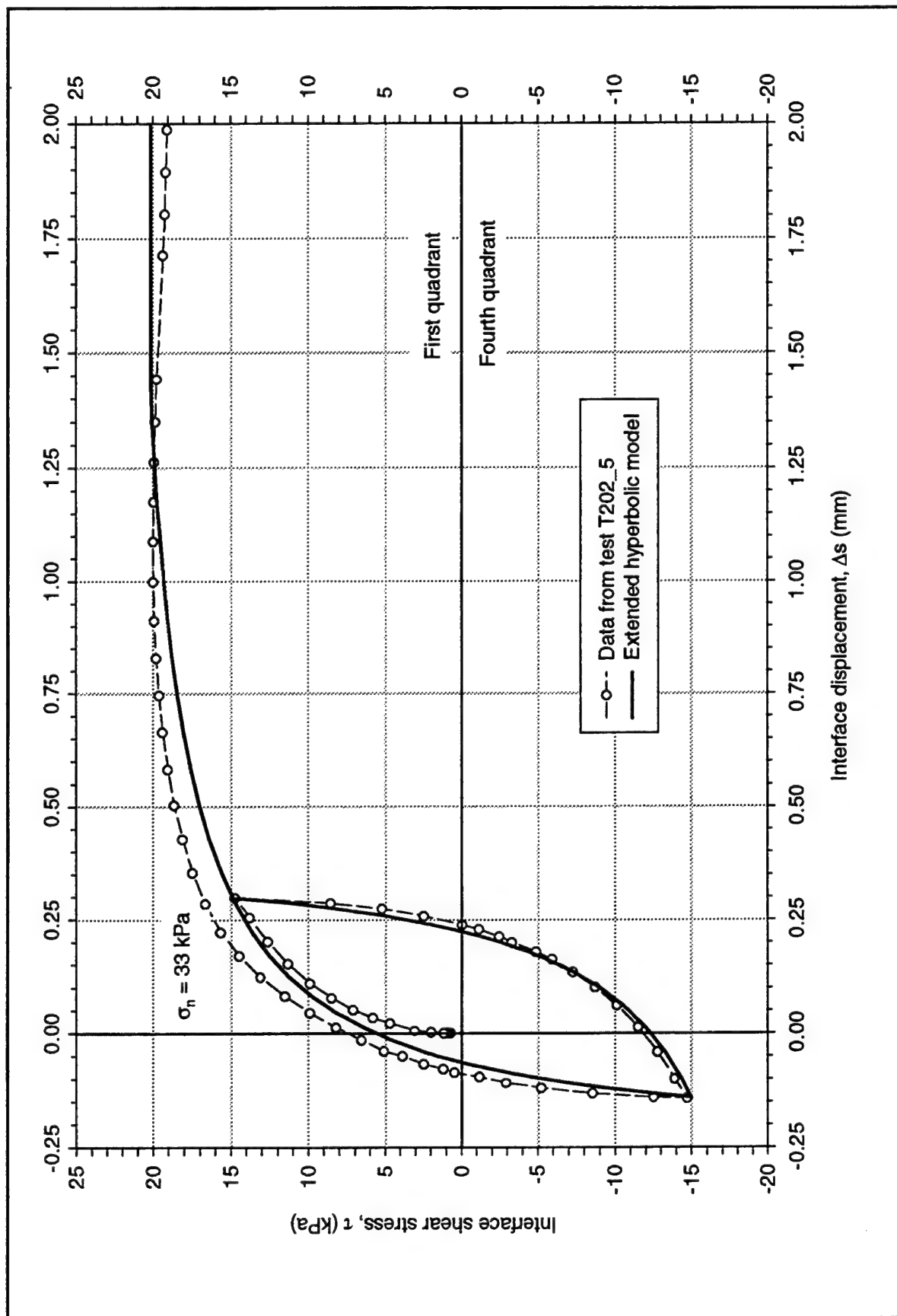


Figure 4-12. Comparison between the extended hyperbolic model and unload-reload data from test T202_5

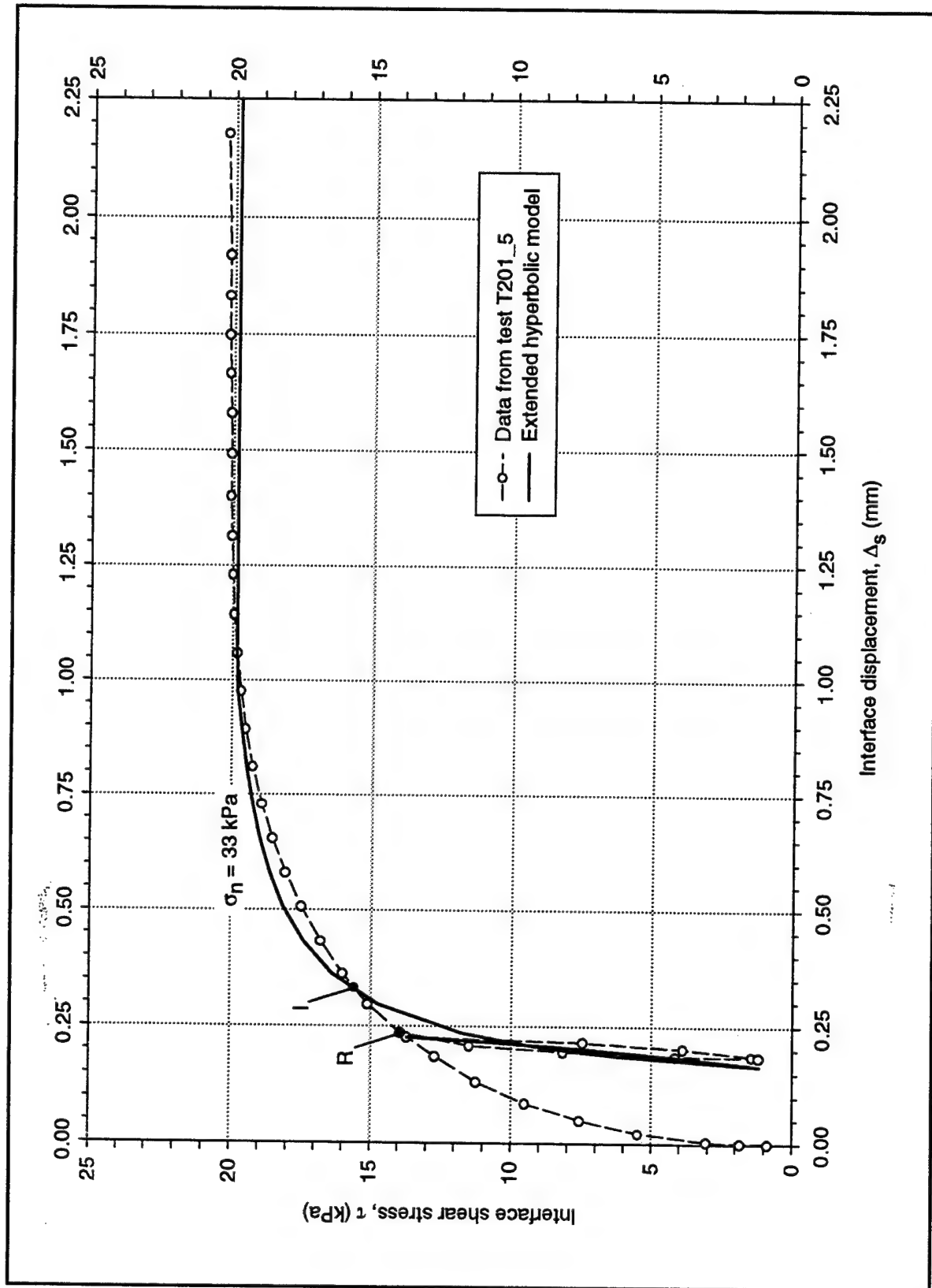


Figure 4-13. Comparison between the extended hyperbolic model and unload-reload data from test T201_5

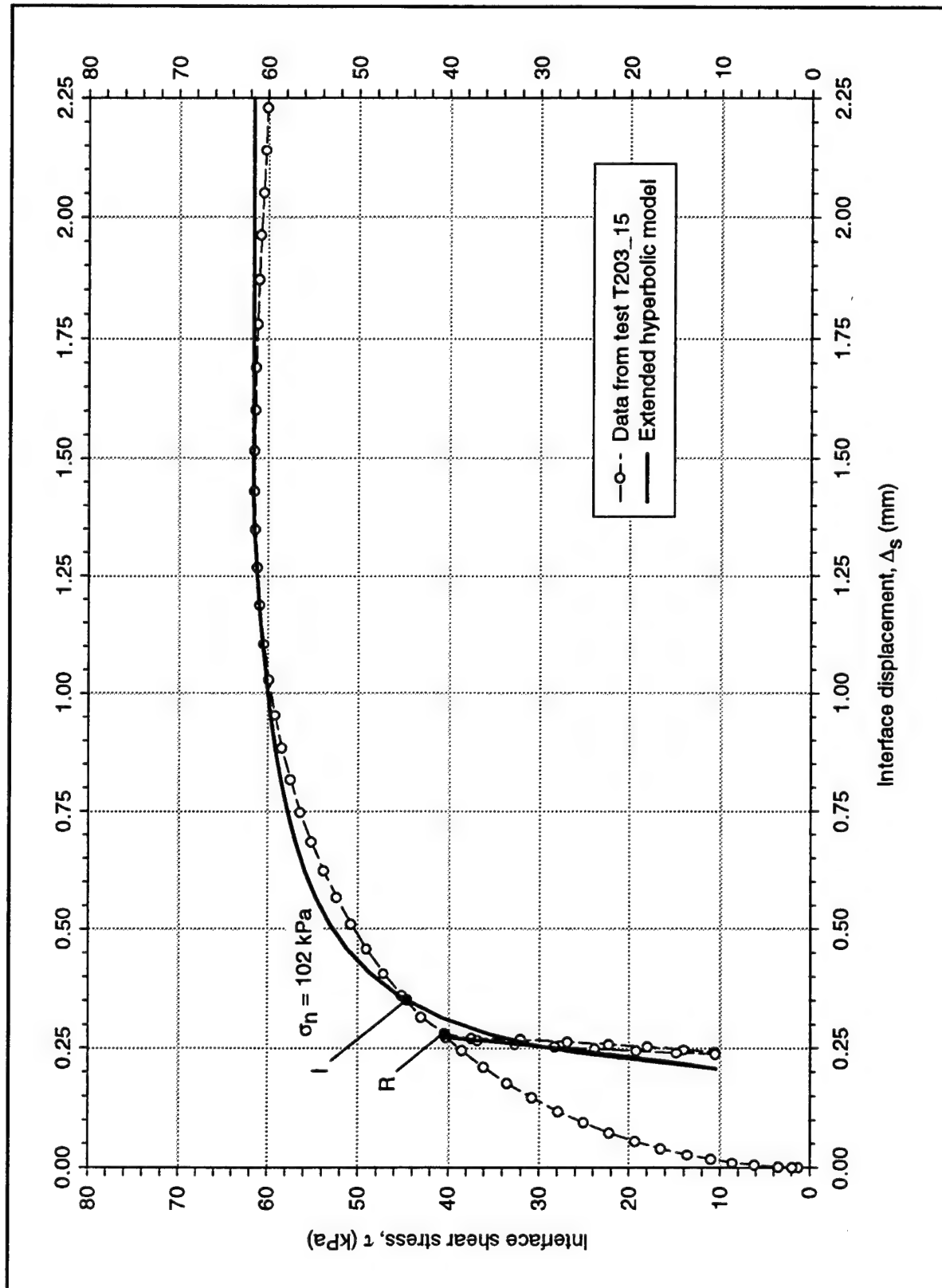


Figure 4-14. Comparison between the extended hyperbolic model and unload-reload data from test T203_15

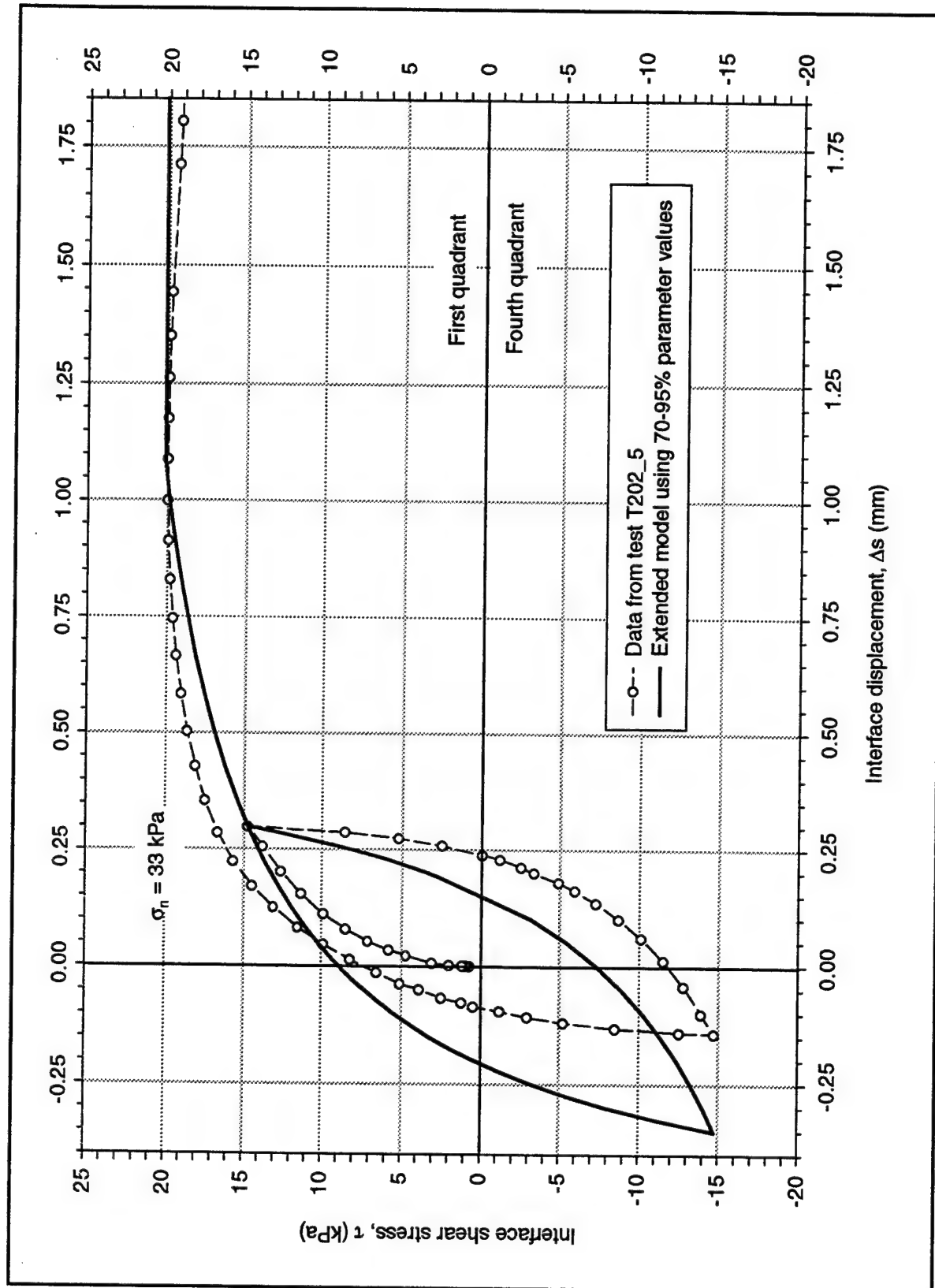


Figure 4-15. Extended hyperbolic model calculated with 70-95% parameters and comparison with unload-reload data from test 202_5

4.3.4 Limitations of the hyperbolic model extended to unload-reload cycles

The main limitation of this model is that the actual response of the interface does not follow a hyperbolic, shear stress-displacement relationship. As a result, neither the 70-95% criterion nor the SID criterion gives an exact value of initial interface shear stiffness. For the case of the dense Density Sand-to-concrete interface used in this investigation, the measured initial shear stiffness is always higher than that obtained from either criterion. Consequently, the extended model gives an interface response during unloading and reloading that is softer than the actual response.

The main consequence arising from the inaccuracy in the estimation of the initial shear stiffness is shown in Figures 4-13 and 4-14. In each figure, the reloading curve obtained from the tests and the reloading curve obtained from the model intersect the primary loading curve at points *R* and *I*, respectively. In both figures, point *I* is located to the right of *R*; therefore, the extended hyperbolic model overestimated the net interface displacement after the complete unload-reload cycle.

For the cases presented in Figures 4-12 to 4-14, the error introduced by the lower values of initial shear stiffness was not significant because the initial shear stiffness K_{si} was obtained using the SID criterion, and only one unload-reload cycle was applied on the interface.

A hypothetical interface test is presented in Figure 4-16, where two consecutive unload-reload cycles are applied within the first quadrant. The error in the displacement value obtained from the model after each loading cycle may result in a significant overestimation of the final interface displacement.

In the following section, a modified formulation is presented that may yield a better estimate of the total interface displacements after a number of unload-reload cycles.

4.3.5 Optional beta-formulation for repeated unload-reload cycles in the first quadrant

In the extended hyperbolic formulation, it is assumed that the initial interface shear stiffness is the same for both unloading and reloading. In the previous section, it was shown that, for repeated unload-reload cycles, this assumption might lead to an overestimation of the interface displacement. For cases such as the one illustrated in Figure 4-16, a formulation has been developed where different initial shear stiffness values are assumed for unloading and for reloading. This formulation is intended as an option for cases where a more precise estimation of displacements under repeated loading is required.

In this formulation, the hyperbolic parameters for unload-reload are first determined as in the extended formulation, according to Equations 4-19 or 4-20.

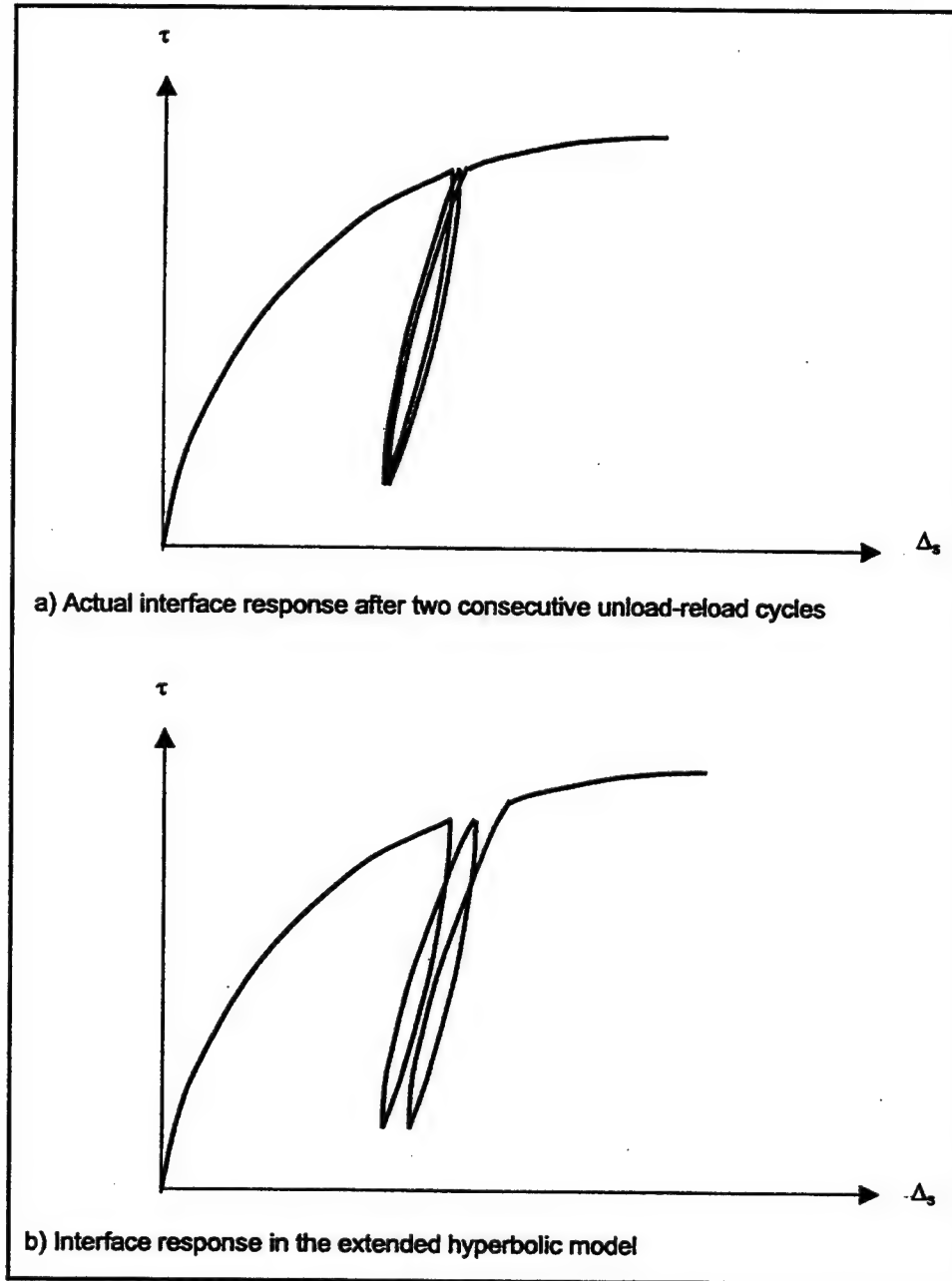


Figure 4-16. Response of interface subjected to consecutive unload-reload cycles

Then, the values of the stiffness numbers for unload and reload are calculated using the following expressions:

$$K_{lul} = \beta_{ul} \cdot K_{lur} \quad (4-23)$$

$$K_{lrl} = \beta_{rl} \cdot K_{lur} \quad (4-24)$$

where β_u and β_r are nondimensional coefficients for unloading and reloading, respectively. All the other hyperbolic parameters remain the same as in the extended formulation.

Finally, the hyperbolic parameters are introduced in Equations 4-16 and 4-17 for unloading and reloading, respectively. There is no rational procedure to estimate the values of the coefficients β_u and β_r , but they may be found with relative ease by trial and error. For unloading, the value of β_u is modified until the hyperbolic shear stress-displacement relationship for unloading passes through the unload and reload points. For reloading, the value of β_r is modified until the shear stress-displacement relationship passes through the reload point and through point R in Figures 4-13 and 4-14. The unload and reload points and point R are therefore the control points for the hyperbolic fit in this formulation.

This formulation was applied to tests T201_5 and T203_15, discussed in the previous section, as shown in Figures 4-17 and 4-18. The values were adopted for the coefficients: $\beta_u = 1.92$ and $\beta_r = 3.2$. These values are valid only for the tests performed and cannot be used for modeling other interfaces.

The β -formulation gives an excellent fit to the test data for the unload-reload cycles. It may be observed that the hyperbolic reload curve intersects the primary loading curve very close to the unloading point. Therefore, this model may be useful for cases of repeated unload-reload cycles where the extended hyperbolic formulation, discussed in the previous section, may yield excessive displacements.

It can be observed that, after intersecting the primary loading curve, the reloading curve departs significantly from the test data. Therefore, for the implementation of the model in SSI analyses, an additional, Massing-type rule (Kramer 1996) is required: *If the reload curve intersects the primary loading curve, it will follow the primary loading curve until the next unloading occurs.*

This formulation was developed only for unload-reload cycles contained in the first quadrant, or within the quadrant where primary loading takes place. For unload-reload cycles extending from the first to the fourth quadrant, as in Figure 4-12, analyses showed that the β -formulation is not accurate.

It must also be noted that the parameters β_u and β_r do not have any physical meaning, but are only a means of fitting the data. The values given herein are applicable only to the Density Sand-to-concrete interface, subjected to the particular loading conditions imposed during the tests.

Additional tests will be performed during the next phase of this investigation to assess the validity and practical applications of this formulation for repeated interface loading.

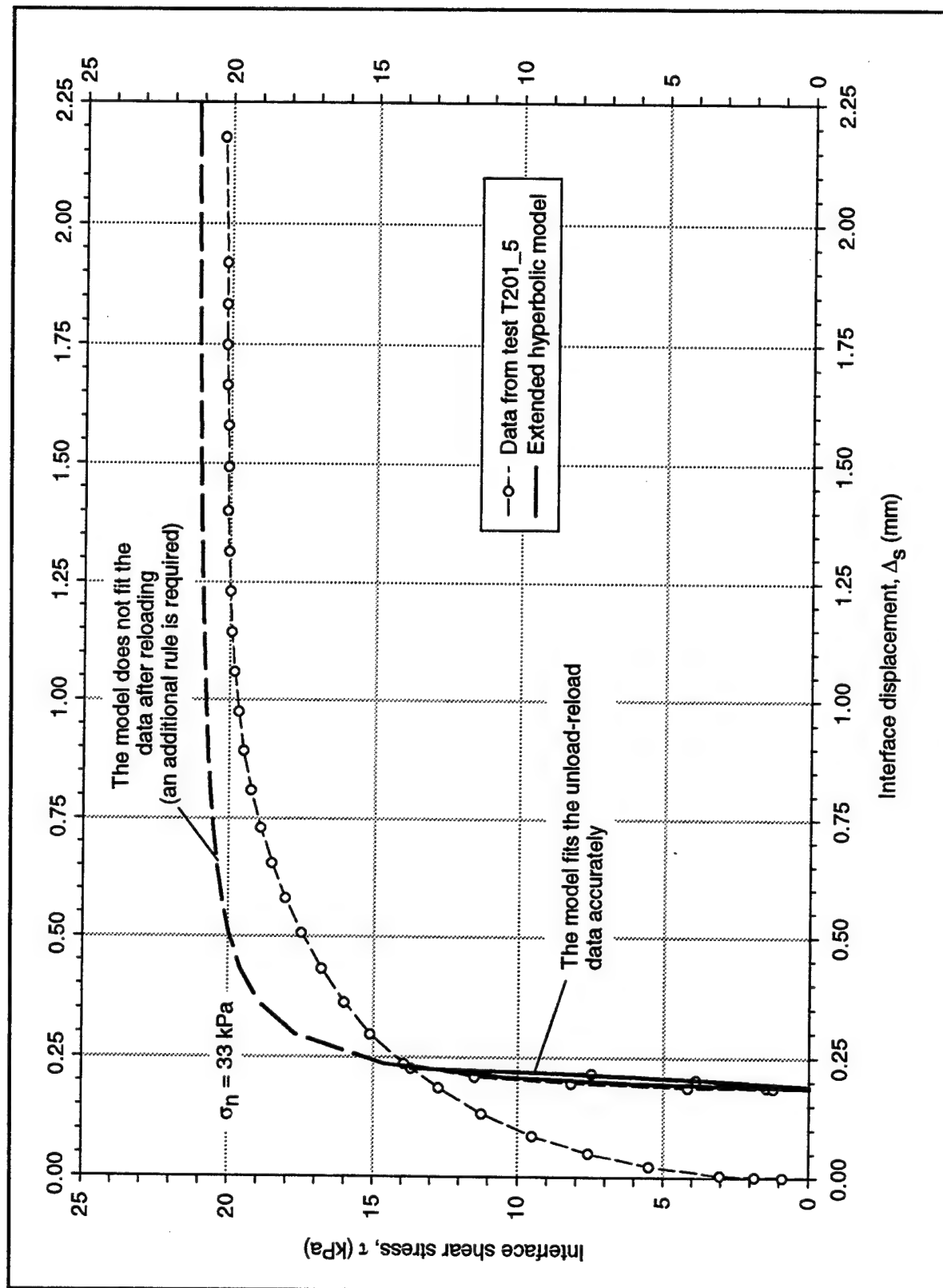


Figure 4-17. Comparison between the β -formulation of the extended hyperbolic model and unload-reload data from test T201_5

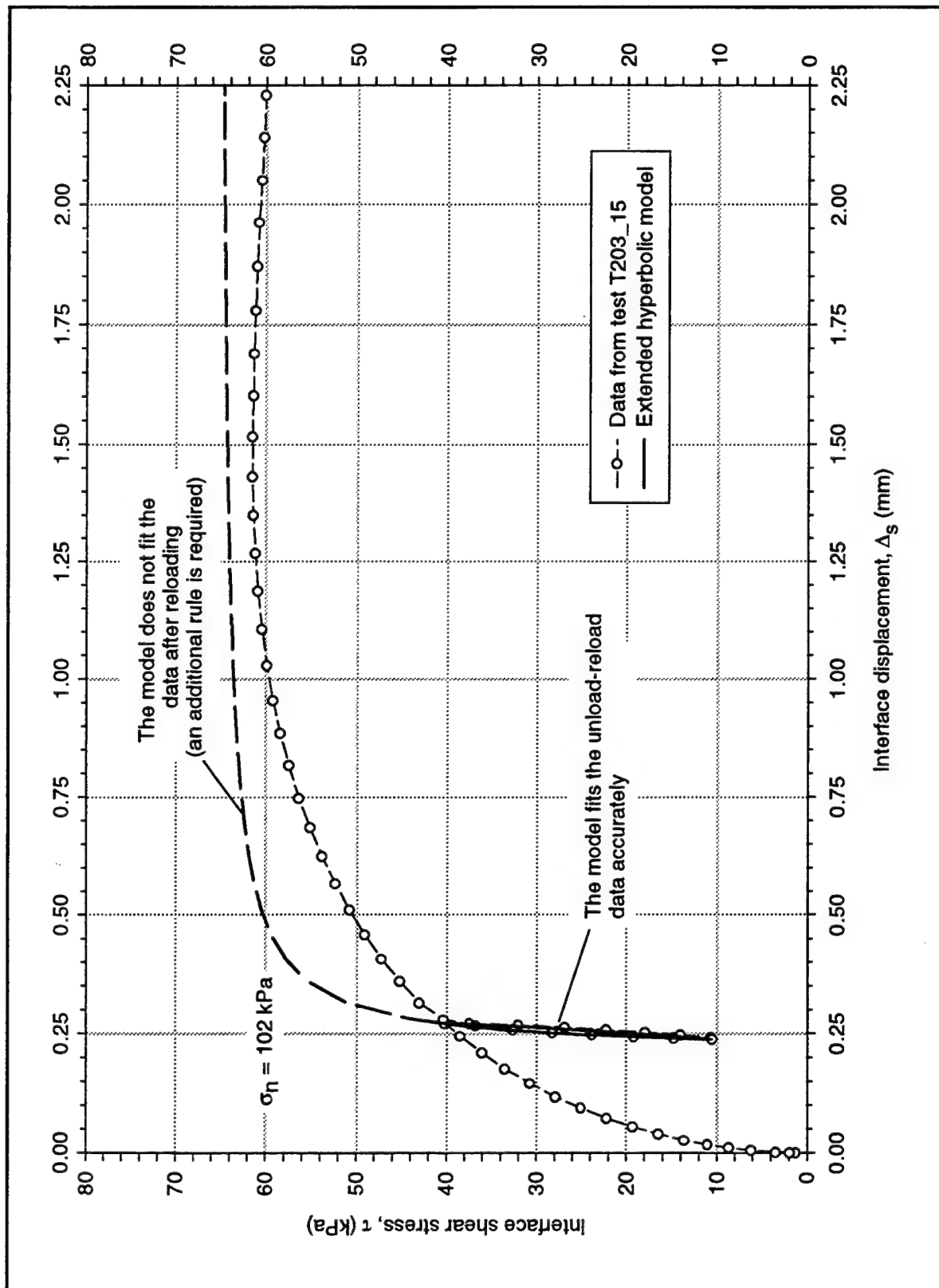


Figure 4-18. Comparison between the β -formulation of the extended hyperbolic model and unload-reload data from test T203_15

4.4 Hyperbolic Model Extended to Staged Shear

As discussed in Chapter 1, the soil-structure interface in a lock wall may be subjected to simultaneous changes of shear and normal stresses, which may occur during placement of the backfill and operation of the lock. In this investigation, the hyperbolic formulation by Clough and Duncan (1971) has also been extended to cases of staged shear where the normal pressure *increases* during shear.

4.4.1 Formulation

Figure 4-19 shows a hypothetical case where the interface is initially sheared, under a normal stress σ_1 , to a point S with coordinates (Δ_{st}, τ_{st}) in the shear stress-displacement plane. At point S , the normal stress is increased instantaneously to a final value σ_2 . A set of relative coordinate axes has been defined at point S . If the response of the interface to shearing beyond point S is assumed to be hyperbolic, a derivation, similar to that presented in the previous sections, yields the following expression:

$$\tau = \tau_{st} + \frac{|\Delta_s - \Delta_{st}|}{\frac{1}{K_{lst} \cdot \gamma_w \cdot \left(\frac{\sigma_n}{p_a}\right)^{n_{st}}} + \frac{R_{fst} \cdot |\Delta_s - \Delta_{st}|}{\alpha_{st} \cdot \sigma_n \cdot \tan \delta}} \quad (4-25)$$

where

K_{lst} = stiffness number

n_{st} = stiffness exponent

R_{fst} = failure ratio

The parameters are valid for staged shear of the interface as denoted by the subscript *st*. The nondimensional scaling factor α_{st} is defined as:

$$\alpha_{st} = |1 - SL_{st}| \quad (4-26)$$

where SL_{st} is the stress level determined after the increase of normal stress from σ_1 to σ_2 .

The hyperbolic model extended to staged shear is represented by Equations 4-25 and 4-26. It may be noted that comparing these expressions to Equations 4-18 and 4-22 shows that the formulations for unload-reload and staged shear are mathematically identical. The hyperbolic parameters for staged shear, however, differ from the unload-reload parameters as described in the following section.

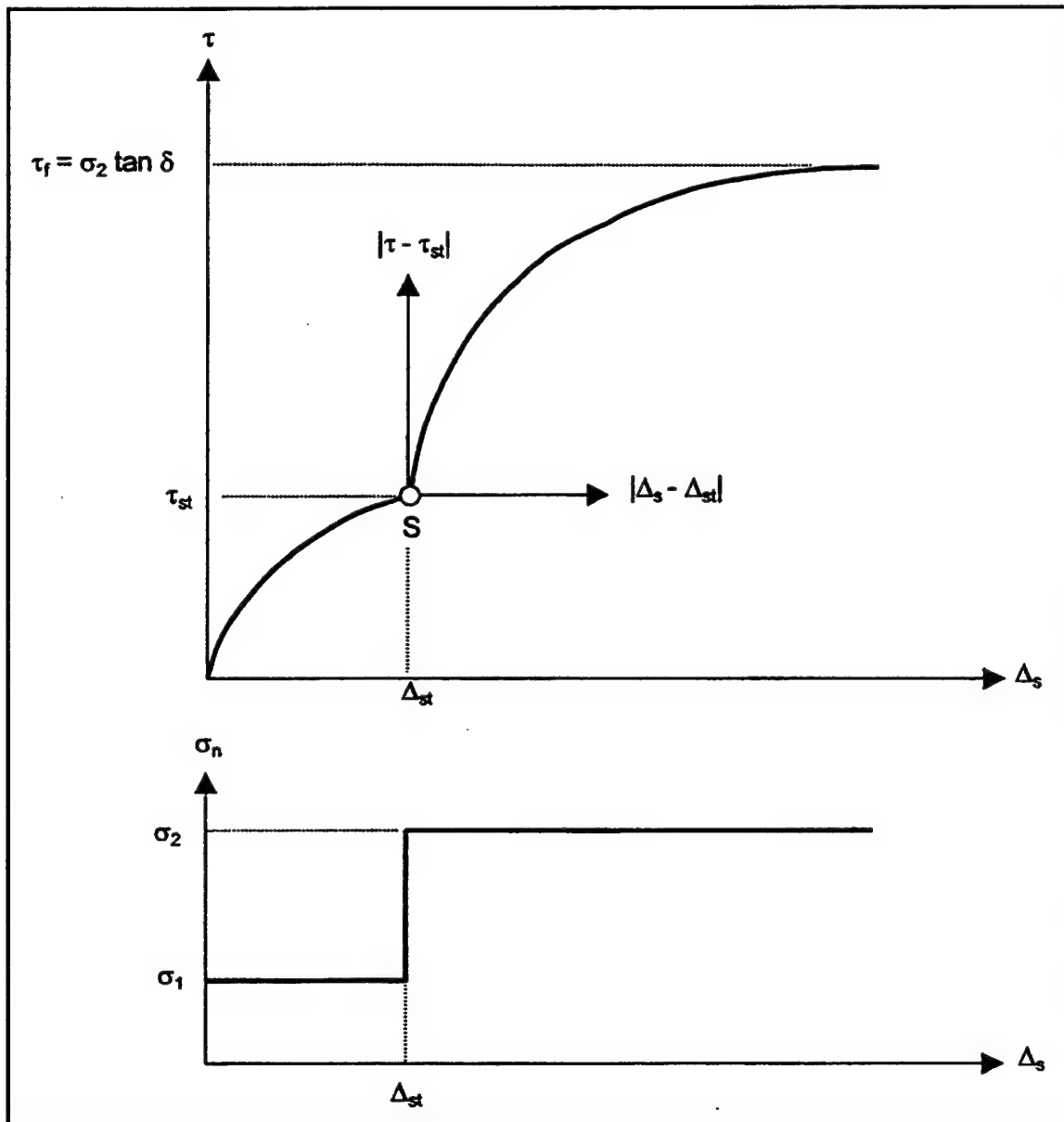


Figure 4-19. Definition of relative coordinate axes in staged shear

4.4.2 Hyperbolic parameters for staged shear

Some guidelines are presented in Figure 4-20 for the selection of the hyperbolic parameters in staged shearing. If the pressure increment is applied *before* mobilization of the peak strength, the following expressions may be used:

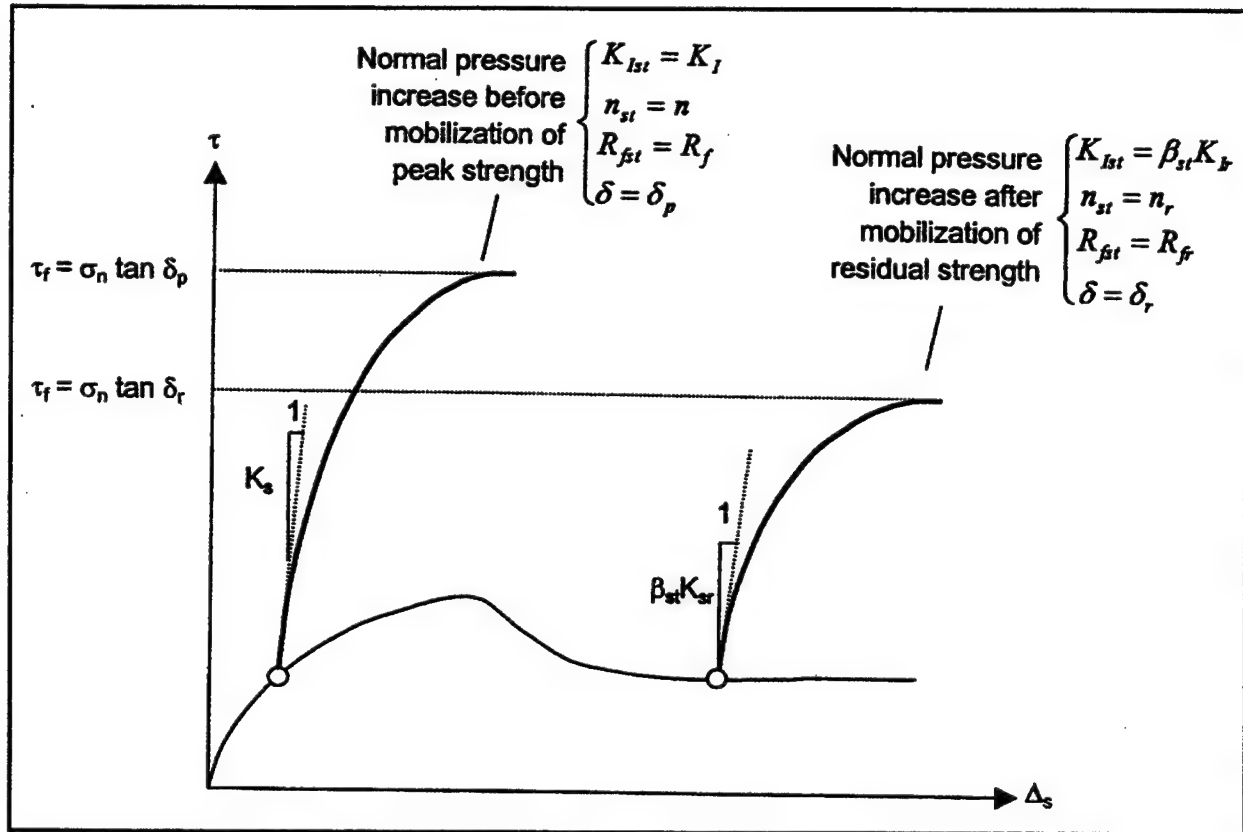


Figure 4-20. Guidelines for selection of parameters for hyperbolic model extended to staged shear

$$\begin{aligned}
 K_{fst} &= K_I \\
 n_{st} &= n \\
 R_{fst} &= R_f \\
 \delta &= \delta_p
 \end{aligned}
 \tag{4-27}$$

If the normal stress is increased *after* mobilization of the residual strength, the following expressions may be used:

$$\begin{aligned}
 K_{fst} &= \beta_{st} K_{Ir} \\
 n_{st} &= n_r \\
 R_{fst} &= R_{fr} \\
 \delta &= \delta_r
 \end{aligned}
 \tag{4-28}$$

where β_{st} is a nondimensional coefficient with no physical meaning and is used only to adjust the value of K_{Ir} according to the actual initial stiffness observed in the tests.

4.4.3 Evaluation of the model against results of staged tests

A comparison between the interface response predicted by the model and the results of the staged shear tests described in Chapter 3 is presented in Figures 4-21 through 4-25. Figures 4-21 and 4-22 show the data from staged tests where the pressure increment was applied before mobilization of the peak strength. Following Equation 4-27, the hyperbolic interface response was calculated using the parameters for initial loading in Table 4-1.

Figures 4-23 through 4-25 show the data from staged tests where the increment in normal stress was applied after mobilization of the residual strength. According to Equation 4-28, the stress-displacement response from the model was calculated using the hyperbolic parameters from Table 4-3. The value adopted for the nondimensional coefficient β_{st} found by trial and error, was $\beta_{st} = 5$.

It may be observed that the model provides a good fit to the data from all the tests. The analyses performed showed that the parameters from either the 70-95% criterion or the SID criterion may be introduced in Equations 4-27 and 4-28; in both cases, the results obtained were reasonable. The 70-95% parameter values were used to generate the model curves in Figures 4-21 through 4-25.

For comparison, the type of interface response commonly assumed in SSI analyses is also presented in Figures 4-21 through 4-25. The traditional model yields an interface response that is softer than the actual response observed in the tests. Consequently, the predicted displacements are larger than the measured displacements.

4.5 Advantages and Limitations of the Extended Hyperbolic Model

The extended hyperbolic formulation presented in previous sections provides a reasonable estimate of the response of the Density Sand-to-concrete interface under unloading-reloading and staged shear. The model conveys important aspects of the behavior of the interface, and provides a more accurate estimate of the interface response under those types of loading than the Clough and Duncan (1971) hyperbolic formulation.

The hyperbolic parameters for the model may be determined from simple interface tests. For loading such as one unloading-reloading cycle or staged shear applied before the mobilization of the peak strength, only the hyperbolic parameter values for monotonic initial loading of the interface are required. These can be determined from simple interface tests or can be found in published databases (e.g., Peterson et al. 1976). For the cases of unloading-reloading and staged shear applied after mobilization of the residual strength, some additional information

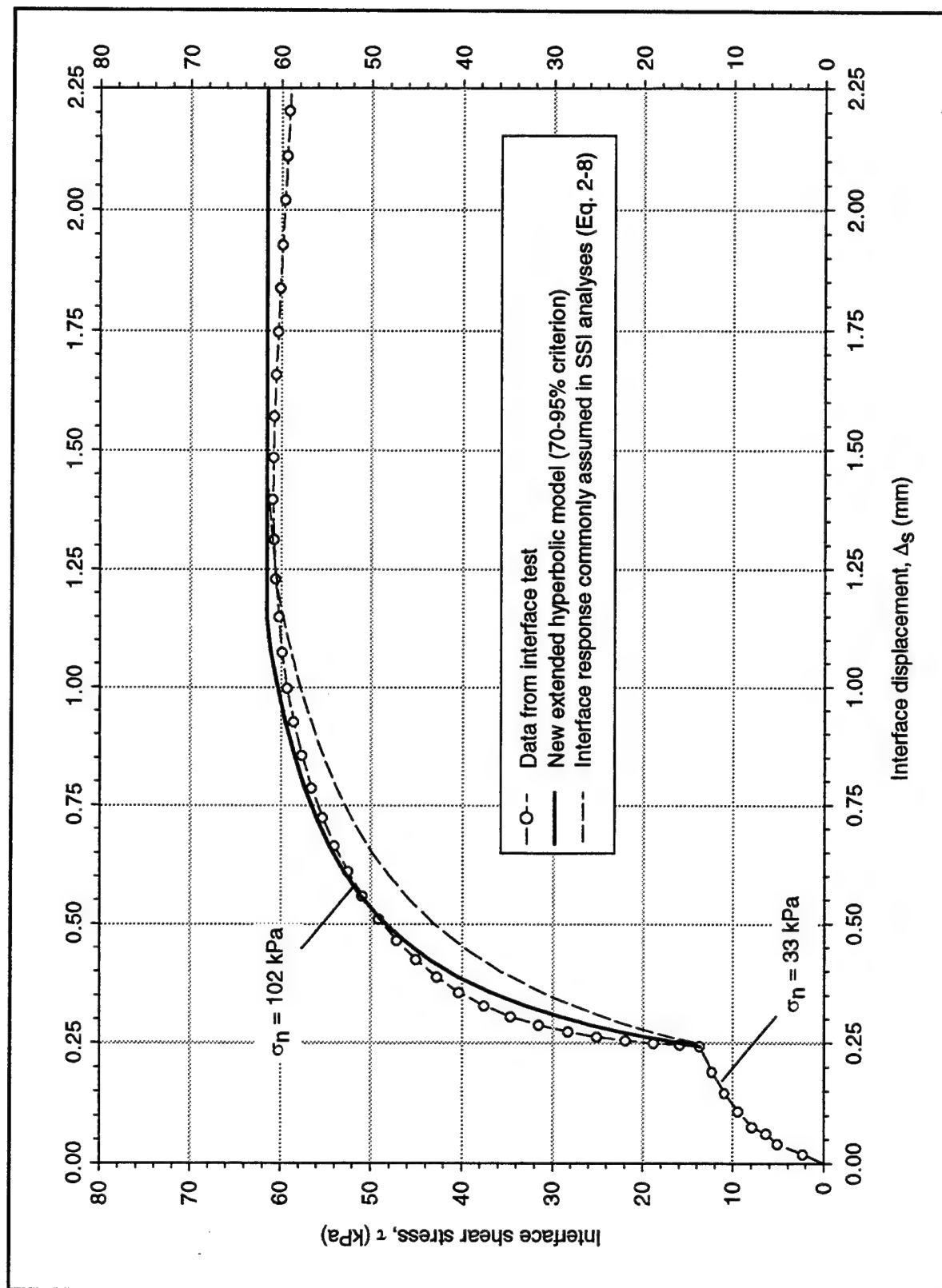


Figure 4-21. Comparison between the extended hyperbolic model and data from staged test T106_15

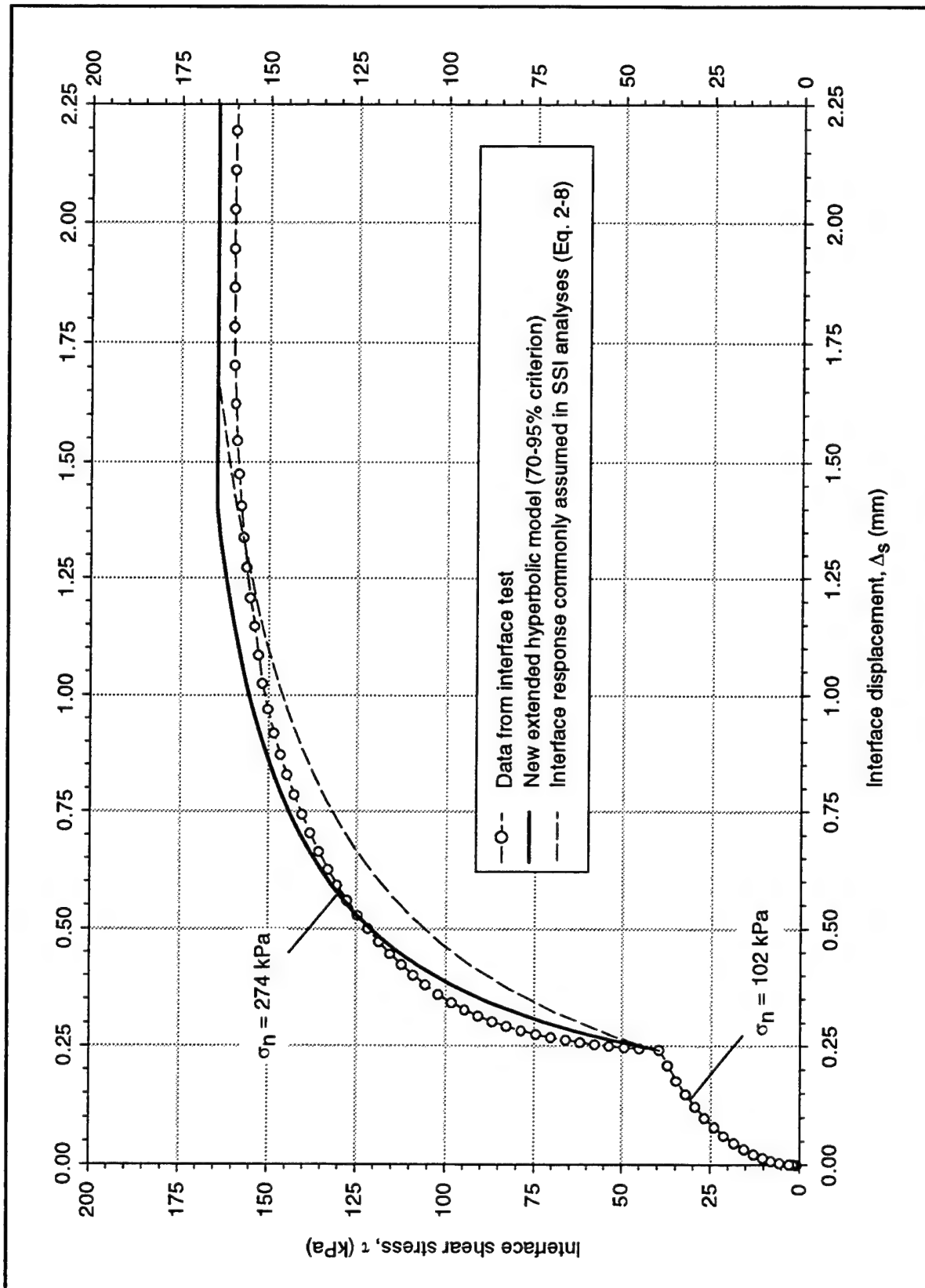


Figure 4-22. Comparison between the extended hyperbolic model and data from staged test T105_40

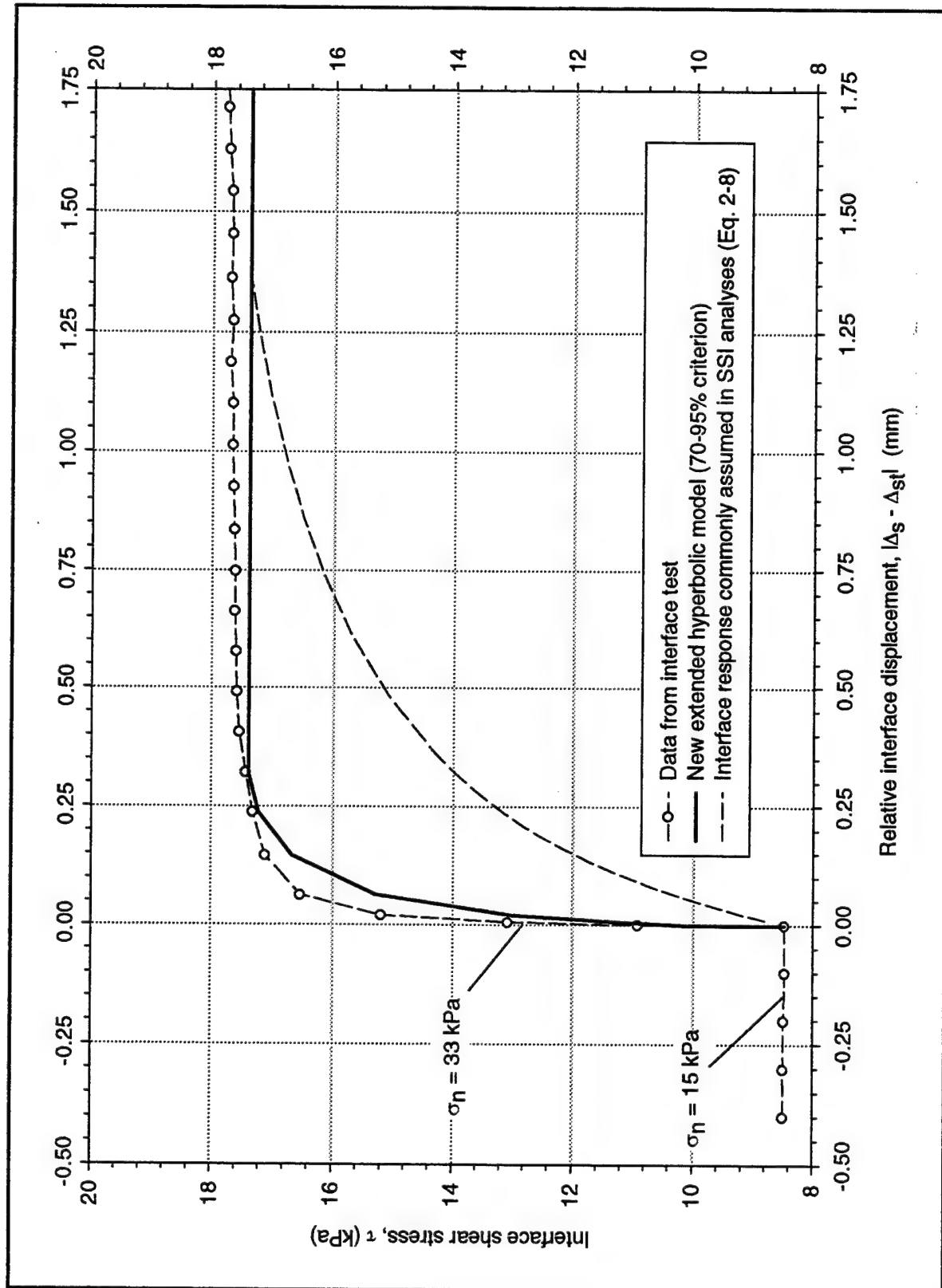


Figure 4-23. Comparison between the extended hyperbolic model and data from staged test T101_5

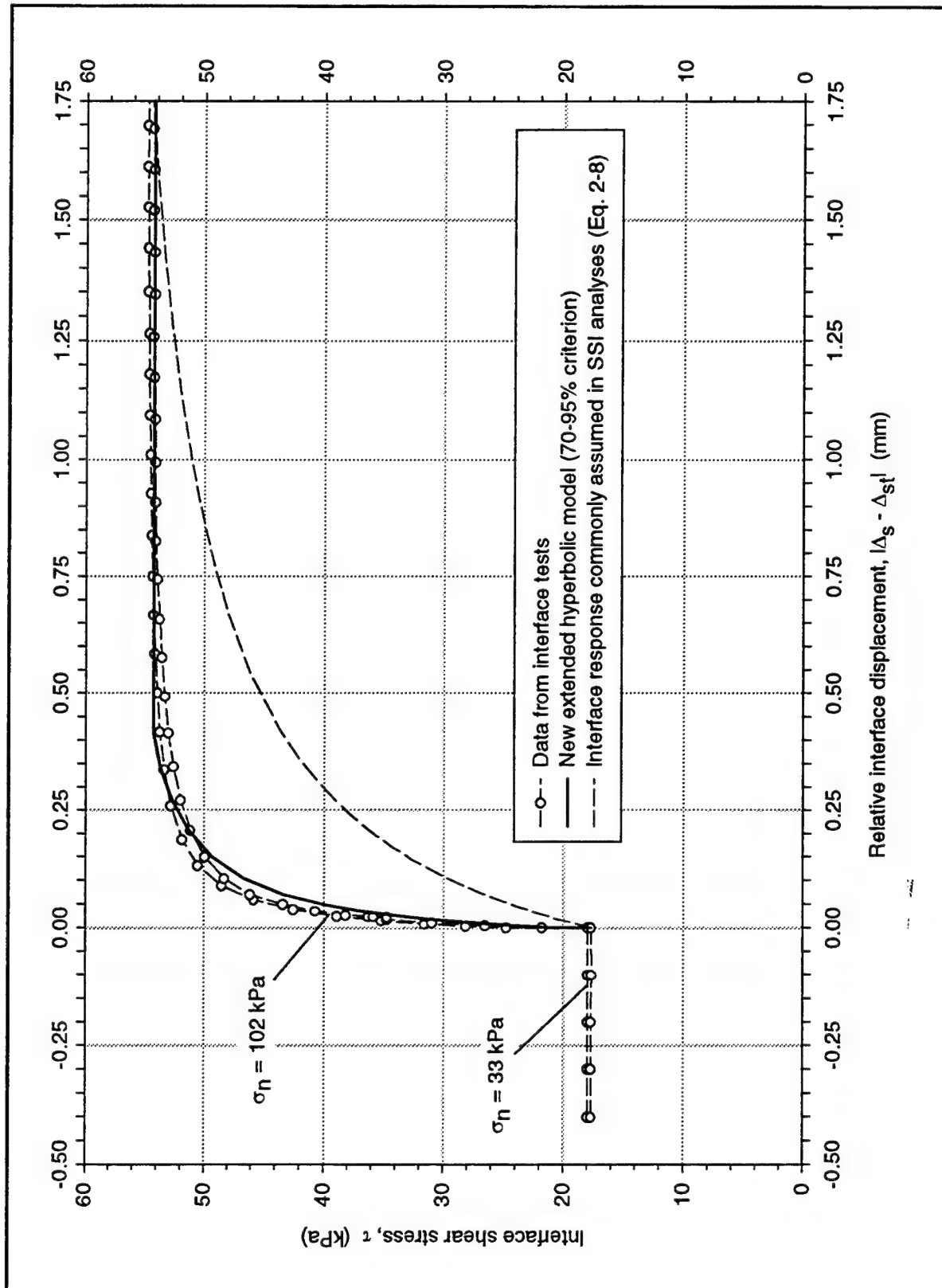


Figure 4-24. Comparison between the extended hyperbolic model and data from staged tests T101_15 and T102_15

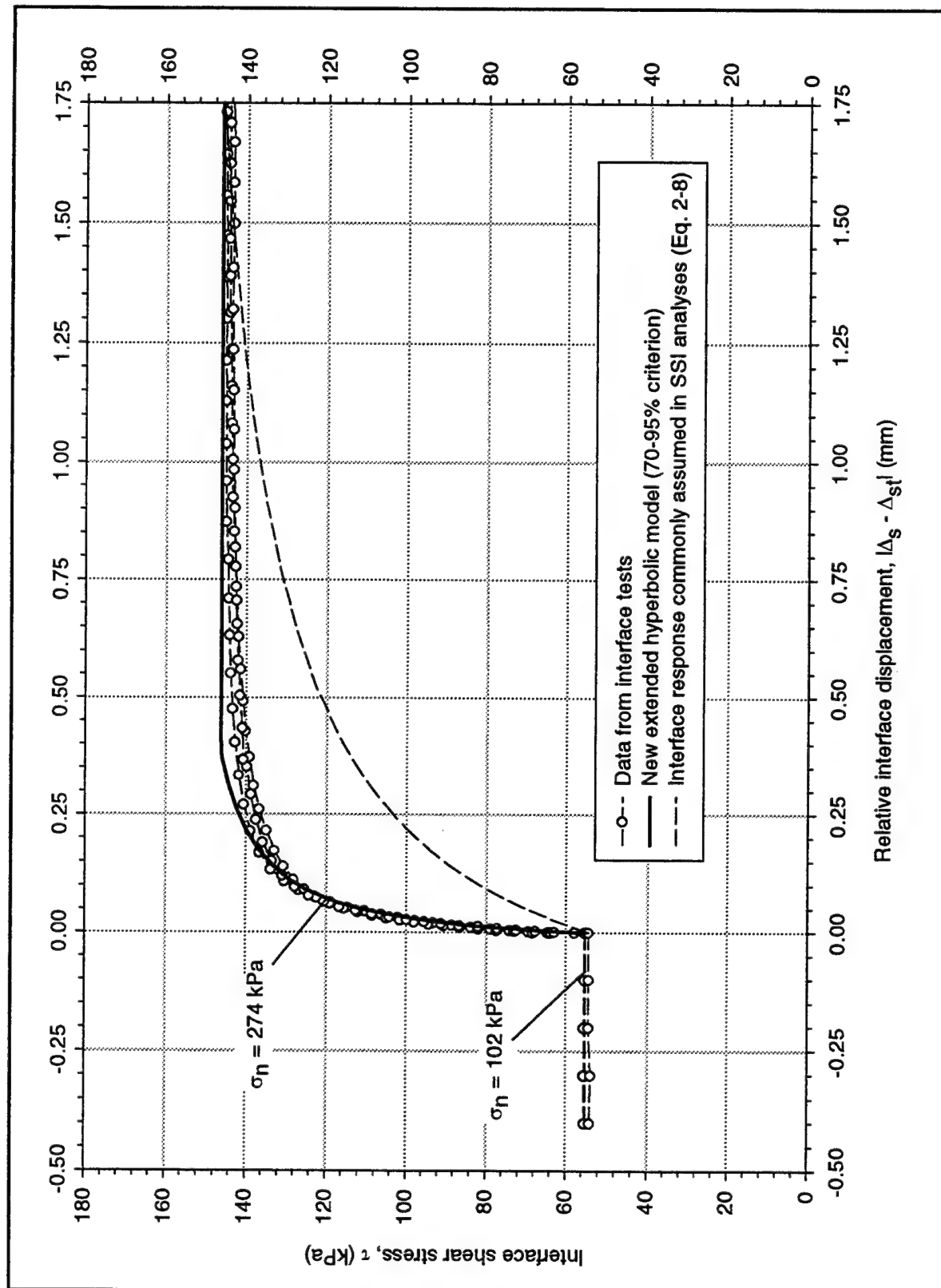


Figure 4-25. Comparison between the extended hyperbolic model and data from staged tests T101_40, T102_40, and T103_40

from the interface tests is required for application of the extended hyperbolic model.

It was noted that the interface response measured in the tests does not follow exactly a hyperbolic shear stress-displacement relationship. If the hyperbolic parameters determined from the SID criterion are used, the model appears to provide reasonable answers for the types of loading considered in the tests. However, it may be inaccurate for other cases, such as repeated unloading-reloading of the interface. The optional β -formulation presented may be useful for modeling repeated unloading-reloading, but there are not enough experimental data to assess its practical applicability.

In lock walls during backfill placement or operation of the lock, the normal stresses may change continuously during shear of the interface. Although the model provides a reasonable estimation of interface response under staged shear, where the normal stress increases instantaneously in a large increment, it has not been evaluated against results of tests where more continuously increasing normal stress is applied. For continuous change in normal stress, the extended hyperbolic model would continuously adjust the value of K_{si} to the initial shear stiffness value K_{si} calculated for the normal stress applied at each instant. Since the initial shear stiffness increases with increasing normal stress, it follows that the resulting shear stress-displacement response given by the model will present an upward concavity. Additional testing will be performed in the next phase of this investigation to determine the actual interface response to such loading conditions.

The extended hyperbolic model does not apply to cases of staged shear where the normal stress decreases during shear. Further testing is required to determine the interface response to this type of loading.

Finally, the model has not been evaluated against the results of tests performed on other interfaces, nor has it been implemented for SSI analyses of lock walls. Therefore, the extended hyperbolic model, as described in this report, must be considered preliminary and subject to further improvements.

4.6 Summary

A preliminary version of an extended hyperbolic formulation for interfaces was developed during this investigation. It is based on the hyperbolic model developed by Clough and Duncan (1971), which was extended to shear stress reversals, unload-reload, and staged shear. A summary of the formulation and its application is presented in Figure 4-26. The extended hyperbolic formulation was evaluated against the results of interface tests performed on the Density Sand-to-concrete interface, which were described in Chapter 3. It appears to provide a reasonable estimate of interface response under the types of loading considered.

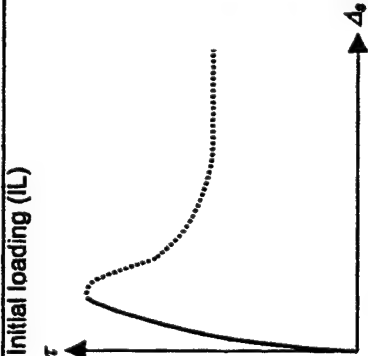
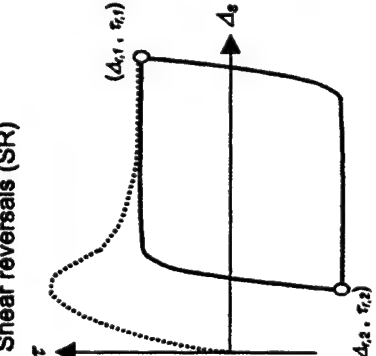
| Type of loading | Formulation of the model | Determination of hyperbolic parameters |
|--|---|---|
| <p>Initial loading (IL)</p>  | $\tau = \frac{\Delta_s}{\frac{1}{K_I \cdot \gamma_w \cdot \left(\frac{\sigma_z}{p_a}\right)^n} + \frac{R_I \cdot \Delta_s}{\sigma_n \cdot \tan \delta}}$ <p>This is the original Clough and Duncan (1971) hyperbolic formulation for interfaces. It is only applicable to initial loading.</p> | <ul style="list-style-type: none"> Hyperbolic parameters K_I, n, R_I, and δ_s must be determined from initial loading tests using either the 70-95% criterion or the SID criterion as described in this chapter. Use the SID parameter values for modeling interface response to initial loading when the stress level is not expected to exceed 50% during shear. Use the 70-95% parameter values for modeling interface response to initial loading when the stress level is expected to exceed 50% during shear. |
| <p>Shear reversals (SR)</p>  | $\tau = \tau_{r,i} \pm \frac{ \Delta_s - \Delta_{r,i} }{1 + \frac{R_p \cdot \Delta_s - \Delta_{r,i} }{K_{rp} \cdot \gamma_w \cdot \left(\frac{\sigma_z}{p_a}\right)^n} + 2 \cdot \sigma_n \cdot \tan \delta_r}$ <p>This formulation is applicable to the i^{th} shear reversal applied at the point of coordinates $(\Delta_{r,i}, \tau_{r,i})$ in the shear stress-displacement plane. This type of loading is a particular case of unloading-reloading after mobilization of the residual strength where the scaling factor α is 2</p> | <ul style="list-style-type: none"> Hyperbolic parameters K_{rp}, n, R_p, and δ must be determined from shear reversal tests using either the 70-95% criterion or the SID criterion. Use the SID parameter values for modeling interface response to shear reversal when the relative stress level is not expected to exceed 50% during shear. Use the 70-95% parameter values for modeling interface response to shear reversal when the relative stress level is expected to exceed 50% during shear. |
| <p>Symbols:</p> <p>Stresses and displacements: Δ_s = interface displacement τ = interface shear stress σ_n = normal stress on interface</p> | <p>Constants: γ_w = unit weight of water p_a = atmospheric pressure</p> | <p>Hyperbolic parameters: K_I; K_{rp}; K_{Iw}; K_{Ist} : stiffness number n; n_r; n_w; n_{st} : stiffness exponent R_I; R_p; R_{Iw}; R_{Ist} : failure ratio δ; δ_s : interface friction angle (subscripts denote type of loading)</p> <p>Subscripts: r : shear reversals ur : unloading-reloading st : staged shear</p> |

Figure 4-26. Summary of the extended hyperbolic model and its application to different types of loading (continued)

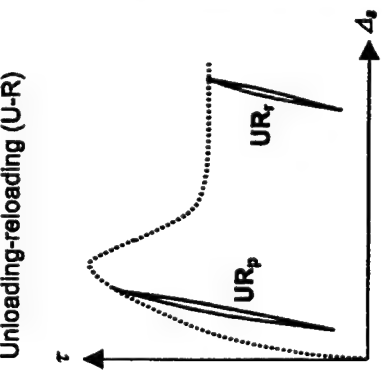
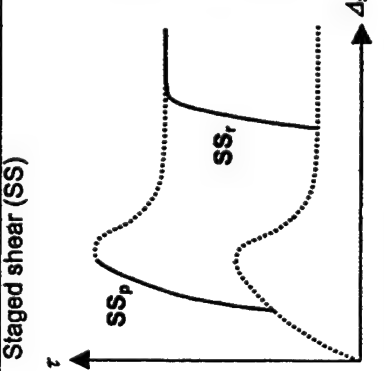
| Type of loading | Formulation of the model | Determination of hyperbolic parameters |
|---|---|---|
|  | $\tau = \tau_o \pm \frac{ \Delta_s - \Delta_o }{1 + \frac{R_{ur} \cdot \Delta_s - \Delta_o }{K_{ur} \cdot \gamma_w \cdot \left(\frac{\sigma_n}{p_n}\right)^{n_{ur}}}} + \alpha \cdot \sigma_n \cdot \tan \delta$ $\alpha = \pm 1 - SL_{ur}$ <p>This formulation applies to unloading or reloading cycles such as UR_p and UR_r. For repeated unload-reload cycles use the optional β-formulation (Figure 4-27) Δ_o and τ_o are the coordinates of the last unload or reload point in the shear stress-displacement plane. SL_{ur} is the stress level at the last unload or reload point</p> | <ul style="list-style-type: none"> UR_p: Determine SID hyperbolic parameters from IL tests $\begin{cases} K_{ur} = K_l \\ n_{ur} = n \\ R_{ur} = R_f \\ \delta = \delta_p \end{cases}$ UR_r: Determine SID hyperbolic parameters from SR tests $\begin{cases} K_{ur} = K_{lr} \\ n_{ur} = n_r \\ R_{ur} = R_{fr} \\ \delta = \delta_r \end{cases}$ |
|  | $\tau = \tau_{st} + \frac{ \Delta_s - \Delta_{st} }{1 + \frac{R_{st} \cdot \Delta_s - \Delta_{st} }{K_{st} \cdot \gamma_w \cdot \left(\frac{\sigma_n}{p_n}\right)^{n_{st}}}} + \alpha_{st} \cdot \sigma_n \cdot \tan \delta$ $\alpha_{st} = 1 - SL_{st} $ <p>This formulation applies to staged shear such as SS_p and SS_r, where the normal pressure is increased instantaneously. Δ_{st} and τ_{st} are the coordinates of the point in the shear stress-displacement plane at which the normal pressure is increased. SL_{st} is the stress level when the normal pressure is increased. σ_n is the final value of normal stress</p> | <ul style="list-style-type: none"> SS_p: Determine 70-95% or SID hyperbolic parameters from IL tests $\begin{cases} K_{st} = K_l \\ n_{st} = n \\ R_{st} = R_f \\ \delta = \delta_p \end{cases}$ SS_r: Determine 70-95% or SID hyperbolic parameters from SR tests $\begin{cases} K_{st} = \beta_{st} K_{lr} \\ n_{st} = n_r \\ R_{st} = R_{fr} \\ \delta = \delta_r \end{cases}$ β_{st} is determined from SS_r tests |
| General remarks: <ul style="list-style-type: none"> The extended hyperbolic formulation does not model the displacement softening behavior observed during the interface tests For repeated unload-reload cycles the optional β-formulation should be applied (Figure 4-27) The extended hyperbolic formulation does not model the interface response under a reduction in the normal stress during shear Upon unloading, reloading, or staged shear, applied before mobilization of the peak strength, the model assumes an initial interface stiffness equal to the initial interface stiffness on initial loading, which is given by: $K_{st} = K_l \cdot \gamma_w \cdot \left(\frac{\sigma_n}{p_n}\right)^n$ (Clough and Duncan 1971) Upon unloading, reloading, or staged shear, applied after mobilization of the residual strength, the model assumes an initial interface stiffness equal to the initial shear stiffness upon shear reversal, which is given by: $K_{st} = K_{lr} \cdot \gamma_w \cdot \left(\frac{\sigma_n}{p_n}\right)^{n_r}$ | | |

Figure 4-26. (Concluded)

A new criterion for determination of the hyperbolic parameters was included in the extended hyperbolic model. This new SID criterion yields an estimate of initial shear stiffness that is closer to the actual initial shear stiffness observed in the tests. It is particularly useful for unload-reload cases, where the hyperbolic parameters determined using the 70-95% procedure yield inaccurate answers. It is anticipated that a simple correlation may be obtained between the SID parameters and the traditional 70-95% parameters. This would allow the use of the hyperbolic parameters from published databases in the new formulation.

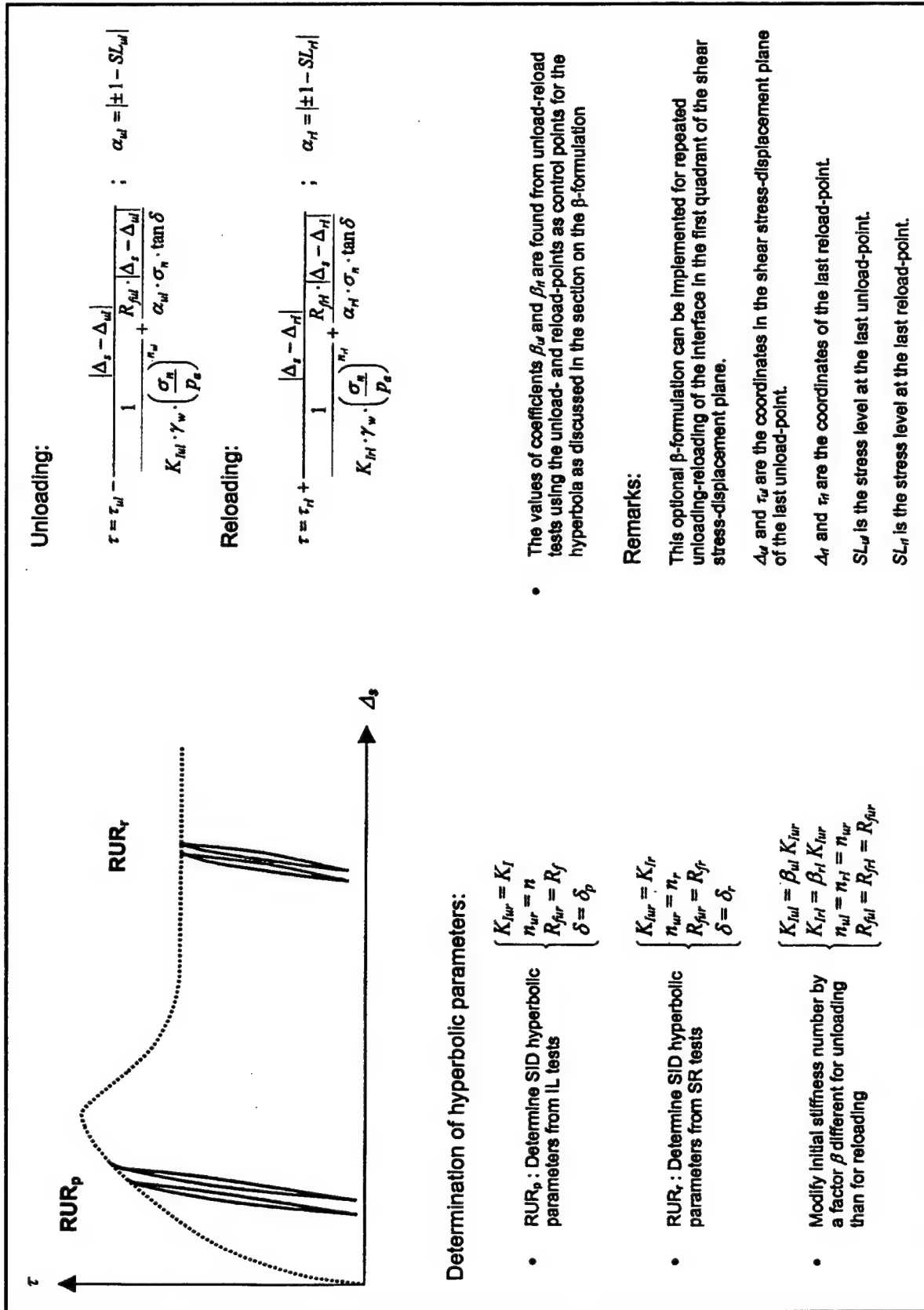
Although the model provides reasonable results for cases in which one unload-reload cycle is applied, it is not believed to be accurate for cases of repeated unloading-reloading. The optional β -formulation (Figure 4-27), also developed during this investigation, may provide accurate answers for this type of loading. However, there are still not enough experimental data for calibration and evaluation of this formulation.

The extended hyperbolic model gives reasonable estimates of interface response in cases of staged shear, where finite normal stress increments are applied instantaneously during shear. It is more accurate than the type of interface response commonly assumed in SSI analyses. However, its performance has not been evaluated against results of tests in which the normal stress is increased continuously during shear.

The following are main limitations of the extended hyperbolic model:

- a.* The stress-displacement interface response is assumed to be hyperbolic.
- b.* It does not model the postpeak displacement softening behavior observed during the interface tests.
- c.* It has not been tested under loading paths with continuously increasing normal stress.
- d.* It does not model staged shear with reductions in normal stress.

The extended hyperbolic model is still in its initial stages of development. Further testing is required to evaluate the performance of the model for other types of interfaces. Additionally, implementation of the proposed model in SSI analyses of lock walls is required for a complete assessment of the issues related to practical applications of the formulation.

Figure 4-27. Summary of the optional β -formulation for repeated unload-reload cycles in the first quadrant

5 Summary and Conclusions

Earth retaining structures such as lock walls may be subjected to a significant downdrag force that is generated during placement of the backfill and acts on the backfill-to-structure interface. This downdrag force has a stabilizing effect that could produce substantial economies if accounted for in the design of the lock wall. The accurate estimation of the downdrag force requires an appropriate model for the response of the backfill-to-structure interface to the type of loading applied during placement of the backfill, inundation of the lock, and subsequent operational stages.

The hyperbolic formulation developed by Clough and Duncan (1971) has been used extensively in SSI analyses for modeling the interface response under monotonic loading. However, it is not applicable to cases where the interface undergoes unloading-reloading or simultaneous changes in shear and normal stresses such as in the backfill-to-structure interface in lock walls. In this investigation, an extended hyperbolic formulation was developed that can model the interface response under initial loading, unloading-reloading, reversal in the direction of shear, and staged shear.

The performance of the extended hyperbolic model was evaluated against the results of a series of interface tests performed for this investigation. It was found that the model provides an accurate approximation of the interface response. However, this formulation is in its initial stages of development; it must be validated against the results of additional tests on several types of interfaces, and must be implemented in SSI analyses to verify its applicability.

This chapter summarizes the activities performed for this phase of the investigation. Additionally, some conclusions are presented on the advantages and limitations of the extended hyperbolic model, as well as recommendations regarding the work to be performed during the final phase of this research.

5.1 Summary of Activities

This section summarizes all the activities completed for this Phase 1 report. It is divided into three subsections: literature review, laboratory testing, and the extended hyperbolic model.

5.1.1 Literature review

The literature review focused on previous work concerning relevant issues for this phase of the investigation: interface testing, interface modeling, and SSI analyses of retaining walls. It will be extended as needed for the final report.

In the experimental work reviewed, the direct shear box (DSB) device and the direct simple shear (DSS) device are used most frequently in sand-to-concrete and sand-to-steel interface testing. All the testing devices described in the literature present interface sizes that range from 105 by 105 mm to a maximum of 305 by 305 mm. The smaller interface sizes may induce errors in the determination of the prepeak interface response due to end effects, and do not allow the determination of the residual interface strength in all cases. The Large Direct Shear Box (LDSB) at Virginia Tech allows testing of interfaces as large as 711 by 406 mm under monotonic or cyclic shear. The size of the interface minimizes end effects and permits maximum interface displacements of 305 mm, allowing the determination of the residual interface strength. The large displacement capabilities of the LDSB also make possible shearing of the interface in several stages with changing normal stress.

Most of the previous work on interface testing corresponds to monotonic shear of the interface under constant normal stress. Only a few interface tests that include unloading-reloading of the interface under constant normal stress have been reported. No test results are available on interface response under staged shear.

The hyperbolic model by Clough and Duncan (1971) has been commonly implemented in the Goodman, Taylor, and Brekke (1968) joint element formulation for modeling the interface response to monotonic shear under constant normal stress. It is a simple model that conveys important aspects of interface behavior using parameters that have physical meaning. However, it does not provide accurate approximations to interface response under cyclic loading or staged shear. None of the other interface models found in this literature review accounts for simultaneous changes in shear and normal stresses.

Most of the studies on SSI analyses of lock walls that were reviewed for this report conclude that the downdrag force, acting on the back of a retaining wall, may contribute significantly to the stability of the structure. In typical lock walls, the downdrag develops as a consequence of fill placement. During fill placement, the shear and normal stresses acting on the backfill-to-structure interface are changing simultaneously. During submergence and operation of the lock, the shear stresses may be reduced or even reversed. Hence, it is important to model accurately the interface response under staged shear, unloading-reloading, and shear reversals.

A simplified method (Appendix F in HQUSACE 1997) to estimate the downdrag force was described. The simplified method is useful to illustrate the importance of an adequate estimation of the downdrag force in design.

5.1.2 Laboratory testing

The following laboratory and field activities were performed during this phase of the investigation:

- a. Modifications to the LDSB.
- b. Design and construction of a soil box and concrete slab.
- c. Selection of the sand for interface tests.
- d. Grain size distribution, minimum/maximum density, and triaxial testing on the Density Sand.
- e. Field survey of existing concrete retaining walls to determine a range of representative surface textures for the concrete specimen.
- f. Development of appropriate testing procedures.
- g. Interface testing following stress paths that model field conditions in lock walls.

The LDSB was modified specifically to accommodate soil-to-concrete interfaces, and a special aluminum soil box was designed and constructed that allows compaction of the sand sample directly onto the concrete specimen. A concrete specimen was prepared with surface features that are representative of field conditions observed during a survey of existing retaining walls. The concrete specimen is contained in a structural frame that minimizes its deformations during interface shear.

A fine, rounded, silica sand (Density Sand) was selected for interface testing. A series of laboratory tests were performed on this sand: minimum/maximum density, grain size analyses, specific gravity, and consolidated drained triaxial tests. A set of hyperbolic parameter values was developed for the Density Sand, based on the results of the triaxial tests. The parameter values obtained are consistent with those reported by Duncan et al. (1980) for a similar material.

An intensive interface testing program was carried out that included initial loading tests, staged shear tests, unload-reload tests, and shear reversal tests. The initial-loading interface tests were performed after compaction of the sample of Density Sand against the concrete specimen. The tests progressed until the residual strength was mobilized. Subsequently, reversal tests were performed on the interface, and the residual strength was mobilized in two directions of shear. In the staged shear tests, the normal pressure was increased in steps during shear. Staged shear tests were performed both before and after mobilization of the peak strength. Several unload-reload tests were performed, where a complete loading cycle was applied between two predetermined stress levels during initial loading of the interface.

The staged shear tests modeled field stress paths in which both normal and shear stresses change simultaneously. Both the reversal tests and the unload-reload tests were representative of field stress paths in which the shear stresses may be reduced, or even reversed, as a consequence of a rise of the water table behind a lock wall.

All the tests were performed on the dry interface between the concrete specimen and the Density Sand compacted to a relative density of approximately 75%. It was observed that the Density Sand undergoes dilation and strain softening during triaxial testing under all the confining pressures applied. Similarly, dilation and displacement softening take place during initial loading of the interface.

The peak interface strength is mobilized at small interface displacements that range between 0.5 and 2 mm. The residual interface strength is mobilized after a displacement of 5 to 15 mm. The initial loading tests yielded a peak interface friction angle of 31 degrees, which is approximately 72 percent of the peak internal friction angle of the sand ($\delta/\phi'_p = 0.72$).

The residual interface friction angle was approximately 28 degrees. The results of the shear reversal tests showed that the value of residual interface strength is not dependent on the direction of shear.

The results of the interface tests obtained were the basis for development of the extended hyperbolic formulation presented in Chapter 4. The extended hyperbolic formulation models the interface response under stress paths similar, but not identical, to those occurring at backfill-to-structure interfaces in lock walls.

5.1.3 Extended hyperbolic model

A preliminary version of an extended hyperbolic formulation for interfaces was developed during this investigation. It is based on the hyperbolic model developed by Clough and Duncan (1971), which was extended to shear stress reversals, unload-reload, and staged shear. A summary of the formulation and its application was presented in Figure 4-26. The extended hyperbolic formulation was evaluated against the results of interface tests performed on the Density Sand-to-concrete interface. It appears to provide a reasonable estimate of interface response under the types of loading considered.

A new criterion for determination of the hyperbolic parameter values was included in the extended hyperbolic model. It has been referred to as the small initial displacement criterion (SID) in this report and considers all the data points in the zero to 95 percent stress level range for the determination of the hyperbolic parameter values. The SID criterion yields an estimate of initial shear stiffness that is closer to the actual initial shear stiffness observed in the tests. It is particularly useful for unload-reload cases, where the hyperbolic parameter values determined using the 70-95% procedure yield inaccurate answers. It is

anticipated that a simple correlation may be obtained between the SID parameters and the traditional 70-95% parameters. This would allow the use of the hyperbolic parameters from published databases in the new formulation.

Although the model provides reasonable results for cases in which one unload-reload cycle is applied, it is not believed to be accurate for cases of repeated unloading-reloading. An optional β -formulation was also developed during this investigation that may provide accurate answers for this type of loading. However, there are still not enough experimental data for calibration and evaluation of this formulation.

The extended hyperbolic model gives reasonable estimates of interface response in cases of staged shear, where finite normal stress increments are applied instantaneously during shear. It is more accurate than the type of interface response commonly assumed in SSI analyses. However, its performance has not been evaluated against results of tests in which the normal stress is increased continuously during shear.

The model presents some important limitations: (a) the stress-displacement interface response is assumed to be hyperbolic, (b) it does not model the post-peak displacement softening behavior observed during the interface tests, (c) it has not been evaluated for conditions of continuously increasing normal stress, and (c) it does not model staged shear with reductions in normal stress.

The extended hyperbolic model is still in its initial stages of development. Further testing is required to evaluate the performance of the model for other types of interfaces. Additionally, implementation of the proposed model in SSI analyses of lock walls is required for a complete assessment of the issues related to practical applications of the formulation.

5.2 Conclusions

The downdrag force acting on a retaining structure such as a lock wall often has an important stabilizing effect on the structure, and it should be accounted for in design. The estimation of the magnitude of the downdrag requires an accurate modeling of the backfill-to-structure interface under the loading conditions occurring in the field.

The extended hyperbolic formulation developed for this Phase 1 report allows modeling of the interface under staged shear, unloading-reloading, and shear reversals. The formulation is simple and the model parameter values can generally be determined from a few interface tests in a straightforward manner. Based on the results of the interface tests performed for this investigation, it was found that the model provides an accurate approximation of the measured response of the Density Sand-to-concrete interface.

This extended hyperbolic model is in its initial stages of development and requires further evaluation against the results of additional tests on other types of

interfaces. The extended hyperbolic formulation does not model staged shear with reductions in normal stress, nor does it model the displacement softening behavior observed in the tests. There are also some questions regarding the accuracy of the interface response predicted by the model under field loading conditions where the normal stress increases continuously during shear and not in finite steps as in the interface tests. Furthermore, the model must be implemented in SSI analyses of retaining walls to assess its applicability and accuracy in practical situations.

5.3 Recommended Work

The development of a complete version of the extended hyperbolic model requires some additional work consisting of (a) additional laboratory interface tests on the same and different types of interfaces, (b) validation of the preliminary version of the model against the results of these tests, (c) implementation of the extended hyperbolic model in an SSI analysis program, and (d) use of the SSI program to evaluate the applicability and accuracy of the new interface model for analysis of retaining walls.

It is recommended that additional laboratory interface tests be performed for the final phase of this investigation, including the following: tests on the Density Sand-to-concrete interface where the normal pressure is increased continuously and not by steps, staged tests where the normal stress is reduced during shear, and tests on other types of interfaces.

Tests with continuous increase in normal pressure would allow the evaluation of the performance of the extended hyperbolic formulation when modeling interface response under field loading conditions in lock walls. It is anticipated that some modifications to the model presented in this report would result from such tests.

The interface response under a reduction of the normal stress during shear has not been studied at this point. It is, however, an important issue for SSI analysis of lock walls, where oscillations in the water table behind the wall may induce a simultaneous decrease in the shear and normal stresses at the backfill-to-structure interface. Interface tests may be performed to study the interface response of the Density Sand-to-concrete interface under this type of loading.

The extended hyperbolic model should be validated against other types of interfaces. Additional tests can be performed on the Density Sand-to-concrete interface in which the sand will be compacted to a medium dense condition. Tests can be carried out on the interfaces between concrete and sands of different angularity and gradation. For each of the sands to be used in the interface tests, a complete set of laboratory tests should be performed that includes grain size gradation, minimum/maximum density, and consolidated drained triaxial tests. A final version of the extended hyperbolic model would be developed based on the results of these additional interface tests. Additionally, a database of hyperbolic

parameters can be created to allow the implementation of the extended hyperbolic model in SSI analyses of lock walls.

It is recommended that the final version of the extended hyperbolic model be implemented in an SSI computer program such as SOILSTRUCT. The computer program could then be used in analyses of retaining walls. A test can be performed in the Instrumented Retaining Wall Facility (IRW) at Virginia Tech where a sandy backfill is compacted in lifts and then inundated. The vertical and horizontal forces acting on the wall are measured, and their values compared to the results obtained from implementation of the model in SSI analyses of the IRW. The accuracy of the model and the issues regarding its practical implementation in SSI analyses may be evaluated based on the results of such a test.

It is anticipated that additional analyses will be performed for some typical cases of Corps of Engineers lock walls, using the extended hyperbolic model. The results of these analyses may be compared to those obtained using the simplified procedure (HQUSACE 1994) described in Chapter 2 of this report. This may allow the implementation of some additions to this simplified procedure for a more accurate design without the need of sophisticated SSI analyses.

References

- Acar, Y. B., Durgunoglu, H. T., and Tumay, M. T. (1982). "Interface properties of sand," *Journal of the Soil Mechanics and Foundations Division*, ASCE, 108(GT4), 648-654.
- American Society for Testing and Materials. (1990). "Standard test method for classification of soils for engineering purposes," Practice No. D2487-90, *1990 Book of ASTM Standards*, 04.08, Philadelphia, PA.
- _____. (1991). "Standard test method for minimum index density and unit weight of soils and calculation of relative density," ASTM D4254-91, West Conshohocken, PA.
- _____. (1992). "Standard test method for specific gravity of soils," ASTM D854-92, West Conshohocken, PA.
- _____. (1993a). "Standard classification of soils for engineering purposes (Unified Soil Classification System)," ASTM D2487-93, West Conshohocken, PA.
- _____. (1993b). "Standard practice for description and identification of soils (visual-manual procedure)," ASTM D2488-93, West Conshohocken, PA.
- _____. (1993c). "Standard test method for maximum index density and unit weight of soils using a vibratory table," ASTM D4253-93, West Conshohocken, PA.
- Bosscher, P. J., and Ortiz, C. (1987). "Frictional properties between sand and various construction materials," *Journal of Geotechnical Engineering*, ASCE, 113(9), 1035-1039.
- Brummund, N. F., and Leonards, G. A. (1973). "Experimental study of static and dynamic friction between sand and typical construction materials," *Journal of Testing and Evaluation*, ASTM, 1(2), 162-165.

- Clough, G. W., and Duncan, J. M. (1969). "Finite element analyses of Port Allen and Old River Locks," Report No. TE-69-3, U.S. Army Engineer Waterways Experiment Station, Vicksburg, MS.
- Clough, G. W., and Duncan, J. M. (1971). "Finite element analyses of retaining wall behavior," *Journal of the Soil Mechanics and Foundations Division*, ASCE, 97(SM12), 1657-1673.
- Desai, C. S., and Rigby, D. B. (1997). "Cyclic interface and joint shear device including pore pressure effects," *Journal of Geotechnical and Geoenvironmental Engineering* 123(6), 568-579.
- Desai, C. S., Drumm, E. C., and Zaman, M. M. (1985). "Cyclic testing and modeling of interfaces," *Journal of Geotechnical Engineering*, ASCE, 111(6), 793-815.
- Desai, C. S., Muqtadir, A., and Scheele, F. (1986). "Interaction analyses of anchor-soil systems," *Journal of Geotechnical Engineering*, ASCE, 112(5), 537-553.
- Desai, C. S., Zaman, M. M., Lightner, J. G., and Siriwardane, H. J. (1984). "Thin-layer elements for interfaces and joints," *International Journal for Numerical and Analytical Methods in Geomechanics* 8(1), 19-43.
- Duncan, J. M., and Chang, C. Y. (1970). "Nonlinear analysis of stress and strain in soils," *Journal of the Soil Mechanics and Foundations Division*, ASCE, 96(SM5), 1629-1653.
- Duncan, J. M., and Clough, G. W. (1971). "Finite element analyses of Port Allen Lock," *Journal of the Soil Mechanics and Foundations Division*, ASCE, 97(SM8), 1053-1067.
- Duncan, J. M., Byrne, P., Wong, K. S., and Mabry, P. (1980). "Strength, stress-strain and bulk modulus parameters for finite element analyses of stresses and movements in soil masses," Report No. UCB/GT/80-01, Department of Civil Engineering, University of California, Berkeley.
- Ebeling, R. M., and Filz, G. M. "Soil-structure interaction analyses of rock founded gravity and cantilevered walls" (in preparation), U.S. Army Engineer Waterways Experiment Station, Vicksburg, MS.
- Ebeling, R. M., and Mosher, R. L. (1996). "Red River U-Frame Lock No. 1 backfill-structure-foundation interaction," *ASCE Journal of Geotechnical Engineering* 122(3), 216-225.
- Ebeling, R. M., and Wahl, R. E. (1997). "Soil-structure-foundation interaction analysis of new roller-compacted concrete North Lock Wall at McAlpine Locks," Technical Report ITL-97-5, U.S. Army Engineer Waterways Experiment Station, Vicksburg, MS.

- Ebeling, R. M., Duncan, J. M., and Clough, G. W. (1990). "Methods of evaluating the stability and safety of gravity earth-retaining structures founded on rock - phase 2 study," Technical Report ITL-90-7, U.S. Army Engineer Waterways Experiment Station, Vicksburg, MS.
- Ebeling, R. M., Pace, M. E., and Morrison, E. E. (1997). "Evaluating the stability of existing massive concrete gravity structures founded on rock," Technical Report REMR-CS-54, U.S. Army Engineer Waterways Experiment Station, Vicksburg, MS.
- Ebeling, R. M., Peters, J. F., and Mosher, R. L. (1997). "The role of non-linear deformation analyses in the design of a reinforced soil berm at Red River U-Frame Lock No. 1," *International Journal for Numerical and Analytical methods in Geomechanics* 21, 753-787.
- Ebeling, R. M., Clough, G. W., Duncan, J. M., and Brandon, T. L. (1992). "Methods of evaluating the stability and safety of gravity earth retaining structures founded on rock," Technical Report REMR CS-29, U.S. Army Engineer Waterways Experiment Station, Vicksburg, MS.
- Ebeling, R. M., Mosher, R. L., Abraham, K., and Peters, J. F. (1993). "Soil-structure interaction study of Red River Lock and Dam No. 1 subjected to sediment loading," Technical Report ITL-93-3, U.S. Army Engineer Waterways Experiment Station, Vicksburg, MS.
- Esterhuizen, J. J. (1997). "Progressive failure of slopes in lined waste impoundments," Ph.D. Diss., Geotechnical Engineering Division, Department of Civil Engineering, Virginia Polytechnic Institute and State University, Blacksburg.
- Evgin, E., and Fakharian, K. (1996). "Effect of stress paths on the behaviour of sand-steel interfaces," *Canadian Geotechnical Journal* 33(6), 853-865.
- Fakharian, K., and Evgin, E. (1995). "Simple shear versus direct shear tests on interfaces during cyclic loading." *Proceedings Third International Conference on Recent Advances in Geotechnical Earthquake Engineering and Soil Dynamics*, St. Louis, MO, April 2-7, 1995. S. Prakash, ed., University of Missouri at Rolla, III, 13-16.
- Fakharian, K., and Evgin, E. (1996). "An automated apparatus for three-dimensional monotonic and cyclic testing of interfaces," *Geotechnical Testing Journal* 19(1), 22-31.
- Fakharian, K., and Evgin, E. (1997). "Cyclic simple-shear behavior of sand-steel interfaces under constant normal stiffness condition," *Journal of Geotechnical and Geoenvironmental Engineering* 123(12), 1096-1105.

- Filz, G. M. (1992). "An analytic and experimental study of earth loads on rigid retaining walls," Ph. D. Diss., Geotechnical Engineering Division, Department of Civil Engineering, Virginia Polytechnic Institute and State University, Blacksburg.
- Filz, G. M., and Duncan, J. M. (1997). "Vertical shear loads on nonmoving walls. I: Theory," *ASCE Journal of Geotechnical Engineering* 123(9), 856-862.
- Filz, G. M., Duncan, J. M., and Ebeling, R. M. (1997). "Vertical shear loads on nonmoving walls. II: Applications," *ASCE Journal of Geotechnical Engineering* 123(9), 863-873.
- Goodman, R. E., Taylor, R. L., and Brekke, T. L. (1968). "A model for the mechanics of jointed rock," *Journal of the Soil Mechanics and Foundations Division, ASCE*, 94(SM3), 637-659.
- Headquarters, U.S. Army Corps of Engineers. (1994). "Stability of gravity walls, vertical shear," Engineer Technical Letter 1110-2-352, Washington, DC.
- Headquarters, U.S. Army Corps of Engineers. (1997). "Stability analysis of concrete structures," Engineer Circular 1110-2-291 (Expires 30 September 1999), Washington, DC.
- Heuze, F. E., and Barbour, T. G. (1982). "New models for rock joints and interfaces," *ASCE Journal of the Geotechnical Engineering Division*, 108(GT5), 757-776.
- Hryciw, R. D., and Irsyam, M. (1993). "Behavior of sand particles around rigid ribbed inclusions during shear," *Soils and Foundations* 33(3), 1-13.
- Huck, P. J., and Saxena, S. K. (1981). "Response of soil-concrete interface at high pressure," *Proceedings of the Tenth International Conference on Soil Mechanics and Foundation Engineering*, Stockholm, 15-19 June 1981. A. A. Balkema, Rotterdam, 2, 141-144.
- Kishida, H., and Uesugi, M. (1987). "Tests of the interface between sand and steel in the simple shear apparatus," *Géotechnique* 37(1), 45-52.
- Kondner, R. L. (1963). "Hyperbolic stress-strain response: Cohesive soils," *Journal of the Soil Mechanics and Foundations Division, ASCE*, Proc. Paper 3429, 89(SM1), 115-143.
- Kondner, R. L., and Zelasko, J. S. (1963). "A hyperbolic stress-strain formulation for sands," *Proceedings, 2nd Pan-American Conference on Soil Mechanics and Foundations Engineering*, Sao Paulo, Brazil, July 16-24 1963. I, 289-324.

- Kramer, S. L. (1996). *Geotechnical earthquake engineering*. Prentice-Hall, Upper Saddle River, NJ.
- Kulhawy, F. H., and Peterson, M. S. (1979). "Behavior of sand-concrete interfaces," *Proceedings of the 6th Panamerican Conference on Soil Mechanics and Foundation Engineering*, Lima, Peru, December 2-7, 1979. II, 225-236.
- Lee, P. A., Kane, W. F., Drumm, E. C., and Bennett, R. M. (1989). "Investigation and modeling of soil-structure interface properties," *Foundation engineering: Current principles and practice*, ASCE Geotechnical Special Publication 22, 580-587.
- Matsui, T., and San, K. C. (1989). "An elastoplastic joint element with its application to reinforced slope cutting," *Soils and Foundations* 29(3), 95-104.
- Morrison, C. S. (1995). "The development of a modular finite element program for analyses of soil-structure interaction," Ph.D. Diss., Geotechnical Engineering Division, Department of Civil Engineering, Virginia Polytechnic Institute and State University, Blacksburg.
- Peterson, M. S., Kulhawy, F. H., Nucci, L. R., and Wasil, B. A. (1976). "Stress-deformation behavior of soil-concrete interfaces," Contract report B-49 to Niagara Mohawk Power Corporation, Syracuse, NY.
- Potyondy, J. G. (1961). "Skin friction between various soils and construction materials," *Géotechnique* 11(4), 339-353.
- Pyke, R. (1979). "Nonlinear soil models for irregular cyclic loadings," *ASCE Journal of the Geotechnical Engineering Division* 105(GT6), 715-726.
- Sehn, A. L., and Duncan, J. M. (1990). "Experimental study of earth pressures on retaining structures," Ph.D. Diss., Geotechnical Engineering Division, Department of Civil Engineering, Virginia Polytechnic Institute and State University, Blacksburg.
- Shallenberger, W. C., and Filz, G. M. (1996). "Interface strength determination using a large displacement shear box." *Proceedings of the Second International Congress on Environmental Geotechnics*, Osaka, Japan, 5-8 November 1996. M. Kamon, ed., A. A. Balkema, Rotterdam.
- Stark, T. D., Ebeling, R. M., and Vettel, J. J. (1994). "Hyperbolic stress-strain parameters for silts," *Journal of Geotechnical Engineering*, ASCE, 120(2), 420-441.
- Stark, T. D., Williamson, T. A., and Eid, H. T. (1996). "HDPE geomembrane/geotextile interface shear strength," *Journal of Geotechnical Engineering* 122(3), 197-203.

- Uesugi, M., and Kishida, H. (1985). "Discussion: Cyclic testing and modeling of interfaces," *Journal of Geotechnical Engineering*, ASCE, 113(9), 1086-1087.
- _____. (1986a). "Frictional resistance at yield between dry sand and mild steel," *Soils and Foundations* 26(4), 139-149.
- _____. (1986b). "Influential factors of friction between steel and dry sands," *Soils and Foundations* 26(2), 33-46.
- Uesugi, M., Kishida, H., and Tsubakihara, Y. (1988). "Behavior of sand particles in sand-steel friction," *Soils and Foundations* 28(1), 107-118.
- _____. (1989). "Friction between sand and steel under repeated loading," *Soils and Foundations* 29(3), 127-137.
- Uesugi, M., Kishida, H., and Uchikawa, Y. (1990). "Friction between dry sand and concrete under monotonic and repeated loading," *Soils and Foundations* 30(1), 115-128.
- Wilson, E. L. (1977). "Finite elements for foundations, joints and fluids." *Finite elements in geomechanics*. G. Gudehus, ed., John Wiley, London.
- Wong, P. C., Kulhawy, F. H., and Ingraffea, A. R. (1989). "Numerical modeling of interface behavior for drilled shaft foundations under generalized loading," *Foundation Engineering: Current Principles and Practice*, ASCE Geotechnical Special Publication 22, 565-579.
- Yoshimi, Y., and Kishida, T. (1981). "A ring torsion apparatus for evaluating friction between soil and metal surfaces," *Geotechnical Testing Journal* 4(4), 145-152.
- Yuan, Z., and Chua, K. M. (1992). "Exact formulation of axisymmetric-interface-element stiffness matrix," *Journal of Geotechnical Engineering* 118(8), 1264-1271.
- Zaman, M. M., Desai, C. S., and Drumm, E. C. (1984). "Interface model for dynamic soil-structure interaction," *Journal of Geotechnical Engineering* 110(9), 1257-1273.

Appendix A

Notation

| | |
|------------|--|
| a | Reciprocal of the initial shear stiffness of the interface K_{si} under initial loading |
| a_r | Reciprocal of the initial shear stiffness K_{sr} upon shear reversal |
| b | Reciprocal of the asymptotic shear stress t_{ult} under initial loading |
| b_r | Reciprocal of the relative-asymptotic shear stress t_{ur} upon shear reversal |
| c' | Cohesion intercept in terms of effective stresses |
| C_c | Coefficient of curvature |
| C_N | Correction factor for the number of steps in the back side of a rock-founded gravity wall |
| C_s | Correction factor for a rock-founded gravity retaining wall with an inclined backfill surface |
| C_u | Uniformity coefficient |
| C_θ | Correction factor for inclination of the back side of a rock-founded gravity wall |
| D_R | Relative density |
| D_1 | Thickness of the backfill above the hydrostatic water table |
| D_2 | Thickness of the submerged backfill above the heel of the wall |
| D_{10} | Particle size diameter corresponding to 10%, 30%, or 60%, respectively, passing in the grain size distribution curve |

| | |
|---------------|--|
| E_i | Initial tangent modulus |
| F_v | Vertical force or downdrag per unit length of wall |
| F_x' | Effective horizontal force per unit length of wall |
| g | $(\sigma_1 - \sigma_3)/2$ |
| G_s | Specific gravity |
| H | Height measured along a vertical plane passing through the heel of the wall and extending through the backfill |
| H_b | Total backfill height as measured in Figure 2-5 |
| k_n | Normal interface stiffness |
| k_s | Interface shear stiffness |
| K_{f-line} | Line joining the failure points in the p' - g plane |
| K_h | Earth pressure coefficient for effective horizontal forces |
| K_l | Dimensionless interface stiffness number for initial loading |
| K_{lr} | Dimensionless interface stiffness number for shear reversals |
| K_{lrl} | Dimensionless interface stiffness number for reloading |
| K_{lst} | Dimensionless interface stiffness number for staged shear |
| K_{lul} | Dimensionless interface stiffness number for unloading |
| K_{si} | Dimensionless interface initial shear stiffness of the interface |
| K_{sr} | Initial shear stiffness for shear for initial loading of the interface reversals |
| K_{st} | Interface tangent stiffness |
| K_v | Earth pressure coefficient for vertical forces |
| $K_{v,q}$ | Vertical shear force coefficient for sloping backfill and surcharge |
| $K_{v,q,ref}$ | Reference value of $K_{v,q}$ obtained for a value of $S = 0$ |
| $K_{v,soil}$ | Vertical shear force coefficient for self-weight of the backfill |

| | |
|------------------|---|
| $K_{v,soil,ref}$ | Reference value of $K_{v,soil}$ obtained for an inclination of the back of the wall, θ , of 90 degrees |
| N | Number of steps in the back of a stepped wall |
| n | Dimensionless interface stiffness exponent for initial loading |
| n_r | Dimensionless interface stiffness exponent for shear reversals |
| n_{rl} | Dimensionless interface stiffness exponent for reloading |
| n_{st} | Dimensionless interface stiffness exponent for staged shear |
| n_{ul} | Dimensionless interface stiffness exponent for unloading |
| p' | $(\sigma'_1 + \sigma'_3)/2$ |
| p_a | Atmospheric pressure |
| q | Applied surcharge pressure |
| r | Subscript denoting shear reversal |
| R_f | Failure ratio for initial loading |
| R_{fr} | Failure ratio for shear reversals |
| R_{fri} | Failure ratio for reloading |
| R_{fst} | Failure ratio for staged shear |
| R_{ful} | Failure ratio for unloading |
| st | Subscript denoting staged shear of the interface |
| S | Horizontal distance from the vertical plane through the wall heel to the top of the backfill slope |
| Sl_r | Relative stress level |
| Sl_{ur} | Stress level at the unload or reload points |
| ur | Subscript denoting that a parameter has the same values for both unloading and reloading of the interface |
| α_{rl} | Dimensionless scaling factor for reloading |
| α_{ul} | Dimensionless scaling factor for unloading |

| | |
|------------------------------|--|
| β_{ub}, β_{rl} | Nondimensional coefficients for unloading and reloading, respectively |
| γ_b | Buoyant unit weight of submerged backfill |
| $\gamma_{max}, \gamma_{min}$ | Maximum and minimum density, respectively |
| γ_{moist} | Moist unit weight of the backfill above the water table |
| γ_w | Unit weight of water |
| δ | Angle of interface friction |
| δ_p | Peak interface friction angle |
| δ_r | Residual interface friction angle |
| Δ_{act} | Actual sliding displacement between soil particles and concrete |
| Δ_{dis} | Deformation of the sand mass due to distortion during interface shear |
| Δ_{meas} | Displacement measured between the soil box and concrete specimen |
| Δ_n | Displacement normal to the interface |
| Δ_o | Interface displacement at the unload or reload point |
| $\Delta_{r,l}, \tau_{r,l}$ | Coordinates in the shear stress-displacement plane at the shear reversal point <i>RI</i> |
| Δ_{rl} | Interface displacement at the reload point <i>RL</i> |
| Δ_s | Displacement along the interface |
| Δ_v | Vertical displacement during interface testing |
| Δ_{ul} | Interface displacement at the unload point <i>UL</i> |
| ϵ | Axial strain |
| σ_n | Normal stress acting on the interface |
| σ_v' | Effective vertical stress |
| σ_1 | Major principal total stress |
| σ_1' | Major principal effective stress |

| | |
|-------------------------------|--|
| σ_3 | Total confining stress |
| σ_3' | Effective confining stress |
| $(\sigma_1 - \sigma_3)_f$ | Deviator stress at failure |
| $(\sigma_1 - \sigma_3)_{ult}$ | Asymptotic strength in triaxial testing |
| τ | Interface shear stress |
| τ_f | Interface shear strength for initial loading |
| τ_{fr} | Interface relative shear strength for shear reversals |
| τ_o | Interface shear stress at the unload or reload point |
| τ_{rl} | Interface shear stress at the reload point <i>RL</i> |
| τ_{ur} | Relative-asymptotic interface shear stress for shear reversals |
| τ_{ul} | Interface shear stress at the unload point <i>UL</i> |
| τ_{ult} | Asymptotic interface shear stress value for initial loading |
| ϕ'_p | Peak friction angle |
| ϕ'_{cv} | Friction angle at a strain of 15% |

REPORT DOCUMENTATION PAGEForm Approved
OMB No. 0704-0188

Public reporting burden for this collection of information is estimated to average 1 hour per response, including the time for reviewing instructions, searching existing data sources, gathering and maintaining the data needed, and completing and reviewing the collection of information. Send comments regarding this burden estimate or any other aspect of this collection of information, including suggestions for reducing this burden, to Washington Headquarters Services, Directorate for Information Operations and Reports, 1215 Jefferson Davis Highway, Suite 1204, Arlington, VA 22202-4302, and to the Office of Management and Budget, Paperwork Reduction Project (0704-0188), Washington, DC 20503.

| | | | | |
|--|---|--|---|--|
| 1. AGENCY USE ONLY (Leave blank) | | 2. REPORT DATE January 1999 | 3. REPORT TYPE AND DATES COVERED Final report | |
| 4. TITLE AND SUBTITLE Development of an Improved Numerical Model for Concrete-to-Soil Interfaces in Soil-Structure Interaction Analyses; Report 1, Preliminary Study | | | 5. FUNDING NUMBERS Work Order 31589 | |
| 6. AUTHOR(S) Jesús E. Gómez, George M. Filz, Robert M. Ebeling | | | | |
| 7. PERFORMING ORGANIZATION NAME(S) AND ADDRESS(ES) Virginia Polytechnic Institute and State University, Blacksburg, VA 24061-0105; U.S. Army Engineer Waterways Experiment Station, 3909 Halls Ferry Road, Vicksburg, MS 39180-6199 | | | 8. PERFORMING ORGANIZATION REPORT NUMBER Technical Report IITL-99-1 | |
| 9. SPONSORING/MONITORING AGENCY NAME(S) AND ADDRESS(ES) U.S. Army Corps of Engineers Washington, DC 20314-1000 | | | 10. SPONSORING/MONITORING AGENCY REPORT NUMBER | |
| 11. SUPPLEMENTARY NOTES Available from National Technical Information Service, 5285 Port Royal Road, Springfield, VA 22161. | | | | |
| 12a. DISTRIBUTION/AVAILABILITY STATEMENT Approved for public release; distribution is unlimited. | | | 12b. DISTRIBUTION CODE | |
| 13. ABSTRACT (Maximum 200 words) <p>Soil-Structure Interaction (SSI) analyses have proven to be powerful tools for use in analyzing, designing, and monitoring geotechnical structures. SSI analyses are particularly useful in problems of complex geometry and loading conditions such as lock walls.</p> <p>Several SSI analyses of Corps of Engineers lock walls have shown that the behavior of the soil-structure interface has a significant influence on the magnitudes of the loads acting against a lock wall. They have also illustrated that the pre- and post-construction field stress paths followed by interface elements often involve simultaneous changes in normal and shear stresses, as well as shear stress reversals. The hyperbolic formulation for interfaces, used commonly in SSI analyses, models interface behavior in the primary loading stage very closely. However, it has not been extended to accurately model simultaneous changes in shear and normal stresses, reduction of shear stress, reversals in the direction of shear, or unload-reload cycles at the interface.</p> <p>The purpose of this research is to develop an interface model capable of giving accurate predictions of the interface response under field loading conditions. In order to develop the necessary test data, the Large Displacement Shear Box (LDSB) at Virginia Polytechnic Institute and State University, Blacksburg, VA, was modified to permit soil-to-concrete</p> <p style="text-align: right;">(Continued)</p> | | | | |
| 14. SUBJECT TERMS Earth retaining structures Interface constitutive model Interface testing | | | 15. NUMBER OF PAGES 153 | |
| | | | 16. PRICE CODE | |
| 17. SECURITY CLASSIFICATION OF REPORT UNCLASSIFIED | 18. SECURITY CLASSIFICATION OF THIS PAGE UNCLASSIFIED | 19. SECURITY CLASSIFICATION OF ABSTRACT | 20. LIMITATION OF ABSTRACT | |

13. (Concluded).

interface testing. A concrete specimen for interface testing was prepared with a surface texture similar to that of concrete retaining walls in service. A number of tests were performed on the interface between this concrete specimen and a uniform dense sand: initial loading, shear reversals, staged shear, and unloading-reloading of the interface.

This research is being conducted in two phases. This report presents the results of the testing performed for the Phase I research. It also contains a preliminary version of an improved numerical model for interfaces, which was developed according to the results of the interface tests performed. This preliminary model is based on the hyperbolic formulation, which has been extended to model shear reversals, load-unload cycles, and staged shear. It was found that the model gives accurate approximations to the interface response under these loading conditions.

A more complete version of this model will evolve as the laboratory testing progresses and as other variables are investigated. For this purpose, additional tests will be performed to investigate the influence of the following variables on interface behavior: density, gradation, and angularity of sand. The final version of the new interface model will be developed, based on the results of these additional tests, during Phase 2 of this investigation.